3 – The Kara-Bom Upper Paleolithic variant

3.1 KARA-BOM: SITE DESCRIPTION AND TECHNOLOGICAL ANALYSIS

3.1.1 GEOGRAPHICAL SETTING

Kara-Bom (N 50° 43'; E 85° 42') is located in the Yelo Basin in the intermountain depression system of Central Altai (Siberia, Russia). The elevation of this area reaches 1100 m asl between mountains composed mainly of Middle Devonian metamorphic rocks and ranging to around 2300 m asl. Lying on the foothills of a schist cliff, Kara-Bom is located adjacent to a fresh water spring. At about 700 m from the site is a natural amphitheatre and a low pass to the neighboring valley. These topographic features could have been attractive for hunters as they provide a natural trap (Figure 17).

3.1.2 BACKGROUND

The excavation started in 1980 under the supervision of Okladnikov (Figure 20, Area 1). As it was first thought that the deposits were heavily disturbed by water circulation, the initial phase of excavation was executed by digging arbitrary spits of 25-30 cm thickness over a surface of 16 m² (Figure 19). Following the discovery of an artifact bearing horizon starting from the second spit (Okladnikov, 1983: 6)

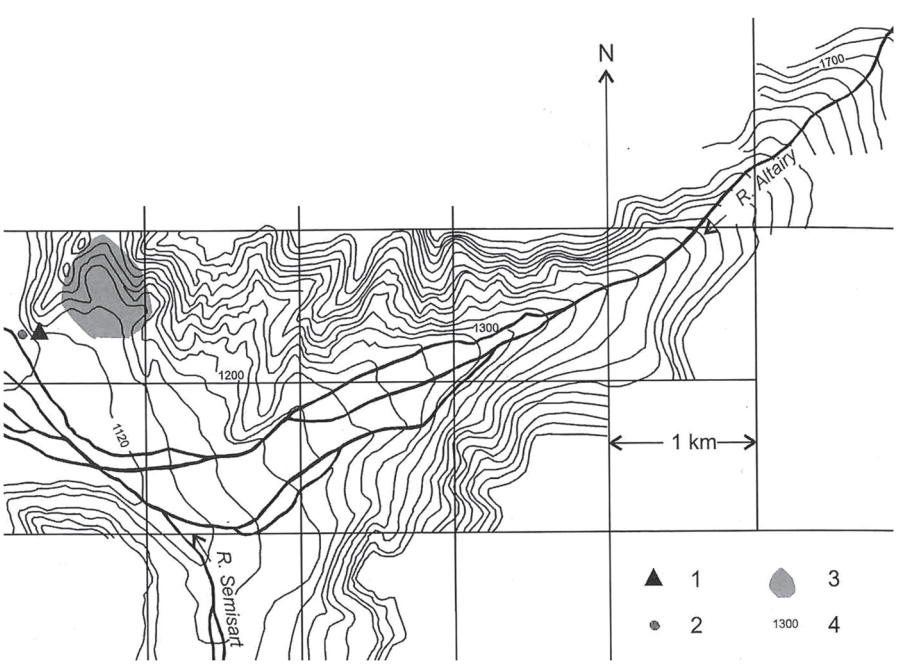

Figure 17: Topographic map. 1: Kara-Bom site; 2: spring; 3: amphitheatre; 4: absolute elevation asl. (after Derevianko and Rybin, 2003)

Figure 18: Kara-Bom, A.P. Okladnikov (center) at Kara-Bom during the 1980s excavations (courtesy of E.P. Rybin)

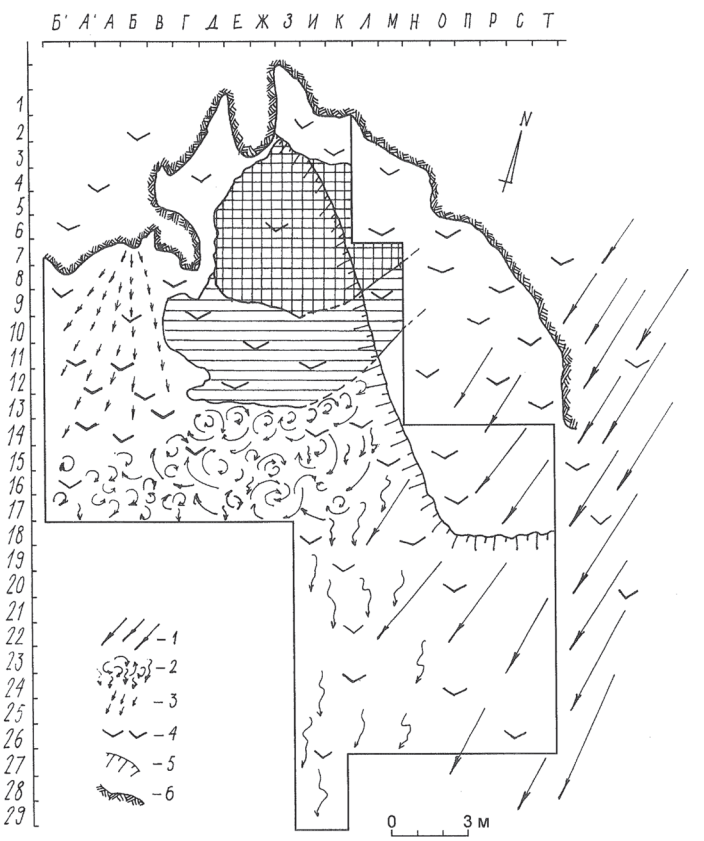

Figure 19: Kara-Bom, analytical reconstruction of post-depositional processes affecting the Kara-Bom site. 1: direction of the melting snow; 2: spring activity; 3: rain water flow; 4: gravitational disturbances (rockfall); 5: underground limit of the cliff; 6: visible limit of the cliff (after Derevianko *et al.*, 1998)

excavators proceeded following stratigraphic layers. The so-called workshop is located in the third spit (Level 3 of Okladnikov's scheme) in a yellowish-brown sandy loam that contains large plates of schist. In 1980, although other parts of Area 1 were excavated deeper, the workshop was not completely excavated (Okladnikov, 1983). According to Okladnikov's report, the western part of the workshop was excavated to a maximum absolute depth of -411 cm, which corresponds to the top of the MPH1.

In 1987, the Altai team of the North Complex Archaeological Expedition (Institute of Archaeology and Ethnography) started the second phase of excavations under the direction of Derevianko and Petrin. Between 1987 and 1993, no fewer than 300 m² were excavated following an extended Cyrillic grid system based on the one used by Okladnikov (Figure 20: area 1-4). Similar datum points and square divisions were used, allowing comparisons based on absolute altitudes (Okladnikov, 1983: 6). In 1991, excavation in Area 1 was completed. A fire-place was found in quadrants I-K/8-9 and a new excavation was made in squares L, M/7-9 corresponding to the stratigraphic position of Okladnikov's workshop. There after, excavation in Area 4 established a new lithological and archeological stratigraphic scheme. Six artifact bearing horizons were recognized, two of which were attributed to the Middle Paleolithic (Derevianko, Petrin, *et al.*, 1998). More recently, Areas 1 and 4 were correlated on the basis of stratigraphic and archeological elements. The workshop (1980 and 1987 excavations, squares Z-L/7-9 from Area 1, including the I-K/8-9 fireplace) is associated with Occupation Horizons (OH) 5 and 6 from the newly excavated Area 4 (Derevianko and Rybin, 2003).

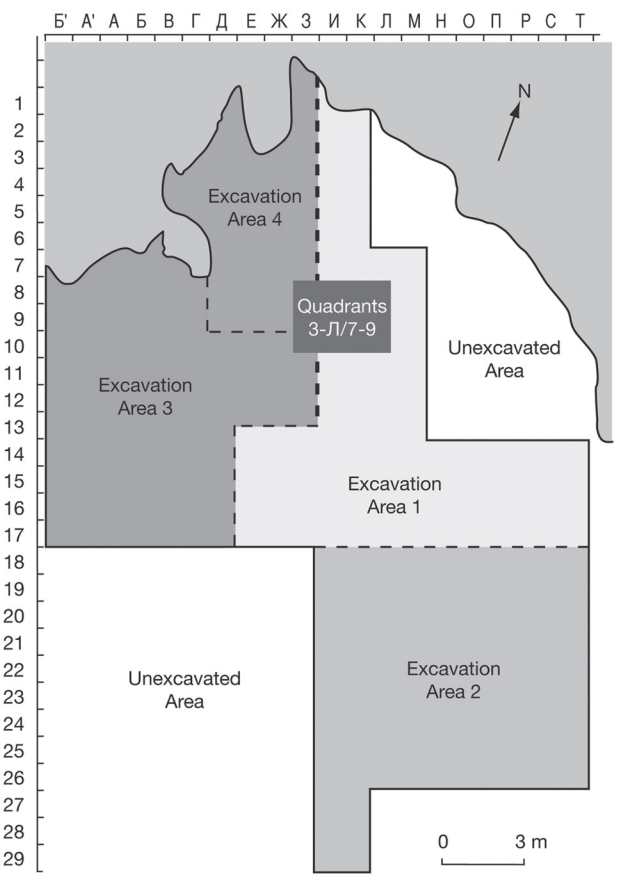

Figure 20: Kara-Bom, map showing excavated and unexcavated areas (modified after Derevianko *et al.*, 1998)

3.1.3 STRATIGRAPHY

The lithological and cultural divisions are briefly described following the section I-1/11. The 3.5 m thick sequence was subdivided into three major units (Figure 21). Unit 1 includes lithological strata 1-8, unit 2 corresponds to stratum 9 and unit 3 to strata 10 and 11. Slope deposits from the lithological uppermost unit 1 contain fine aeolian sediments and grayish yellow sandy loam and debris. Strata 4 to 2 were identified close to the cliff, as they were washed out by erosion starting approximately 3 m from the wall. The uppermost portion of stratum 4 has yielded the Occupation Horizon 1 (OH1). Stratum 5 is composed of brownish-gray loam and is subdivided into 5a and 5b, the later yielding more *debris*. Occupation Horizons 2 (OH2) and 3 (OH3) are respectively associated with strata 5a and 5b. Stratum 6 consists of gray coarse rock fragments, schist elements and gravels cemented by sandy-loam. The uppermost portion of stratum 6 shows the admixture of humic sediment and includes (OH4). This could correspond to a buried soil in secondary position. Starting from the central part of the stratum, schist slabs occur in horizontal position and they increase in density as one moves deeper. OH5 was identified in the central part of the stratum and OH6 is located close to the lowermost portion. OH4, 5 and 6 are attributed the to Upper Paleolithic. Stratum 9 is composed of a homogenous deposit and is subdivided in three substrata. Separated from the OH6 by three sterile strata (7, 8 and 9a), the first Middle Paleolithic Horizon (MPH1) is associated with sub-stratum 9b and MPH2 with sub-stratum 9B. Humic sediments occur in sub-stratum 9B. The bottom of the sequence is composed of cryoturbated slumping deposits overlying the bedrock (strata 10-11) and is archeologically sterile (Derevianko, Nikolayev, and Petrin, 1993; Derevianko, Petrin, *et al.*, 1998; Derevianko, Petrin, and Rybin, 2000; Derevianko and Rybin, 2003). According to Okladnikov's report, the western part of the workshop was originally excavated to a maxi-

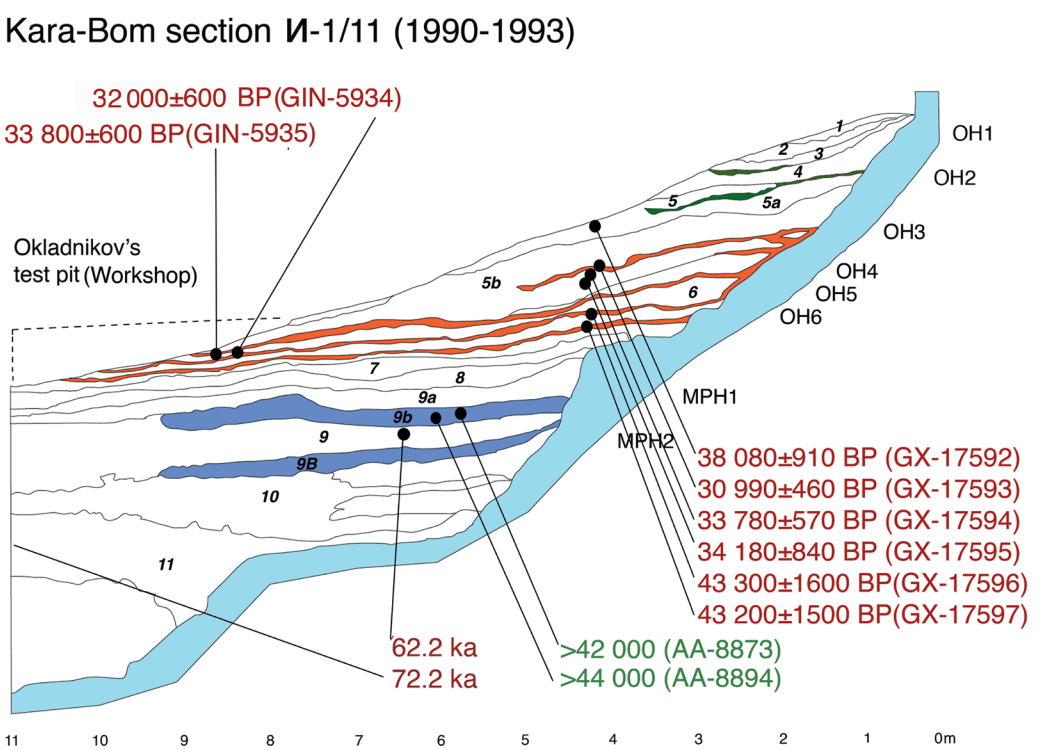

Figure 21: Kara-Bom, I-1/11 section with dated sample locations, numbers are lithological strata (modified after Derevianko and Rybin, 2003)

mum absolute depth of -411 cm in square Z12, which corresponds to the top of the MPH1 (Okladnikov, 1983: 6). It seems, therefore, unlikely that the Okladnikov test pit reached the Middle Paleolithic occupation layers in this area. Between squares B-N/14-17, the test pit was excavated deeper. This area was described, however, by Nikolaiev as disturbed due to spring water circulation (Derevianko, Petrin, *et al.*, 1998).

3.1.4 CHRONOLOGY

The first attempt to date the sequence yielded two conventional radiocarbon results. The first is 32,000 ± 600 ^{14}C BP (GIN-5934) on a bone collagen sample coming from stratum 4, but for which the cultural association with OH4 remains unclear. The second, 33,800 ± 600 ^{14}C BP (GIN-5935), comes from a wood charcoal sample associated with a fireplace located in quadrants I-K/8-9, between OH4 and OH5. In 1991, Goebel excavated a small column within the section exposed by Petrin. The sequence has been dated by AMS, conventional ^{14}C, and by Electro Paramagnetic Reasonance (EPR) (calendar age, uptake unspecified)(Derevianko, Nikolayev, and Petrin, 1993; Goebel *et al.*, 1993). Two infinite dates were obtained for the MPH 1; > 44 ka ^{14}C BP (AA-8894) and > 42 ka ^{14}C BP (AA-8873), both coming from bone collagen as no charcoal was found associated with this level. In addition, lithological stratum 8 (below the MPH1) and 11 (below MPH2) yielded EPR results of 62.2 ka and 72.2 ka respectively. These results mainly bracket MPH2, however, the upper sample was taken within a sandy loam sediment matrix from stratum 9, just underneath the interface with the MPH1 that the geologist Nikolayev recognizes as 'rather hypothetical' (Derevianko, Nikolayev, and Petrin, 1993). The small profile exposed does not include OH5 and OH6, as the section starts from stratum 7. The MPH1 occurs at mid-section, separated from OH6 by more than 50 cm of sterile sediment, in which Nikolayev recognizes two clear interfaces (7/8, and 8/9). Although he was excavating by 50 cm thick spits, Okladnikov previously mentioned this hiatus (Okladnikov, 1983; Derevianko, Nikolayev, and Petrin, 1993). The OH6 and OH5 have AMS ages of 43,200 ± 1,500 ^{14}C BP (GX-17597) and 43,300 ± 1,600 ^{14}C BP (GX-17596) respectively, both on wood charcoal, with the latter being directly associated with a fireplace from quadrant I4/5 within OH5 (Goebel *et al.*, 1993). Two ^{14}C dates were obtained on charcoal coming from above OH4 and yielding 34,180 ± 640 ^{14}C BP (GX-17595) and 33,780 ± 570 ^{14}C BP (GX-17594). OH3 has yielded a date of 30,990 ± 460 ^{14}C BP (GX-17593). In this series, only the following result does not fit with the stratigraphic succession. A 38,080 ± 910 ^{14}C BP (GX-17592) date was obtained on a charcoal sample collected close to the surface and in the vicinity of a frost crack. It was the only sample of the 1991's series not associated with archeological material. Among the results obtained during the first dating campaign, the result coming from OH5 is clearly younger then Goebel's results. In this case, the latter are considered reliable as they are directly linked with the I4/5 fireplace. Coming from above a step in the bedrock, these results are very unlikely contaminated by material from MPH1. The two results obtained on OH5 and OH6 samples indicate an age between 46 and 40 ka BP at a two-sigma range. It is noteworthy that they are very close to the limits of the ^{14}C method, and Goebel notes that they could also indicate a minimum age. The stratigraphic position of the I-K7/9 fireplace (downslope) and its conventional ^{14}C date do not rule out an association of this feature with the OH4. The occurrence of *Coelodonta antiquitatis* (woolly rhinoceros) coming from the fire structure from quadrants I-K7/9 (Derevianko and Rybin, 2003) seems to indicate an occupation during a rather cold phase. In OH6 and OH5, fauna is generally badly preserved. In OH6, the presence of *Equus hidruntinus* (wild ass), *Equus sp.* (horse/ass), *Capra sibirica* (ibex) and *Crocuta spelaea* (hyena) are reported. *Bison sp.* (bison) occurs in OH5 but also in OH4 together with *Equus sp*.(Vasiliev, 2003).

3.1.5 TAPHONOMIC APPROACH

This study focuses on the material associated with OH5 and OH6 and starts by trying to assess the integrity of the assemblage within the stratified part of the site excavated according to stratigraphic layers. For this, breakage refits on broken laminar elements and short sequence refits are used. Artifacts are plot-

Squares	OH4	OH4/OH5	OH5	OH5/OH6	OH6	Type	ID
Z7/Z8	1					Break	h
Z7		1				Break-X/Y?	n
Z5/Z6			1			Sequence	p
Z7			1			Break	m
J8			1			Break	g
I9/Z8			1			Break	e
Z8			1			Break-X/Y?	f
I9/Z9			1			Break	b
I9			1			Break	a
Z6			1			Break	o
I9/E8				1		Sequence	c
Z9				1		Break	d
Z7/Z9				1		Sequence	i
I8					1	Break	j
Z7/E7					1	Sequence	l
Z8					1	Break	k
	1	1	8	3	3		N=32

Table 1: Kara Bom, distribution of inter-(shaded rows) and intra-OH refits.

ted on I-1/11 section according to their positions following the coordinate system used during the excavation (*e.g.* Hofman, 1986; Cziesla, 1990; Bordes, 2000). The purpose of this work was not to refit long technological sequences to tackle behavioral issues, but rather to test movement between layers.

The refitted group of artifacts can be divided into three main categories. The first group includes broken elements for which it was possible to rule out breakage due to excavation methods (Figure 22). On some of the snapped sections, mineral concretions testify to the ancient character of the breakage.The second category deals with the technological refits, testifying to knapping activities (Figure 23). The third one can be either on breakage or technological, but for these spatial information within the square was missing. For these, an arbitrary position was chosen, generally in the middle of the square.

The majority of the refits are attributed to OH5 (Table 1). Among the two refits involving OH4, one connects it with OH5 from lateral a distance of 2 m. Among six refits involving OH6, three connect it with OH5. These connections between the levels do not show substantial vertical movement (Figure 24). They seem to suggest a rather good integrity of the OH5, showing inter-level contacts downslope with OH6 (quadrant 7/9), where OH5 and 6 are very close to each other. However, the good preservation of the I5/4 fireplace seems to indicate a low-energy sedi-

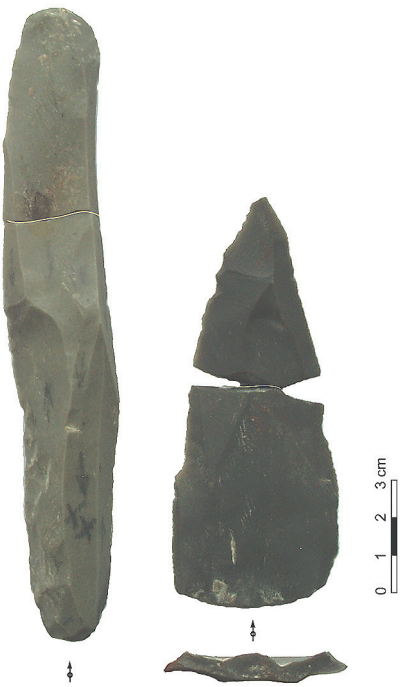

Figure 22: Refits on breakage. Left: O; Right: K

Figure 23: Technological refit (I): side blade refitted on a retouched blade

mentation rate where both OH5 and 6 are separated by maximum 25 cm thickness.

All in all, it seems that the material from OH4, OH5 and OH6 should be treated as independent stratigraphic units at least for the E-K/1-11 excavation units. However, four refits show some occasional problems downslope, along lines 7-9. In all cases, artifacts were found at the same depth showing no vertical movements. According to previous studies on the 1980-1991s collection, it is also worth noting that no refits were found between artifacts from MPH1 and OH6. Although further efforts could be devoted on this specific issue, the occurrence of intervening sterile levels reinforces the idea that those cultural horizons were distinct. However, one technological refit of a laminar core, including nine artifacts, indicates some mixing between OH at the bottom of the slope. Among nine artifacts, four were attributed to OH4, three to 'the periphery of OH5', downslope, and two to the Okladnikov's workshop (Slavinsky and Rybin, 2007). Given that the archeological layers are stretched in this part of the site, and given the good preservation of the hearth feature at the bottom of OH6, this situation does not reflect a large scale high energy process. No connections have been found between OH6 and OH4 and the idea that the fire structure is an intrusion from OH4 to OH6 seems unlikely. The available data rather suggest localized slope processes combined with minor mixing during the excavation or during the labeling. Refits between OH4, OH5 and OH6 have been tested but given the nature of the raw material and the time devoted to this type of analysis, it is unlikely that all possibilities of refits have been tested.

3.1.6 SAMPLE COMPOSITION

During the second phase of excavation, 20 m² were excavated in MPH1. A total of 104 artifacts, including 9 potential preforms, 3 cores, 41 tools and 46 flakes. This material was described as a Mousterian

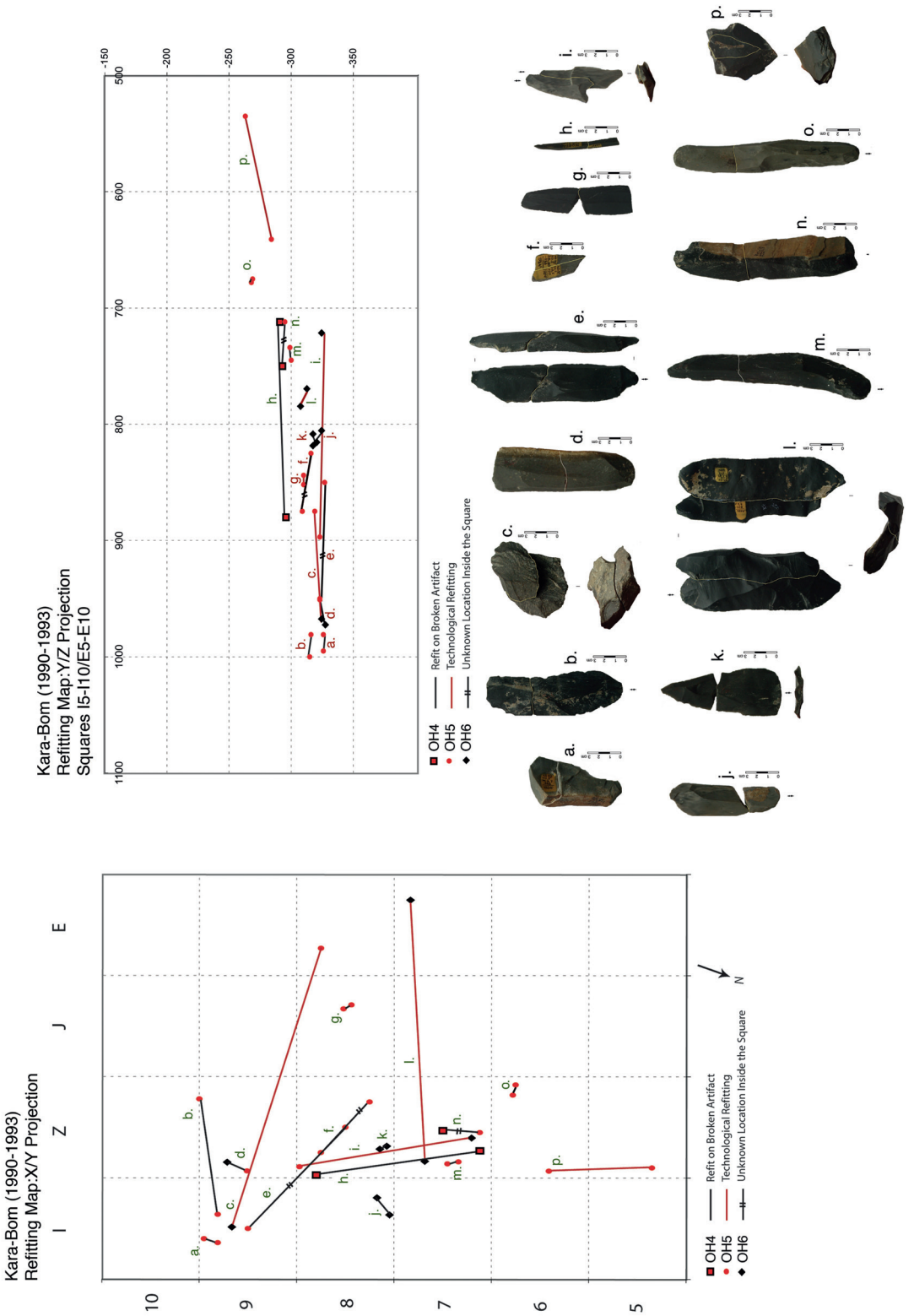

Figure 24: Kara-Bom: refitted artifact plot in section (right) and in plan (left)

	MPH1		OH6		OH5		OH4		1980–1991	
	N	*f*	N	*f*	N	*f*	N	*f*	N	*f*
Blade	15	44%	126	61%	123	65%	34	62%	0	0%
Bladelet	0	0%	36	17%	22	12%	5	9%	0	0%
Microblade	0	0%	0	0%	3	2%	0	0%	0	0%
Flake	5	15%	4	2%	4	2%	0	0%	0	0%
Core	2	6%	14	7%	10	5%	0	0%	21	100%
Tool	12	35%	28	13%	26	14%	16	29%	0	0%
	34	100%	208	100%	188	100%	55	100%	21	100%

Table 2: Kara-Bom, general structure of the sample

assemblage. OH6 yielded 878 artifacts from a 12 m² surface including 351 blades, 339 flakes, and 143 tools (Derevianko, Petrin, *et al.*, 1998). For OH5, 14 m² were excavated yielding a total of 594 lithic artifacts, with a concentration in squares Z-I/5-9. 282 blades (mainly fragments), 215 flakes, and 81 tools are reported in the original publication. OH4 was excavated over a surface of 11 m², yielding 214 lithic artifacts, among which 4 are preform/cores, 73 are blades and 39 are listed as tools (Derevianko, Markin, *et al.*, 2001). Although it was sometimes described as chert (*e.g.* Goebel, 1993; Brantingham *et al.*, 2000; Derevianko *et al.*, 2001) or as cryptocristaline silicate (Goebel, 2004), the raw material in use mostly consist in metamorphic rock . The primary outcrops are located in the surrounding mountains (*e.g.* Mt Aptyrga) along tectonic cracks and are carried by the Altairy River on a relatively short distance (1-2 km away). Tabular blocks offer the necessary volume for the production of massive blades. The homogeneity, the fine-grained texture and the hardness (6.5 on the Mohs scale) make this highly suitable material convenient (Derevianko *et al.*, 2000; Derevianko and Shunkov, 2005). It represents 98% of the raw material used in both Middle and Upper Paleolithic levels in Kara-Bom (Brantingham *et al.*, 2000). The material from OH6-OH4 was previously described as a transitional technology showing a shift between a Levallois parallel blade reduction towards prismatic and narrow-face cores. This change is linked with the predominance of blade production over flake production and with the first appearance of 'microblades' (Petrin and Chevalkov, 1992). These small laminar elements are said to be produced from the narrow face of exhausted blade cores (Petrin and Chevalkov, 1992) or on massive *débordant* flakes (Derevianko, Petrin, *et al.*, 1998, 1999; Derevianko and Rybin, 2003; Derevianko and Volkov, 2004).

The general structure of the sample studied here is described in Table 2. Mainly laminar elements from the stratified part of the site and bearing an unambiguous level label were selected. Some of the artifacts showing inconsistency between their altitude and their stratigraphic attributions have been either removed or described separately. For example, three blades (including two naturally backed blades) were labeled as MPH1 but have an altitude corresponding to OH5 in the relevant squares. These artifacts were, therefore, removed from consideration. Another core (KB-92.YO5.Z6.1) was published as belonging to OH5 (Derevianko *et al.*, 1998, Fig.41, num. 4) but with an altitude of -398. Given that the lowest artifact in that square has an altitude of -343, the core is described in the 'Additional artifacts' section.

The numeric differences between the sample considered here and the material reported in the original publication can be explained in various ways. Although all material that was available at the time of the study have been sampled, large differences in terms of tools can be observed. First, this is due

to the fact that only laminar artifacts bearing clear intentional retouch are considered here, so that numerous tools on flake blanks, *'notches'* or '*naturally backed knife'*, although belonging to the Bordes's type list (Bordes, 1961), have been left out of the tool category. These categories of tool represent a significant part of the original artifact list. For example, the sum of denticulates, notches, knives and blanks bearing irregular or sporadic retouch represent 83 artifacts in OH6 and 42 artifacts in OH5. Second, for some of the assemblages, almost all burins have been described as cores (Mode B) in various stages of reduction.

3.2 LAMINAR TECHNOLOGY: MPH1

3.2.1 BLANK ATTRIBUTES

Breakage

Leaving out the complete elements, mesioproximals and mesial fragments are the most common among the blade set (Table 3). For analytical purposes, a minimum number of individual blanks (MNI) is calculated. It includes all artifacts which have a platform (complete, proximal and mesioproximal fragments). The MNI reduces the risk that artifact breakage introduces a bias in the dataset. For MPH1, an MNI of 15 artifacts is calculated on a total sample of 20 artifacts.

Platform: size and preparation

Taken as a whole, blade platforms have a mean thickness of 3.7 ± 1 mm and a mean width of 9.4 ± 5.2 mm. Flakes have a mean thickness of 9.4 ± 2.3 mm. Flake platform widths have a mean of 30.8 ± 10.2 mm. In spite of the small sample size, blade platform thickness (Mann-Whitney, T=Ub=0, p=<.05) and width (Mann-Whitney, T=Ub=1, p=<.05) are significantly lower than for flakes. This trend can also be observed when disentangling morphological categories; however, the sample sizes become too small to be statistically tested. Blades with facetted platforms (N=3) have a mean thickness of 3.8 ± 2.8 mm and mean width of 9.3 ± 2.3 mm, and the only one flake has a facetted platform of 6.4 mm thick and 15 mm wide. Plain platforms tend to be less thick and less wide.

Blank size attributes

Length

As only four artifacts are complete, it is not possible to observe any trend in MPH1. The two blades are 36.4 and 87.9 mm long and the two laminar flakes are 77.8 and 42.4 mm long.

	Total		Blade		Flake	
	N	*f*	N	*f*	N	*f*
Distal	0	0%	0	0%	0	0%
Mesiodistal	1	5%	1	7%	0	0%
Mesial	4	20%	4	27%	0	0%
Mesioproximal	8	40%	6	40%	2	40%
Proximal	3	15%	2	13%	1	20%
Complete	4	20%	2	13%	2	40%
	20	100%	15	100%	5	100%

Table 3: Kara-Bom, MPH1, breakage

	Total		Blade		Flake	
	N	*f*	N	*f*	N	*f*
Plain	6	40%	4	40%	2	40%
Facetted	4	27%	3	30%	1	20%
Dihedral	3	20%	1	10%	2	40%
Undetermined	2	13%	2	20%	0	0%
	15	100%	10	100%	5	100%

Table 4: Kara-Bom, MPH1, platform preparation

Plain platform	Total		Blade		Flake	
	Thickness	Width	Thickness	Width	Thickness	Width
Sample size	6		4		2	
Mean (mm)	5.2	15.8	3.2	6.6	9.1	34
Standard deviation (mm)	3.3	15	0.8	2.8	2.4	10
Range (mm)	2.2 to 10.8	2.6 to 41.1	2.2 to 3.9	2.6 to 8.8	7.5 to 10.8	27 to 41.1

Table 5: Kara-Bom, MPH1, plain platform size

	Total sample			MNI		
	Total	Blade	Flake	Total	Blade	Flake
Sample size	20	15	5	13	8	5
Mean (mm)	26.7	22.2	40.2	28.6	21.3	40.2
Standard deviation (mm)	10.7	8.1	1.4	10.7	5.7	1.4
Range (mm)	12.8 to 42.5	12.8 to 41.4	35.4 to 42.5	15.2 to 42.5	15.2 to 33.1	35.4 to 42.5

Table 6: Kara-Bom, MPH1, blank width

Width

The mean width of blade and flake categories are different (Table 6), in both total sample and MNI, reflecting the fact that the categories are defined on the basis of shape attributes.

Thickness

In spite of the effect of the small sample size, flakes tend to be significantly thicker than the total blade sample (Mann-Whitney, T=Ub=10, p=<.05) and the blade MNI (Mann-Whitney, T=Ub=1, p=<.05) (Table 7).

	Total sample			MNI		
	Total	Blade	Flake	Total	Blade	Flake
Sample size	20	15	5	13	8	5
Mean (mm)	7.7	6.7	10.4	7.7	6	10.4
Standard deviation (mm)	2.7	2	1.3	2.9	0.9	1.3
Range (mm)	3.9 to 14.5	3.9 to 11.3	7.4 to 14.5	4.6 to 14.5	4.6 to 7.8	7.4 to 14.5

Table 7: Kara-Bom, MPH1, blank thickness

Dorsal scar pattern

Laminar blanks are mainly unidirectional although when considering the only two complete artifacts, one is bidirectional and the other one unidirectional. Two of the flakes show the same picture, one being unidirectional and the other bidirectional. Two of the flakes show a radial dorsal patterning and are not included in the Table 8 as they do not fit in any of the defined categories. Among the laminar blanks, one is a neo-crest blade fragment.

Cross-section

Cross-sections are mainly trapezoidal, indicating that the removals were detached following several ridges (Table 9). Two of the flakes showing a radial dorsal patterning have a polyhedral section. When considering the MNI, the main trends are unchanged. Trapezoidal sections dominate (N=10), followed by triangular (N=3).

	Total		Blade		Flake	
	N	*f*	N	*f*	N	*f*
Unidirectional	8	44%	7	47%	1	33%
Unidirectional and cortex	1	6%	1	7%	0	0%
Bidirectional	4	22%	3	20%	1	33%
Bidirectional and cortex	0	0%	0	0%	0	0%
Crest	0	0%	0	0%	0	0%
Second Crest	0	0%	0	0%	0	0%
Neo-crest	1	6%	1	7%	0	0%
Undetermined	4	22%	3	20%	1	33%
	18	100%	15	100%	3	100%

Table 8: Kara-Bom, MPH1, dorsal scar pattern

	Total		Blade		Flake	
	N	*f*	N	*f*	N	*f*
Flat	0	0%	0	0%	0	0%
Rectangular	1	5%	1	7%	0	0%
Triangular	5	25%	5	33%	0	0%
Trapezoidal	12	60%	9	60%	3	75%
Polyhedral	2	10%	0	0%	2	25%
	20	100%	15	100%	5	100%

Table 9: Kara-Bom, MPH1, blank cross-section

Profile

In the total sample and in the MNI, profiles are mainly straight in both flake and blade categories (Table 10). Slightly curved profiles are also quite frequent.

Orientation

Blanks are mainly axial although given the small sample size and the number of undetermined values; this trend is not significant (Table 11). In fact, when considering the blade MNI, values are equal (N=3) except for the undetermined category (N=1).

	Total		Blade		Flake	
	N	*f*	N	*f*	N	*f*
Straight	11	61%	8	57%	3	75%
Slightly Curved	4	22%	3	21%	1	25%
Curved	0	0%	0	0%	0	0%
Twisted	2	11%	2	14%	0	0%
Undetermined	1	6%	1	7%	0	0%
	18	100%	14	100%	4	100%

Table 10: Kara-Bom, MPH1, blank profile

	Total		Blade		Flake	
	N	*f*	N	*f*	N	*f*
Right	3	15%	3	20%	0	0%
Left	4	20%	3	20%	1	20%

… continue page 66

None	7	35%	4	27%	3	60%
Undetermined	6	30%	5	33%	1	20%
	20	100%	15	100%	5	100%

Table 11: Kara-Bom, MPH1, blank orientation

3.2.2 CORES: REDUCTION PATTERNS AND SIZE ATTRIBUTES

Two cores and two core-like tools are described in this section. The core-like tools are also included in the retouched tools list. Flake cores do not fit in our Mode classification system as it was designed for laminar reduction systems.

Core description

Flake cores (N=2)

∗ KB-92.M1.J11.3.2348
This core is produced on a block/slab blank (Figure 25). The back is mainly cortical and is prepared by a series of radial removals around the periphery, giving the flaking surface a sub-triangular shape. Some of the removals appear deeper and more invasive when they correspond to striking platform preparations associated with the last dorsal removal negatives. The dorsal face illustrates the alternate use of two platforms perpendicular to each other. Assuming that one of these platforms is mainly used to shape the flaking surface, this core can be classified as unidirectional recurrent Levallois.

∗ KB-92.M1.Z11.1.2347
This core is produced on a block/slab blank and displays a combination of cortex and natural surfaces on its back (Figure 26). The contour of the ventral face shows a series of radial removals, some of which are striking platform preparations. The dorsal face displays a series of radial removals, the last phase of reduction being a three-step sequence (left, right and middle) which give to the last removal a triangular shape. The general morphology of the core suggests Levallois affinities.

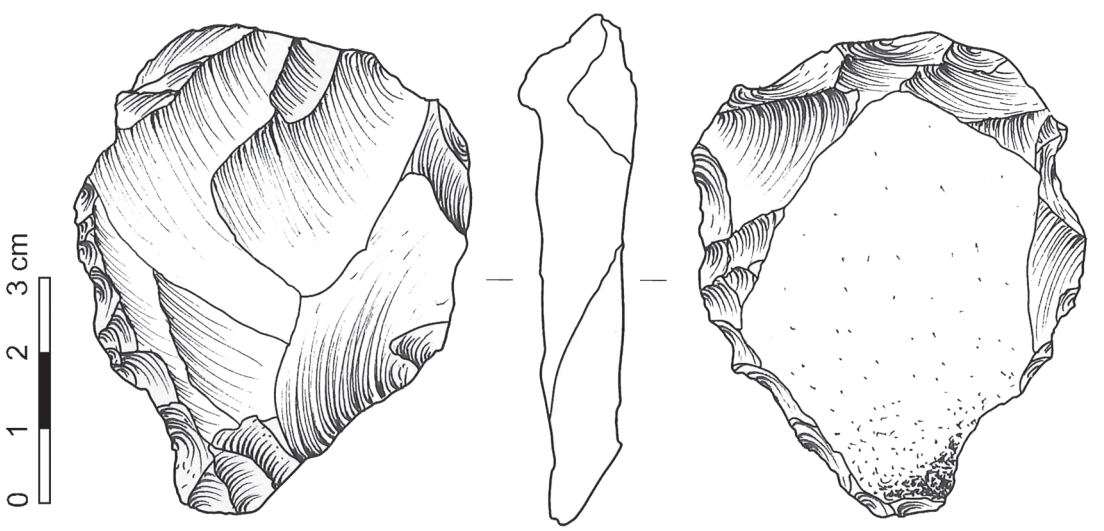

Figure 25: Kara-Bom, MPH1, KB-92.M1.J11.3.2348

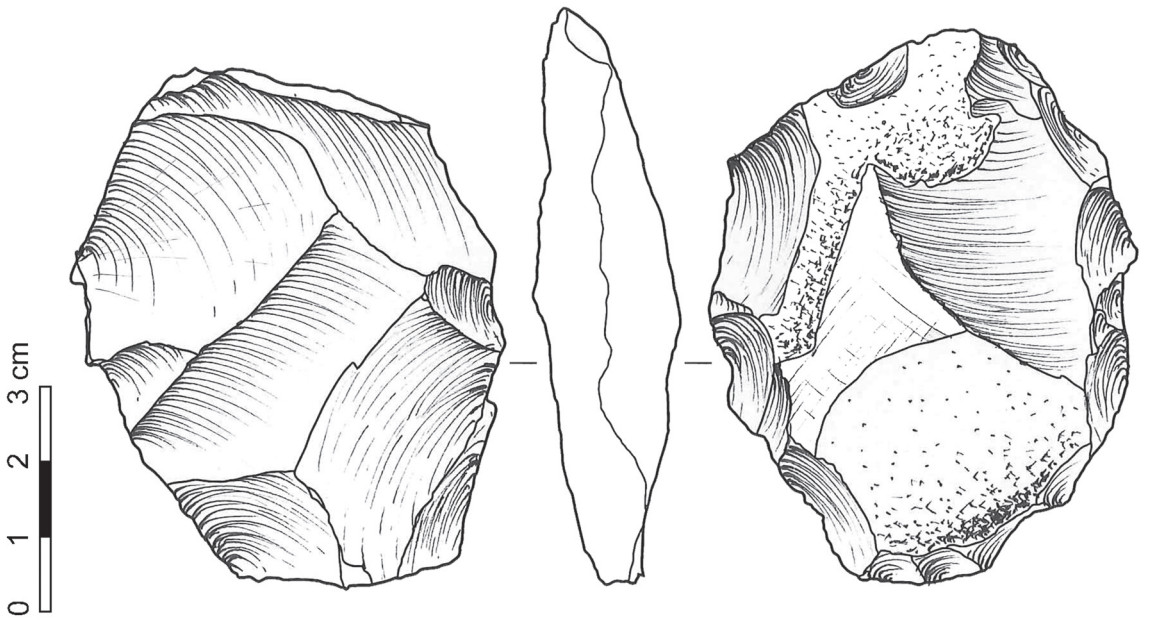

Figure 26: Kara-Bom, MPH1, KB-92.M1.Z11.1.2347

Core-like tools (N=2)

* KB-92.M1.D11.7.2327
This artifact is on a unidirectional blade blank with an inverse truncation on the proximal part (Figure 27). Two possible removals are located along the left edge of the blank. For one of the surfaces, it was not possible to determine the direction of the removal. It is not clear if the removals are posterior or anterior to the detachment of the core blank as no bulb negative is preserved. Therefore, this artifact is typed as a truncated blade and included in the retouched blade category.

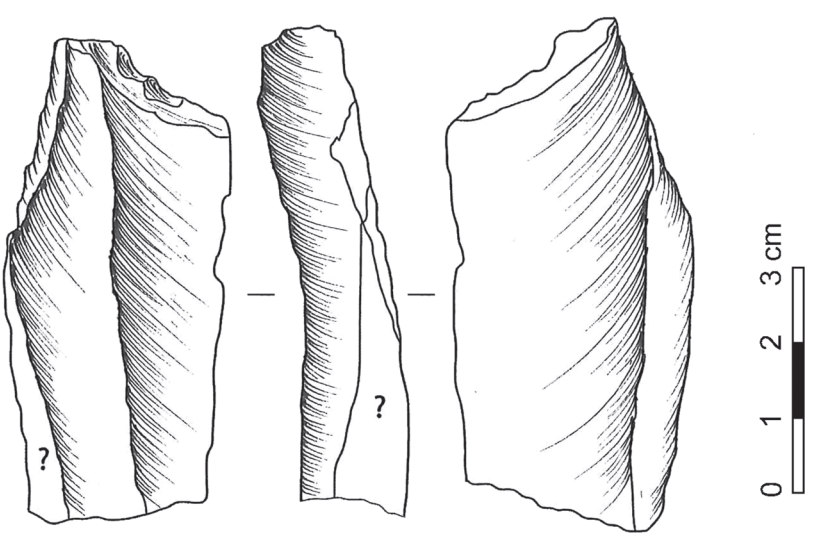

Figure 27: Kara-Bom, MPH1, KB-92.M1.D11.7.2327

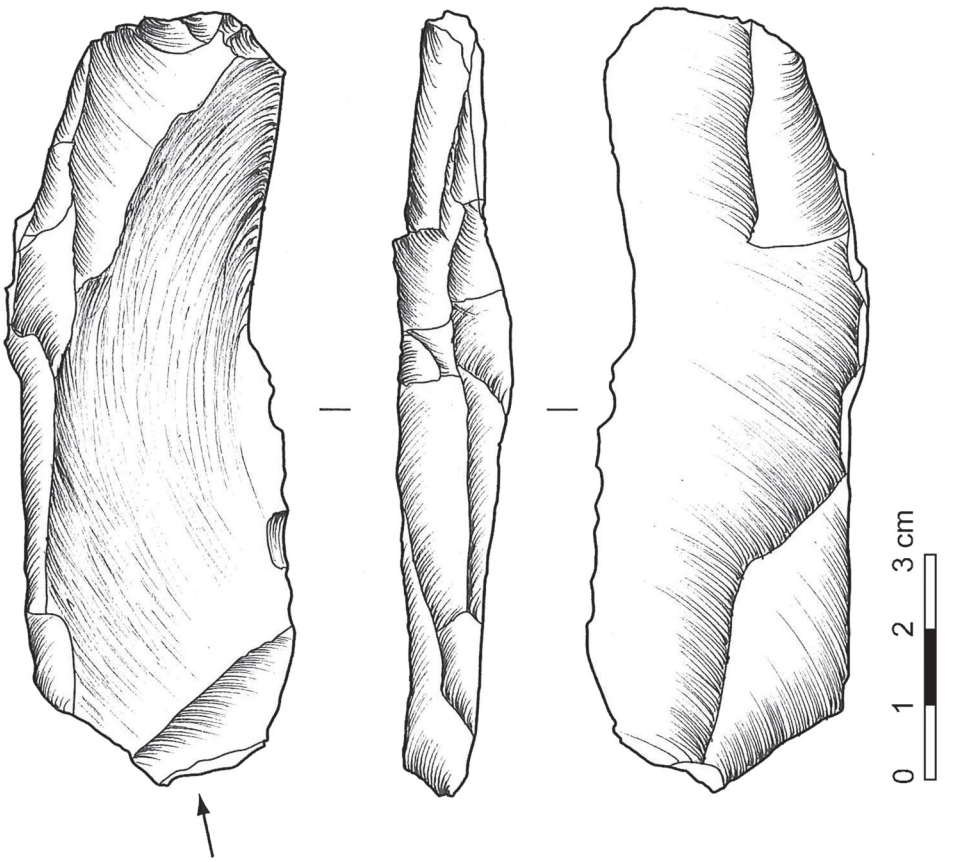

Figure 28: Kara-Bom, MPH1, KB-92.M1.Z11.13.2344

∗ KB-92.M1.Z11.13.2344

This artifact is produced on a laminar blank detached from the corner of the flaking surface of a large blade core (Figure 28). It shows a series of laminar negatives along the left edge, the right edge being sharp and thin. Two flake removals were detached from opposed platforms and extend mainly on the ventral face of the blank. They make it impossible to determine if the laminar removals from the edge are posterior to the detachment of the blank or not. In this context, this artifact cannot be considered as a Mode B core, and is instead typed as a burin and classified in the broader category of retouched blades.

3.2.3 REDUCTION SEQUENCE RECONSTRUCTION

Giving the small sample size, the reduction sequence cannot be reconstructed on a robust, quantified basis. However, some general observations can be proposed. The blanks can be classified into three main morphological categories: blades with parallel edges, and flakes with convergent edges, and flakes.

Laminar blanks with parallel edges

Blades show a combination of unidirectional and bidirectional reduction sequences but also facetted and plain striking platforms. Some of the largest laminar artifacts illustrate a bidirectional reduction system

with two opposed platforms (Figure 29, num. 5 and 6). The morphology of large/ medium size cores is unknown as they are absent in the sample. The occurrence of a neo-crested blade (Figure 29, num. 3), however, indicates that, at least occasionally, the management of the flaking surface by the removal of a thicker blank at the intersection between two surfaces. A production of small size blades/bladelets is also possible as one of the blanks displays two natural backs and is, therefore, detached from a core with a narrow flaking surface. However, the two core-like tools described above are rather atypical and cannot be directly associated with this type of production.

Convergent blanks

The convergent blanks are mainly flakes, but their shape attributes indicate an intermediate position between the flake and blade category. From a qualitative point of view, some of them can be designated as laminar flakes. They show both unidirectional

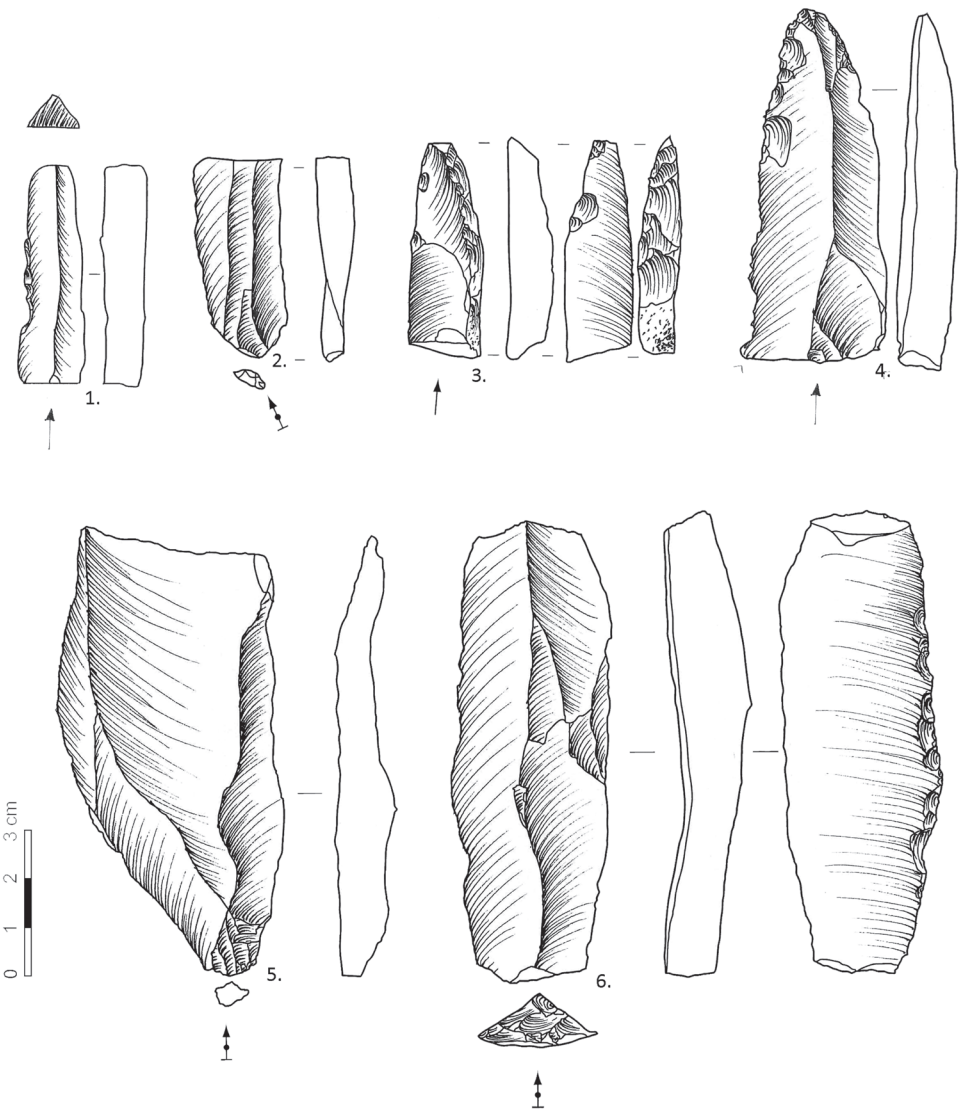

Figure 29: Kara-Bom, MPH1, Laminar blanks and retouched tools

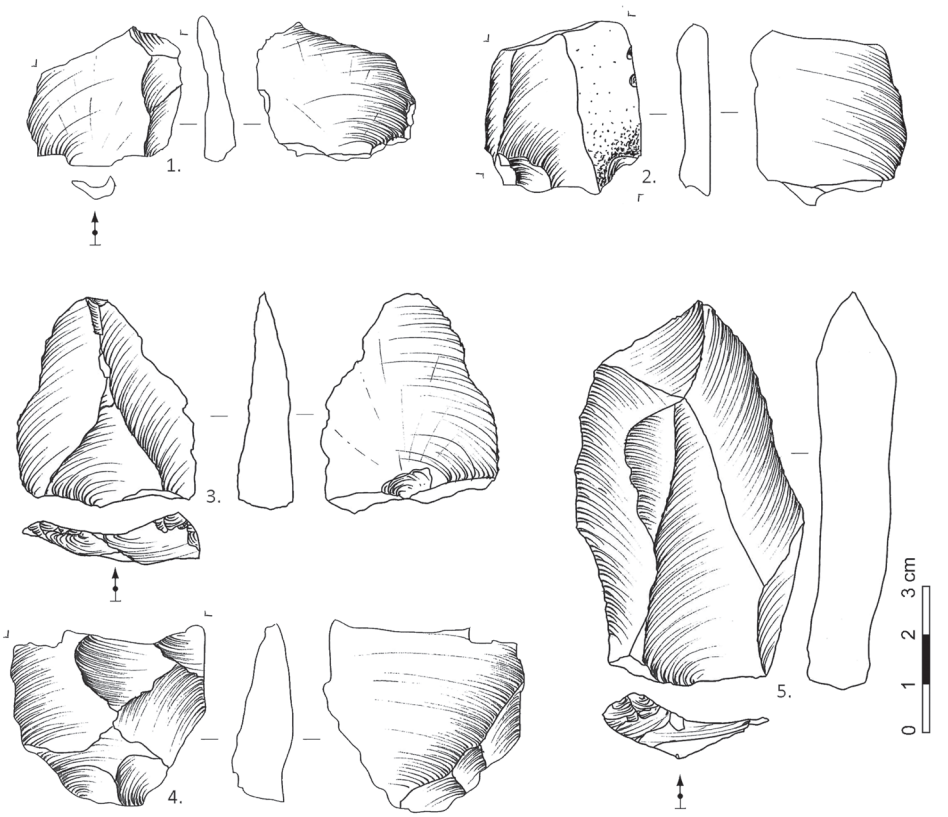

Figure 30: Kara-Bom, MPH1, convergent and flake blanks

and bidirectional scar patterning. Some are similar to Levallois points, but the central removals visible on their dorsal face can sometimes precede the lateral ones. Given the sample size, this may indicate a certain degree of variability in the method of production. Generally, these blanks are rather short and have a thick platform. One artifact shows some flaking on the side of a dihedral platform (Figure 30: 3). Another artifact has a plain platform slightly modified due to an aborted removal (Figure 30: 5). The convergent blanks could be associated with flake cores such as KB-92.M1.Z11.1.2347 (Figure 26).

Flake blanks

Some flakes in the assemblage may be linked with the Levallois flake cores. They have a roughly circular shape and a dorsal scar pattern showing radial removals (Figure 30: 4).

Platform preparation and percussion technique

The percussion technique is difficult to assess given the size and the nature of the sample. The mean platform thickness of the total sample is more than 4 mm, but this is partly due to the presence of flakes that have significantly thicker platforms than the blades. Moreover, no sign of abrasion has been observed on the blanks. So, in this case, it is assumed that the flakes are detached with a hard hammer. For the blades, the question is still open although no features usually associated with the use of a soft hammer have been observed.

	N	*f (among tools)*	*f (from total, N=55)*
Retouched blade	10	91%	29%
Retouched bladelet	0	0%	0%
Retouched Point	0	0%	0%
Endscraper	0	0%	0%
Other	1	9%	3%
	11	100%	32%

Table 12: Kara-Bom, MPH1, main types of retouch tool

Retouched tools

The retouched toolkit is mainly composed of retouched blades and of a single retouched flake (Table 12). As a general observation, differences in patina and the occurrence of edge damage on several blanks (N=2) and tools (N=3) suggest that some of the irregular retouch, notches and denticulations perhaps related to post-depositional processes. Following a conservative approach, 11 artifacts are selected. Only three have a platform preserved, one is plain, one is unidentified and the third is facetted. The platform thickness varies from 2.1 to 9.8 mm and the width between 4.2 and 18.9mm.

	N	*f*
Distal	0	0%
Mesiodistal	1	9%
Mesial	6	55%
Mesioproximal	1	9%
Proximal	0	0%
Complete	3	27%
	11	100%

Table 13: Kara-Bom, MPH1, retouched tool breakage

One blade fragment shows bilateral retouch on the distal end and displays a small burin-spall like removal starting from the tip (Figure 29: 4). This feature also occurs on a non-retouched convergent blank (Figure 30: 3). In a Middle Stone Age context, burin-like removals are listed by Villa and Soressi (2009) as diagnostic for impact fractures. In MPH1, the size of the spalls is reduced and the length of the step-scar is too short to be convincing. One notch is produced on a Levallois flake displaying bidirectional dorsal scar patterns (Figure 31).

The notch bears at least two generations of retouch and some and an inverse truncation is visible on the proximal end of the ventral face.

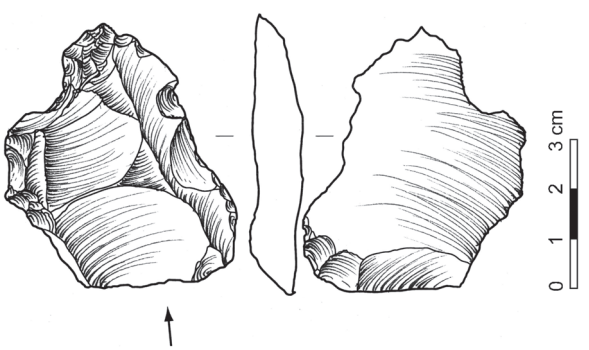

Figure 31: Kara-Bom, MPH1, retouched tool on Levallois flake

The retouch is mainly direct (Table 14), and is located on the mesial (N=4), on the proximal (N=3) and on the distal part (N=2) of the dorsal face, and

on the mesial (N=2) and proximal part (N=1) of the ventral face.

	N	*f*
Direct	7	64%
Inverse	2	18%
Alternate	2	18%
	11	100%

Table 14: Kara-Bom, MPH1, retouch location (face)

One artifact has a curved profile and one has a twisted one. The rest of the tools have a straight profile. Except for three artifacts, oriented on the right, none of the tool orientations could be determined.

3.3 LAMINAR TECHNOLOGY: OH6

3.3.1 BLANK ATTRIBUTES

Breakage

The distribution of both blades and bladelets indicates a majority of mesial and mesioproximal fragments, with a clear lack of distal elements. Based on these observations, an MNI of 82 blades and 18 bladelets is calculated on a total sample of 162 laminar artifacts recorded (Table 15).

Platform: size and preparation

Based on observations from the MNI sample, OH6 blades show similar frequencies of plain and facetted platforms and a minor occurrence of flat dihedral platforms (Table 16). As for the bladelets, facetted platforms dominate but the sample is reduced by the presence of numerous undetermined platform types. Considering all categories together, the mean platform thickness is 5.7 ± 3.7 mm and the mean width is 12.9 ± 6.6 mm. When separating blade and bladelet categories, the results show a different picture. Blade mean platform thickness is 6.2 ± 3.7 mm and bladelets have a mean of 2.8 ± 1.5 mm. In the following tables, measurements are grouped per morphological types. Two plain and one facetted platform are discarded due to damage.

It appears that facetted platforms have a higher platform thickness than the mean of the overall assemblage. There is a clear overlap between blade and bladelet platform thickness (Table 17).

For the plain platforms, mean thickness differences between the blades and the bladelets can be related

	Total		Blade		Bladelet	
	N	*f*	N	*f*	N	*f*
Distal	4	2%	3	2%	1	3%
Mesiodistal	21	13%	15	12%	6	17%
Mesial	36	22%	25	20%	11	31%
Mesioproximal	31	19%	23	18%	8	22%
Proximal	6	4%	6	5%	0	0%
Complete	64	40%	54	43%	10	28%
	162	100%	126	100%	36	100%

Table 15: Kara-Bom, OH6, blank preservation

	Total		Blade		Bladelet	
	N	*f*	N	*f*	N	*f*
Plain	39	39%	35	43%	4	22%
Facetted	41	41%	33	40%	8	44%
Dihedral Flat	7	7%	6	7%	1	6%
Undetermined	13	13%	8	10%	5	28%
	100	100%	82	100%	18	100%

Table 16: Kara-Bom, OH6, platform preparation

Facetted platform	Total		Blade		Bladelet	
	Thickness	Width	Thickness	Width	Thickness	Width
Sample size	40		32		8	
Mean (mm)	6.5	13	7.3	14.6	3.4	6.6
Standard deviation (mm)	4	7.3	4.1	7.2	1.2	2.6
Range (mm)	1.5 to 23.1	2.3 to 30.8	1.8 to 23.1	4.9 to 30.8	1.5 to 4.7	2.3 to 9.6

Table 17: Kara-Bom, OH6, facetted platform size

Plain platform	Total		Blade		Bladelet	
	Thickness	Width	Thickness	Width	Thickness	Width
Sample size	37		33		4	
Mean (mm)	4.9	10.1	5.3	10.8	1.3	3.8
Standard deviation (mm)	3.5	5.6	3.4	5.4	0.7	0.6
Range (mm)	0.7 to 17.4	2.3 to 25.4	1.1 to 17.4	2.3 to 25.4	0.7 to 2.3	3.2 to 4.6

Table 18: Kara-Bom, OH6, plain platform size

to the small sample size of the latter (Table 18). Nevertheless, blade plain platforms are statistically less thick than facetted platforms (Mann-Whitney, T=Ub=357.5, p=<.05), a trend that is also observed when considering blades and bladelets as a whole (Mann-Whitney, T=Ub=544.5, p=<.05). Dihedral platforms are not numerous (blade N=6, bladelet N=1) and show a flat morphology. They have a mean thickness of 4.7 ± 2.8 mm (ranging from 0.8 to 9.4 mm) and a mean width of 13.7 ± 7.6 mm (ranging from 4.7 to 27.5 mm). It appears that dihedral platforms are closer in size to the plain than to the facetted ones. No traces of abrasion occur on the external ridge of the platforms except in a few cases (N=6), where an intensive abrasion totally smoothed the external platform angle.

	Total	Blade	Bladelet
Sample size	64	54	10
Mean (mm)	71.7	78.2	36.6
Standard deviation (mm)	30.2	28.1	10.2
Range (mm)	17.1 to 152.9	27.9 to152.9	17.1 to 51.6

Table 19: Kara-Bom, OH6, blank length

Blank size attributes

Length

As length is measured only on complete elements, the results presented are based on a smaller sample. Blade and bladelet length ranges clearly overlap but the two categories have different means and standard deviations (Table 19). When considered as a whole, the distribution of length measurement appears to be normally distributed around a mean of 71.7 mm (Shapiro-Wilk, W=0.96, p= .06) (Figure 32).

Width

Means and standard deviations for the total sample are generally lower than for the MNI, with the exception of the bladelets which display a slightly lower means and standard deviations (Table 20). However, none of the observed differences are statistically significant. It suggests that there is no direct relationship between the width of the blank and the rate of breakage. In this case, repeating measurements on fragments coming from a same artifact would not affect the general trends visible in the overall popu-

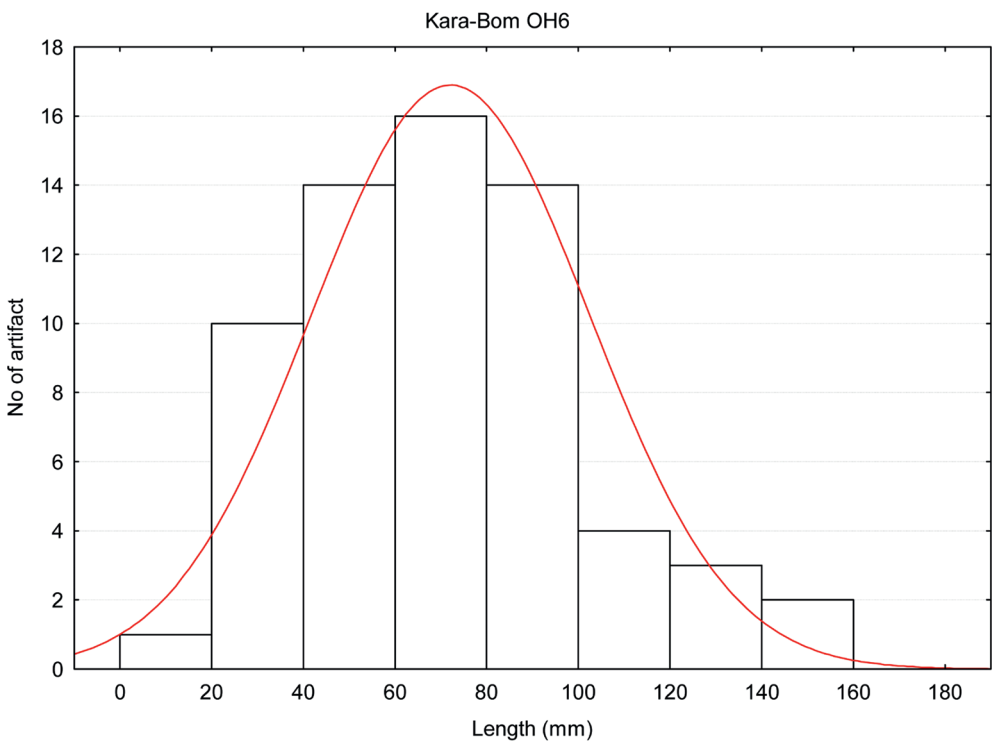

Figure 32: Kara-Bom, OH6, blank length distribution

	Total sample			MNI		
	Total	Blade	Bladelet	Total	Blade	Bladelet
Sample size	162	126	36	100	82	18
Mean (mm)	22	25.6	9.4	23.3	26.1	10.2
Standard deviation (mm)	11.2	10.1	1.7	11.2	10.4	1.5
Range (mm)	6.9 to 66.9	10.8 to 66.9	6.9 to 12.5	7.7 to 66.9	10.8 to 66.9	7.7 to 12.5

Table 20: Kara-Bom, OH6, blank width

lation. The width means of blade and bladelet categories appear different in both MNI and total sample, reflecting the arbitrary character of the classification of these two types.

However, the histogram of width measurements from the total sample and the MNI shows a bimodal distribution (Figure 33). The first mode is between 10-15 mm width and the second between 25-20 mm width. With respect to the smaller sample size, the two modes are also visible in the MNI distribution although in a less clear fashion. The positive skewness of the histograms (respectively 0.89 and 0.99 for the whole population and for the MNI) can be partly explained by an apparent size cut-off of 5 mm. After looking at the shatter from OH6 assemblage, it appears that it is not due to a selection or artificial cut-off post-excavation, but rather to the lack of systematic screening. As described in the following sections, it seems anyway unlikely that a large part of

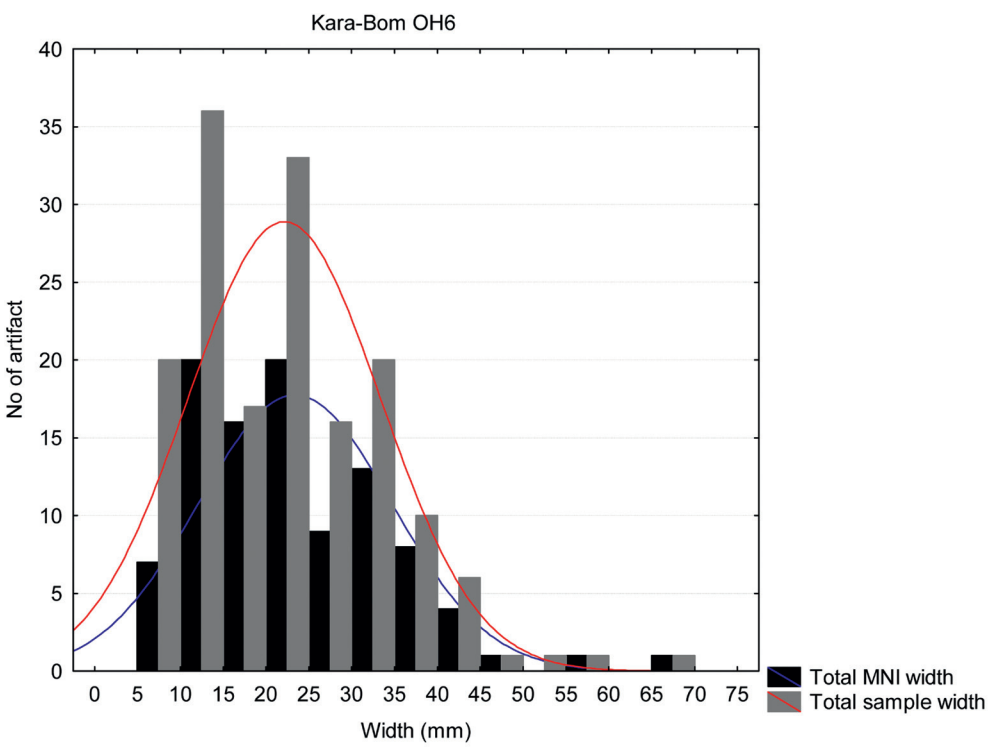

Figure 33: Kara-Bom, OH6, blank width distribution

	Total sample			MNI		
	Total	Blade	Bladelet	Total	Blade	Bladelet
Sample size	162	126	36	100	82	18
Mean (mm)	7.9	9.1	4	8.3	9.1	4.5
Standard deviation (mm)	4.4	4.3	1.6	2.1	3.9	1.7
Range (mm)	2.1 to 29.4	2.5 to 29.4	2.1 to 7.7	2.1 to 21.8	2.5 to 21.8	2.1 to 7.7

Table 21: Kara-Bom, OH6, blank thickness

the assemblage is missing, as cores that could testify of a systematic production of microblades are absent.

Thickness

Compared with the total population, MNI blank thickness shows equal or slightly higher mean values and also sometimes a smaller standard deviation (Table 21), although not significantly. As for the width, it seems that breakage does not influence significantly the main trends observed in terms of thickness in the sample considered. Blade and bladelet thickness clearly differ. The thickness histogram is unimodal and shows a positive skewness (respectively 1.45 and 0.85 for the whole population and for the MNI). The MNI, although based on less numerous measurements, shows a similar distribution to that of the total sample population (Figure 34).

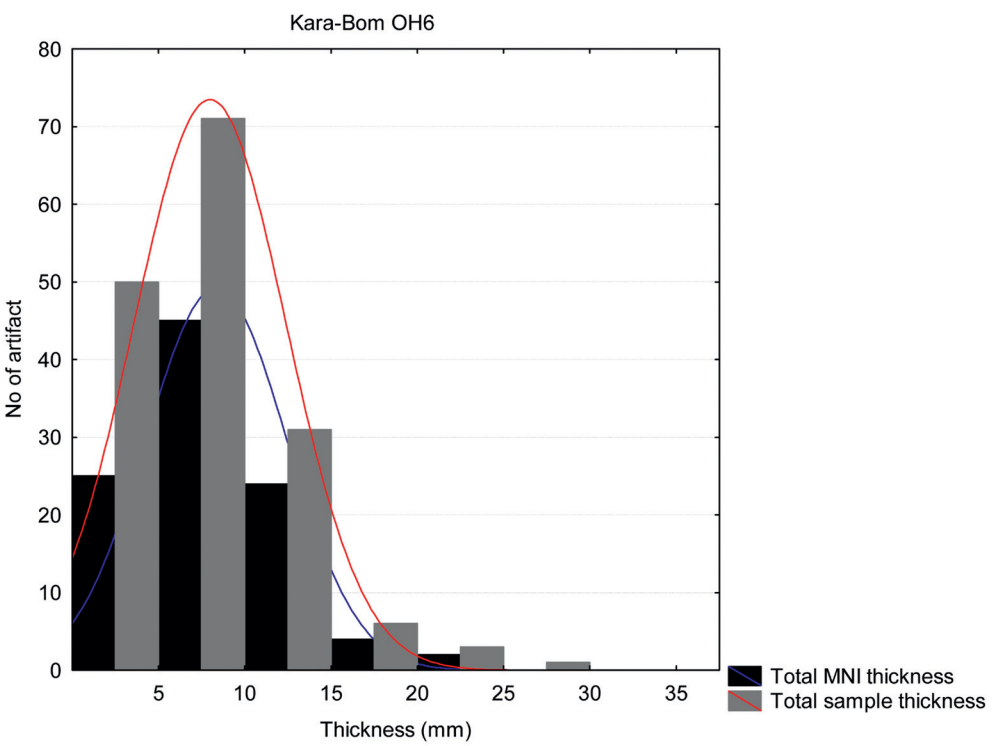

Figure 34: Kara-Bom, OH6, blank thickness distribution

Dorsal scar pattern

In spite of the quasi absence of cortex on the blanks, the occurrence of technical elements of various sizes, such as crested blanks, second crest *(sous-crete)* and neo-crest, shows that maintenance operations occur at different stages of the reduction sequence (Table 22). Unidirectional and bidirectional scar patterns have similar frequencies in the total sample (χ^2 (6)= 8.46, p=.21), and differences observed between unidirectional and bidirectional within blade and bladelets categories are not statistically significant. This coexistence of both bidirectional and unidirectional elements suggests that the main reduction sequences are not strictly unidirectional or alternate bidirectional.

However, the frequency of breakage of the blanks may bias this observation. In other words, blade fragments are more likely to be described as unidirectional (Bar-Yosef and Van Peer, 2009). When only complete elements are considered, the sample is reduced to 64 blanks.

Statistically, there are no significant changes when one compares the total sample with only the complete blanks. However, it appears that the unidirectional patterns are slightly overestimated in the total sample. Among the complete blanks, a shift of approximately 10% from unidirectional to bidirectional is observed, the sharpest change occurring in the bladelet category (Table 23). Within the latter, bidirectional patterning becomes significantly dominant

	Total		Blade		Bladelet	
	N	*f*	N	*f*	N	*f*
Unidirectional	78	48%	65	52%	13	36%
Unidirectional and cortex	1	1%	1	1%	0	0%
Bidirectional	67	41%	47	37%	20	56%
Crest	2	1%	2	2%	0	0%
Second Crest	5	3%	4	3%	1	3%
Neo-crest	8	5%	7	6%	1	3%
Undetermined	1	1%	0	0%	1	3%
	162	100%	126	100%	36	100%

Table 22: Kara-Bom, OH6, dorsal scar pattern

	Complete blank		Complete blade		Complete bladelet	
	N	*f*	N	*f*	N	*f*
Unidirectional	24	38%	22	41%	2	20%
Bidirectional	33	52%	25	46%	8	80%
Crested	7	11%	7	13%	0	0%
	64	100%	54	100%	10	100%

Table 23: Kara-Bom, OH6, dorsal scar patter frequencies among complete blanks

(χ^2 (1)= 7.2, p= <.05) although this observation is balanced by a reduction of the sample size.

Cross-section

A majority of triangular and trapezoidal cross-sections is observed in both blade and bladelet categories, which are equally represented when considering the total sample from OH6 and show minor differences within the blade category (Table 24).

However, in the bladelet category, triangular elements are significantly dominant, indicating the frequent use of a single ridge during the production of small laminar blanks.

Profile

Straight profiles clearly dominate the sample, directly followed by slightly curved and curved blanks. This trend is expressed in both categories. Twisted profiles are almost totally absent (Table 25).

As for the dorsal scar pattern, profile frequencies can be biased by breakage. The trends observed on the total sample are present in the MNI sample (Table 26) and show that breakage does not affect the profile determination.

	Total		Blade		Bladelet	
	N	*f*	N	*f*	N	*f*
Flat	3	2%	2	2%	1	3%
Rectangular	1	1%	0	0%	1	3%
Triangular	80	49%	58	46%	22	61%
Trapezoidal	77	48%	65	52%	12	33%
Polyhedral	1	1%	1	1%	0	0%
	162	100%	126	100%	36	100%

Table 24: Kara-Bom, OH6, type of cross-section

	Total		Blade		Bladelet	
	N	*f*	N	*f*	N	*f*
Straight	117	72%	94	75%	23	64%
Slightly Curved	33	20%	25	20%	8	22%
Curved	7	4%	4	3%	3	8%
Twisted	4	2%	2	2%	2	6%
Undetermined	1	1%	1	1%	0	0%
	162	100%	126	100%	36	100%

Table 25: Kara-Bom, OH6, type of profile

	Total		Blade		Bladelet	
	N	*f*	N	*f*	N	*f*
Straight	71	71%	60	73%	11	61%
Slightly Curved	19	19%	16	20%	3	17%
Curved	5	5%	3	4%	2	11%
Twisted	4	4%	2	2%	2	11%
Undetermined	1	1%	1	1%	0	0%
	100	100%	82	100%	18	100%

Table 26: Kara-Bom, OH6, type of profile based on MNI

Orientation

It appears that axial blanks are the most common within the blade sample, with only 19% of the blanks being off-axis. Bladelets seems to show a similar pattern although for a large part of the fragments, the orientation could not be determined (Table 27).

When looking at the MNI, the frequencies of undetermined orientation sharply decrease as the orientation can be determined more easlily when the platform is preserved. It appears that the trends observed on the total sample are confirmed by the observations on the MNI, showing that in this case, the fragmentation of blanks does not significantly affect

	Total		Blade		Bladelet	
	N	*f*	N	*f*	N	*f*
Right	11	7%	8	6%	3	8%
Left	20	12%	17	13%	3	8%
None	95	59%	80	63%	15	42%
Undetermined	36	22%	21	17%	15	42%
	162	100%	126	100%	36	100%

Table 27: Kara-Bom, OH6, blank orientation

	Total		Blade		Bladelet	
	N	*f*	N	*f*	N	*f*
Right	10	10%	8	10%	2	11%
Left	17	17%	14	17%	3	17%
None	70	70%	58	71%	12	67%
Undetermined	3	3%	2	2%	1	6%
	100	100%	82	100%	18	100%

Table 28: Kara-Bom, OH6, blank orientation based on MNI

the determination of orientation. Moreover, differences become larger in spite of the reduction of the sample size (Table 28).

3.3.2 CORES: REDUCTION PATTERNS AND SIZE ATTRIBUTES

From a general point of view, cores are not numerous within the OH6 sample. Among 14 cores identified, four are produced on small blocks or slabs (Mode A): two being flat-faced bidirectional cores with two independent flaking surfaces and two being semi-turning bidirectional cores. The majority of the cores are produced on blade blanks (Mode B), with six of them being unidirectional, and four of them being bidirectional (Figure 35).

	n	%
A1		
A2		
A3		
A4		
A5		
A6	2	14%
A7		
A8		
A9		
A10	2	14%
A11		
A12		
B1	3	21%
B2		
B3		
B4		
B5	6	43%
B6		
B7	1	7%
	14	100%

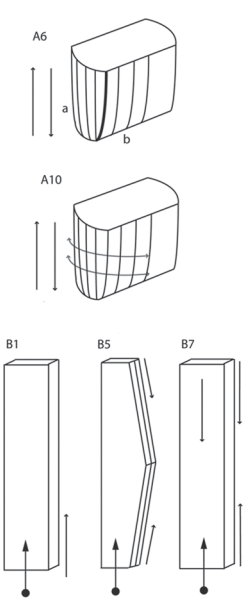

Figure 35: Kara-Bom, OH6, frequencies of cores per Mode

Size attributes

All measurements are recorded according to the system described in Chapter 2 which does not change based on the type of blank on which the core is produced. As a result, measurements are comparable, but in the case of Mode B cores, the thickness corresponds to the length of the blade blank, and the length of the core represents the thickness of the blade. No differences observed are statistically significant, except core length (Mann-Whitney, T=Ub=0, p=<.05) and the flaking surface width (Mann-Whitney, T=Ub=3, p=<.05) both of which are smaller in Mode B cores. With small sample sizes, Mann-Whitney U test has little power and tends to produce Type II errors. In this case, the results are not biased by the sample size. Differences in core length and flaking surface width reflect the fact that Mode B cores have their flaking surface located on the narrow edge of a blade blank, the latter, although relatively thick, remains generally thinner than a Mode A core on block. It is, however, clear that the rest of the values have a quite similar mean. When leaving out KB-92. YO6.J8.3.1761 (Figure 49) (although being a core on blade blank, it is technologically similar to Mode A6 cores), the size differences between the two Modes are more clearly expressed, reflecting different constraints in flaking surface size depending on the type of core blank.

Striking platform preparation

Striking platforms are mainly facetted with a frequency equal to the sum of the other categories (Table 30). The situation is similar when looking at the Mode B cores but is more balanced than in the Mode A cores. Based on such a small sample size, it is not possible to draw any definite conclusions; however, facetted platforms seem more represented in the bladelet category although there is no clear relationship between blank size and type of preparation. Profiles of the Mode A last removals are curved (N=1), slightly curved (N=1), straight (N=1) and undetermined (N=1). In Mode B, they are straight (N=4), twisted (N=1), slightly curved (N=1) and undetermined (N=4). From a general point of view, core management consists in occasional rejuvena-

	Mode A			Mode B		
	Mean	σ	N	Mean	σ	N
Core length	65.2	19.3	4	14.2	4	10
Core width	39.4	19.3	4	28.7	9.6	10
Core thickness	37.1	19.6	4	60.4	11.9	8
Flaking surface length	61	18	4	55.1	9.3	7
Flaking surface width	37	22.3	4	17.3	2.6	7
Last removal length	60	12.5	3	39.3	8.3	7
Last removal width	14.3	4.4	3	14.2	2.8	7

Table 29: Kara-Bom, OH6, general size values (mm) per core Mode

	Total		Mode A		Mode B	
	N	*f*	N	*f*	N	*f*
Plain	1	7%	1	25%	0	0%
Facetted	7	50%	1	25%	6	60%
Reshaped	4	29%	2	50%	2	20%
Undet	2	14%	0	0%	2	20%
	14	100%	4	100%	10	100%

Table 30: Kara-Bom, OH6, type of striking platform preparation

tions of the striking platform by faceting, or by removing a complete or a partial tablet. As described in the following section, the use of neo-crests or *débordant* blades is rather often observed on the cores at the intersection of two surfaces, with the occasional occurrence of a posterior crest. The latter can be to prepare a new flaking surface but is also known in various UP contexts as a procedure to prepare lateral convexities of a volumetric blade core (*e.g.* Pigeot, 1987). Distal shaping of flaking surfaces is almost absent and the general reduction pattern is rather parallel. In fact, all cores show parallel reduction patterns except two of the Mode B type, one shows convergent removals (KB-92.YO6. Z8.58) and one remains undetermined.

Core descriptions

Mode A6 (N=2)

∗ KB-92.Y06.J8.31.1698

This core is produced on a block showing two independent flaking surfaces and two opposed platforms. The right side and the back of the block are still fully cortical. The first flaking surface shows a succession of two laminar removals (1 and 2) struck from the lower platform followed by a switch to the upper platform. A first blade is detached from the junction between the two flaking surfaces (3), followed by a series of three hinged removals (4-6). The second flaking surface shows a single clear blade removal (1) followed by three hinged removals struck from

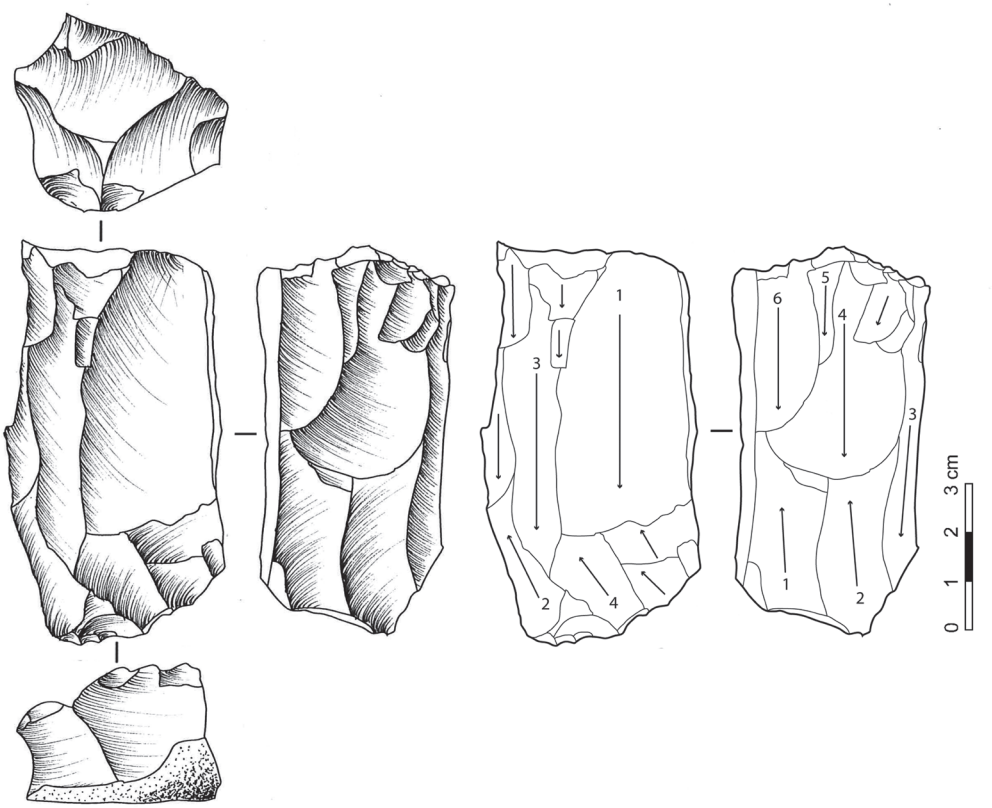

Figure 36: Kara-Bom, OH6, KB-92.Y06.J8.31.1698

the lower platform, one of which (4) is interpreted as an attempt to remove a side blade from the junction of the two flaking surfaces. Two additional small removals indicate another attempt to remove a blade from the same ridge but from the upper platform.

The upper striking platform is shaped by radial flaking removing several partial tablets. The lower platform shows less intense preparation, the surface being shaped by two sub-cortical hinged removals.

∗ KB-92.YO6.Z7.12.513

This core presents two flaking surfaces opposed to a cortical back prepared by radial flaking (Figure 37). The larger surface displays negatives of a bidirectional blade production following a short series of 3-4 relatively wide removals detached from two opposed platforms. The second flaking surface is located on the left narrow side, as shown by a series of laminar removals detached from two opposed platforms.

The striking platforms are shaped by flake removals opening a plain surface and creating an acute angle at the junction between the flaking surface and the back of the core. As far as it can be observe, early stages of the reduction indicate (1) the use of two opposed platforms at the junction between the right lateral and the broad flaking surface and on its left ends. The second phase takes place in the middle of the broad flaking surface (2) and is followed by a removal in the middle (3), both struck from the lower platform. It is followed by a switch to the upper platform with a small flake and a more elongated removal (4) and by a hinged central blade removal (5). Then, following a hinged removal (6), two removals (7) are likely attempts to remove the negatives left by the previous knapping accident. The last stages of reduction take place on the narrow flaking surface on the left side of

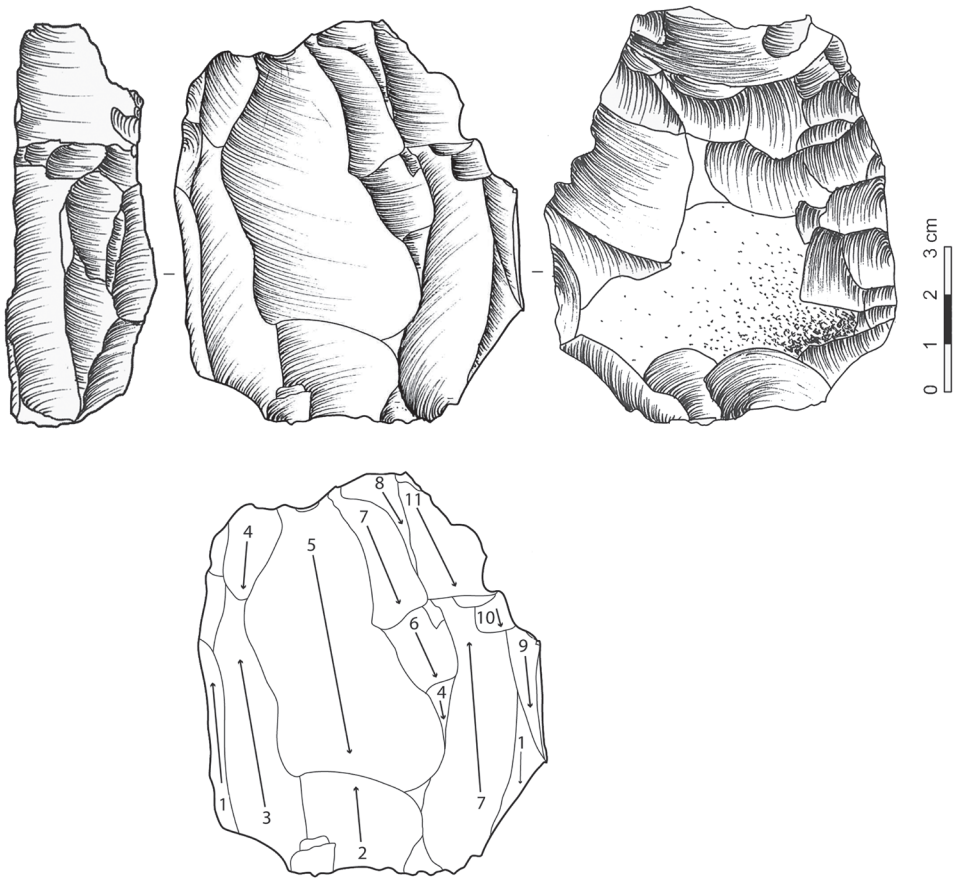

Figure 37: Kara-Bom, OH6, KB-92.YO6.Z7.12.513

the core. A lateral removal scar (9) is followed by severe hinged fractures (10 and 11) struck from the upper platform. At first glance, the core seems to show two independent flaking surfaces (cfr. Mode A6). The radial preparation of the back suggests a surface approach similar to the Levallois method (Boëda, 1994). However, the last removals are located at the junction between the two surfaces. Hinge fractures illustrate a significant number of attempts to remove a side blade, reshaping the lateral convexity of the wider flaking surface. Thus, considering the possible interaction between the two surfaces, the reduction is not only based on the treatment of a surface (like in a Levallois blade core) but rather illustrates a sub-volumetric approach. The general orientation of removals indicates a parallel pattern of reduction.

Mode A10 (N=2)

* KB-92.YO6.Z9.9.67

This core is produced on a slab preserving both cortical lateral surfaces (Figure 38). The back of the core is crested by alternate removals. It displays a single flaking surface located on the narrow edge of the slab. Removals are detached from two opposed platforms, the earliest being located at the intersection between the right lateral face and the main flaking surface. The reduction sequence reconstruction shows frequent platform switches with the two first removals (1 and 2) showing a change from the upper to the lower platform. Although it is not possible to establish a precise chronology of the platform switches, it seems likely that the reduction progressed by short sequences of several removals

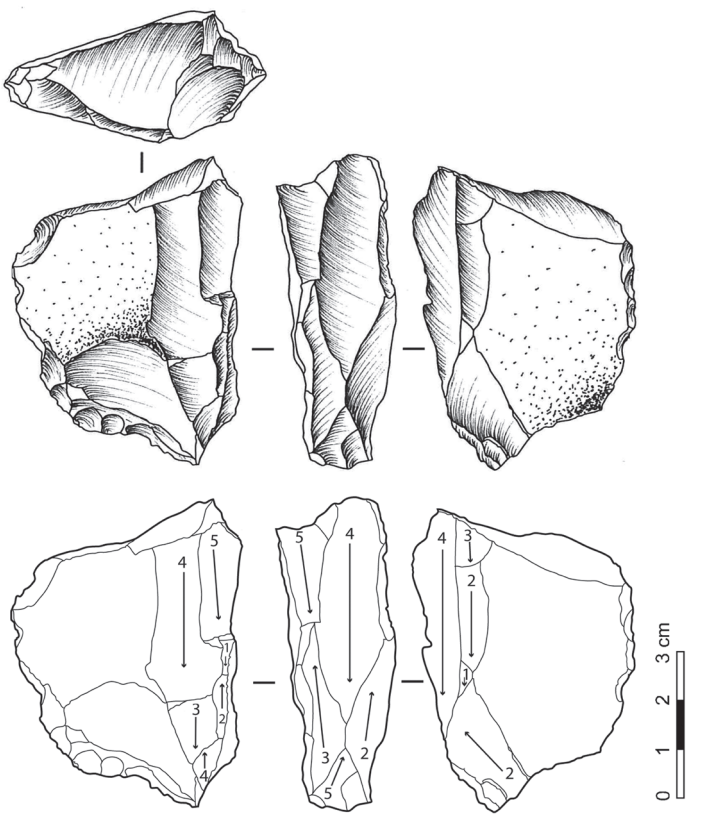

Figure 38: Kara-Bom, OH6, KB-92.YO6.Z9.9.67

rather than by a strict alternate bidirectionality. The lower platform is missing due the last series of removals, the upper platform shows several removal scars which most likely indicates several phases of rejuvenation, as well the remaining part of a preparation by faceting. A clear negative correspond to a small blade removal of 46 mm length for a minimum of 13 mm width. The latter follows the ridge produced by the two opposed removals detached from the lower platform. The cross-section of the core indicates a semi-turning reduction pattern as described by Pigeot (1987). Orientation of the removals seems to indicate a sub-parallel reduction, which ends on the upper platform by a hinge fracture.

∗ KB-92.YO6.Z7.50.948

This core of a rather small size is produced on an unknown blank type (Figure 39). The sides have been shaped by lateral and longitudinal flaking that may have been linked with a first flaking surface. It shows two platform switches. A first removal is detached from the upper platform followed by two removals from the lower platform and a last one struck from the upper platform. All removals are detached along the longitudinal axis, but the flaking surface tends to extend from a broad toward a narrow flaking surface.

Mode B1 (N=3)

∗ KB-92.YO6. Z8.58.58

This core is produced on cortical laminar blank bearing negatives of anterior removals on its back (Figure 40). A single flaking surface shows a series of three removals struck from a single platform and following the longitudinal axis of the blank. Two last hinged negatives follow a perpendicular flake removal and likely represent the final stage of the reduction at the right corner of the flaking surface. A

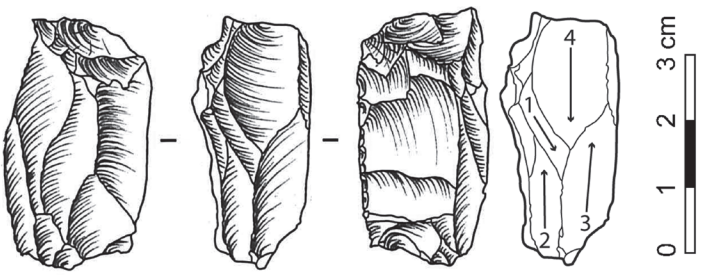

Figure 39: Kara-Bom, OH6, KB-92.YO6.Z7.50.948

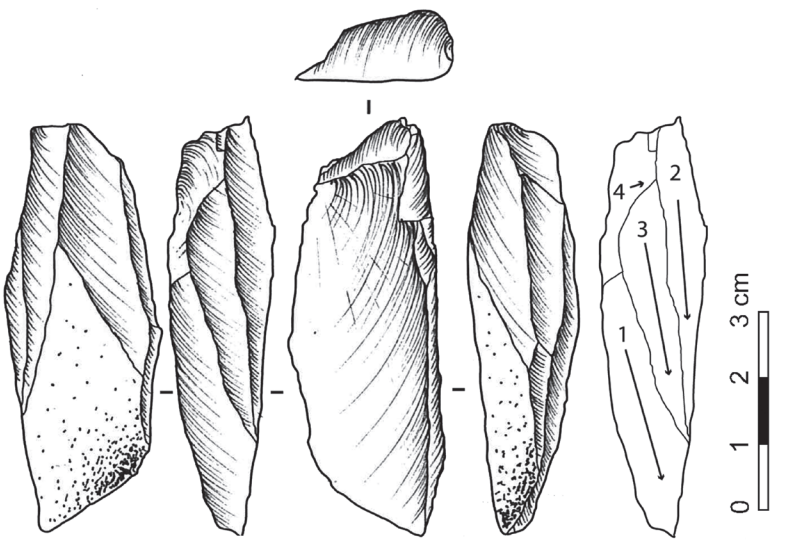

Figure 40: Kara-Bom, OH6, KB-92.YO6. Z8.58

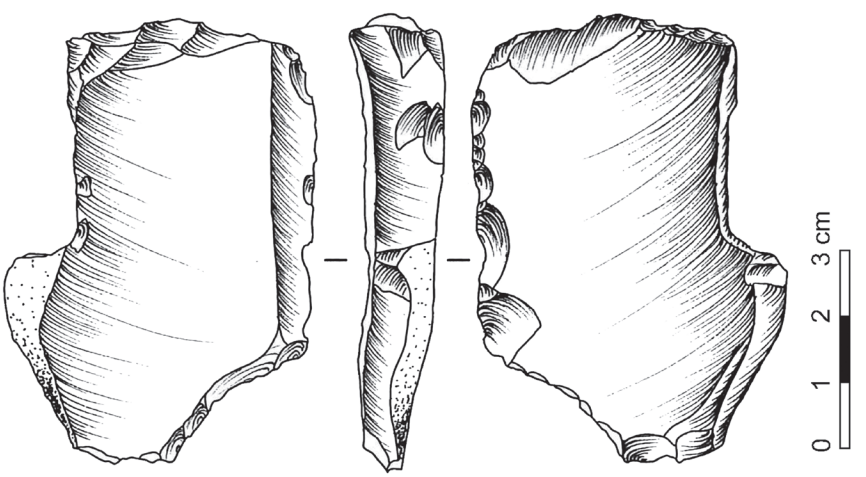

Figure 41: Kara-Bom, OH6, KB-92.YO6.I9.5.1280

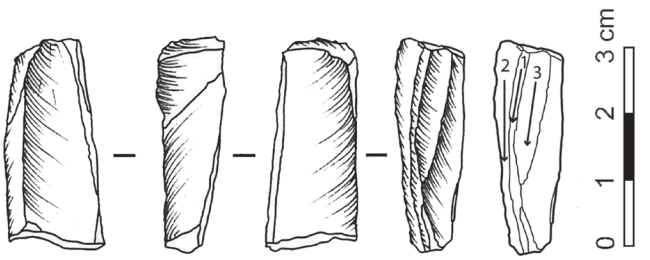

Figure 42: Kara-Bom, OH6, KB-92.YO6.I8.12.48

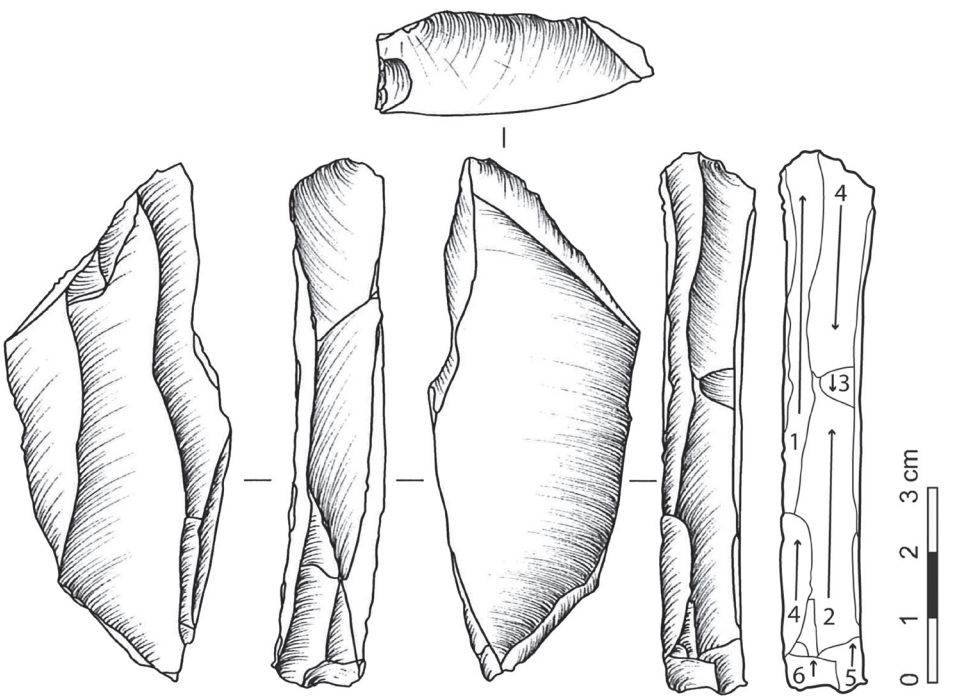

Figure 43: Kara-Bom, OH6, KB-92.YO6.J6.6. 1987

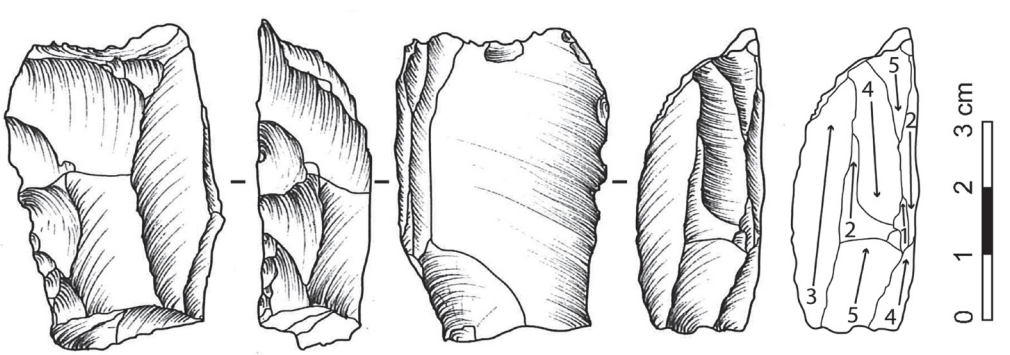

Figure 44: Kara-Bom, OH6, KB-92.YO6. Z7.38.168

single removal negative represents the only visible management of the striking platform.

∗ KB-92.YO6.I9.5.1280

This artifact is a wide laminar cortical blank bearing unidirectional negatives on the dorsal face (Figure 41). It bears a distal truncation and inverse irregular retouch. Two removals were detached from the upper platform along the cortical right edge, followed by two hinged removals ending the reduction process. Judging by the dorsal scar pattern, the blank was likely a larger blade and typologically could be described as a burin on a truncation (Demars and Laurent, 1992).

∗ KB-92.YO6.I8.12.48

This artifact is described as a fragment of a core produced on a laminar blank (Figure 42). Three removals detached from the proximal end of the blank can be observed. They follow the longitudinal axis of the blank. This core shows some of the smallest last removals observed within the OH6 sample.

Mode B5 (N=6)

∗ KB-92.YO6.J6.6. 1987

This artifact is produced on a unidirectional blade blank showing removal scars along the right edge (Figure 43). A relatively narrow flaking surface displays negatives of a bidirectional reduction system operated from two opposed platforms. The upper platform displays clear waves caused by a snapping event above which small negatives from the preparation of the platform by faceting are still visible. The lower platform shows a minimum of three removals associated with the detachment of a partial tablet. Chronological reconstruction seems to suggest that at least sometimes; removals are covering the whole length of the flaking surface (1). A short sequence of two removals starts from the lower platform (1 and 2) before switching to the upper platform (3). The next phase is characterized by the occurrence of two hinged negatives (4) from both platforms, ending the reduction process. Typologically, this piece is close to the polyhedral burin *(burin polyedrique)* described in Late Gravettian context (*e.g.* Hahn, 1969; Klaric *et al.*, 2009).

∗ KB-92.YO6. Z7.38.168

This artifact is produced on a blade blank and is remarkable for its reduced size (Figure 44). The back shows a crested morphology anterior to the last rejuvenation of the lower platform. It is not clear if it has to be considered as a morphological feature occurring on the blank prior to when the reduction started or if it corresponds to a later preparation. A single flaking surface is located along the right edge of the blank. Removal are detached from two opposed striking platforms and following a longitudinal axis.

The earliest visible removals are detached from the lower platforms from right to left in two sequences (1-3 and 3-5) before a switch to the upper platform. A single removal (2) seems to have successfully covered the whole length of the flaking surface and is followed by a hinged fracture (4) and a very small removal (5). The second platform switch starts by an attempt to detach a blade from the left corner of the flaking surface followed by another hinged fracture (5) that marks the end of the reduction process. Both striking surfaces have been reshaped by a single (upper) or several removals (lower).

∗ KB-93.YO6. E8.1.4321

This is another example of small sized cores produced on thick laminar blanks showing two opposed striking platforms (Figure 45). Small laminar blanks are detached along the longitudinal axis, by alternate bidirectional reduction. The ventral side of the core blank displays perpendicular flake scars. By following a single ridge, one of the removals is naturally pointed and likely has a triangular cross-section. Both striking platforms have been reshaped by radial removals.

∗ KB-92.YO6.Z6.14.758

The core is produced on a segment of neo-crested blade removed from a large blade core (Figure 46). It displays two opposed plain platforms. Platforms bear clear traces of snapping events, especially on

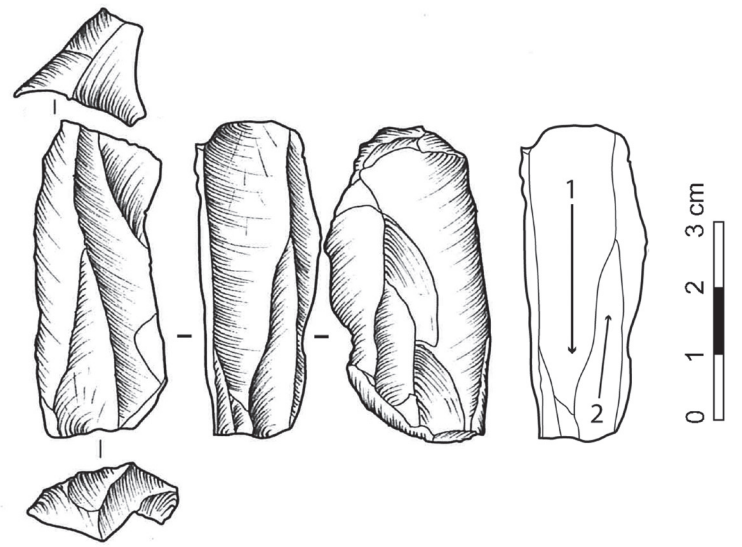

Figure 45: Kara-Bom, OH6, KB-93.YO6. E8.1.4321

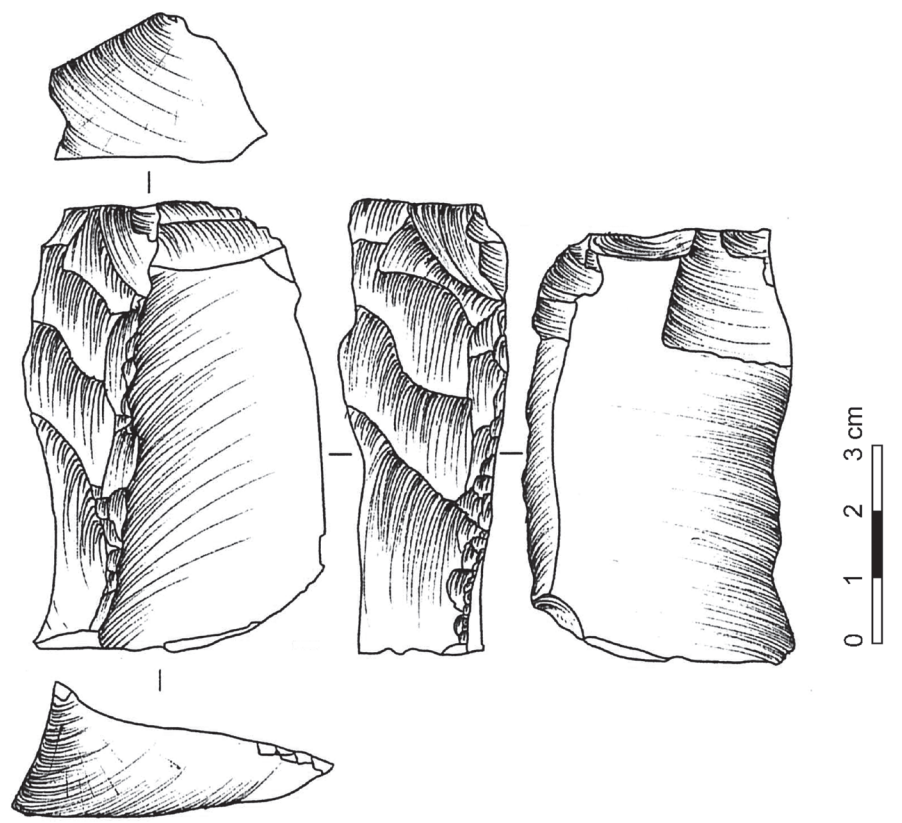

Figure 46: Kara-Bom, OH6, KB-92.YO6.Z6.14.758

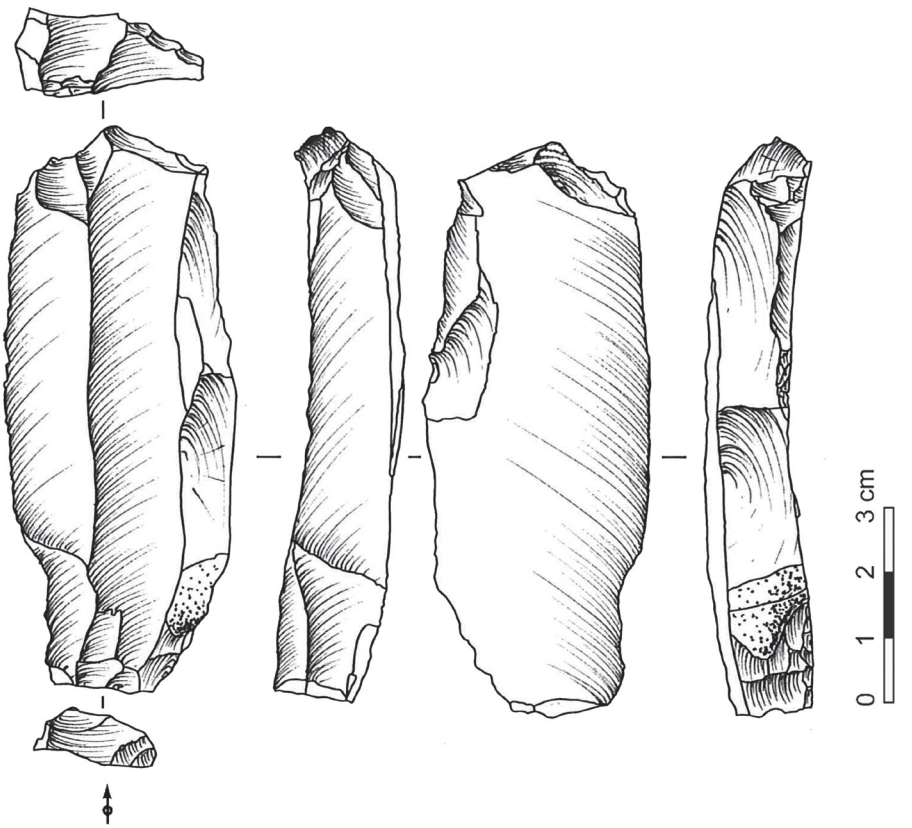

Figure 47: Kara-Bom, OH6, KB-92.YO6. I9.5.1280

the lower platform on which an impact is still visible. One laminar removal is detached from the lower platform and follows the longitudinal axes along the left edge of the blank. At least two more attempts failed as shown by the succession of hinged removals detached from the upper platform. Another hinged flake is visible on the ventral face of the blank.

∗ KB-92.YO6. I9.5.1280

This core is produced on a second crest blade bearing unidirectional dorsal scar patterns (Figure 47). Although little evidence of reduction can be observed, the preparation of a striking platform struck from the ventral side, at the distal end of the blank, and the perpendicular flake removed from the ventral face prior to the detachment of thin spall illustrate the initial stages of reduction. The lower striking platform is set up by the removal of the core blank platform from which two hinged flakes are struck. This artifact is typologically a *burin dièdre d'angle* (Demars and Laurent, 1992).

∗ KB-92.YO6.I8.12.48

This artifact is likely a fragment of a larger core produced on a blade blank. It displays a preparation of the striking platform as shown by the dihedral morphology of the distal end (Figure 48). The right edge shows several removal negatives, showing that the longitudinal edge is used as a flaking surface.

In this case, it is however not possible to push further the description and many questions remain regarding the original size and the stage of reduction of the core prior to the breakage event.

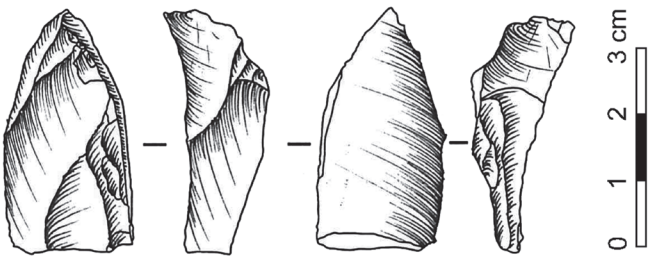

Figure 48: Kara-Bom, OH6, KB-92.YO6.I8.12.48

Mode B7 (N=1)

∗ KB-92.YO6.J8.3.1761

Produced on a blade blank, this core shows two flaking surfaces, one on the dorsal face and one located on the right lateral edge (Figure 49). The broader surface shows bidirectional removals of laminar flakes struck from two opposed platforms prepared by faceting (truncation). The narrow one shows the remains of a crest on the upper platform, independent of the platform on the broader flaking surface. This crest is posterior to a removal detached from the upper platform and is likely guiding a laminar removal struck from the lower platform. The ventral face bears removals detached prior to the last preparation of the lower platform.

The general pattern of reduction is parallel. The relationship between the two flaking surfaces, however, is not as clear as for larger blade cores. It cannot be excluded that the side removals play a role in the management of the lateral convexities. Such management operation may occur as a laminar reduction of a broad flaking surface necessarily lead to a flattening of the core. This artifact shows numerous similarities with blade cores or with the general reduction pattern of bladelet core of 'Kostenki technique' (*e.g.* Slimak and Lucas, 2005). Similar objects are classified by Dibble and McPherron (2007) and as flake cores, but typologically, they fit in the truncated-facetted category (Schroeder, 1969, 2007), Nar-Ibrahim truncation (Solecki and Solecki, 1970) or Kostenki knives (Efimenko, 1958; Turq and Marcillaud, 1976; Escutenaire, 1997).

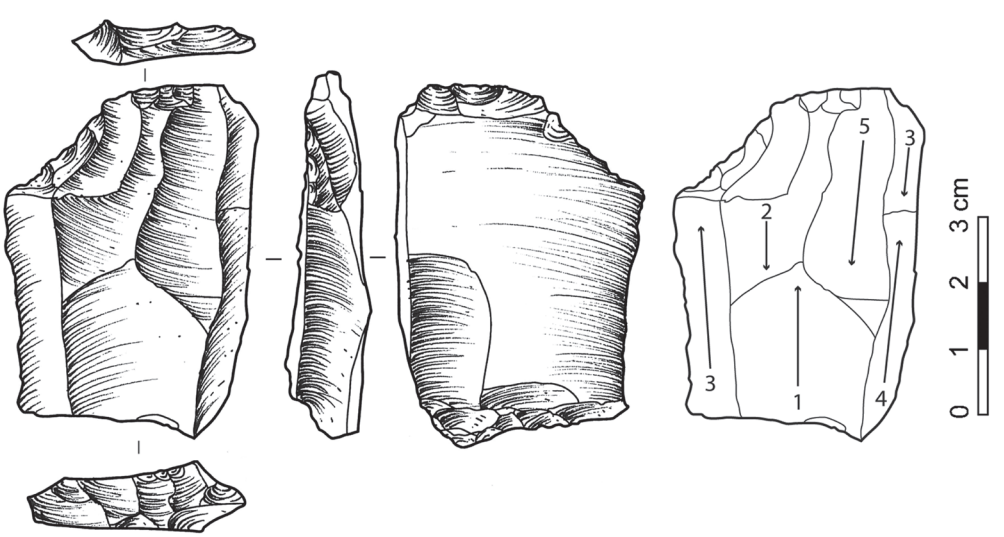

Figure 49: Kara-Bom, OH6, KB-92.YO6.J8.3.1761

3.3.3 REDUCTION SEQUENCE RECONSTRUCTION

Following the results of the blank attribute analysis and the core descriptions, an analytical reconstruction of the individual reduction sequences is proposed in the following section.

Laminar blanks with parallel edges

From a morphological point of view, two main types of blade are observed. The first category corresponds to artifacts displaying parallel edges starting from the mesial part. This type of blank covers the whole range of length and width observed in the OH6 sample. Dorsal scar patterns show a coexistence of uni- and bidirectional reduction process. The largest complete examples show that the maximum length of such blades sometimes exceeds 160 mm. Starting from the earliest stage of reduction, crested blades are used to enhance or create the first guiding ridge but also to maintain a certain degree of lateral convexities of the flaking surfaces. These management operations occur all along the reduction process, as shown by the various sizes of neo-crested blanks (Figure 50).

Although not numerous and heavily reduced, large/medium size blade cores are mainly produced on blocks or nodules (Mode A). The reduction sequence reconstruction illustrates a succession of short unidirectional sequences followed by a change to the opposed platform. This situation is reflected by the roughly equivalent frequency of uni- and bidirectional dorsal scar patterns. Strict alternate bidirectionality (showing a platform switch after each removal) seems unusual on Mode A cores. Blank cross-sections are mostly triangular or trapezoidal showing a frequent use of multiple ridges guiding the detachment of laminar blanks. The short unidirectional sequences do not follow a clear systematic path, although the largest blade core presents a series of 2-3

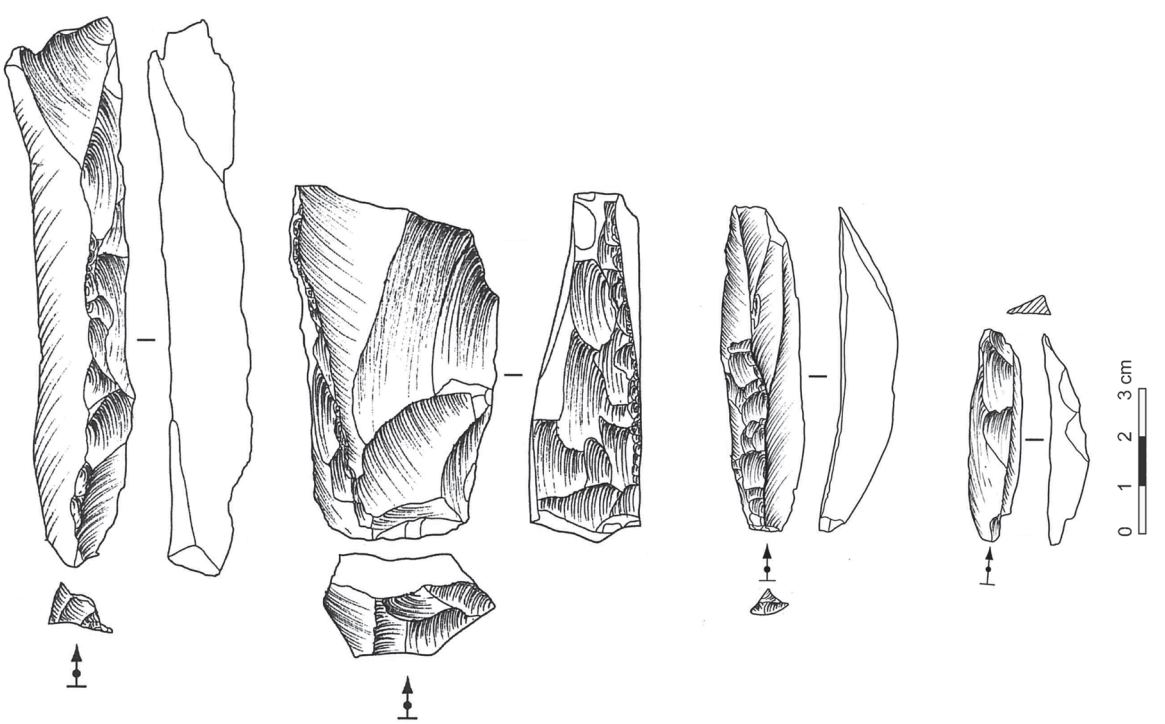

Figure 50: Kara-Bom, OH6, crested blanks

removals from left to right, using the previous scar as a ridge (see Figure 36). All Mode A cores show a use of two flaking surfaces, either independently (Mode A6) or in continuity (Mode A10). These two variants are, however, very similar and may reflect different stages of reduction. From time to time, a thick blade (crested or not) is detached from the intersection of two surfaces in order to reshape the lateral convexity of the core. Although blanks can be produced from both surfaces, diacritic reconstructions show that the reduction takes place mainly on the broader surface and extends to the narrow face during the final phase (see Figure 36 and Figure 37). This could indicate a secondary role of the narrow face, mainly used to remove the crested elements necessary to reshape the convexity of the broader surface. In this case, the two flaking surfaces are not strictly independent nor in continuity (semi-turning reduction), but rather inter-dependent. In addition, the presence of *débordant*, facetted platforms on thin blades indicates that the reduction can also takes place at the junction of the two surfaces.

The situation is slightly different for the small size blade/bladelet production. This type of blank is mainly detached from cores on blades (Mode B). Core blanks are selected among the thickest laminar blanks. As illustrated on Figure 51, the distribution of core blank thickness for Mode B overlaps with the thickest 25% of the total sample of blades and with the blade MNI. Statistically, the medians of core blank thickness differ from overall blade thickness (Mann-Whitney, T=Ub=186.5, p=<.05) and MNI blade thickness (Mann-Whitney, T=Ub=133.5, p=<.05) showing that they belong to a different population. In other words, the thickest byproducts from the large blade production are selected and transformed into cores for the production of smaller blanks. The thickest blades are mainly crested blanks, or *débordant* blades, removed from the intersection of the flaking surface and the lateral side of the blade core.

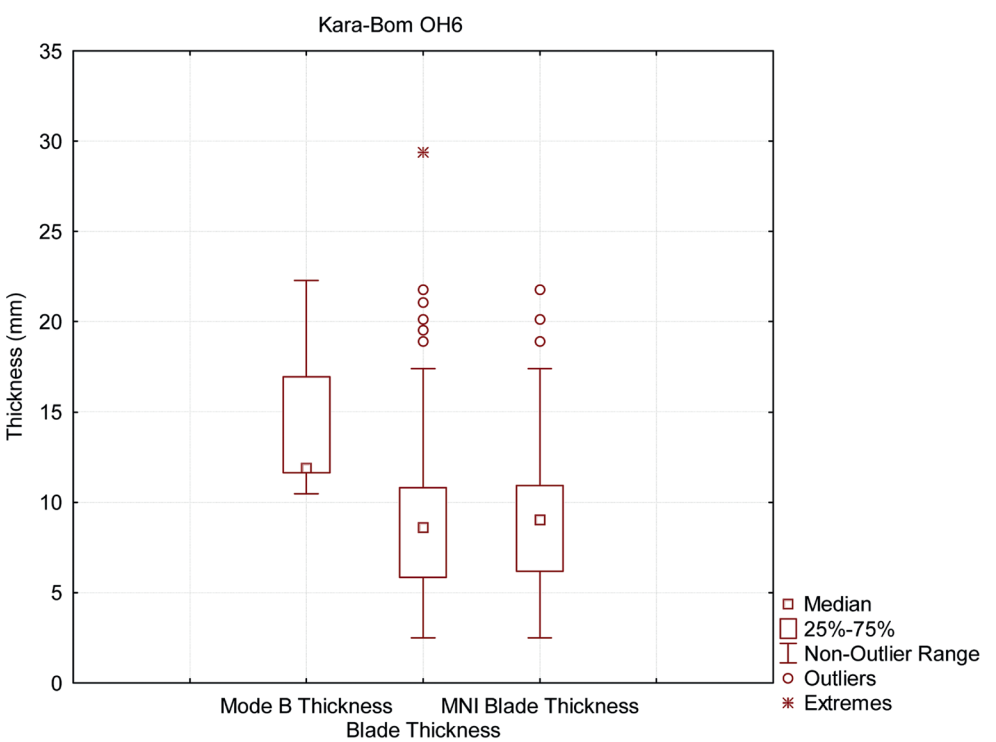

Figure 51: Kara-Bom, OH6, thickness of Mode B blanks compared with the overall blade thickness (total sample and MNI)

If necessary, the blade is snapped prior starting the Mode B reduction. This allows a certain control on the length of the removals, but also offers the possibility to select the thickest part of the blank to obtain a minimum 10 mm wide flaking surface. Within the OH6 sample, some of the features observed on the internal surface of broken pieces seem to indicate a snapping by percussion (see Figure 9 and 12). However, this behavior is likely opportunistic as it cannot be regarded as a systematic process unless it occurs in higher frequency. Reduction is systematically taking place along one edge of the blank, following its longitudinal axis. As for the Mode A cores, it tends to follow short sequences of 2-3 removals (Mode B1) before a platform switch occurs. A few small size cores show alternate bidirectional removals at the last stage of the reduction process. Unless a knapping accident (such as hinged fractures) happens, removals seem to cover the whole length of the flaking surface. Thus, although a use of two relatively independent platforms is attested too, the flaking surface is considered as a whole and not as the sum of two distinct surfaces.

The reduction is mainly frontal, but in some cases, an expansion on the lateral side of the core approaches a semi-turning progression. This latter fact may be accentuated by the method itself as the narrow morphology of the core blank makes it difficult to obtain a long lasting reduction. As shown by the occurrence of small-sized crested blades, core management is also taking place on Mode B cores.

The morphology of the blanks obtained varies according to their initial position on the flaking surface. On very narrow flaking surfaces, blanks are generally removed from the corner of the flaking surface, resulting in either a natural back and/or a triangular section. When the flaking surface is wide enough, blanks may be detached from the middle part of the flaking surface, and therefore, show a thinner triangular section. A few removals display a rectangular section. As most of the time they bear negatives of hinged fractures on their dorsal face, they could be interpreted as flaking surface management operations. As observed on some of the complete blanks, a distinction can be made between pointed elements and the rest. The pointed small blades show both triangular but also trapezoidal cross-sections. This latter fact is clearly linked with the bidirectionality of the reduction. As the general orientation of the removal is parallel, laminar blanks with a trapezoidal section can only be pointed by using two opposed platforms. All in all, the common denominator between these blanks is that they are relatively narrow, elongated, axial and have a straight profile.

By comparing the width of the flaking surfaces, differences between Mode A and Mode B core distributions can be observed (Figure 53). Mode A, although poorly represented, covers the whole range of widths observed within the blank population. However, Mode B shows a skewed distribution with the mean corresponding to one of the peaks of the blank bimodal distribution. This situation reflects the coexistence of two technological schemes. One of these focuses on the use of a narrow edge of thick blades as a flaking surface in order to produce small-size laminar blanks. Only one Mode B core of truncated-facetted morphology has one of its flaking surfaces wider than 20 mm. The overlap between flaking surface width of Mode A and Mode B could explain why the bimodality of the distribution is not fully visible. In spite of the small number of observable last removals on the cores (N=10), a difference between the modes is visible with Mode A tending to produce wider blanks than Mode B (see Table 29).

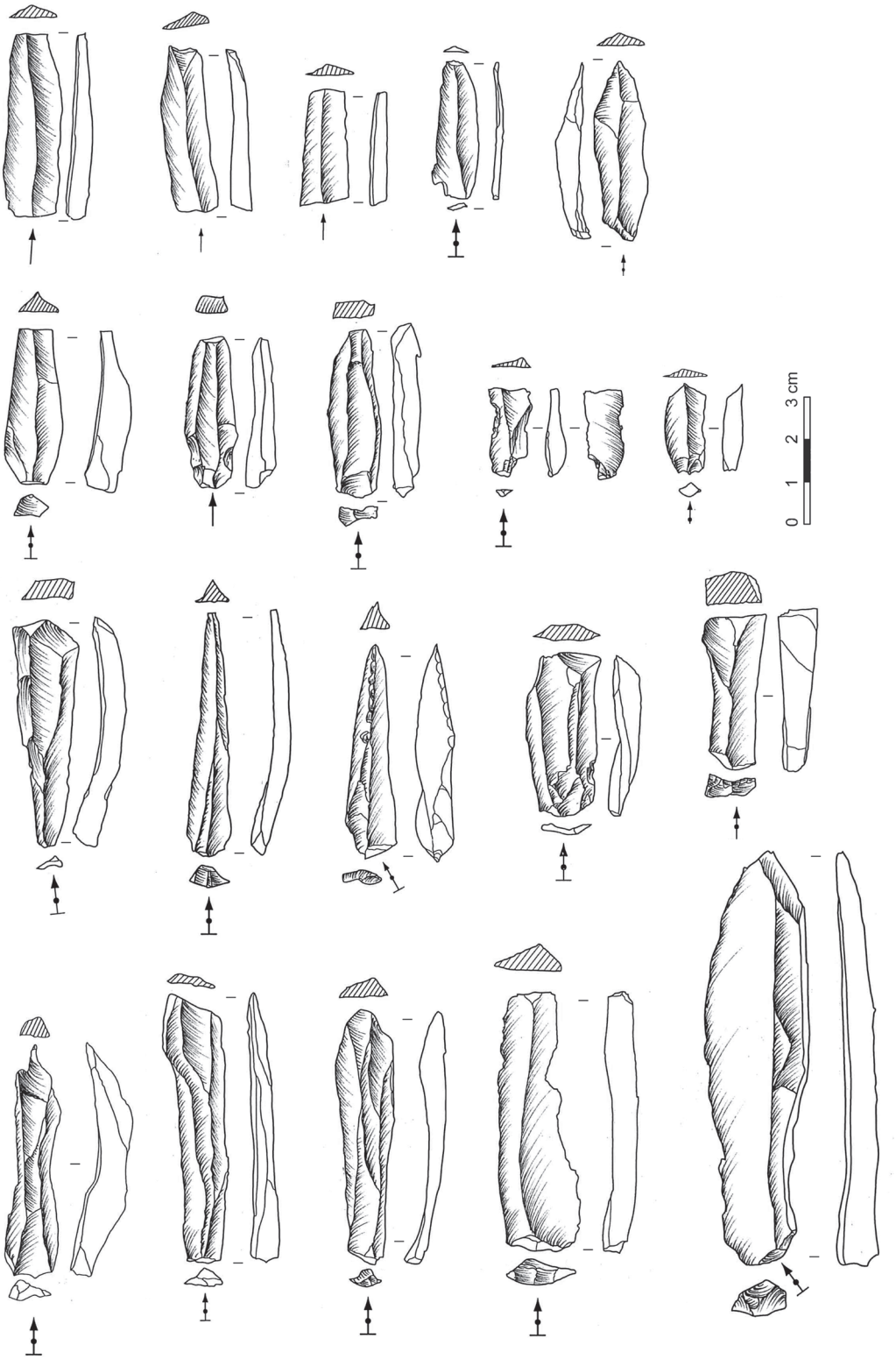

Figure 52: Kara-Bom, OH6, laminar blanks

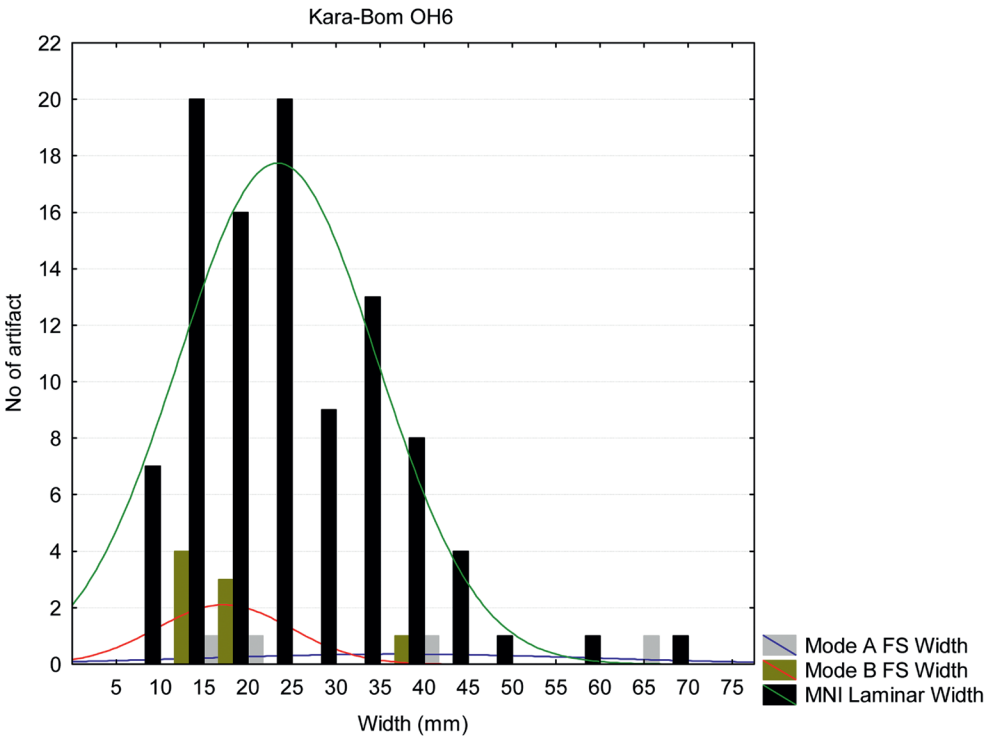

Figure 53: Kara-Bom, OH6, Mode A and Mode B flaking surface width and MNI width

Convergent blanks

A second type of laminar blank showing convergent mesio-distal edges is present (N=10). Five blanks are complete, three are mesioproximal and two are distal and mesiodistal fragments. Except for one, they all have bi-directional removal scars on the dorsal face and all show trapezoidal sections. Their profiles are straight or slightly curved. The majority (N=8) have a width between 25 and 40 mm for a length between 60 and 110 mm, and a maximum thickness around 1cm. Two artifacts are of a smaller size with a width of 9.5 and 12.9 mm. The size of their platform does not differ from the variability observed on the overall blade sample regardless of whether their morphology is plain (N=5) or facetted (N=3). Two of these blanks show clear traces of an extreme abrasion of the external platform edge. The bladelet category also includes this kind of blank although they are less numerous (N=2). The convergent blades are all axial.

The reduction sequence leading to the production of such blanks implies a minimum of 3 laminar removals given the number of scars visible on their dorsal face. The largest convergent blade displays a width that indicates a rather large core or a core reduced on its wider face. The straight profile and the relatively flat dorsal face seem to indicate that they are detached from cores such as Modes A3 to A6, presenting at least one broad flaking surface. In the OH6 sample, only one core (see Figure 37) seems to correspond to this description. The chronological reconstruction shows at least one sequence of three unidirectional removals, which given the previous scars associated with the opposed platform, could easily yield a bidirectional dorsal scar patterning. The trapezoidal section of these elements suggests that in the case of a unidirectional reduction, a clear convergent orientation of removals is required to obtain pointed blanks. As most of these unretouched artifacts show bidirectional scar patterns, the largest convergent blanks are likely produced on wide-faced cores. However, without long refitted sequences,

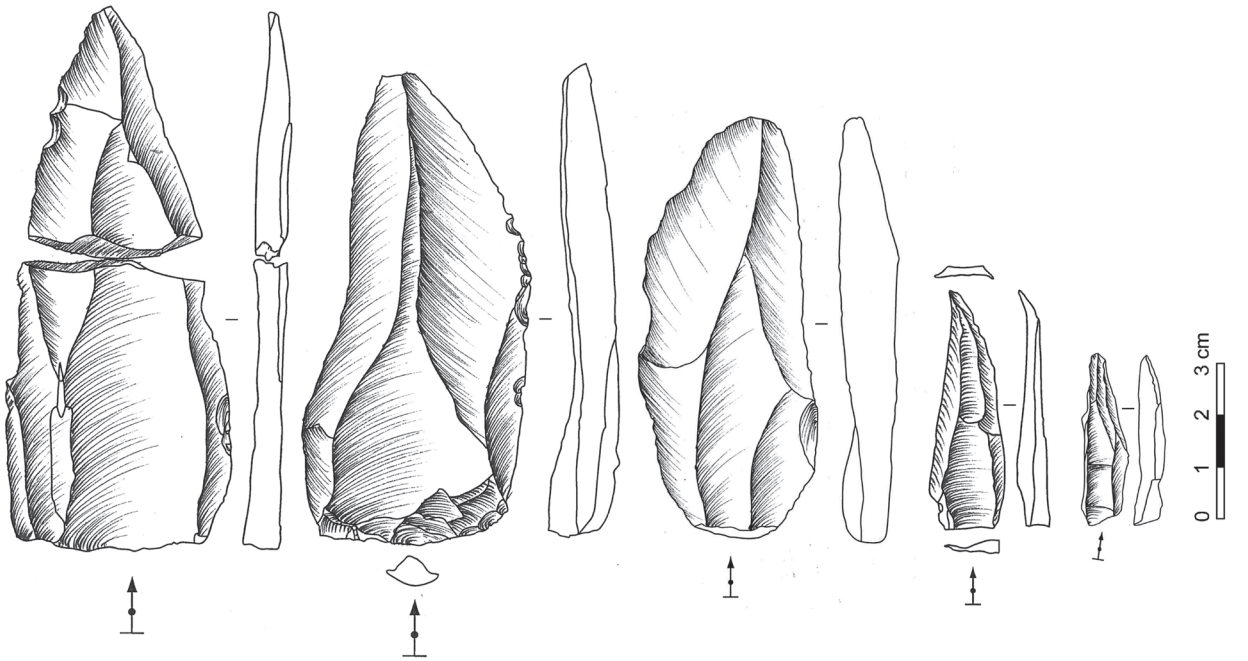

Figure 54: Kara-Bom, OH6, convergent laminar blanks

other possibilities cannot be ruled out. In fact, these artifacts could also be occasionally produced during a bidirectional blade production from larger cores. The smallest convergent blanks are less demanding in terms of flaking surface width. It is assumed that some of them could be produced on truncated-facetted cores (Figure 54, second from the right), as they appear to be technologically similar to the wide-faced core described above. However, one of the smallest convergent blanks is rather narrow and displays multiple laminar scars detached from an opposed platform in its mesiodistal part. In addition, a clear natural back is visible. In this case, the blank was likely detached from a Mode B core (Figure 54: first from the right).

Platform preparation and percussion technique

As previously mentioned, no traces of thin abrasion have been recognized on cores or on blanks. In a few cases, the external platform angle of the blank is heavily smoothed by a strong abrasion. Plain and facetted platforms coexist, the latter showing morphological variability. Beside the classical faceting, two main variants could be observed. The first shows an extension of the faceting on the lateral side of the blank, indicating that the blank was removed close to the junction of two surfaces. The second variant shows a partial faceting of the platform, as a perpendicular preparation flaking to change the external platform angle, but the point of percussion is located on an unprepared plain surface. This preparation is sometimes combined with flaking surface trimming from the platform (Figure 55, left). When considering the blade category, the mean platform thickness is clearly above the 4 mm limit defined by Pelegrin (1995) and characterized as thick platforms *(talon épais)*. More generally speaking, flaking on the bulb (circa 18% of the blade MNI) and lip (circa 13% of the blade MNI) occur sporadically on the blanks.

Considering these elements together, it is assumed that the technique of percussion in use is mainly a stone hammer *sensu lato*. If numerous features are analogous to those described in practical experiments using hard hammer stone on flint, the lack of experiments on the Kara-Bom specific raw material leave the question partly open. However, some features such as extreme abrasion of the EPA, or the flaking

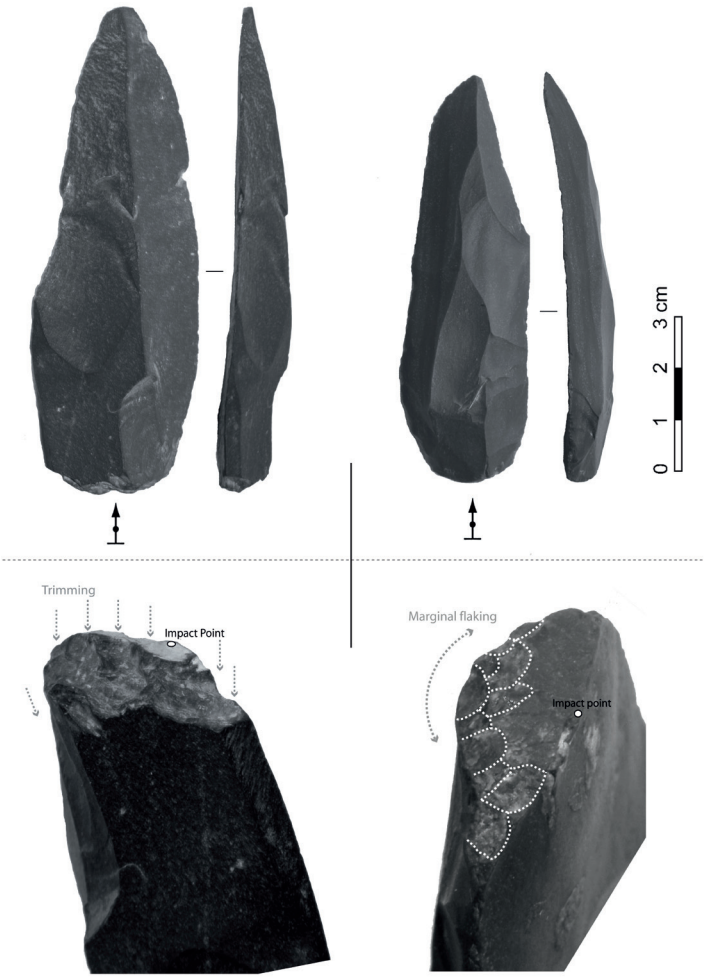

Figure 55: Kara-Bom, OH6. On the right, partial faceting (KB-92.YO6.Z8.22.924). On the left, trimming (KB-92.YO6.Z6.26.1383)

of the bulb, could indicate the occasional use of soft hammer stone (*e.g.* limestone). The quasi-total absence of features typically associated with the use of organic hammer is noteworthy and suggest that the use of stone hammer remains the most parsimonious hypotheses. Similar hammers, displaying traces of percussion, have been reported as associated with OH6 (Derevianko, Petrin, *et al.*, 1998).

Retouched tools

27 retouched tools were recorded in the sample: 21 on blades, 5 on bladelets, and 1 on a laminar flake. Except the later, the sample does not include tools on flakes. A conservative approach is applied here to recognize intentional retouch and to leave out ambiguous artifacts when they fail to exhibit clear evidence for secondary treatments.

	N	*f* (among tools)	*f* (from total, n=189)
Retouched blade	12	43%	6%
Retouched bladelet	6	21%	3%
Retouched point	8	29%	4%
Endscraper	2	7%	1%
Other	0	0%	0%
	28	100%	15%

Table 31: Kara-Bom, OH6, frequency of major retouched tool types

The preservation of the tools shows a different picture than for the blank sample. Complete artifacts dominate the sample, but mesial fragments are less than others, as distal fragment are totally absent. As discussed below, this is related to the position of the retouch, which tends to occur less frequently on the mesial part of the tool.

	N	*f*
Distal	0	0%
Mesiodistal	4	14%
Mesial	1	4%
Mesioproximal	6	21%
Proximal	3	11%
Complete	14	50%
	28	100%

Table 32: Kara-Bom, OH6, retouched tools, breakage

In terms of platform preparation, facetted and dihedral platforms are the most common, with only a few occurrences of plain platforms. When comparing these frequencies with the whole laminar sample, it appears that facetted platforms are not more significantly numerous among the toolkit than in the laminar blanks (χ^2 (1)= 0.104, p=.92). Dihedral platforms are more frequent but not enough to be statistically meaningful. So, the most striking difference is the lack of plain platforms (χ^2 (1)= 9.706, p=<.05). Given that a third of the tools do not show identifiable platforms, these observations might also be biased by the reduced sample size. The mean platform thickness is similar to what is observed on the non-retouched blanks (Mean=5.98 ± 3.36 mm).

	N	*f*
Plain	2	7%
Facetted	12	43%
Dihedral Flat	5	18%
Undet	9	32%
	28	100%

Table 33: Kara-Bom, OH6, retouched tools, platform preparation

In terms of length, or thickness, no clear pattern emerges when comparing the toolkit with the laminar elements. However, it seems that the width of retouched tools shows a bimodal distribution similar to what it is observed in the laminar blanks. Considering that retouch is likely to reduce the width of blanks, such a correspondence is noteworthy (Figure 56).

It seems clear that the OH6 assemblage does not show examples of extreme tool reduction, artifacts being only slightly modified by the secondary treatment. Dorsal scar patterns are highly similar to the non-retouched blanks, with 55% of bidirectional and 44% unidirectional scar patterns, and are mainly axial. The infrequent occurrence of unidirectional convergent dorsal scars is noticed, although this type of patterning is absent from the non-retouched elements.

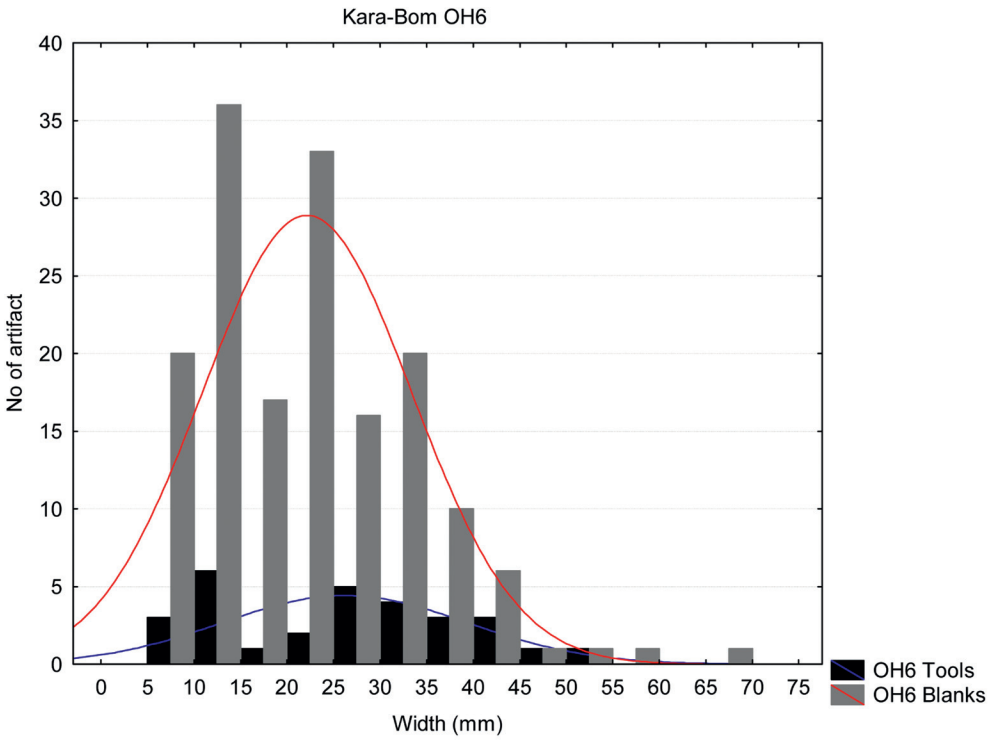

Figure 56: Kara-Bom, OH6, width histogram comparing retouched tools and blanks

	N	*f*
Right	4	14%
Left	2	7%
None	17	61%
Undet	5	18%
	28	100%

Table 34: Kara-Bom, OH6, retouched tools, Orientation

Blades with parallel edges are retouched on the proximal (Figure 26: 9) and distal parts, sometimes into pointed blades (Figure 26: 12), sometimes into endscrapers (Figure 26: 10), with the latter transformed by a direct marginal retouch on the distal end. Convergent or pointed blanks are modified mainly by direct retouch (Table 35) affecting the proximal part of the blanks (Table 36; Figure 26: 2, 3, 11), but also sometimes the distal part (Figure 26: 4, 13), somewhat accentuating the pointed shape of the tip. Tools showing a combination of retouch on the dorsal face (N=2) also show an association of distal and proximal retouch.

	N	*f*
Direct	23	82%
Inverse	5	18%
Alternate	0	0%
	28	100%

Table 35: Kara-Bom, OH6, retouch location (face)

The presence of a single atypical Mousterian point is of note. It is produced on a *débordant* Levallois point blank, for which the right *débordant* edge is accentuated by a short series of inverse steep retouch. The left edge shows continuous thin retouch. No core

	Dorsal		Ventral	
	N	*f*	N	*f*
Distal	5	18%	1	4%
Mesial	2	7%	2	7%
Proximal	10	36%	0	0%
Combination	2	7%	0	0%
Continuous	3	11%	1	4%
Undetermined	6	21%	0	0%
	28	100%	4	15%

Table 36: Kara-Bom, OH6, retouch location (edge)

corresponding to such technology has been found in the OH6 sample.

Most of the retouch is located around the proximal and distal ends of blanks. This is also reflected by the lack of retouched mesial blade fragments although the latter are clearly the most numerous among the unretouched blanks. Among the five blanks showing inverse retouch, two bear thin retouch along the right edge of bladelets showing an unidirectional dorsal scar patterning. They are typologically Dufour bladelets of Dufour sub-type (Demars and Laurent, 1992). One of these likely comes from a Mode B core as the blank displays a part of the core's ventral face (Figure 57: 6). A small blade displaying mesiodistal semi-steep retouch along the right edge also occurs. The blank is a thick, bidirectional, naturally-backed blade detached from a Mode B core (Figure 57: 8). One backed bladelet on an atypical narrow cortical blank occurs in the sample and displays a small truncation at the proximal end.

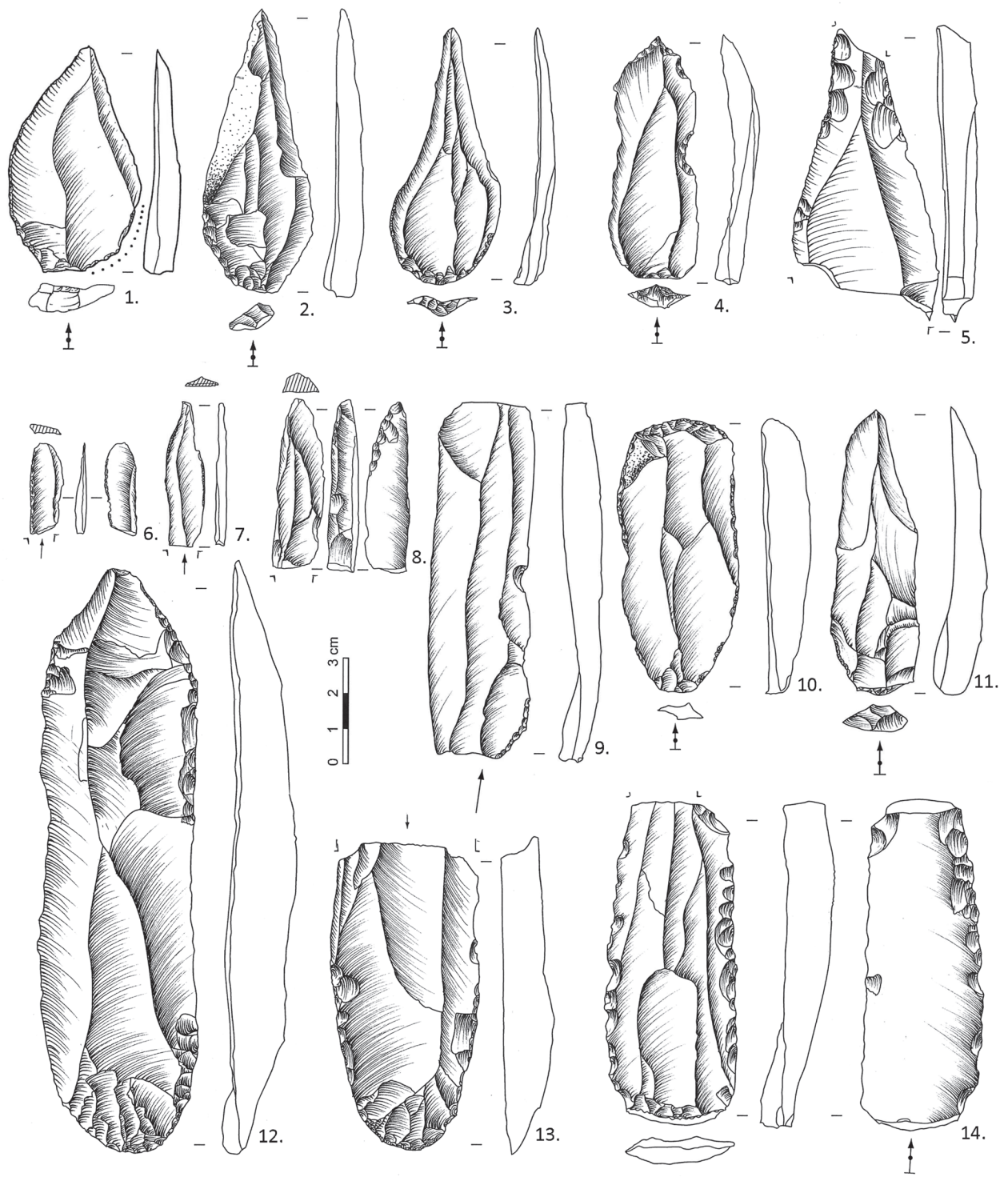

Figure 57: Kara-Bom, OH6, retouched tools

3.4 LAMINAR TECHNOLOGY: OH5

3.4.1 BLANK ATTRIBUTES

Breakage

Complete artifacts, mesial and mesioproximal fragments are the most represented (Table 37). Based on these observations, an MNI of 69 blades and 11 bladelets is calculated on a total of 148 laminar artifacts recorded.

Platform: size and preparation

Considered as a whole, laminar blanks show similar frequencies of facetted and plain platforms (Table 38). This trend is clearly expressed in the blade category, as the majority of bladelet platforms are facetted. The latter observation is balanced by a fairly reduced sample size. The mean platform thickness is 5.3 ± 4.1 mm and mean platform width is 12.4 ± 8 mm. For the blade category, mean platform thickness is 5.7 ± 4.1 mm and mean width is 13.3 ± 7.7 mm. Bladelet mean platform thickness is 2.6 ± 3.2 mm and mean width is 6.4 mm ± 7.5 mm. The small sample of bladelets shows a lot of variability. Here measurements are listed per morphological type.

	Total		Blade		Bladelet	
	N	*f*	N	*f*	N	*f*
Distal	10	7%	6	5%	4	16%
Mesiodistal	17	11%	12	10%	5	20%
Mesial	41	28%	36	29%	5	20%
Mesioproximal	27	18%	25	20%	2	8%
Proximal	14	9%	12	10%	2	8%
Complete	39	26%	32	26%	7	28%
	148	100%	123	100%	25	100%

Table 37: Kara-Bom, OH5, breakage

	Total		Blade		Bladelet	
	N	*f*	N	*f*	N	*f*
Plain	26	18%	24	20%	2	8%
Facetted	32	22%	26	21%	6	24%
Dihedral Flat	8	5%	7	6%	1	4%
Undet	82	55%	66	54%	16	64%
	148	100%	123	100%	25	100%

Table 38: Kara Bom, OH5, platform preparation

Facetted platform	Total		Blade		Bladelet	
	Thickness	Width	Thickness	Width	Thickness	Width
Sample size	32		26		6	
Mean (mm)	5.4	13.7	5.9	15.1	3.3	7.4
Standard deviation (mm)	3.4	8.7	3.2	8.2	3.8	9
Range (mm)	13.5 to 0.5	35.3 to 1.5	13.5 to 1.8	35.3 to 2.6	10.5 to 0.5	25.4 to 1.5

Table 39: Kara-Bom, OH5, facetted platform size

Plain platform	Total		Blade		Bladelet	
	Thickness	Width	Thickness	Width	Thickness	Width
Sample size	26		24		2	
Mean (mm)	4.2	10.4	4.5	11	0.9	2.7
Standard deviation (mm)	2.9	6.9	2.9	6.8	<0.1	1.2
Range (mm)	11.6 to 0.8	28.4 to 1.9	11.6 to 0.8	28.4 to 2.4	0.9 to 0.8	3.6 to 1.9

Table 40: Kara-Bom, OH5, plain platform size

Blade facetted platform are significantly thicker than plain ones (Mann-Whitney, T=Ub=267, p=<.05)(Table 39). This is also visible in the bladelet category, but the small sample size does not allow any further observations. Variance differs between the two morphological categories, as facetted platforms appear slightly more variable in size than plain platforms. These differences are, however, not statistically significant.

A few flat dihedral platforms occur in the sample (blade N=7, bladelet, N=1) (Table 40). The mean thickness is 8 ± 7.8 mm, and mean width is 13.8 ± 7.3 mm. This type of platform is clearly thicker than the whole population but shows a similar mean width as the facetted platforms. From a general point of view, we observe a quasi-total absence of thin abrasion on the blanks external platform edge. The only exceptions are observed on blades (N=5) which show a strong abrasion smoothing of the EPA.

Blank size attributes

Length

As length is measured only on complete elements, the results presented are based on a smaller sample. It appears that blades and bladelets overlap in terms of range and standard deviation. The length is not normaly distributed (Shapiro-Wilk, W=0.90 p=<.05) and the fragmentary nature of the sample show a positive skewness (1.5)(Figure 58).

	Total	Blade	Bladelet
Sample size	39	32	7
Mean (mm)	67.3	73.17	40.7
Standard deviation (mm)	28.9	27.4	19.8
Range (mm)	180 to 25.5	180 to 29.6	83.7 to 25.5

Table 41: Kara-Bom, OH5, blank length

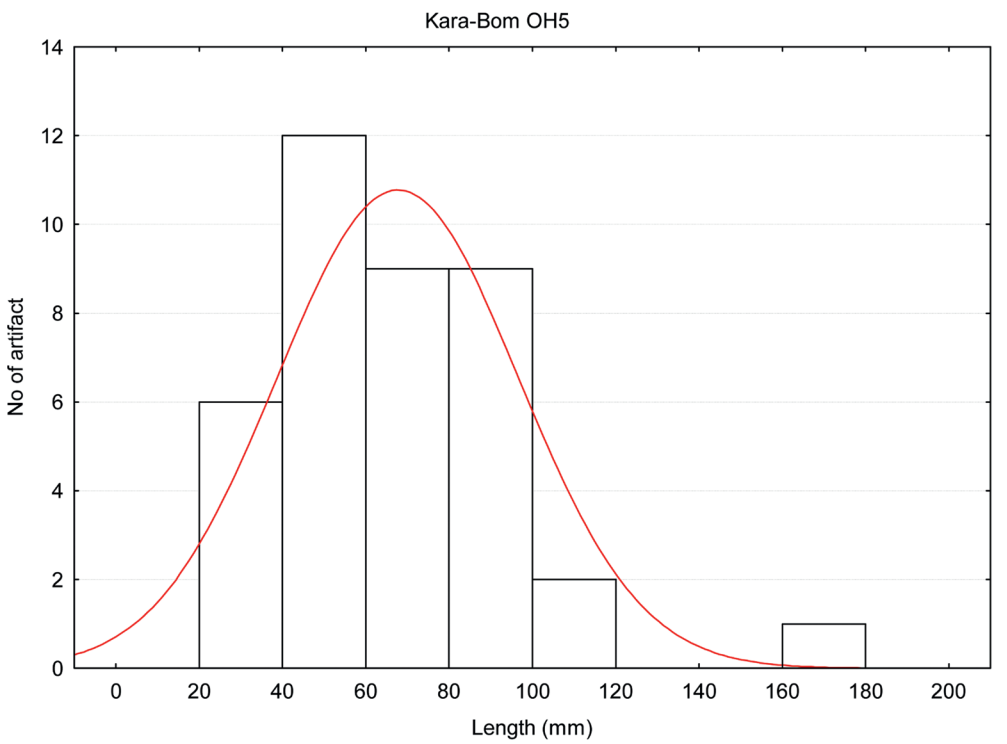

Figure 58: OH5, blank length distribution

Width

In terms of width, when comparing mean and standard deviations from the complete sample and from the MNI, it appears that MNI values are either equal or higher than in the total sample (Table 42).

The distribution of width measurement from the total sample may be bimodal distribution (Figure 59). The first mode would peak between 10-15 mm width and the second corresponds to the mean. However, the two modes are less visible in the MNI distribution, although both MNI (Shapiro-Wilk, W=0.96 p=<.05) and total sample (Shapiro-Wilk, W=0.97 p=<.05) are not normally distributed. The positive skewness of the histograms (respectively 0.61 and 0.88 for the whole population and for the MNI) can be partly explained by an apparent cut-off of 5 mm. The occurrence of two microblades (width < 6mm) is noted but due to their poor representation, they are grouped with the bladelets.

	Total sample			MNI		
	Total	Blade	Bladelet	Total	Blade	Bladelet
Sample size	148	123	25	80	69	11
Mean (mm)	23.1	25.9	9.5	24	26.1	10.8
Standard deviation (mm)	10.5	9	5.3	11.3	10.4	7.5
Range (mm)	64.2 to 4.1	64.2 to 9.8	32.8 to 4.1	64.2 to 4.9	64.2 to 9.8	32.8 to 4.9

Table 42: Kara-Bom, OH5, blank width

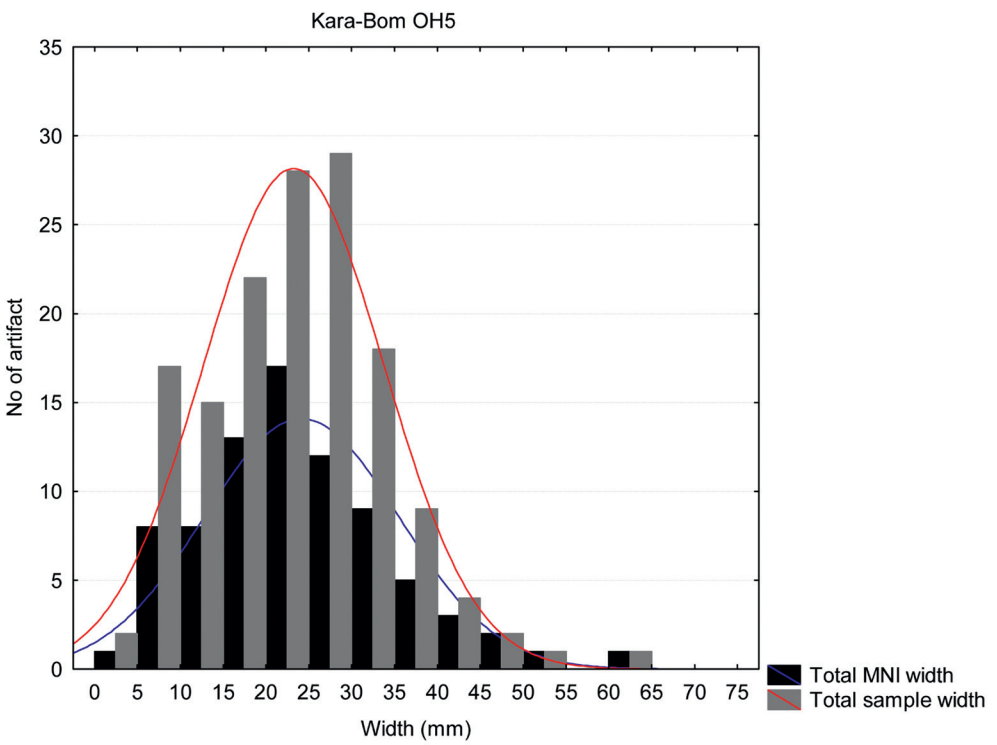

Figure 59: Kara-Bom, OH5, blank width distribution

Thickness

Compared with the total population, MNI thickness shows equal or slightly higher mean values and for bladelets, a higher standard deviation (Table 43; Figure 60). Differences are however not statistically significant. This shows that breakage does not influence significantly the main trends observed in terms of thickness in the sample considered. Blade and bladelet thickness samples clearly differ but their standard deviations overlap. The thickness histogram is perhaps weakly bimodal showing a first mode of less than 10 mm and a second mode of more than 10 mm. The MNI, although based on less numerous measurements, shows a similar distribution to the total sample population.

	Population			MNI		
	Total	Blade	Bladelet	Total	Blade	Bladelet
Sample size	148	123	25	80	69	11
Mean (mm)	7.8	8.5	4	8.1	8.5	5.1
Standard deviation (mm)	4	3.6	3.6	4.2	3.9	5.1
Range (mm)	19.8 to 1	19.8 to 1.9	19.5 to 1	19.8 to 1.7	19.8 to 1.9	19.5 to 1.7

Table 43: Kara-Bom, OH5, blank thickness

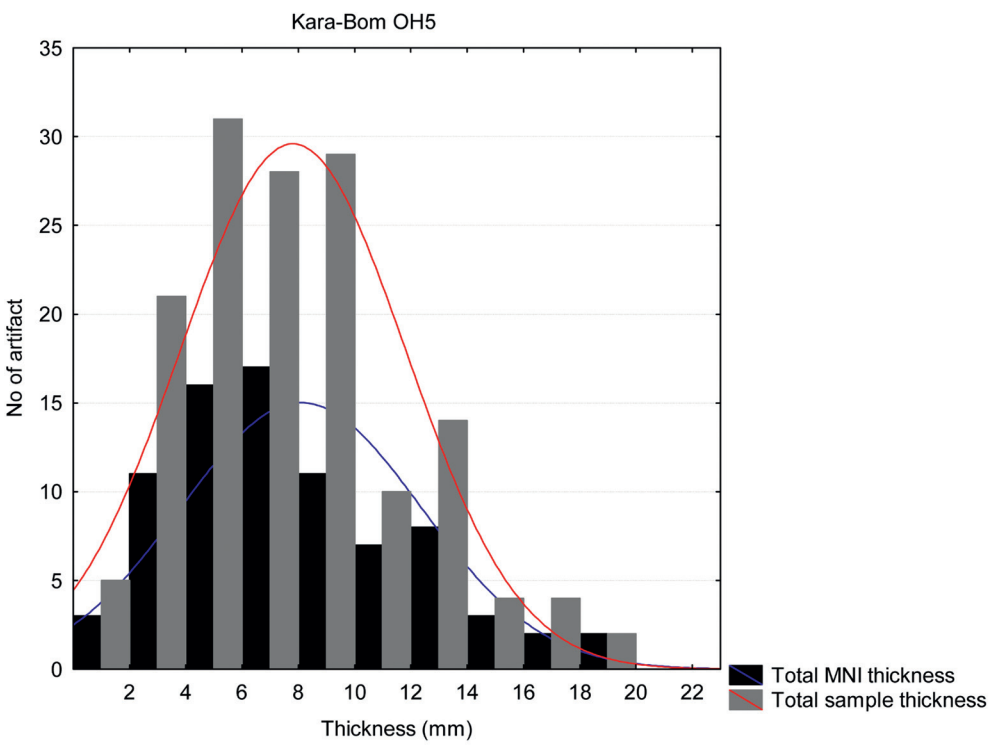

Figure 60: OH5, blank thickness distribution

Dorsal scar pattern

A discrete occurrence of cortex occurs on both unidirectional and bidirectional blanks, indicating that some initial phases of reduction took place on site, which seems to be confirmed by the presence of an initial crested blade and a second bladelet (Table 44). Neo-crested blanks are also well represented, mainly among blades, suggesting that core management operations took place on site. For the total sample, as for the blades, unidirectional dorsal scar patterns dominate. Bladelets show a majority of bidirectional scar patterns, although the difference is minor and mainly visible due to the reduced sample size.

As underlined by others (*e.g.* Bar-Yosef and Van Peer, 2009), blank fragmentation may artificially increase the frequency of unidirectional blanks. So, our

	Total		Blade		Bladelet	
	N	*f*	N	*f*	N	*f*
Unidirectional	71	48%	62	50%	9	36%
Unidirectional and cortex	5	3%	4	3%	1	4%
Bidirectional	52	35%	41	33%	11	44%
Bidirectional and cortex	4	3%	4	3%	0	0%
Crest	1	1%	1	1%	0	0%
Second Crest	1	1%	0	0%	1	4%
Neo-crest	9	6%	8	7%	1	4%
Undetermined	5	3%	3	2%	2	8%
	148	100%	123	100%	25	100%

Table 44: Kara-Bom, OH5, dorsal scar pattern

	Complete blank		Complete blade		Complete bladelet	
	N	*f*	N	*f*	N	*f*
Unidirectional	12	31%	10	31%	2	29%
Bidirectional	20	51%	17	53%	3	43%
Crested	4	10%	4	13%	0	0%
Undetermined	3	8%	1	3%	2	29%
	39	100%	32	100%	7	100%

Table 45: Kara Bom, OH5, dorsal scar pattern of complete blanks

observations are repeated based on complete blanks only, sharply reducing the sample (N=39)(Table 46).

Considering only complete elements, a significant decrease in the unidirectional pattern frequency (χ^2 (1)= 5.2, p= <.05) can be observed. Meanwhile, the decrease of bidirectional is noticeable, but less sharp and not significant in statistical terms. As a result, bidirectional dorsal scar pattern becomes dominant at the expense of the unidirectional ones, but the difference between frequencies remains statistically insignificant.

Cross-section

The cross-sections are mainly trapezoidal in both blade (χ^2 (1)= 27.4, p= <.05) and total sample categories (χ^2 (1)= 13.9, p= <.05) (Table 46).

	Total		Blade		Bladelet	
	N	*f*	N	*f*	N	*f*
Flat	7	5%	5	4%	2	6%
Rectangular	0	0%	0	0%	0	0%
Triangular	53	36%	37	30%	16	44%
Trapezoidal	85	57%	78	63%	7	19%
Polyhedric	3	2%	3	2%	0	0%
	148	100%	123	100%	25	69%

Table 46: Kara-Bom, OH5, type of cross-section

	Total		Blade		Bladelet	
	N	*f*	N	*f*	N	*f*
Straight	96	65%	82	67%	14	56%
Slightly Curved	36	24%	28	23%	8	32%
Curved	5	3%	5	4%	0	0%
Twisted	8	5%	5	4%	3	12%
Undet	3	2%	3	2%	0	0%
	148	100%	123	100%	25	100%

Table 47: Kara-Bom, OH5, type of profile

	Total		Blade		Bladelet	
	N	*f*	N	*f*	N	*f*
Straight	44	55%	39	57%	5	45%
Slightly Curved	25	31%	20	29%	5	45%
Curved	4	5%	4	6%	0	0%
Twisted	6	8%	5	7%	1	9%
Undet	1	1%	1	1%	0	0%
	80	100%	69	100%	11	100%

Table 48: Kara-Bom, OH5, type of profile based on MNI

However, within the bladelet category the triangular elements are significantly dominant ($\chi^2(1)= 6.5$, $p= <.05$), indicating the frequent use of a single guiding ridge during the production of small laminar blanks.

Profile

All categories show a general preference for straight profiles, directly followed by slightly curved profiles (Table 47). This trend is remains visible when looking at the MNI; however, the straight profiles are a little less numerous and the slightly curved profile frequency shows a minor increase (Table 48). Thus, this shows that fragmentation has only a minor effect on the identification of the profiles.

Orientation

Blanks are mainly axially orientated, as shown by the frequencies observed in all categories (Table 49). A few blanks are orientated to the right or to the left, and they are equally represented. However, a large number of blanks have an undetermined orientation.

When considering a sample reduced to MNI, the frequency of undetermined elements decreases (Table 50). However, the trends observed on the total sample does not change significantly. Blanks remain mainly axial, the rest of the sample being equally shared by right and left oriented ones.

	Total		Blade		Bladelet	
	N	*f*	N	*f*	N	*f*
Right	19	13%	18	15%	1	4%
Left	14	9%	13	11%	1	4%
None	88	59%	65	53%	13	52%
Undet	27	18%	27	22%	10	40%
	148	100%	123	100%	25	100%

Table 49: Kara-Bom, OH5, blank orientation

	Total		Blade		Bladelet	
	N	*f*	N	*f*	N	*f*
Right	17	21%	17	25%	0	0%
Left	12	15%	12	17%	0	0%
None	43	54%	33	48%	10	91%
Undet	8	10%	7	10%	1	9%
	80	100%	69	100%	11	100%

Table 50: Kara-Bom, OH5, blank orientation based on MNI

	n	%
A1		
A2		
A3		
A4	1	10%
A5		
A6	1	10%
A7		
A8		
A9		
A10		
A11		
A12		
B1	3	30%
B2		
B3	1	10%
B4		
B5	2	20%
B6	1	10%
B7	1	10%
	10	100%

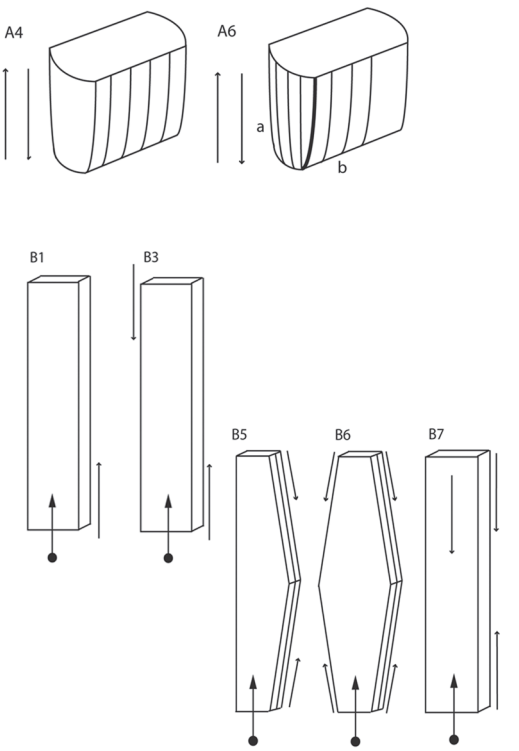

Figure 61: OH5, frequencies of cores per Mode

3.4.2 CORES: REDUCTION PATTERNS AND SIZE ATTRIBUTES

Ten cores have been identified within OH5. Two are on block or flake blanks (Mode A) and the others are on laminar blanks (Mode B) (Figure 61). Mode A cores show the occurrence of bidirectional reduction from a broad face and from two separated flaking surfaces. The Mode B cores illustrate different stages of reduction from single platform and single flaking surface, to cores bearing two platforms and two flaking surfaces.

Size attributes

Measurements and observations on nine cores are presented here, one of the Mode B cores is excluded as it could not be measured (KB-91.L9.3.5.11069). All measurements are recorded according to the system described in Chapter 2 which does not take into account the type of blank on which the core is produced. As a result, measurements are comparable, but in the case of Mode B cores, the thickness corresponds to the length of the blade blank, and the length of the core represents the thickness of the blade. Due to the small sample size of Mode A cores, comparisons with Mode B are not tested statistically. It is, however, possible to make some basic observations (Table 51). Core length appears smaller on Mode B cores as it depends on the thickness of the blade blank. Similar observation can be made

	Mode A			Mode B		
	Mean	σ	N	Mean	σ	N
Core length	37.7	2.1	2	15.5	4.2	7
Core width	43.1	14.5	2	29.2	9.6	7
Core thickness	74.9	9.3	2	73.3	12.9	7
Flaking surface length	63.3	5.2	2	60.6	11.8	7
Flaking surface width	42	17.4	2	12.5	4.7	7
Last removal length	51.3	5.5	2	46.9	10.4	6
Last removal width	17.9	10.4	2	9.3	2	6

Table 51: Kara-Bom, OH5, general size values (mm) per core Mode

regarding the core width with blocks tending to be wider than blades. The thickness values are similar for both Modes, which is confirmed by the flaking surface length. The flaking surface and last removal width are also smaller in Mode B cores, which is due to the fact that flaking surfaces are generally located along a narrow edge of the blade blank. Last removals were measured on five Mode B cores, one of them (KB-92.YO5.18/200.655) providing two measurable removals. The large standard deviation for Mode A last removal width is related to the small sample size, one of the removals being 11 mm wide, and the other being around 30 mm.

Striking platform preparation

Similar frequencies of facetted and plain platforms are observed. The sample size is, however, too small to make comparisons between modes. Profiles of the Mode A last removals are straight (N=2) and in Mode B, they are straight (N=2), twisted (N=1), and undetermined (N=4).

	Total		Mode A		Mode B	
	N	%	N	%	N	%
Plain	4	44%	0	0%	4	57%
Facetted	3	33%	2	100%	1	14%
Reshaped	0	0%	0	0%	0	0%
Undetermined	2	22%	0	0%	2	29%
	9	100%	2	100%	7	100%

Table 52: Kara-Bom, OH5, core striking platform preparation

Core descriptions

Mode A4 (N=1)

∗ KB-92.YO5.Z6.3.802

This core is produced on a block and displays a single flaking surface on the broad side of the core blank (Figure 62). The back is in part shaped by a radial flake removal showing a deep *contre-bulbe*. The rest of the face still shows naturally weathered surfaces and cortex. The flaking surface is shaped by faceting on the external edge; and the rest is still unprepared and naturally flat. The flaking surface illustrates a sequence of five removals (1-4). The first phase is represented by a removal detached from the right side of the flaking surface. The second phase includes two removals (2), one detached from a provisionary opposed platform on the right end of the flaking surface and the other by a removal from the left side of the flaking surface. This phase is followed by a laminar blank struck from the left side of the flaking surface (3) and by a pointed laminar flake detached from the very center of the flaking surface (4). The latter blank was identified within the same assemblage and has been refitted. The last removals are hinged and visible at the left edge of the flaking surface (5-8). They likely represent a failed attempt to remove a thick side blade in order to reshape the flaking surface convexity. This example illustrates the occasional use of a provisionary opposed platform involved in the shaping of a triangular flaking surface. The distal convergence facilitates the production of pointed blanks. However, no bidirectional removals occur on the dorsal face of the blank.

Mode A6 (N=1)

∗ KB-92.YO5.J64.1792

This core is produced on a thick flake blank (Figure 63). A flaking surface is located along the left edge of the flake blank and is reduced from a single striking platform, reshaped by frontal and lateral removals, and prepared by faceting along the external platform edge. The earliest observable removals (1) are located in the central part and on the right edge of flaking surface. This is followed by a series of three remov-

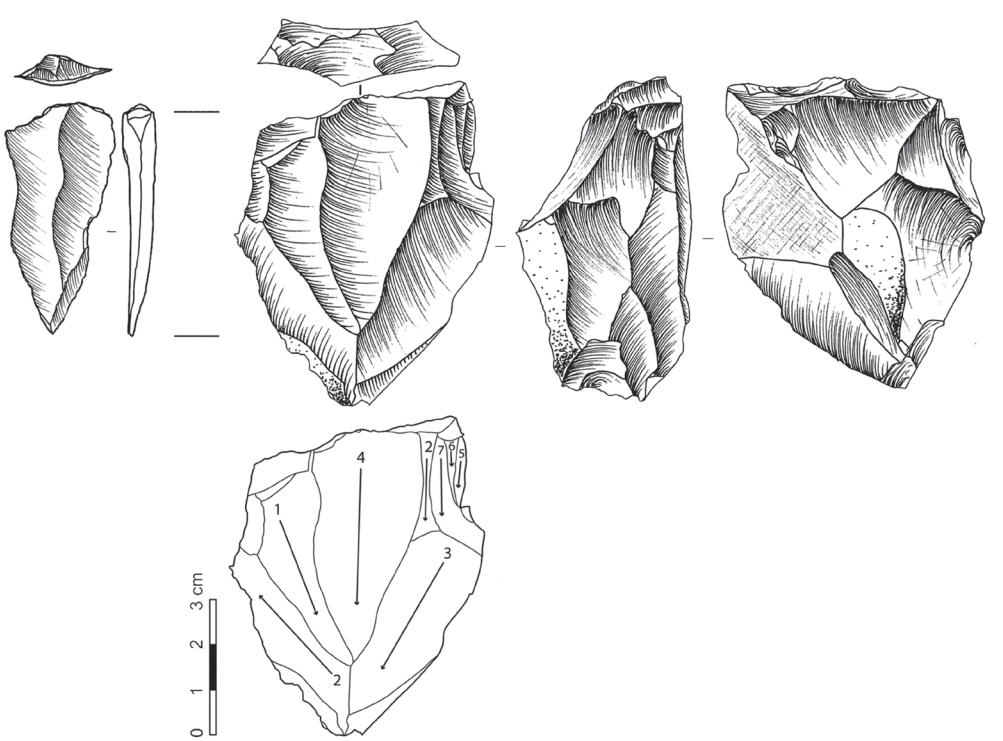

Figure 62: Kara-Bom, OH5, KB-92.YO5.Z6.3.802

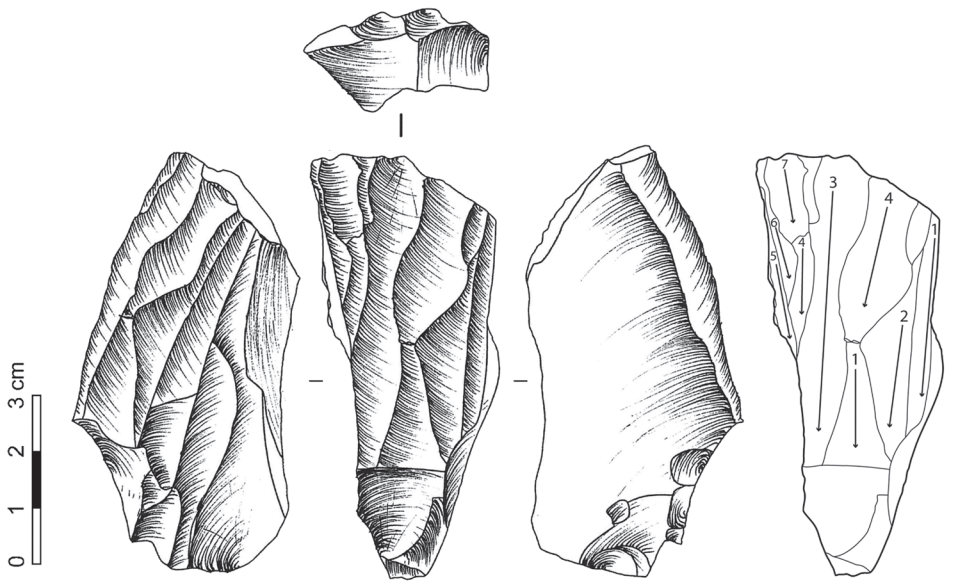

Figure 63: Kara-Bom, OH5, KB-92.YO5.J64.1792

als, respectively on the right (2), on the left (3) and then in the middle (4), following the ridge made by the negative of the previous removal. One additional long removal is detached from the middle part of the flaking surface (3). A second series of three removals (4-6) takes place on the right corner of the flaking surface and the reduction ends by with a hinged fracture (7). A series of removals visible on the left edge were detached from an opposed platform located on the dorsal face of the core blank, and testify to a previous phase of reduction that would have taken place on the broad dorsal face of the core blank. Remains of a crest are observed on the distal part of the flaking surface. This core is remarkable by its volumetric conception and by the triangular shape of the flaking surface. The reduction pattern is slightly convergent. No abrasion is observed on the external edge of the striking platform, the latter being rather irregular due to the presence of relatively deep *contre-bulbe*.

Mode B1 (N=3)

* KB-92.YO5.J8.37.1853

This core shows a single removal detached from the ventral face of a blade blank and struck from the proximal end (Figure 64). The morphology of the negative indicates the production of a narrow and elongated bladelet, pointed at its distal end.

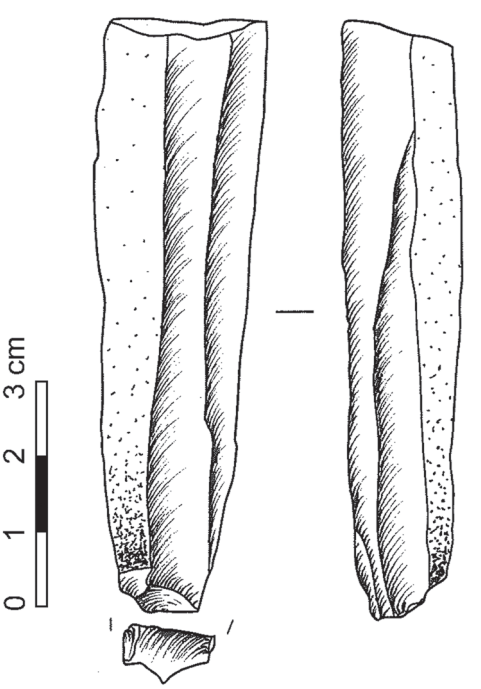

Figure 64: Kara-Bom, OH5, KB-92.YO5.J8.37.1853

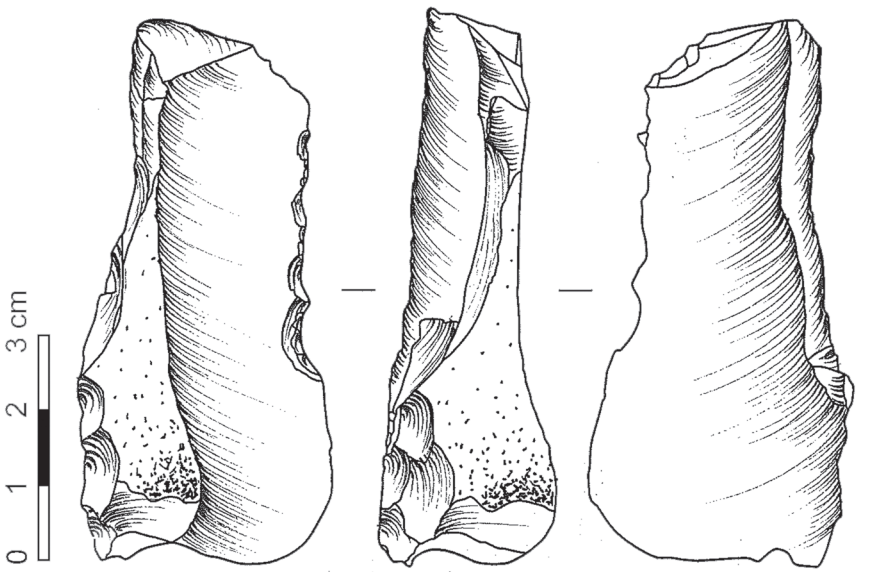

Figure 65: Kara-Bom, OH5, KB-92.YO5.48.28.22

∗ KB-92.YO5.48.28.22

This core is produced on a thick cortical blade and shows a removal negative following two hinged removals along the right edge of the blank (Figure 65). Removals are detached from a plain striking platform located on the proximal part of the blank. The mesiodistal part of the flaking surface displays the remains of an initial crest indicating that the reduction sequence was rather short.

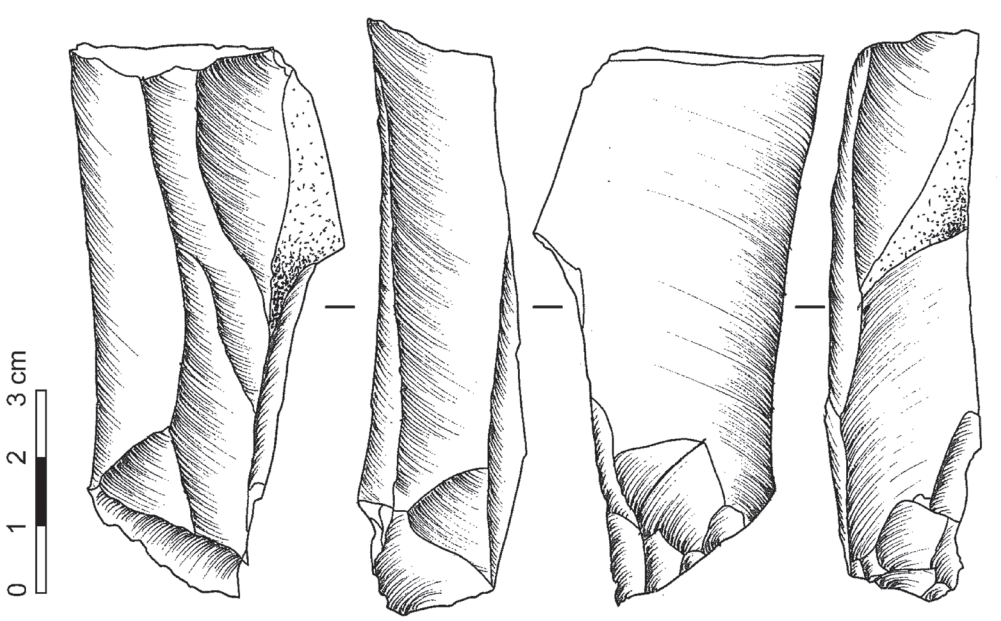

Figure 66: Kara-Bom, OH5, KB-92.YO5.Z8.23.1765

* KB-92.YO5.Z8.23.1765

This artifact illustrates the initial phases of reduction of Mode B cores (Figure 66). A plain striking platform is located on the proximal part of a thick cortical blank. A series of hinged removals are located at the corner between the ventral face and the left edge of the blank.

Mode B3 (N=1)

* KB-92.YO5.18/200.655

This core is produced on a blade blank and shows two opposed facetted striking platforms from which removals are detached following the ridge at the intersection between surfaces (Figure 67). This core was likely discarded due to hinge fractures.

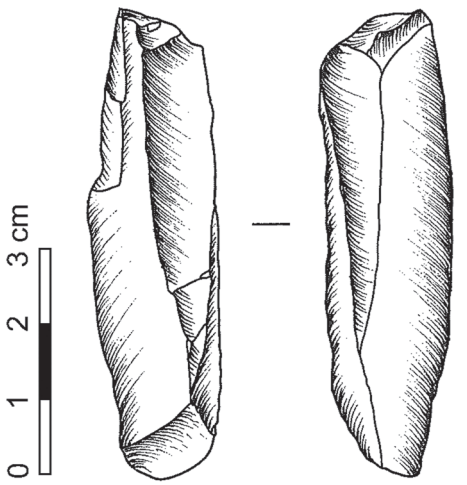

Figure 67: Kara-Bom, OH5, KB-92.YO5.18/200.655

Mode B5 (N=2)

* KB-92.YO5.Z6.12.130

This core is produced on a blade blank that, although showing a significant maximum thickness (19.6 mm), is still relatively thin along the edges (Figure 68). The left edge is used as a flaking surface dis-

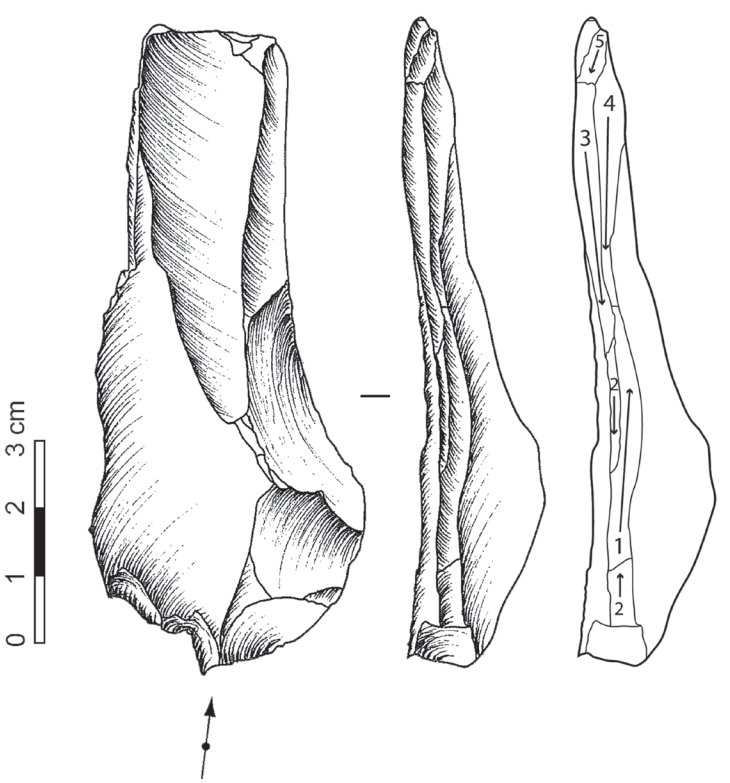

Figure 68: Kara-Bom, OH5, KB-92.YO5.Z6.12.130

playing bladelet removals parallel to the longitudinal axis of the blank and detached from two opposed platforms. The reduction starts from the proximal part of the blank by one removal (1) followed by a hinged fracture (2) and then a switch to the upper platform (2-4), with a series of three removals, ending on another hinged fracture (5).

∗ KB-92.YO5.I6.16.368

This core is on a blade blank showing a single flaking surface along the right edge, reduced from two opposed striking platforms. The flaking surface mainly extends on the dorsal face (1-4) of the blank. The ventral face displays a single bladelet removal (1). It is not possible to determine if the reduction sequence follows an alternate bidirectional path or if it consists of two series of 3-4 removals before the platform switch occurs. The upper platform is shaped by a small flake removal and the lower one by a truncation.

Mode B6 (N=1)

∗ KB-92.Y05.Z7.12.40

This core is produced on a thick laminar blank and reduced from two opposed platforms along both edges (Figure 70). The right edge bear a series of four removals from a proximal platform (1-4), the two last being hinged. The opposed platform shows two small hinged removals that illustrate attempts to resume the reduction sequence. The left edge displays two removals detached from the upper platform followed by severe hinge fractures, some of which are interpreted as removals of crested blanks from the intersection of the two surfaces. Then, a switch to the lower platform occurs with a series of removals detached at the intersection between the narrow edge and the ventral face of the blank. The sequence ends on a deep hinge fracture on the lower platform.

The lower striking platform shows negatives of a partial tablet removal detached laterally, and the upper striking platform shows a lateral impact point that may indicate either a tablet removal or a snapping of the blade blank by percussion.

Mode B7 (N=1)

∗ KB-91.L9.3.5.11069

This core is produced on a laminar blank reduced from two independent flaking surfaces (Figure 71). The narrow face shows an alternate bidirectional reduction with two platform switches for four blanks

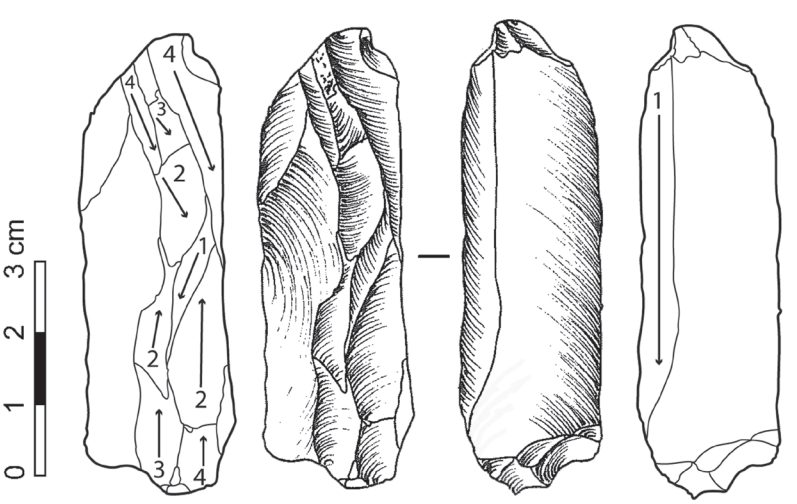

Figure 69: Kara-Bom, OH5, KB-92.YO5.I6.16.368

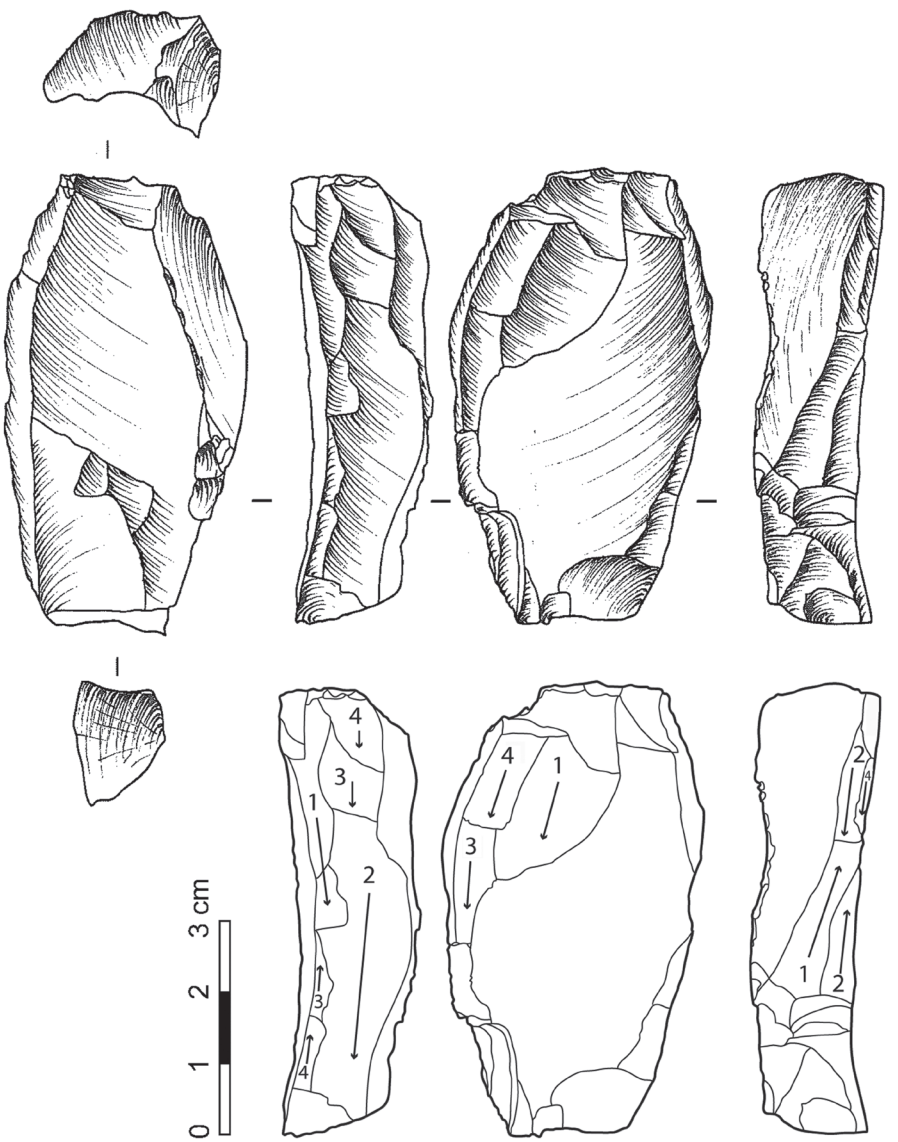

Figure 70: Kara-Bom, OH5, KB-92.Y05.Z7.12.40

detached. The last blank has a rather irregular shape in the distal part. The broad face shows two main negatives detached from the upper platform; however, negatives visible on the distal part of the flaking surface indicate previous phases of reduction from the lower platform. The back, located along the left edge of the blank, is crested and shows removal negatives. The upper platform is prepared by faceting. This pattern of reduction is rather unusual for Mode B cores and could be linked to the advanced stage of reduction.

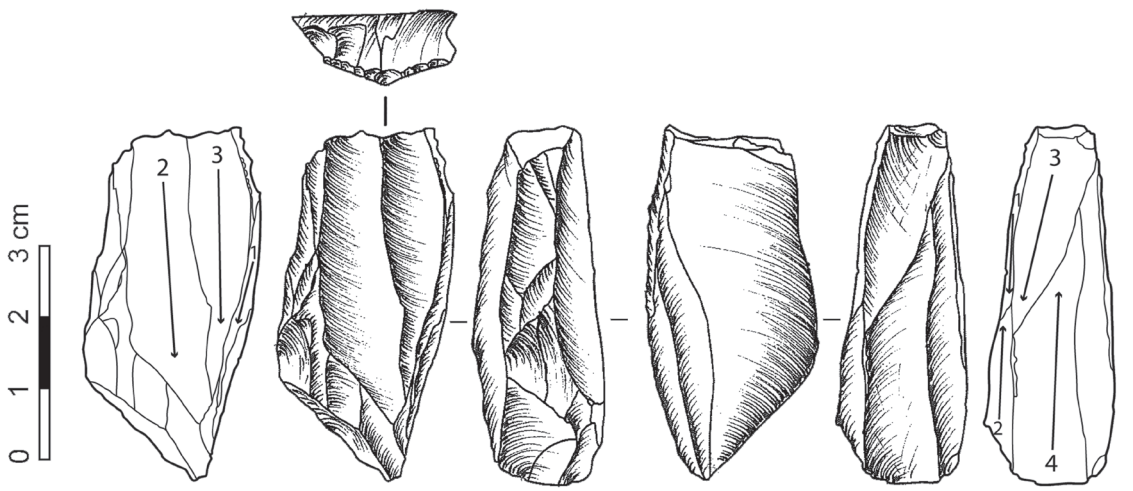

Figure 71: Kara-Bom, OH5, KB-91.L9.3.5.11069

3.4.3 REDUCTION SEQUENCE RECONSTRUCTION

Following the results of the blank attribute analysis and the core descriptions, an analytical reconstruction of the individual reduction sequences is proposed.

Laminar blanks with parallel edges

From a morphological point of view two main types of blades are recognized. The first category corresponds to artifacts displaying parallel edges starting from the mesial part. This represents the majority of the assemblage and shows a coexistence of uni- and bidirectional reduction processes. The largest complete examples show that the maximum length of such blades sometimes reaches 180 mm. A single laminar element presenting up to 80% cortex on its dorsal face, a single two-sided crested blade and a secondary crest on a bladelet illustrate different initial phases of the reduction process. In addition, just a few blanks have cortex preserved on their dorsal face (N=8), indicating that the first cortical blanks detached do not occur in the sample or that blocks were at least partially shaped off-site. Neo-crested elements ranging from 60 to 90 mm in length show that management operation are pursued on relatively small cores. Naturally backed elements, correspond to a more opportunistic exploitation of available edges at the intersection between core surfaces. Some show remains of the ventral face of the core blank (N=10). Only one spall shows a double back, indicating that it was detached from a narrow side (24 mm width flaking surface) of a core on a flake/blade blank. In other cases, the back is cortical (N=3) and is more likely to be detached from a block. In the sample, only one core can be associated with a production of large/medium size blades. It is a Mode A6 core which displays two independent flaking surfaces reduced successively from two opposed striking platforms. However, the last flaking surface is rather convergent and shows two series of unidirectional removals following a three-step path (one from the left, one from the right and then one from the middle). It is then possible that this core, in the last stages of reduction, was more orientated to a production of blanks with convergent edges. The frequencies of bidirectional and uni-directional blanks likely reflect a reduction by short sequences of 2-3 removals between platform switches following one or several ridges.

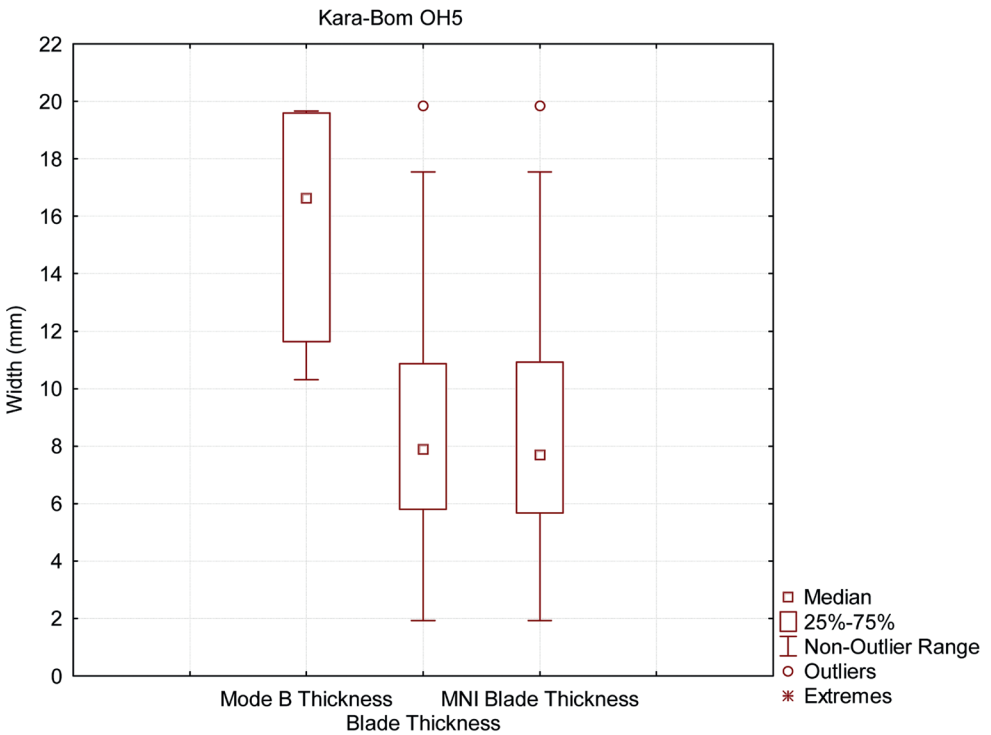

Figure 72: Kara-Bom, OH5, thickness of Mode B blanks compared with the blade thickness (total sample and MNI)

Mode B cores are produced on the thickest of the large/medium size blade blanks. As shown in Figure 72, the blanks are clearly selected among the outliers of the blade population, with a minimum thickness of 10 mm. Mode B1 cores represent the first stages of reduction as generally they bear not more than two removals detached from the thickest edge of the blade blank, following its longitudinal axis, from a striking platform located at its proximal end and using the angle between two surfaces as a ridge. A switch to an opposed striking platform leads to the re-exploitation of the previous flaking surface or to the exploitation of a new one along the other edge of the core blank. This latter fact, together with the length of some of the negatives (Figure 72), indicates that reduction proceeded by short sequences of 2-3 removals before a platform switch occurs. The edge of the core blank is, therefore, used as a single flaking surface, tending to be reduced on its whole length. Only one core illustrates clearly a genuine alternate bidirectional patterning at its last stage of reduction (KB-91.L9.3.5.11069). In this case, even though two opposed removals divide the flaking surface, they tend to extend across the whole length.

The reduction is mainly frontal but several cores display removals either extending on to the dorsal or the ventral face of the core blank. In some cases, it is hard to determine if these removals represent an attempt to detach blanks or if they are linked with core management operations. Such management could reshape the lateral convexity of the flaking surface or could create a ridge enhancing the angle made by the intersection of the two surfaces. Only one core displays evidence for a reduction on a wide and a narrow face of the core, however, the two surfaces are treated independently rather than following a semi-turning reduction pattern. More generally, cores displaying removals extending on to the wide face seem to represent a rather advanced stage of reduction. So, it is assumed that blank production mainly takes place along the edge of the core blank and at its corners. When comparing widths between Mode A and Mode B flaking surfaces and the MNI laminar popu-

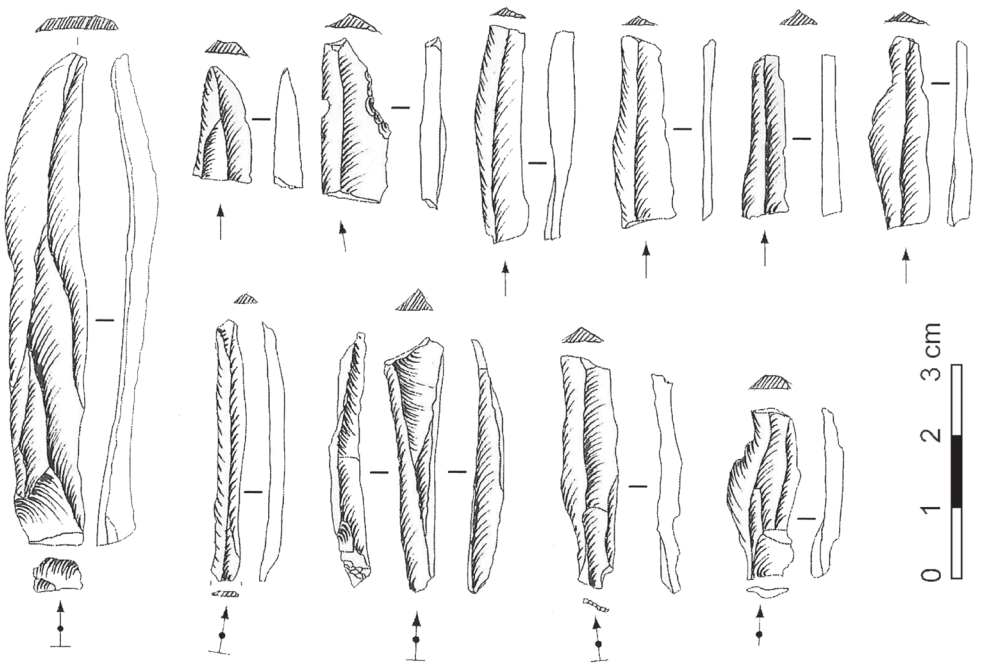

Figure 73: Kara-Bom, OH5, small blade/ bladelet blanks

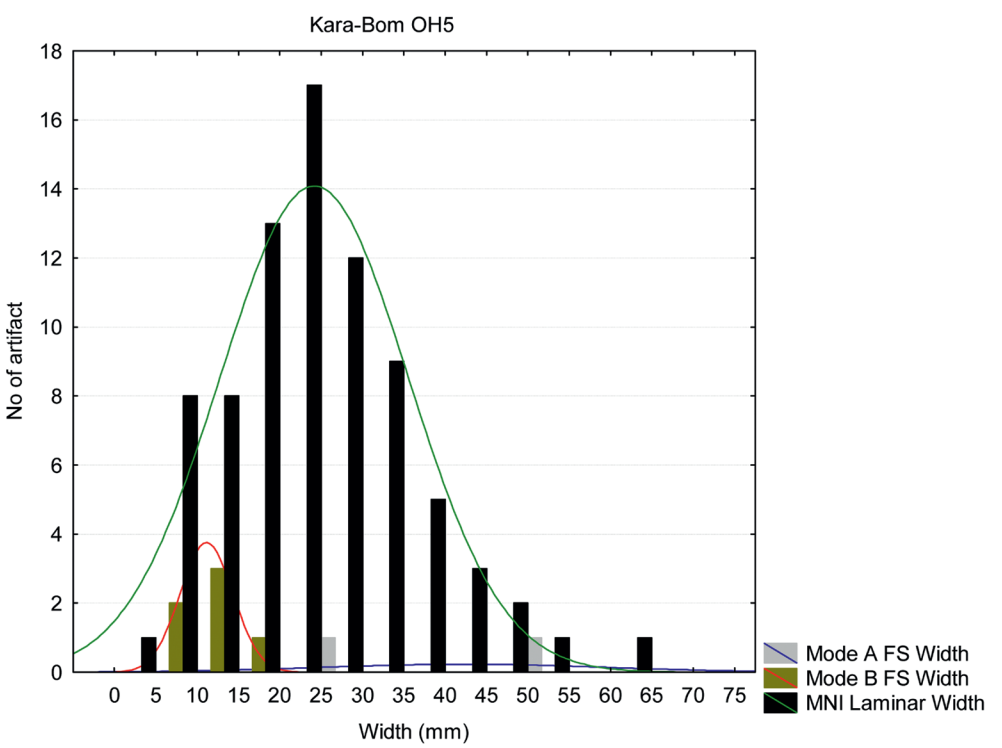

Figure 74: Kara-Bom, OH5, Mode A and Mode B flaking surface width and MNI width

lation width, a distinction between the two modes is visible. Mode A cores, in spite of the sample size, appear more variable and generally larger than the flaking surface from the Mode B cores (Figure 74).

MNI width distribution is not as clearly bimodal as the whole laminar sample, although it still displays a discrete peak between 5 and 15 mm width, which overlaps with the main mode peaking around 25 mm in width. Mode B core flaking surfaces and last removals widths match with the narrowest part of the laminar population. Morphologically, two main types of blank are detached from Mode B cores. Some blanks are naturally backed with thick triangular sections and are struck from a corner of the flaking surface. The second type is detached from the central part of the flaking surface and usually shows a rather flat and thin triangular or trapezoidal section. Both types of blank do not match with arbitrarily defined categories such as blade and bladelet and are not part of a comtinuum of reduction starting with the large blades.

Convergent blanks

Among the laminar elements, a few are characterized by their convergent edges (N=5). Three are complete and two are mesial and mesiodistal fragments. The complete elements have a length between 29 and 60 mm. Four of the five blanks have a width ranging from 21 to 32 mm, the last one having a width circa 13.5 mm. Their thicknesses vary from 4.7 to 6.9 mm, and their section is mostly trapezoidal with two being triangular. Among the observable platforms, two are facetted and one is plain. They all have a straight profile and, except one, they display a bidirectional scar patterning. The only bidirectional blank refits with the Mode A4 core KB-92.YO5.Z6.3.802 (Figure 62). It was struck from a broad side of a bidirectional core. Although a previous removal was struck from the distal part of the flaking surface, it is not visible on the dorsal face of the blank. It has a facetted platform although the impact point is located on a rather prominent and plain facet. This is the only technological refit that provides direct information about the production of the convergent blanks which are likely associated with Mode A cores, as they may display a broad flaking surface. The production of such a blank requires a series of 2-4 removals, some of which give the distal part of the flaking surface a triangular shape. Although in this case the cross-section of the blank is triangular, the previous removals likely create a convergent guiding ridge at the distal end of the flaking surface. Like in Levallois technology, this preparation leads to the production of a naturally pointed blank with convergent edges. However, the core described here differs from the classic Levallois examples as it shows a series of hinged fractures indicating an attempt to produce removals from a narrow edge of the core. This gives to the core a sub-prismatic morphology. Unfortunately, long refitted sequences are lacking and this single example can hardly be generalized to all convergent blanks from the sample.

Platform preparation and percussion technique

Regarding the technique of percussion, several observations can be discussed. First, thin abrasion of the external platform edge is totally absent, although some blanks (N=5) bear traces of a strong abrasion smoothing the EPA until the latter show a rounded edge. Such a preparation occurs on medium/large laminar elements, uni- and bidirectional, with plain and facetted platforms. It is associated with one naturally backed blank. The mean of blade platform thickness is above the 4 mm limit defined by Pelegrin (1995) as a thick platform *(talon épais)*. Third, facetted platforms are at least as frequent as the plain platforms, no matter the size of the blank. Among the facetted platforms, some bear only a partial faceting affecting mainly the EPA and the point of percussion is located on a slightly prominent plain surface. Moreover, flaking on the bulb (circa 17% of the blade MNI) and lip (circa 18% of the blade MNI) occur sporadically on the blanks. Considering all these observations together, it appears that typical features associated with the use of an organic hammer are almost absent. Discrete features associated with the use of a soft-stone hammer occur sporadically and typical features associated with hard hammer occur significantly. Therefore, a general use of hard-hammer likely associated with some soft-stone hammer is proposed as a hypothesis to categorize the technique of percussion used in OH5.

Retouched tools

The main categories of retouched tools include here only tools on laminar elements. For OH5, one of the retouched points was produced from a laminar flake and is included in the list (Table 53). It is then no surprise to see the retouched blades as dominant in the sample. Also, the approach adopted here is conservative and tries to leave out ambiguous tool types such as notches, or denticulates, as they may be the result of mechanical edge damage.

Tool breakage differs from what can be observed on the unretouched blanks. The mesioproximal fragments dominate the set, but for the rest, no clear pattern can be observed (Table 54).

There is no clear pattern of blank size selection regarding the width (Figure 75) or thickness, and the sample is too small to observe such a pattern on the length values.

	N	*f* (among tools)	*f* (from total, n=174)
Retouched blade	18	69%	10%
Retouched bladelet	1	4%	1%
Retouched point	5	19%	3%
Endscraper	2	8%	1%
Other	0	0%	0%
	26	100%	15%

Table 53: Kara-Bom, OH5, frequency of major retouched tool types

Among the retouched blades, the most typical type is the so-called 'sickle-like blade' (N=2). These tools are produced on bidirectional blanks and show a continuous retouch along a convex edge, opposed to a slightly retouched or natural straight/convex edge.

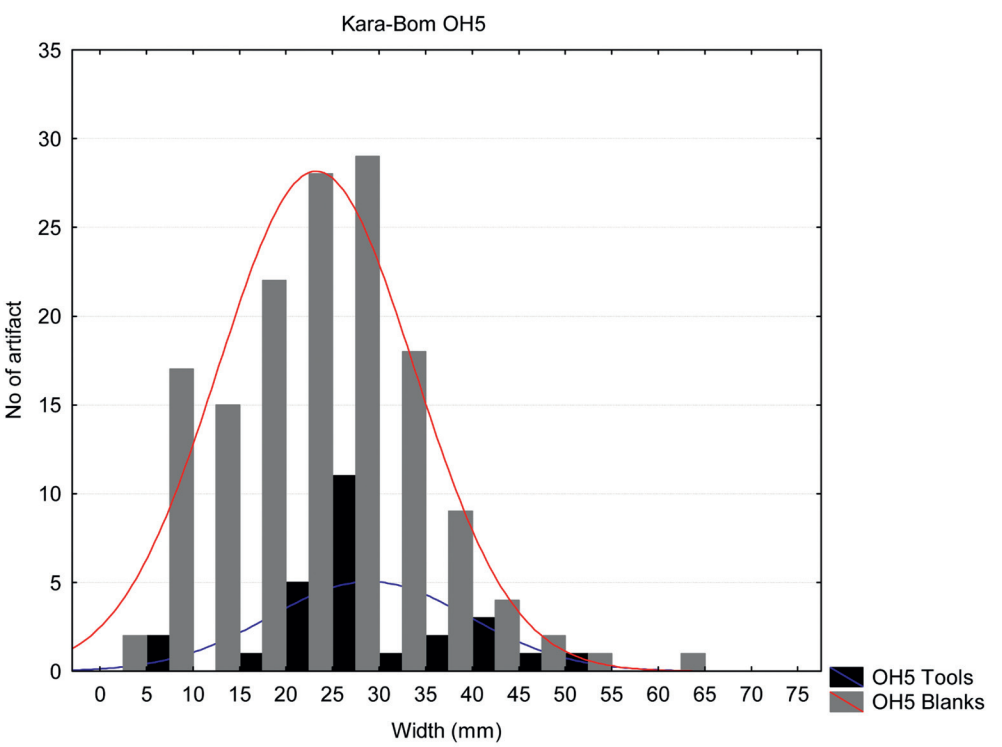

Figure 75: Kara-Bom, OH5, width histogram comparing retouched tools and blanks

	N	*f*
Distal	2	8%
Mesiodistal	5	19%
Mesial	4	15%
Mesioproximal	10	38%
Proximal	1	4%
Complete	4	15%
	26	100%

Table 54: Kara Bom, OH5, retouched tools breakage

The general arched morphology appears roughly similar to the sickle blade from the Neolithic from the Near-East (*e.g.* Rosen, 1982, 1997), although in this case, they do not bear any traces of the typical polish reflecting their intensive use on vegetal material.

These were first named sickle-like blade by Derevianko and colleagues (1993) when they reported the artifact illustrate here in Figure 76, num.4, but the refit of two artifact fragments (Figure 76: 5), previously considered as a point and a tool on blade (Derevianko *et al.*, 1998, Fig. 43, num. 3 and 9), illustrate a second complete sickle blade of circa 180 mm long, 25 mm width and 12 mm thick. One additional mesioproximal fragment (KB-92.Y05.E8.7) likely belongs to the same category. It is produced on a side blade showing a 20 mm thick natural back along a slightly convex right edge showing irregular scaled retouch opposed to a convex edge bearing continuous steep/semi-steep retouch (see Derevianko *et al.*, 1998, Fig. 42 num. 6). This type of artifact occurs only within the OH5 sample and, therefore, can be considered as typical for this assemblage. One genuine notched blade also occurs among the retouched blades. Among the set of tools, convergent laminar elements are also present, including two Mousterian points on bidirectional blanks, one of which shows a notch on the left side of the proximal part, struck

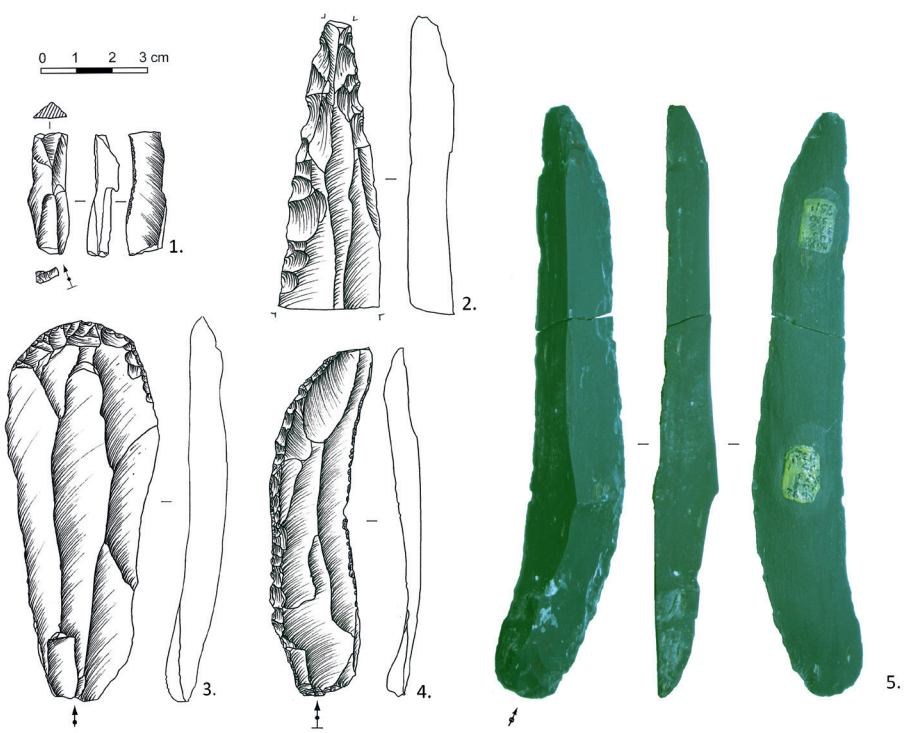

Figure 76: Kara-Bom, OH5, retouched tools

from the ventral side, and a direct continuous thin retouch along the right edge (see Derevianko *et al.*, 1998, Fig. 43, num. 6). Another point is represented by the mesioproximal end of a bidirectional laminar blank modified by a semi-invasive scaled retouch (Figure 76: 2). Two endscrapers are also listed, one being on a mesioproximal cortical and bidirectional blade fragment, with a combination of thin and semi-steep retouch on the proximal end. The second one is complete and produced on an unidirectional blade with a semicircular front located on the distal end with scaled and thin retouch (Figure 76: 3). Burins are absent, those previously illustrated are either considered as cores, or have the removal of the burin spall is anterior to the removal of the blank.

	N	*f*
Plain	5	19%
Facetted	5	19%
Dihedral Flat	1	4%
Undetermined	15	58%
	26	100%

Table 55: Kara Bom, OH5, retouched tools, platform preparation

Plain and facetted platform frequencies are equal but the number of undetermined platforms is relatively high due to missing or retouched platforms (Table 55). In fact, the tool MNI (N=15) includes identifiable (N=11), retouched (N=1) and undetermined platforms (N=3). A single artifact shows a smoothed EPA. Dorsal scar patterns are mostly bidirectional (85 %). A low frequency of unidirectional (8%) is observed. Although a large number of undetermined orientations may blur the trends, axial tools dominate the set but not significantly (Table 56).

Retouch is mainly direct with only two blades showing inverse retouch (Table 57). One is a small size bidirectional blank bearing thin semi-continuous retouch along the right edge. The blank is rather atypical as it shows a deep hinge fracture on the dorsal face. The other tool with inverse retouch is a larger

	N	*f*
Right	6	21%
Left	3	10%
None	8	28%
Undetermined	9	31%
	26	100%

Table 56: Kara Bom, OH5, retouched tools, orientation

blade displaying scaled retouch. Types of direct retouch vary from steep to thin but a frequent use of the scaled retouch is noticeable. This type of retouch also occurs combined with thin retouch (*e.g.* Figure 76: 3-5). One notched blade and two denticulate pieces (including one on a Mousterian point) are part of the toolkit. One borer is shaped on the distal end of a bidirectional blank by steep retouch (Derevianko *et al.*, 1998, Fig.43, num. 5).

	N	*f*
Direct	24	92%
Inverse	2	8%
Alternate	0	0%
	26	100%

Table 57: Kara Bom, OH5, retouche location (face)

There is no apparent pattern of retouch distribution along edges. However, continuous retouch is well represented compared to the other categories (Table 58).

Among the smaller blanks, some of them have been left out of the tool category as the intensity and regularity of their retouch is questionable. However, some of them are intriguing by the location of their 'pseudo-retouch'. The three examples presented in Figure 77 are pointed blanks showing notches made by single blows located on their proximal and mesial ends. In the context of an assemblage with pointed

	Dorsal		Ventral	
	N	*f*	N	*f*
Distal	4	17%	0	0%
Mesial	6	25%	1	0%
Proximal	4	17%	0	50%
Combination	1	4%	0	0%
Continuous	9	38%	1	50%
Undermined	0	0%	0	0%
	24	100%	2	100%

Table 58: Kara Bom, OH5, retouch location (edge)

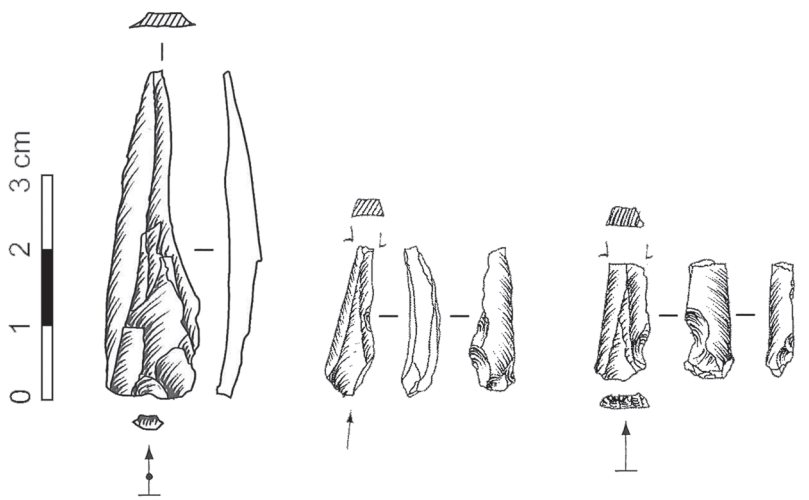

Figure 77: Kara-Bom, OH5, small laminar elements with possible proximal retouch

elements and frequent proximal modifications, perhaps these artifacts are worth mentioning; however, their tool status remains uncertain. Similar artifacts may occur in OH6 (see Figure 52, second row, second from the left).

3.5 LAMINAR TECHNOLOGY: OH4

3.5.1 BLANK ATTRIBUTES

The OH4 sample is significantly smaller than OH5 and OH6. The quantitative aspects of the analysis should, therefore, be interpreted accordingly. Some of the statistical tests used on other samples are absent in this section, as the sample size does not fit with their requirements.

	Total		Blade		Bladelet	
	N	*f*	N	*f*	N	*f*
Distal	2	5%	1	3%	1	20%
Mesiodistal	2	5%	1	3%	1	20%
Mesial	12	31%	11	32%	1	20%
Mesioproximal	9	23%	9	26%	0	0%
Proximal	0	0%	0	0%	0	0%
Complete	14	36%	12	35%	2	40%
	39	100%	34	100%	5	100%

Table 59: Kara-Bom, OH4, breakage

Breakage

Laminar blanks are mainly mesial and mesioproximal fragments (Table 59). Based on these observations, an MNI of 19 blades and 4 bladelets is calculated on a total of 39 laminar blanks recorded.

Platform: size and preparation

Considered as a whole, laminar blank platforms show similar frequencies although plain platforms occur more often than facetted ones (Table 60). This observation is balanced by the small sample size. A few dihedral platforms occur among the blades, and the bladelets are exclusively plain. The mean platform thickness is 5.2 ± 4.1 mm and the mean platform width is 11.8 ± 8.3 mm. For the blade category, the mean platform thickness is 6.2 ± 4.1 mm and the mean width is 13.9 ± 8.3 mm. Bladelet mean platform thickness is 2.2 ± 0.7 mm and the mean width is 4.6 ± 2.1 mm. Measurements are listed per morphological types.

The thickness of facetted platforms is described for the blades only as no bladelets show such a platform (Table 61).

Plain platforms are significantly less thick than the facetted platforms (Mann-Whitney, T=Ub=9, p=<.05), although due to the small sample size, this observation is hard to interpret (Table 62). No traces of abrasion could be observed on the blanks external

	Total		Blade		Bladelet	
	N	*f*	N	*f*	N	*f*
Plain	9	39%	5	26%	4	100%
Facetted	6	26%	6	32%	0	0%
Dihedral Flat	2	9%	2	11%	0	0%
Undetermined	6	26%	6	32%	0	0%
	23	100%	19	100%	4	100%

Table 60: Kara-Bom, OH4, platform preparation

Facetted platform	Total (=blade)	
	Thickness	Width
Sample size	6	
Mean (mm)	7.9	16.2
Standard deviation (mm)	5.3	8.2
Range (mm)	2.9 to 15.7	7.3 to 30.1

Table 61: Kara-Bom, OH4, facetted platform size

Plain platform	Total		Blade		Bladelet	
	Thickness	Width	Thickness	Width	Thickness	Width
Sample size	9	5	4			
Mean (mm)	3.2	8.2	4.6	11.1	1.6	4.6
Standard deviation (mm)	2.7	7.8	3.2	9.7	0.7	2.1
Range (mm)	0.8 to 8.7	1.7 to 26.1	0.8 to 8.7	26.1 to 55.7	0.8 to 2.2	1.7 to 6.7

Table 62: Kara-Bom, OH4, plain platform size

platform edge, with the only exception of a single blade showing a strong abrasion smoothing the EPA.

Blank size attributes

Length

Due to the sample size, the data set is rather poor but still provides a general idea of the variability in OH4 blanks ranging from 20 to 153 mm long and averaging 75 mm (Table 63, Figure 78).

Width

When comparing mean width and standard deviations from the total sample and from the MNI, it appears that MNI values are either equal or higher than the total sample (Table 64). However, differences are not statistically significant. In other words,

	Total	Blade	Bladelet
Sample size	14	10	4
Mean (mm)	74.6	89.1	38.1
Standard deviation (mm)	41.2	39.5	13.3
Range (mm)	20.1 to 152.5	49.8 to 152. 5	20.1 to 52

Table 63:Kara-Bom, OH4, blank length

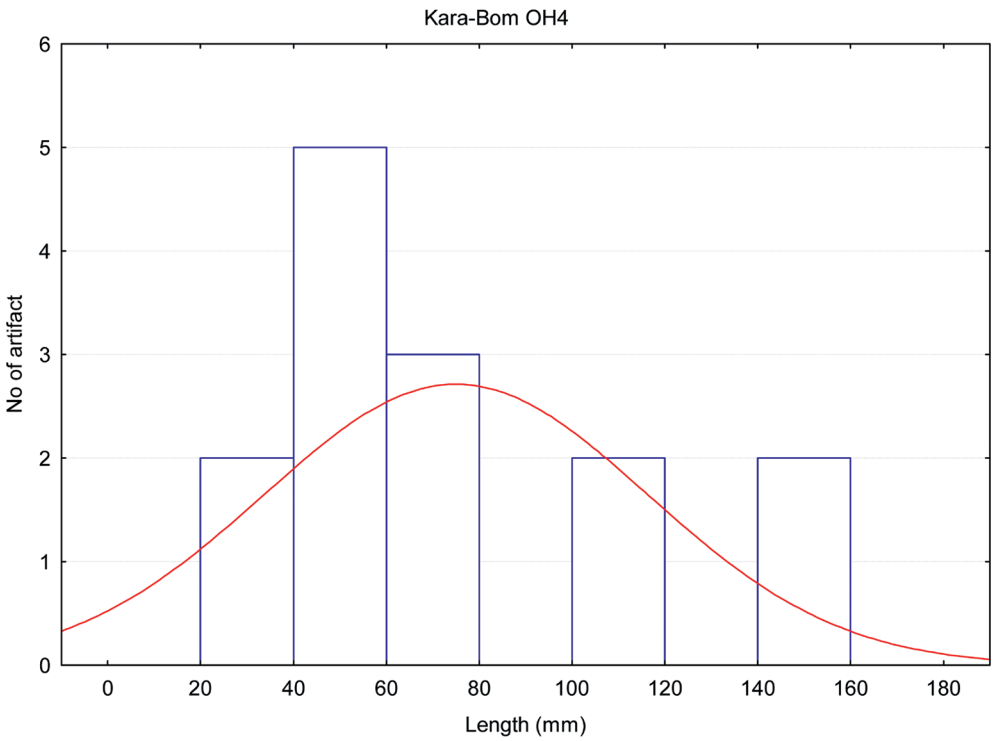

Figure 78: Kara-Bom, OH4, blank length distribution

	Population			MNI		
	Total	Blade	Bladelet	Total	Blade	Bladelet
Sample size	39	32	7	23	19	4
Mean (mm)	23.6	26.9	8.9	24.8	28.1	9.4
Standard deviation (mm)	12.1	11	1	12.4	11.1	1
Range (mm)	7.7 to 51.2	12.6 to 51.2	7.7 to 10.6	8.6 to 49	12.6 to 49	8.6 to 10.6

Table 64: Kara-Bom, OH4, blank width

measurements of the maximum blank width are not significantly affected by breakage. The distribution is bimodal with a cut-off point around 20 mm (Figure 79). The first mode is between 5-15 mm, and the second is close to the mean.

Thickness

Compared with the total population, MNI thickness shows equal or slightly higher mean values. Differences are, however, not statistically significant (Table 65). This shows that breakage does not influence significantly the main trends observed in thickness in the sample considered (Figure 80).

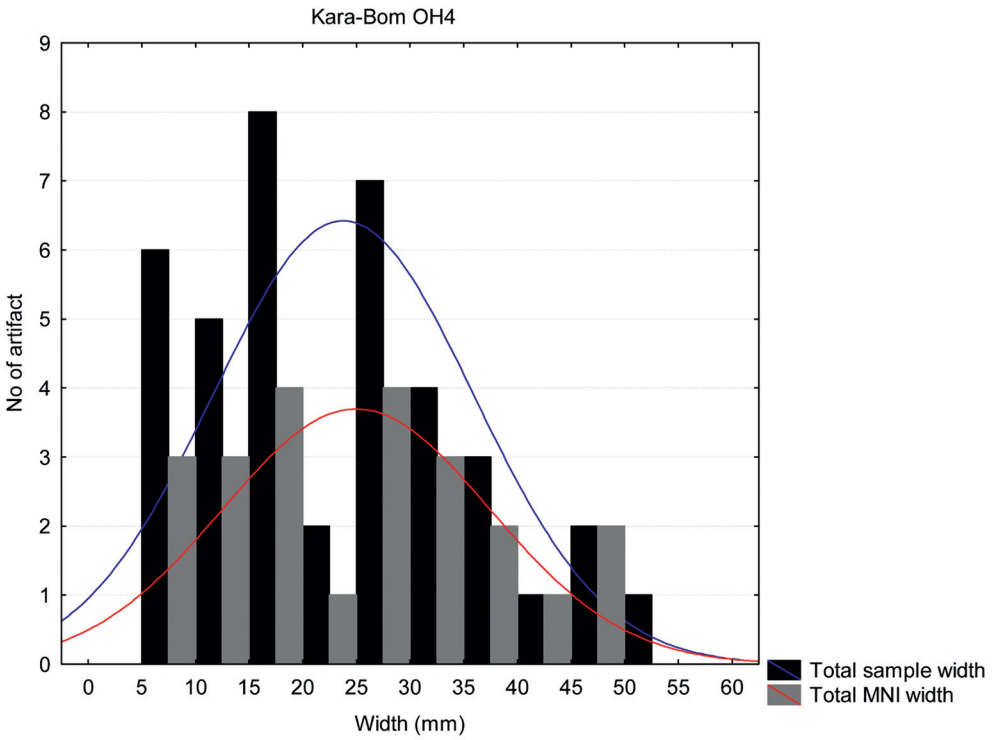

Figure 79: Kara-Bom, OH4, blank width distribution

	Population			MNI		
	Total	Blade	Bladelet	Total	Blade	Bladelet
Sample size	39	32	7	23	19	4
Mean (mm)	9.8	11.2	3.7	10.8	12.3	3.5
Standard deviation (mm)	6	5.8	1.6	6.7	6.3	1.5
Range (mm)	1.6 to 24.9	5.2 to 24.9	1.6 to 5.8	2.3 to 24.9	6.5 to 24.9	2.3 to 5.54

Table 65: Kara-Bom, OH4, blank thickness

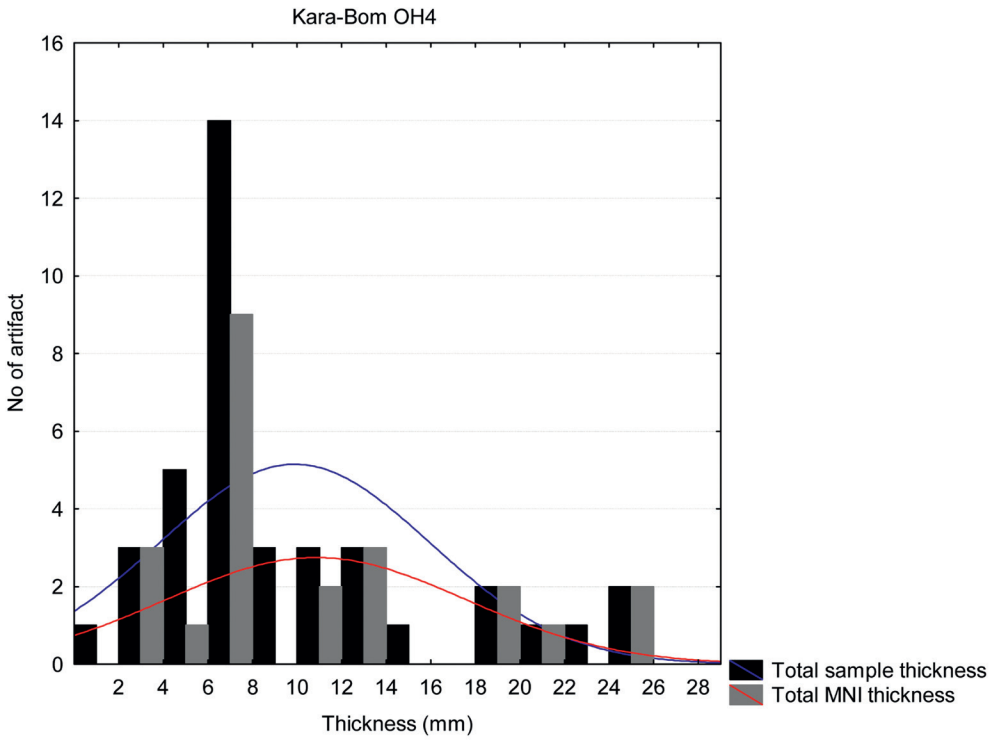

Figure 80: Kara-Bom, OH4, blank thickness distribution

	Total		Blade		Bladelet	
	N	*f*	N	*f*	N	*f*
Unidirectional	7	18%	6	19%	1	14%
Unidirectional and cortex	0	0%	0	0%	0	0%
Bidirectional	25	64%	19	59%	6	86%
Bidirectional and cortex	4	10%	4	13%	0	0%
Crest	0	0%	0	0%	0	0%
Second Crest	2	5%	2	6%	0	0%
Neo-crest	1	3%	1	3%	0	0%
Undet	0	0%	0	0%	0	0%
	39	100%	32	100%	7	100%

Table 66: Kara-Bom, OH4, dorsal scar pattern

	Complete blank		Complete blade		Complete bladelet	
	N	*f*	N	*f*	N	*f*
Unidirectional	3	21%	2	20%	1	25%
Bidirectional	10	71%	7	70%	3	75%
Crested	1	7%	1	10%	0	0%
	14	100%	10	100%	4	100%

Table 67: Kara-Bom, OH4, dorsal scar patter frequencies for the complete blanks

Dorsal scar pattern

The OH4 sample shows a clear dominance of bidirectional scar patterns, a few of them bearing cortex (Table 66). A unidirectional pattern is uncommon, and a few crested elements indicate core management operations. Considering only the complete artifacts, bidirectional scar pattern still dominate in both blade and bladelet categories (Table 67).

Profile

Most of the profiles are straight or only sometimes slightly curved (Table 70). However, the difference is sharply reduced when considering the MNI sample even if the trends remain the same (Table 71). Straight are the most common (N=11), followed by the slightly curved ones (N=8). Two of the bladelets are slightly curved. One is straight and one is twisted.

Cross-section

The majority of the cross-sections are trapezoidal or triangular (Table 68). This trend is mainly expressed in the blade category and appears similar when considering the MNI (Table 69).

Orientation

Artifacts are mainly axial, a few being equally orientated either on the right or on the left (Table 72). This trend is observed in all categories and in both total sample and MNI (Table 73).

	Total		Blade		Bladelet	
	N	*f*	N	*f*	N	*f*
Flat	0	0%	0	0%	0	0%
Rectangular	0	0%	0	0%	0	0%
Triangular	16	41%	11	34%	5	71%
Trapezoidal	23	59%	21	66%	2	29%
Polyhedric	0	0%	0	0%	0	0%
	39	100%	32	100%	7	100%

Table 68: Kara-Bom, OH4, type of cross-section

	Total		Blade		Bladelet	
	N	*f*	N	*f*	N	*f*
Flat	0	0%	0	0%	0	0%
Rectangular	0	0%	0	0%	0	0%
Triangular	9	39%	7	37%	2	50%
Trapezoidal	14	61%	12	63%	2	50%
Polyhedral	0	0%	0	0%	0	0%
	23	100%	19	100%	4	100%

Table 69: Kara-Bom, OH4, type of cross-section based on the MNI

	Total		Blade		Bladelet	
	N	%	N	%	N	%
Straight	26	67%	22	69%	4	57%
Slightly Curved	8	21%	6	19%	2	29%
Curved	4	10%	4	13%	0	0%
Twisted	1	3%	0	0%	1	14%
Undetermined	0	0%	0	0%	0	0%
	39	100%	32	100%	7	100%

Table 70: Kara-Bom, OH4, type of profile

	Total		Blade		Bladelet	
	N	*f*	N	*f*	N	*f*
Straight	11	34%	10	53%	1	25%
Slightly Curved	8	25%	6	32%	2	50%
Curved	3	9%	3	16%	0	0%
Twisted	1	3%	0	0%	1	25%
Undetermined	0	0%	0	0%	0	0%
	23	100%	19	100%	4	100%

Table 71: Kara-Bom, OH4, type of profile based on the MNI

	Total		Blade		Bladelet	
	N	*f*	N	*f*	N	*f*
Right	7	18%	6	19%	1	14%
Left	5	13%	3	9%	2	29%
None	24	62%	21	66%	3	43%
Undetermined	3	8%	2	6%	1	14%
	39	100%	32	100%	7	100%

Table 72: Kara-Bom, OH4, blank orientation

	Total		Blade		Bladelet	
	N	*f*	N	*f*	N	*f*
Right	6	26%	5	26%	1	25%
Left	4	17%	3	16%	1	25%
None	13	57%	11	58%	2	50%
Undetermined	0	0%	0	0%	0	0%
	23	100%	19	100%	4	100%

Table 73: Kara-Bom, OH4, blank orientation based on the MNI

3.5.2 CORES: REDUCTION PATTERNS AND SIZE ATTRIBUTES

Only one core is associated with OH4 sample.

3.5.3 CORE DESCRIPTION

Mode A2 (N=1)

* KB-91.M8.26.10906

The core blank is a Kombewa *débordant* flake which displays a single flaking surface along its left edge, from which blanks are detached from two opposed striking platforms (Figure 81). The two earliest removals (1 and 2) illustrate a platform switch followed by a series of removals for which the chronology could not be determined. Striking platforms are reshaped by frontal or lateral partial tablets. The general morphology of the core blank and the removals visible on the débordant section may indicate that it was originally a core tablet. Although some of the removals extend on the ventral face, the main pattern of reduction is frontal and, therefore, this core is categorized as Mode A2. The core blank by its morphology is comparable to a blade core tablet.

3.5.4 REDUCTION SEQUENCE RECONSTRUCTION

The reconstruction proposed here is mainly based on the laminar blanks, as only one core can be associated with the OH4 assemblage.

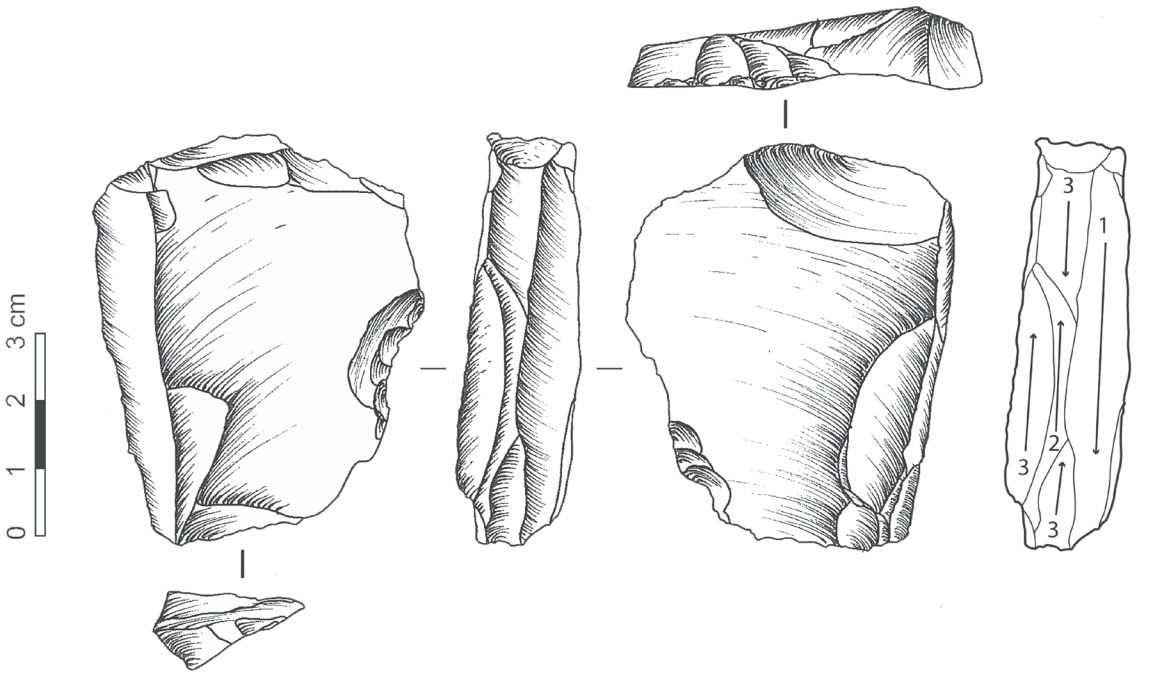

Figure 81: Kara-Bom, OH4, KB-91.M8.26.10906

Laminar blanks with parallel edges

The majority of the sample is composed of laminar elements displaying parallel edges, mainly produced by bidirectional reduction sequences. Some of these sequences may have been initiated on the site, as shown by the presence of a cortical secondary crest. Blanks are struck from two opposed platforms from the earliest stages of reduction, as indicated by blanks displaying a combination of bidirectional scar patterns and cortex. Judging by the significant frequency of bidirectional dorsal scar patterns, platform switches may have been relatively frequent, indicating short unidirectional sequences and maybe occasional alternate bidirectionality. The occurrence of crested elements indicates occasional core management taking place at the corner of the flaking surface. Removals are mostly detached following multiple ridges, especially in the blade category. Some of the small blades and bladelets (N=4) present a natural back, which may indicate that they were detached from a relatively narrow flaking surface, or from the corner of a wider one. One is clearly similar to a classic burin spall with a thick triangular section and a ventral face opposed to a two-sided dorsal face that partially preserves the ventral side of the core-blank. The majority of the blanks have a straight profile and an axial orientation.

Convergent blanks

A single artifact is categorized as a convergent blank (KB-92.Y04.I8.25) (Derevianko *et al.*, 1998, Fig. 46, num. 5). The blank is 68 mm long, 34 mm wide and 14 mm thick and bears unidirectional dorsal scar patterns. The platform is plain, 9 mm thick, and 26 mm wide.

Platforms are plain and facetted, the mean thickness of facetted platforms is above 4 mm and can be qualified as thick *(talon épais)* (Pelegrin, 1995). The mean thickness of plain platforms is lower than 4 mm. No abrasion of the external platform edge is observed except in one case where the blade shows a strong abrasion. Based on such as small sample size, it is difficult to identify the technique of percussion,

although the features observed on the blanks seem to indicate a frequent use of hard hammer.

Retouched tools

All retouched tools are produced on blades including one endscraper on a blade and one notched blade.

	N	*f* (among tools)	*f* (from total, n=55)
Retouched blade	12	75%	22%
Retouched bladelet	0	0%	0%
Retouched point	2	13%	4%
Endscraper	1	6%	2%
Other	1	6%	2%
	16	100%	29%

Table 74: Kara-Bom, OH4, frequency of major retouched tool types

One blade has a mesiodistal truncation giving the distal end an asymmetric pointed shape (Figure 83, center); however, only two artifacts had a clear pointed shape before being retouched. Some of the blanks have convergent edges without presenting a sharp pointed distal edge (Figure 83, left). Retouched small laminar blanks are almost absent, the only exception being a fragment of small blade showing a rather irregular continuous inverse retouch along the left edge (Figure 83, right).

	N	*f*
Distal	0	0%
Mesiodistal	4	25%
Mesial	5	31%
Mesioproximal	2	13%
Proximal	0	0%
Complete	5	31%
	16	100%

Table 75: Kara-Bom, OH4, retouched tools breakage

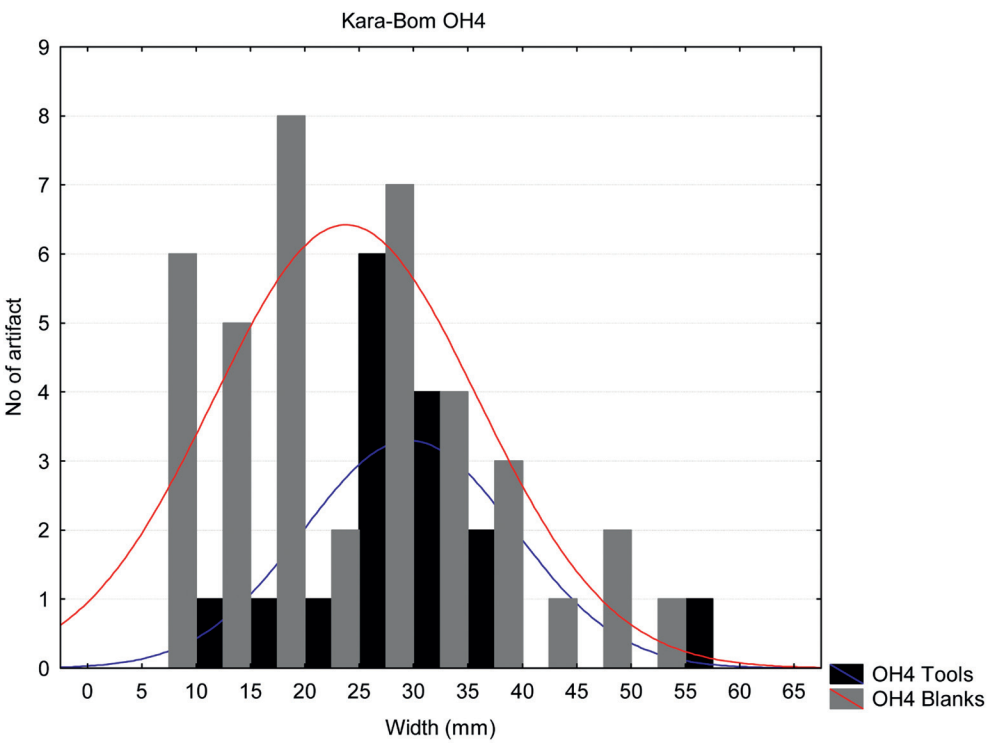

Figure 82: OH4, width histogram comparing retouched tools and blanks

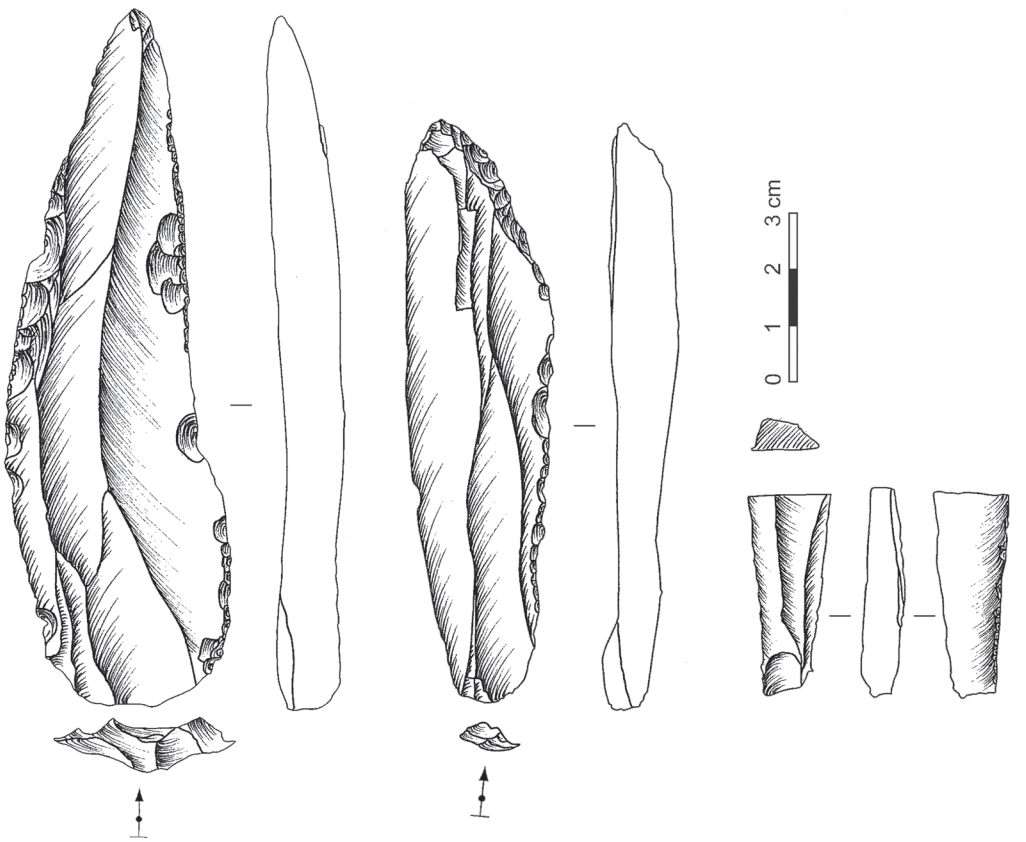

Figure 83: OH4, retouched tools

Along with complete artifacts, mesial and mesio-distal tool fragments are the most common (Table 75). All platforms are facetted except one which is dihedral. The mean thickness is 7.1 ± 5 mm. The mean is strongly influenced by the presence of an outlier (circa 17 mm), as the median is 5.4 mm. The mean platform width is 16 ± 10.2 mm. Half of the cross-sections are triangular, the other half being trapezoidal. Blanks are axial (N=6), oriented on the right (N=3) or on the left (N=1), with the rest being undetermined.

No clear pattern of blank selection related to size is observed. It seems that the tools are slightly wider than the blank mean width (Figure 82).

Retouch is mainly direct, with two examples being inverse and one being alternate (Table 76). Thin retouch is the most common (N=8), a few examples of scaled retouch also occur alone (N=2) or combined with thin retouch (N=1) (Figure 83, left). Semi-steep and steep retouch occurs only in combination with thin retouch (N=3) (Figure 83, center).

	N	*f*
Direct	13	81%
Inverse	2	13%
Alternate	1	6%
	16	100%

Table 76: Kara-Bom, OH4, retouche location (face)

Retouch shows no pattern of location along the edges (Table 77). Although retouch occurs quite often

	Dorsal		Ventral	
	N	*f*	N	*f*
Distal	4	29%	0	0%
Mesial	2	14%	1	33%
Proximal	1	7%	2	67%
Combination	1	7%	0	0%
Continuous	5	36%	0	0%
Undermined	1	7%	0	0%
	14	100%	3	100%

Table 77: Kara-Bom, OH4, retouch location (edge)

along the left edge (N=6), no clear pattern of lateral location can be observed.

3.6 ADDITIONAL ARTIFACTS

Following the description of the material sampled, this section consists of the description of 22 artifacts coming the 1987-1993 excavation campaigns. They could not be localized precisely or come from the 1980's Okladnikov's test pit. Artifacts attributed to Okladnikov's layers 1 to 4 and located between squares Z-N and lines 3-12 are most probably attributed to OH4-OH6, as MPH1 and MPH2 have not been reached in this area (Okladnikov, 1983). These artifacts were selected on the basis of strong similarities with the assemblage from OH5 and OH6. With respect to taphonomic issues, and in light of the results obtained on the sample, it is suggested that this material could be attributed to one of these occupation levels. Although no quantitative data are presented from this old collection, qualitative descriptions are used to illustrate the expectable range of technological variability of the described reduction sequences.

3.6.1 CORES

Core description

Mode A6 (N=2)

∗ KB-92.YO5.Z6.1

This core was previously attributed to OH5 but the spatial coordinates are not consistent with this attribution and likely indicate a problem in the data recording. It is a core on block with a cortical back and two flaking surfaces, one on the broad side of the core and one on the right lateral face. It displays two opposed platforms shaped by crude flaking (Figure 84). The left edge of the broad face show traces of radial flaking probably designed as a preparation of the surface convexity. A series of three removals are detached on the broad flaking surface from the lower platform (1-3), one on the left, one on the right and then one in the middle. The three following removals are detached from different platform. The one from the upper platform is fragmentary and hard to interpret, and the two others are struck for the lower platform, at the intersection between two surfaces (4). One more removal (5) is then detached from the lower platform at the right edge of the lateral flaking surface. The next removals are detached from the upper platform on the narrow flaking surface (6, 7),

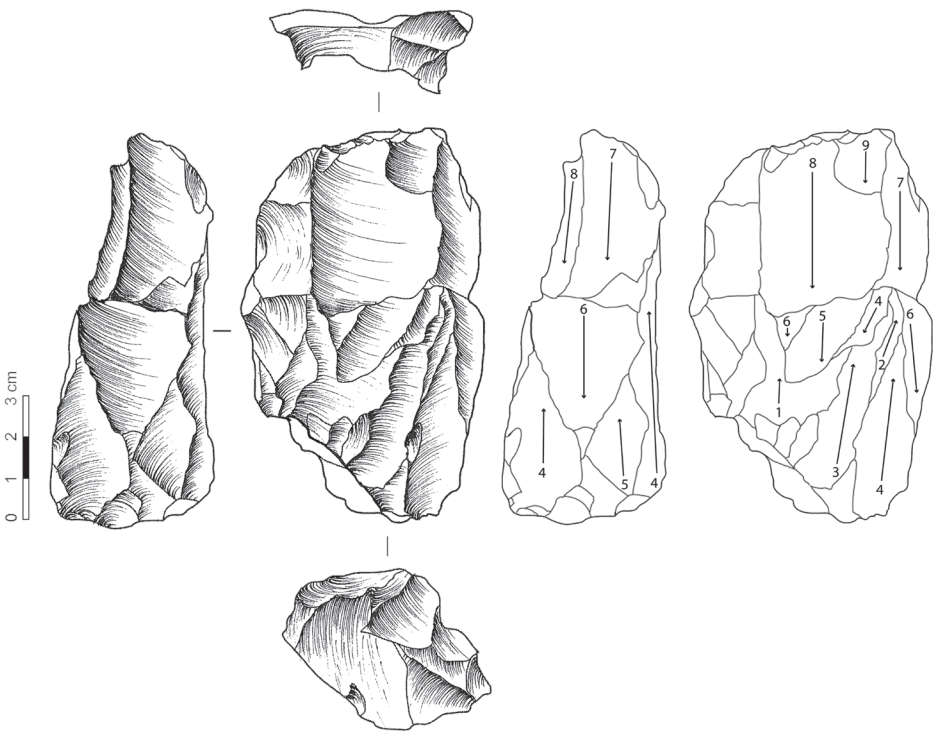

Figure 84: Kara-Bom, KB-92.YO5.Z6.1

the second one being hinged and ending the reduction on the lateral flaking surface. Alternatively, or after stopping on the lateral surface, two removals are detached from the broad surface (5, 6). However, the two last removals are struck from the upper platform on the broad face (7, 8). This core illustrates the alternating use of two related surfaces and two platforms, as opposed to a semi-turning reduction.

∗ KB-80.I11/2A.2381

This core is produced on a block and shows two flaking surfaces and two opposed platforms (Figure 85). The main flaking surface is located on a broad, slightly convex surface. The earliest phase of reduction (1) is located on the two lateral extremities and on the proximal part of the flaking surface, and blanks are struck from both platforms. This is followed by a series of three removals (2-3-4) finishing on a hinged fracture. One removal associated with phase 2 is struck from the upper platform. The reduction ends by two attempts to remove a blade at the left corner of the broad flaking surface (5-6). The second flaking surface is located along the right narrow edge of the core and is posterior to the phase 2 of reduction from the broad surface. It likely represents an attempt to remove a side blade from the right corner after the reduction on the broad face ended, in order to reshape convexities and resume the reduction process. The blanks detached from the broad face are probably flat and elongated with convergent edges as the side removals more likely show a thick triangular trapezoidal section.

Mode B1 (N=1)

∗ KB-88 (RA-80).98Y.I10/2

This artifact is a thick mesioproximal blade fragment with a dorsal patterning showing a cortex-like inclusion which occurs after the detachment of a lateral removal visible along the right mesial part of the blank (Figure 86). Two crest-like blows show attempts to remove it before the blade is detached.

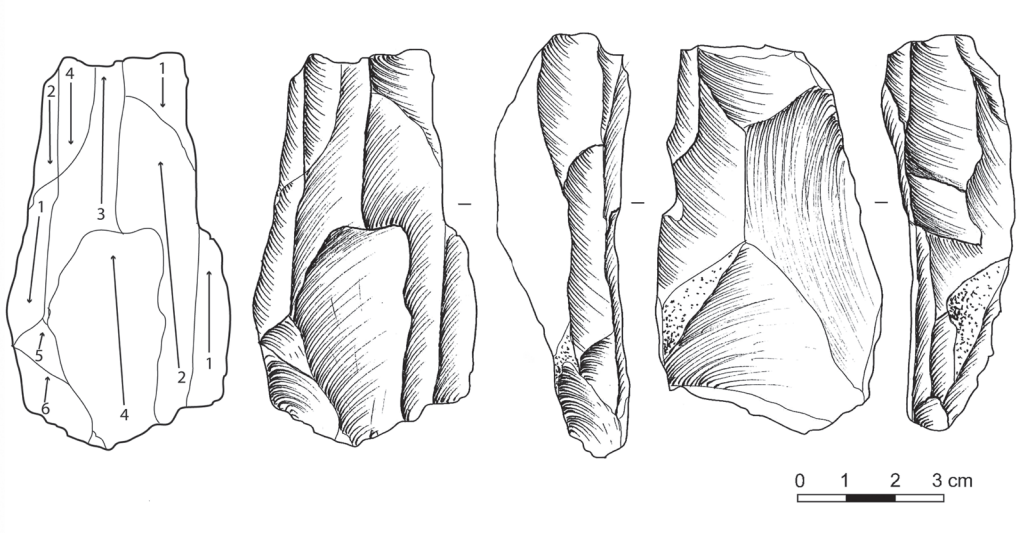

Figure 85: Kara-Bom, KB-80.I11/2A.2381

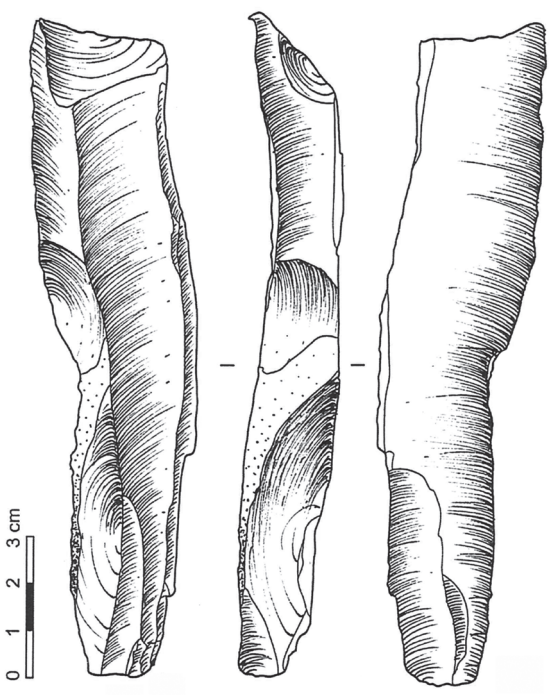

Figure 86: Kara-Bom, KB-88 (RA-80).98Y.I10/2

Three removals show attempts to detach thin spalls along the left edge. In this case, it seems to represent the initial stage of a Mode B reduction.

Mode B2 (N=3)

∗ KB.1043.10/3.1939

This core is made on a thick blade/laminar flake which bear negatives of convergent removals on the dorsal face and a series of sporadic direct retouch along the left edge and on the proximal right end (Figure 87). It also display a distal truncation posterior to a snap/break. Four hinged negatives show repeated attempts to remove spalls along the retouched right edge. This artifact could also be typed as a burin on a truncation.

∗ KB-80.1Hor.I/8.4419

This artifact is on a cortical blade blank with unidirectional convergent removals, a notch, some retouch along the proximal left edge, a series of retouch on the right edge, and a single retouch on the platform (Figure 88). Several sub-cortical hinged removals are visible along the thickest edge of the blank, detached from a plain platform. This artifact is typed as a *burin d'angle*.

∗ KB-80.1Hor.M14.4775

This artifact is on a laminar flake bearing a combination of cortex, natural surface and a single removal

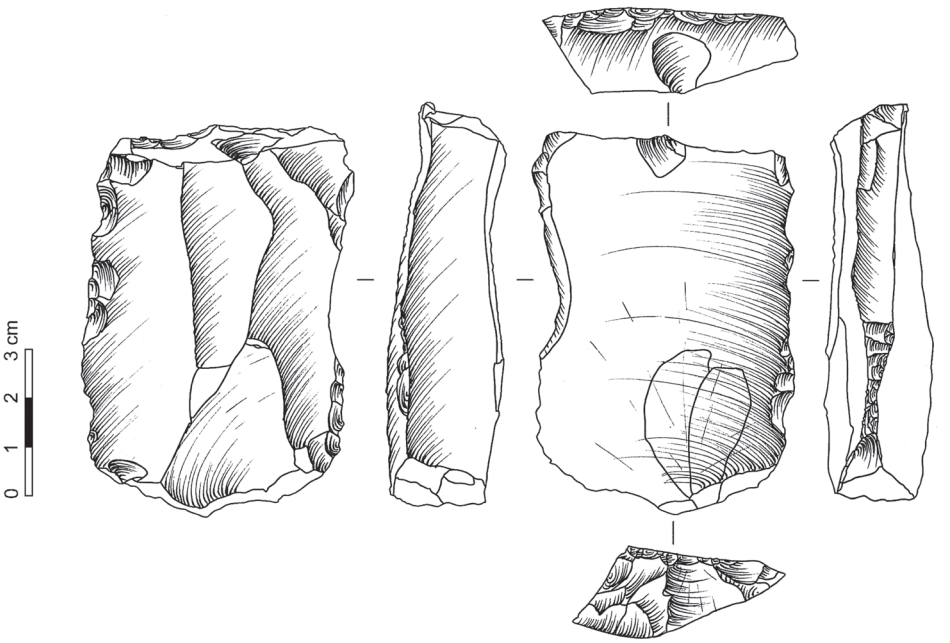

Figure 87: Kara-Bom, KB.1043.10/3.1939

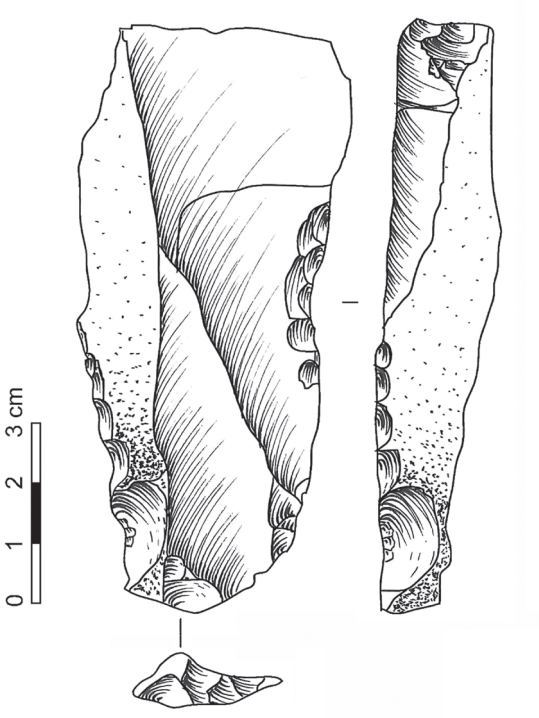

Figure 88: Kara-Bom, KB-80.1Hor.I/8.4419

on its dorsal face (Figure 89). It has a particularly thick hinge removal along the left edge opposed to a right edge bearing a combination of direct retouch and an inverse notch (edge damage?). A striking platform is prepared in the distal part by a series of removals, struck from the dorsal face and from the side, followed by a series of sub-cortical hinged removals. Although typologically it can be considered as a *burin d'angle*, the preparation of the platform and the fact that spalls are detached from the thickest edge indicates instead an initial stage of Mode B core reduction.

Mode B5 (N=10)

* KB.2831.I10/1A.3739

This core is on a second crested blade and shows a single flaking surface along its right edge (Figure 90). Two opposed platforms are used, one of which probably benefits from the thicknes of a core blank plunged morphology. The reduction sequence is mainly conducted from the upper platform and shows a series of unidirectional removals, some of them exploiting the entire length of the flaking surface (1,

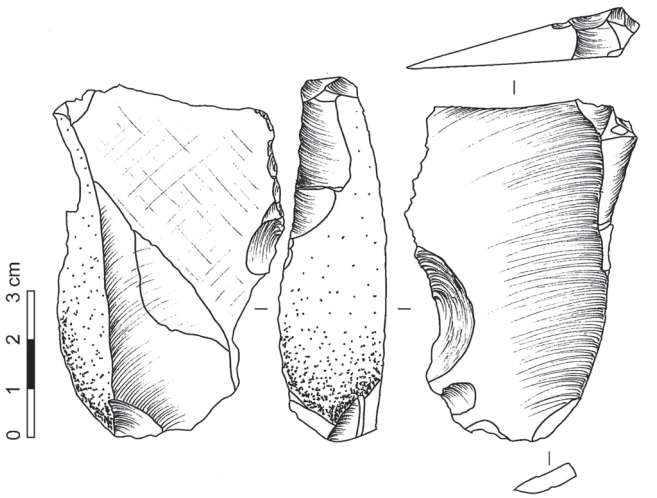

Figure 89: KB-80.1Hor.M14.4775

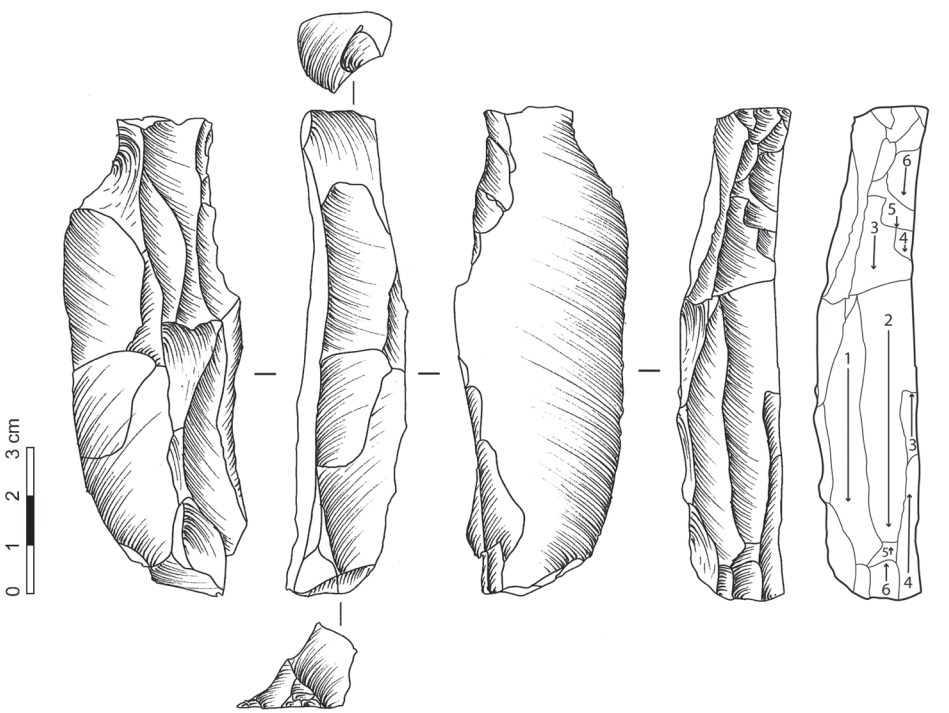

Figure 90: Kara-Bom, KB.2831.I10/1A.3739

2). It is then followed by a series of hinged fractures struck from both striking platforms (3-6) and slightly expanding on the ventral face, although it is not clear when the platform switch occured. The upper striking platform is plain and the lower platform shows preparation and reshaping with flakes being struck from the ventral face.

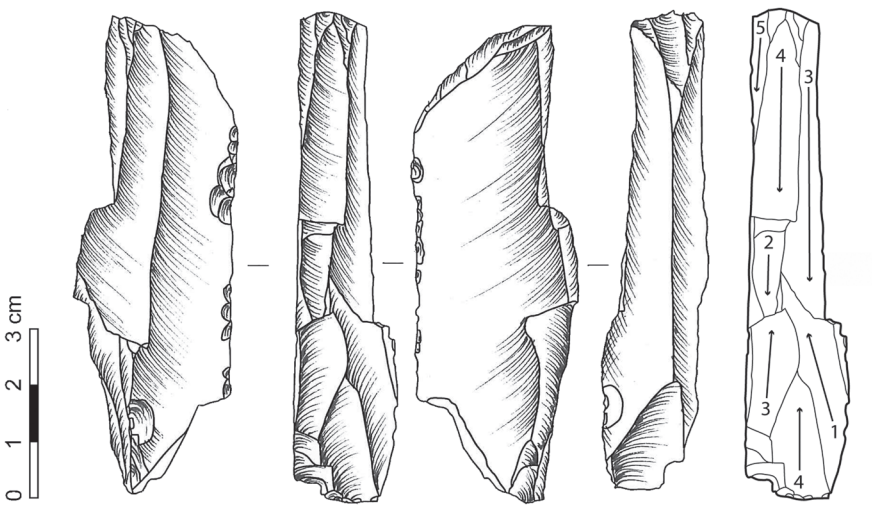

Figure 91: Kara-Bom, KB.RA-87.Sl3.M9.33.10

∗ KB.RA-87.Sl3.M9.33.10

This core is a unidirectional blade with a single flaking surface located along its right edge (Figure 91). The left edge displays alternate retouch. The flaking surface is reduced using two opposed flaking surfaces. The earliest removal is detached from the lower platform and is followed by a platform switch (2). Then a series of removals are struck from the upper platform and from the left edge to the right one (3-5). Two removals are detached from the lower platform (3, 4). The upper platform is shaped by small removals giving it a somewhat carinated morphology. The lower platform is shaped by a single blow.

∗ KB-80.Hor3.I/5.5596

This core is produced on a unidirectional blade which shows a direct truncation at its proximal end (Figure 92). A single flaking surface is located along

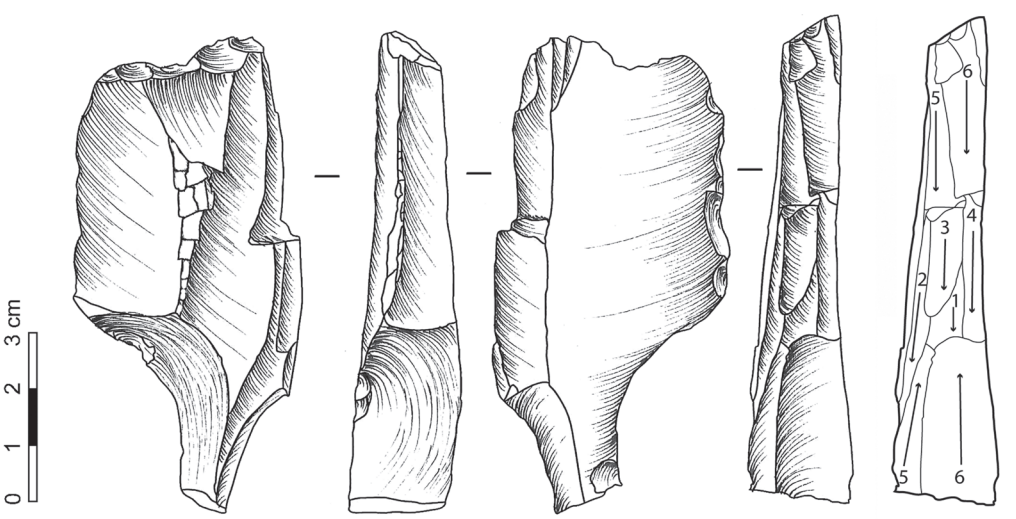

Figure 92: Kara-Bom, KB-80.Hor3.I/5.5596

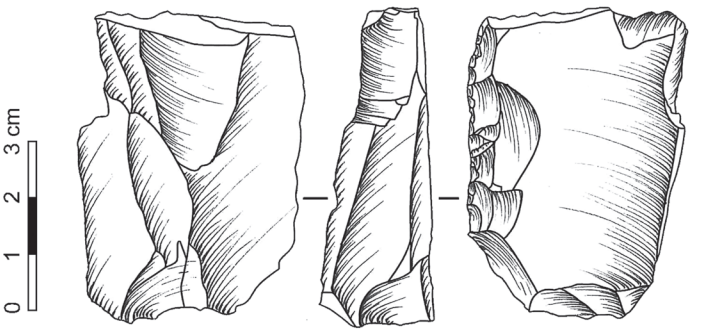

Figure 93: Kara-Bom, KB-80.Hor1.J7.4864

the right edge of the blank and is reduced from two opposed platform. A series of unidirectional removals are struck from the upper platform (1-6), some of them covering the entire flaking surface length (2). Two hinged removals are struck from the lower platform at the end of the reduction sequence. The small removals extending on the ventral face are detached from the upper platform and may indicate the use of the intersection between two surfaces as a natural crest.

∗ KB-80.Hor1.J7.4864

This core is produced on a bidirectional blade blank showing a proximal truncation and bearing a combination of thin and scaled inverse retouch along the right edge (Figure 93). A flaking surface located along the left edge is reduced by bidirectional removals detached from two opposed platforms. The left edge indicates that the first phase of reduction uses the lower platform. The upper platform is shaped by a removal perpendicular to the axis of the blank which is followed by two hinged removals, ending the reduction sequence.

∗ KB-RA-80.2526.I10/1.3444

This core represents initial stages of Mode B reduction on a bidirectional large blade (Figure 94). It shows the remains of a crest along the distal part of the right edge and a single flaking surface along the left edge, reduced from two opposed striking platforms. Three spalls are detached from the lower platform and two hinged removals are struck from the upper one. Platforms are prepared by removals on both ends.

∗ KB-92.450

This core is produced on a second-crest blade blank and displays a flaking surface located on its left edge (Figure 95). Reduction comes from two opposed flaking. The upper one is plain and the lower one is missing. The two earliest (1-2) removals illustrate a platform switch followed by two hinge fractures (3). The upper platform displays a clear impact point on the breakage surface that may indicate snapping by percussion.

∗ KB-80.2039.Z10/2.2955

This core is produced on a thick bi-directional blade blank with a single flaking surface, located along the right edge and reduced from two opposed striking platforms (Figure 96). Earliest phases of reduction show a use of the upper platform (1-2) followed by a switch to the lower platform and a series of hinged removals ending the reduction process. The upper platform shows a plain surface bearing traces of a lateral impact probably linked with the snapping event and a frontal removal corresponding to the detachment of a partial tablet.

∗ KB-80.Hor1.I/9.Y528

This core is on a unidirectional blade blank and shows a single flaking surface located along its left edge (Figure 97). Two opposed facetted striking plat-

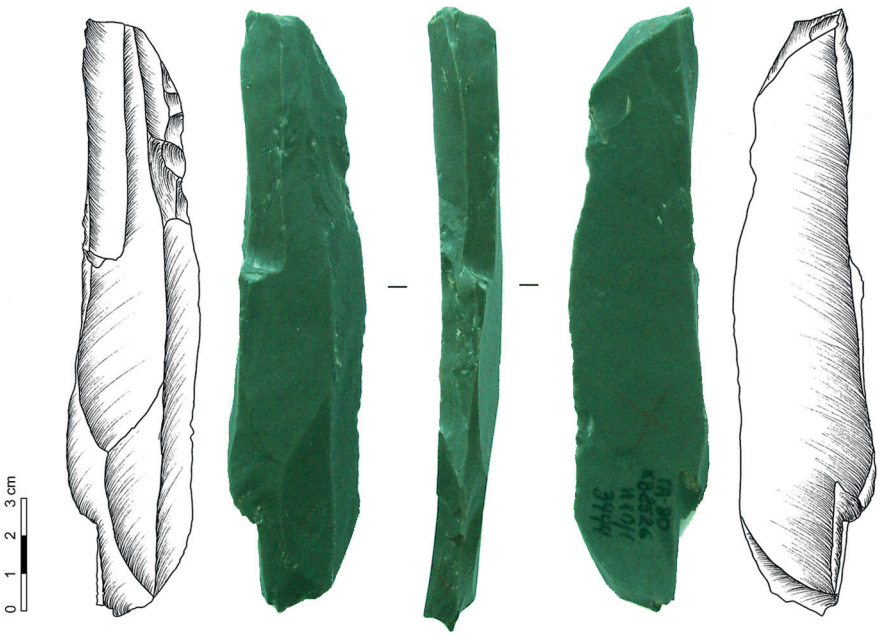

Figure 94: Kara-Bom, KB-RA-80.2526.I10/1.3444

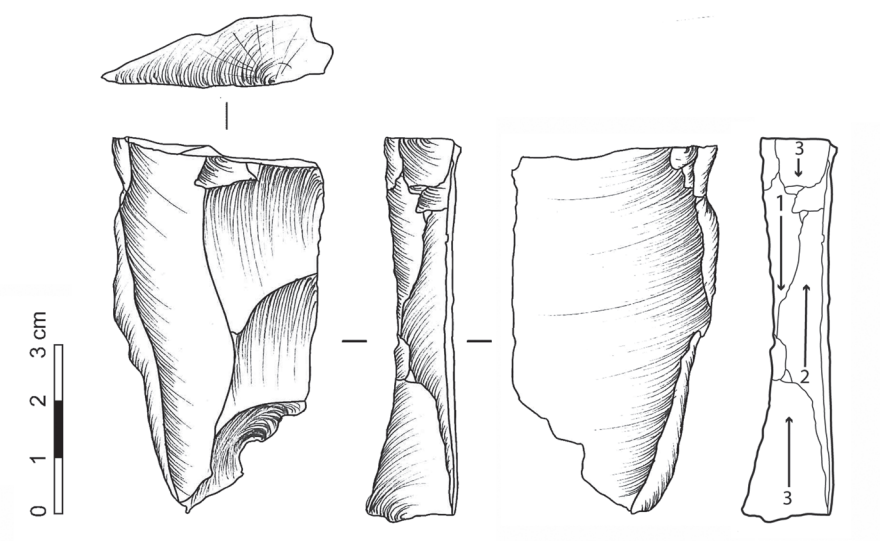

Figure 95: Kara-Bom, KB-92.450

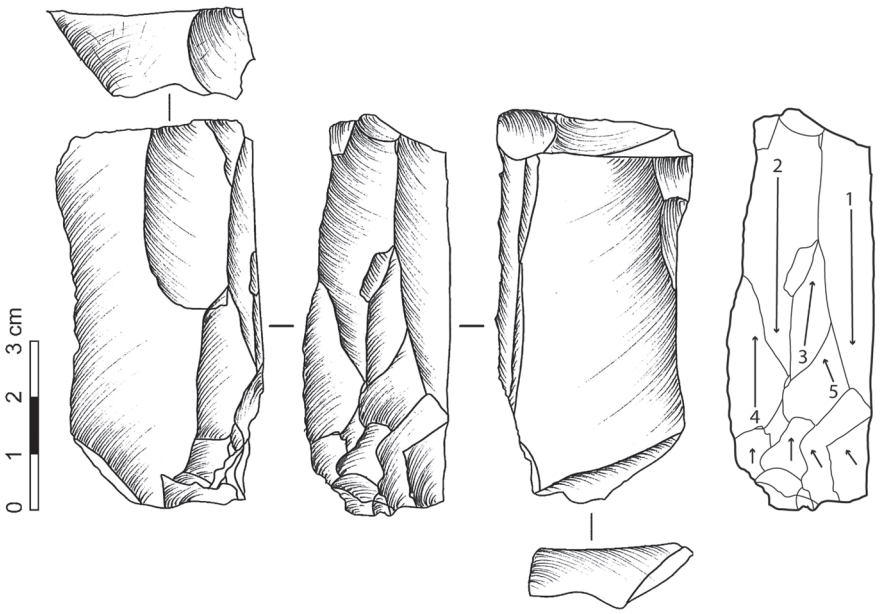

Figure 96: Kara-Bom, KB-80.2039.Z10/2.2955

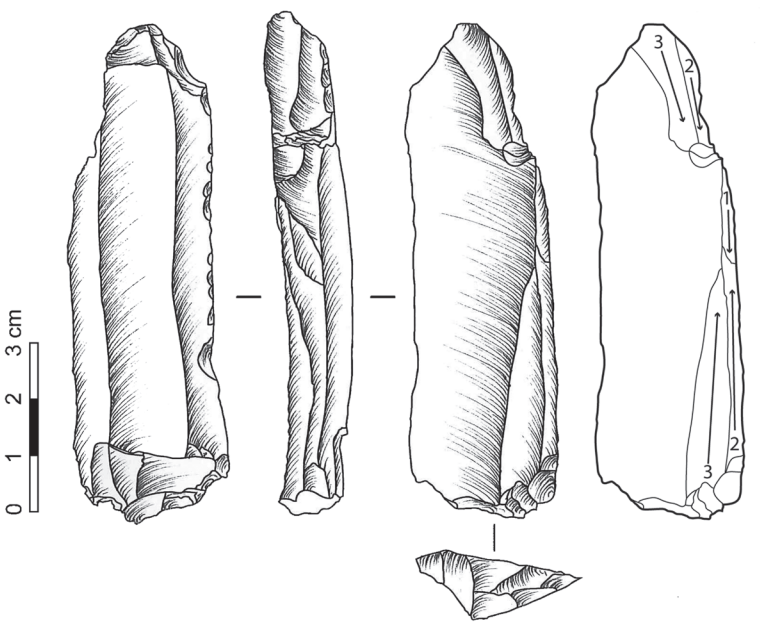

Figure 97: Kara-Bom, KB-80.Hor1.I/9.Y528

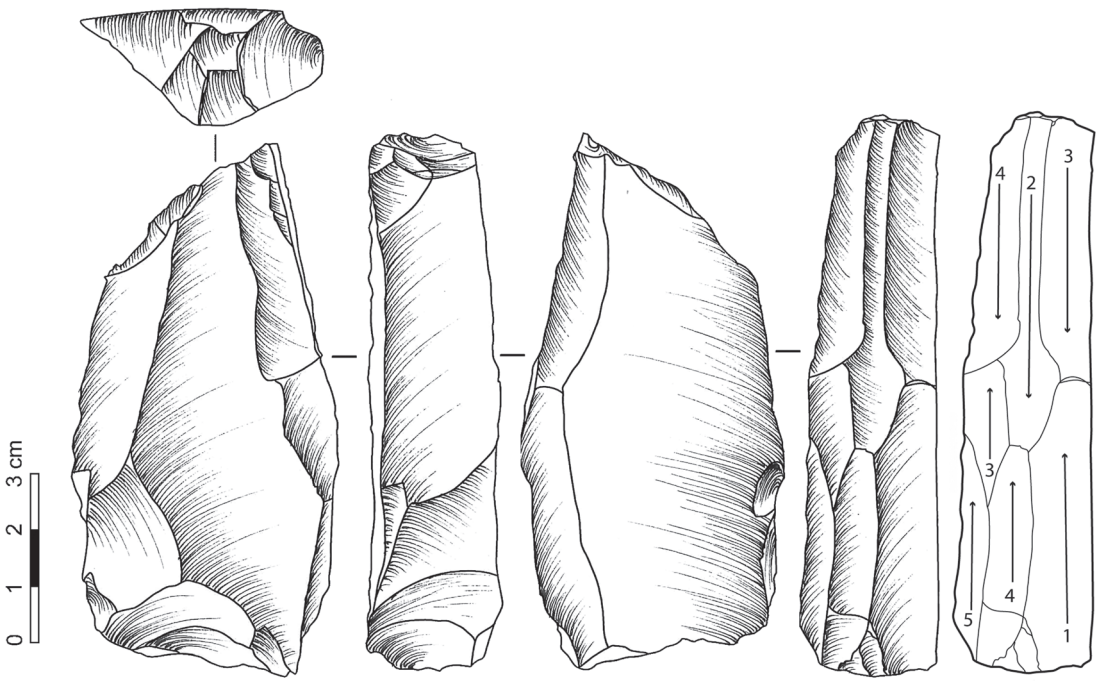

Figure 98: Kara-Bom, KB-80.Hor1.L/9.4378

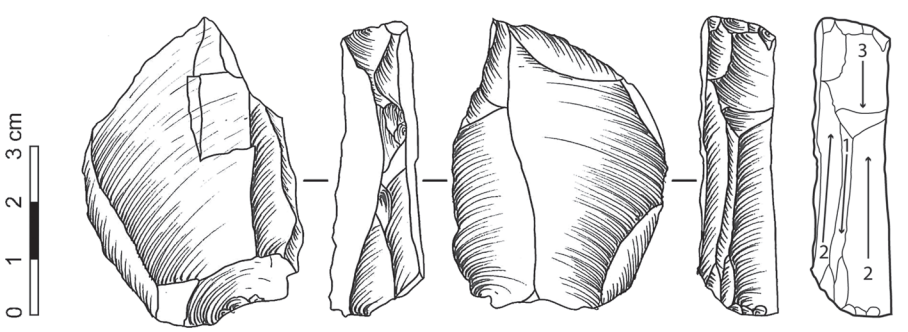

Figure 99:Kara-Bom, KB-87.SL3.I/54.N11.K8.327

forms are used, and removals are detached from the middle part of the flaking surface (1, 2) and from the corner with the ventral face (3). Upper platform reduction ends with two deep, hinged removals.

∗ KB-80.Hor1.L/9.4378

This core is produced on a large laminar blank and shows a single flaking surface located along the right edge (Figure 98). Two opposed striking platforms illustrate a bidirectional reduction sequence. The earliest phase (1) uses the lower striking platform and is followed by a switch to the upper platform (2). This is followed by two series of two and three removals from respectively the upper and the lower platforms (3-5); however, the chronology of the platform switches remains unclear. The upper flaking surface displays negatives of several frontal tablet removals.

∗ KB-87.SL3.I/54.N11.K8.327

This core is made on a laminar flake with a single flaking surface located on its right edge (Figure 99). The flaking surface is reduced from two opposed platforms, with a first removal (1) struck from the upper platform, followed by a platform switch with two more removals (2) detached from the lower platform. One of these clearly extends on the ventral face. Then another platform switch occurs as shown by the final hinged removals (3).

Mode B6 (N=2)

∗ KB-80.2472.I10/1.3890

This core is produced on a thick cortical laminar flake displaying a truncation on the proximal part (Figure 100). It has two independent flaking surfaces parallel to the longitudinal axis of the blank. The flaking surface on the right edge is flaked from two opposed striking platforms. The earliest phase of reduction consists of a series of two removals struck from the lower platform (1, 2) followed by a platform switch (3) and three hinged removals (4, 5). The flaking surface along the left edge shows the preparation of a crest, still visible on the distal end, and two hinged removals detached from both upper and lower platforms. The upper platform is shaped by a lateral removal with a combination of scaled and thin retouch, and the lower platform is shaped by a lateral flake removal and a frontal partial tablet removal.

∗ KB-91.YO5.Z6.1.P8.49.11342

This core is on a cortical bidirectional blade and has two independent flaking surfaces located parallel to its longitudinal axis (Figure 101). Along the right edge, the flaking surface is mainly unidirectional, with three removals tending to cover its whole length. A deep hinged removal is then detached from the lower platform. Both platforms are plain. The second flaking surface displays two hinged removals, struck from the upper platform. The latter is heavily prepared by a series of removals.

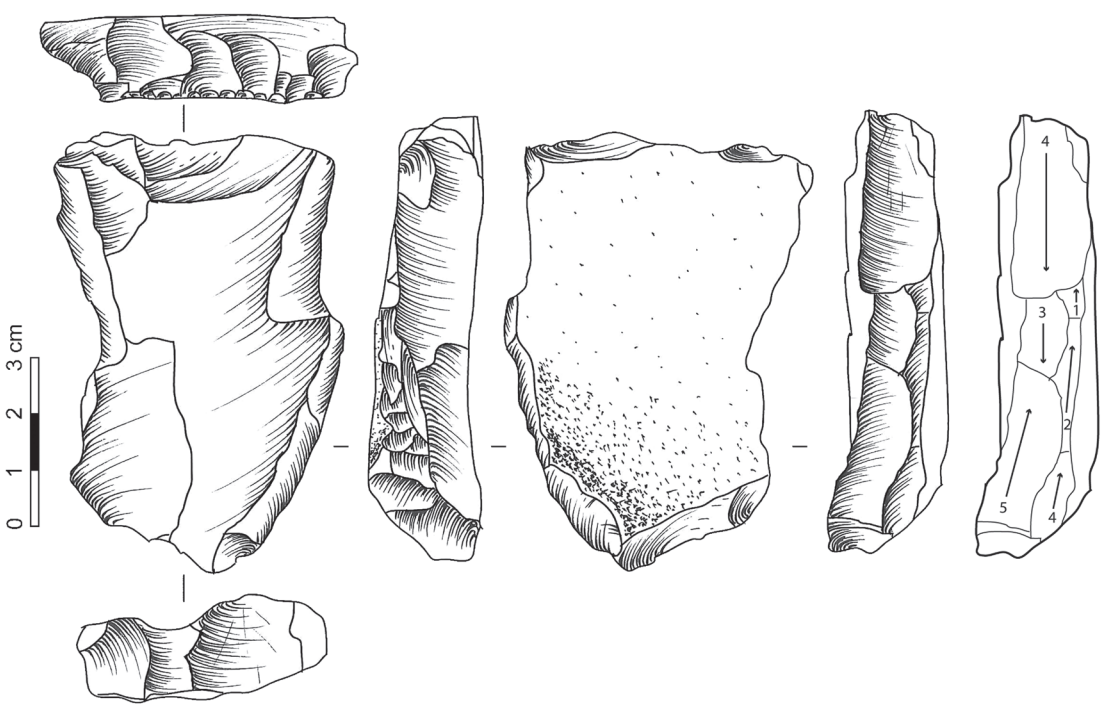

Figure 100: Kara-Bom, KB-80.2472.I10/1.3890

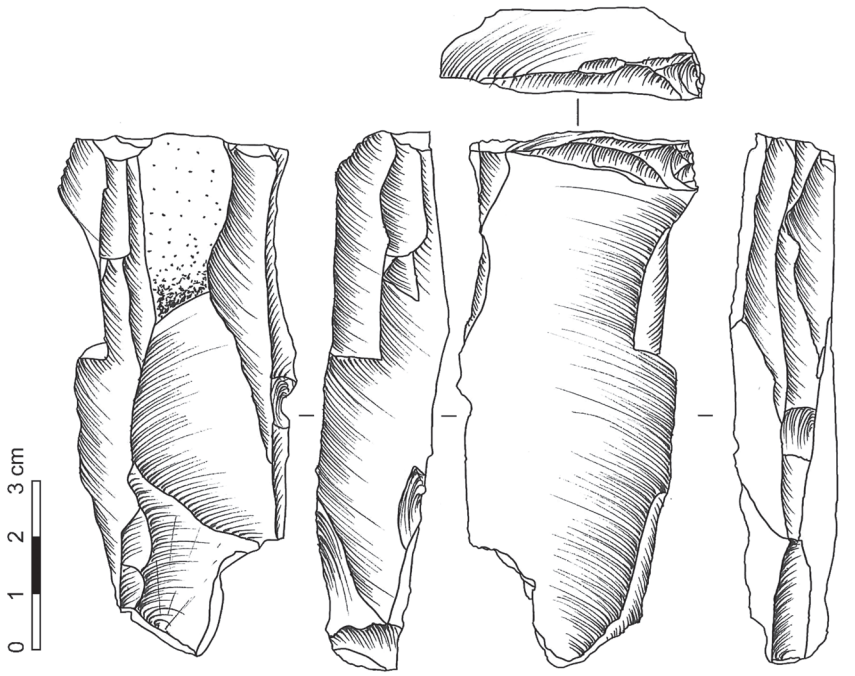

Figure 101: Kara-Bom, KB-91.YO5.Z6.1.P8.49.1134

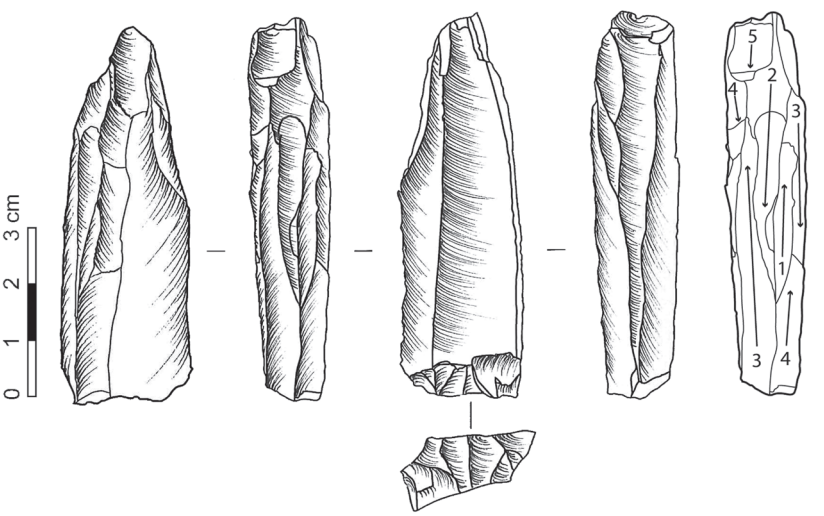

Figure 102: Kara-Bom, KB-80.Hor3.K6/5627

∗ KB-80.Hor3.K6/5627

This core is produced on a unidirectional blade with two flaking surfaces along both the right and left edges (Figure 102). The left edge shows the most intensive reduction from two opposed platforms. An early platform switch (1-2) is followed by three removals from the upper platform and two from the lower (3-5). The last phases clearly extends to the ventral face of the blank. The second flaking surface

shows a succession of three removals, one covering the whole length of the edge. This flaking surface is exploited prior to the left edge and is used as a striking platform for the right one. The lover striking platform is a truncation.

Others (N=1)

* KB.RA87.I/53.K8.SL3.1.RL.323

This core is produced and shows a variant of the A10 Mode on a laminar flake. It shows a bidirectional reduction system on a broad surface in a rather semi-turning fashion. It expands on the left edge of the blank (Figure 103). The earliest removals are struck from both the upper and lower platform, showing an alternate bidirectional sequence. Platforms are mainly truncations, and this artifact can be typed as a truncated-facetted piece.

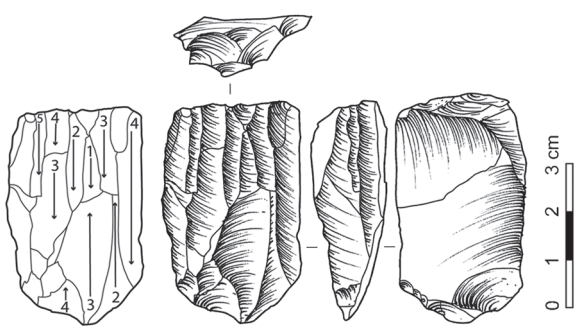

Figure 103: Kara-Bom, KB.RA87.I/53.K8.SL3.1.RL.323

Core-like tool (N=2)

* KB.259.L10/2.1152

This artifact is listed here as a possible core. It is produced on a bidirectional blade blank showing a semi-continuous direct retouch extending from the proximal part along the left edge (Figure 104). An inverse proximal truncation is observed, as the distal part show negatives of hinged removals. In this case, the artifact can be typed as a truncated-facetted piece, but the removals show an irregular morphology that could also be characterized as scaled. So, it illustrates the variability observed among the truncated-facetted pieces, some being tool-like cores and some being clearly cores.

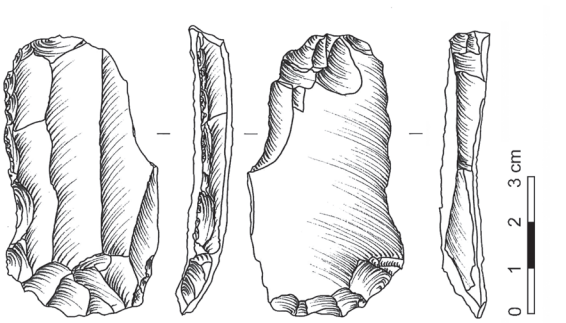

Figure 104: KB.259.L10/2.1152

* KB-80.279.L10/4.1171

This artifact is a blade with a cortical platform, a trapezoidal section and a unidirectional cortical dorsal scar patterning. It has an abrupt cortical right edge. It bears sporadic retouch on both the right and left edges (Figure 105). A striking platform is prepared by a removal perpendicular to the axis of the blank, followed by three sub-cortical, hinged removals. This artifact can be typed a dihedral burin *(burin dièdre d'angle)*.

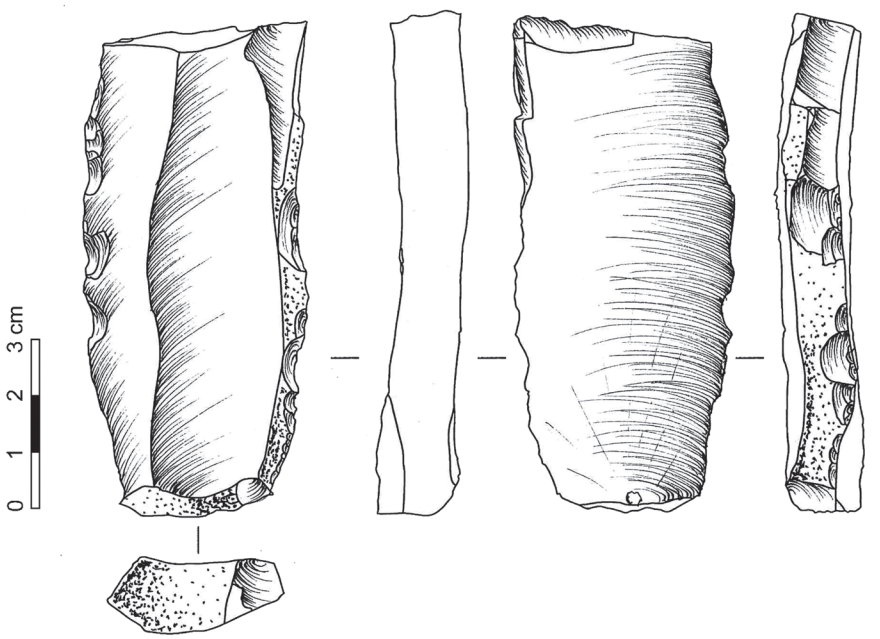

Figure 105: KB-80.279.L10/4.1171

3.7 KARA-BOM: MPH1, OH6, OH5 AND OH4 SAMPLE COMPARISONS

Based on the dataset described in the previous sections, the main characteristic of the archeological assemblages are compared.

3.7.1 BLANK ATTRIBUTES

Platform size and preparation

The platform preparation appears to show an association between plain and facetted platforms in each level. In both OH6 and OH5, the majority of platforms are facetted directly followed by plain platforms. MPH1 and OH4 show a majority of plain platforms followed by facetted ones; however, they both represent the smallest samples. The frequency of facetted (χ^2=(3) 2, p=0.57) and plain (χ^2=(3) 1.28, p=0.73) platforms, although showing variability, do not differ significantly from one assemblage to another. Dihedral platforms also have a similar frequency in all assemblages. Notable is the occurrence of partial faceting in both OH6 and OH5, a platform preparation that is not observed in MPH1 and OH4. Strong abrasion of the external platform is absent from MPH1, but occurs occasionally in OH4. Therefore, from a general point of view, platform preparation is quite similar throughout the described samples, and specific features seem to indicate a higher degree of similarity between OH6 and OH5.

Considered as a whole, the platform thickness between levels does not vary significantly ($F(3, 173) = 0.64$, $p = .59$). OH6 and OH5 tend to have more outliers, which may result from a larger sample size. An opposite situation is observed in MPH1, for which the narrow range of thickness might be linked with the small sample size. As stated in the blank attribute sections, based on medians, plain platforms are statistically less thick than the facetted ones in OH6, OH5 and OH4. The MPH1 sample size is too small to be tested.

Based on the platform surface, OH6 and OH5 are similar in terms of size distribution although the facetted platforms tend to show more variability.

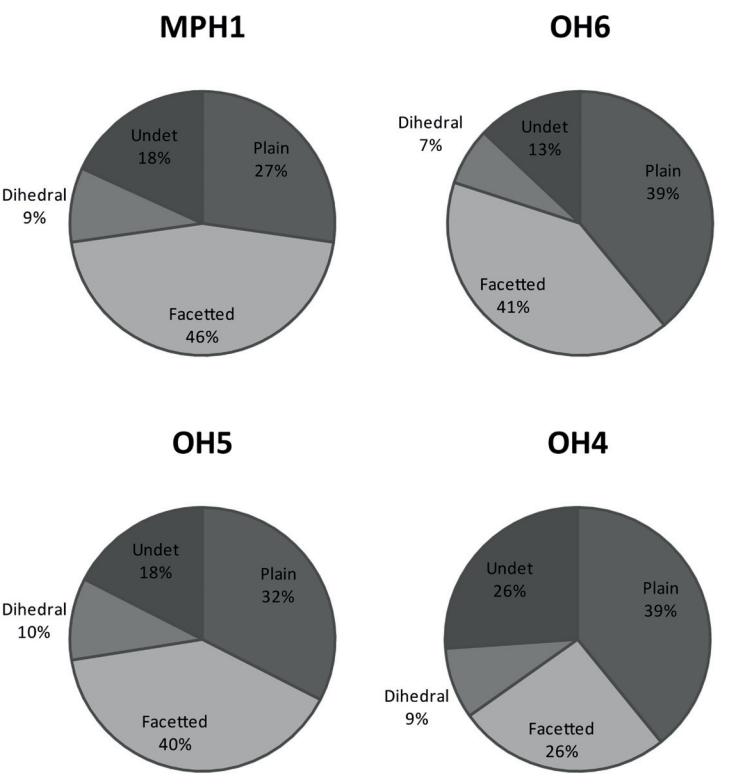

Figure 106: Kara-Bom, comparison of platform preparation between samples

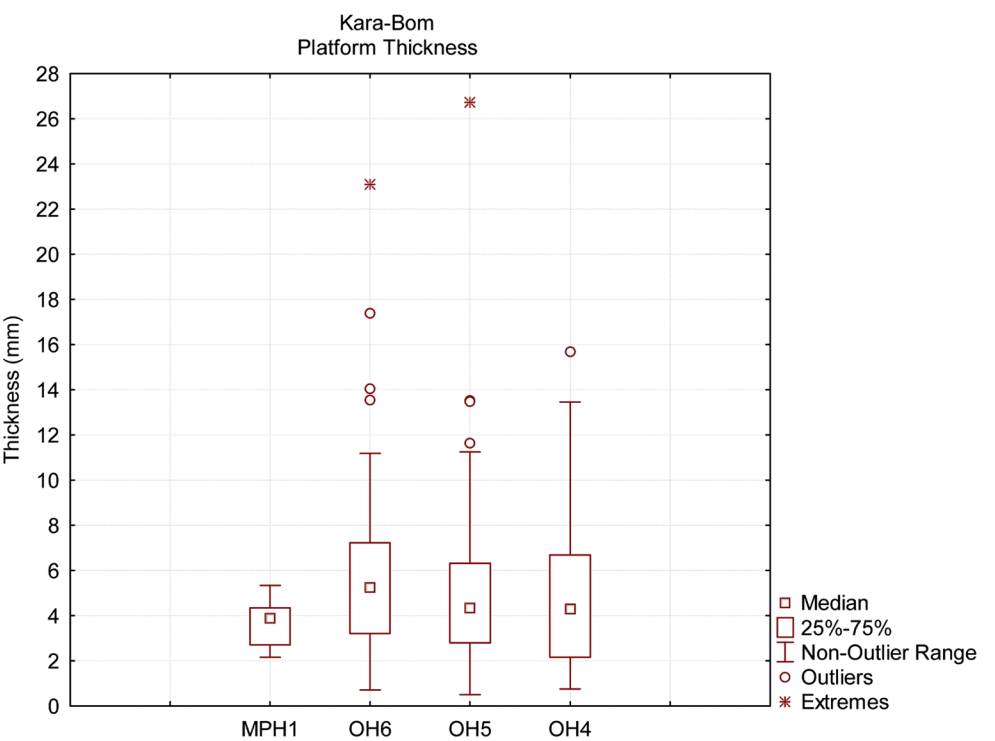

Figure 107: Kara-Bom, platform thickness, comparison between samples

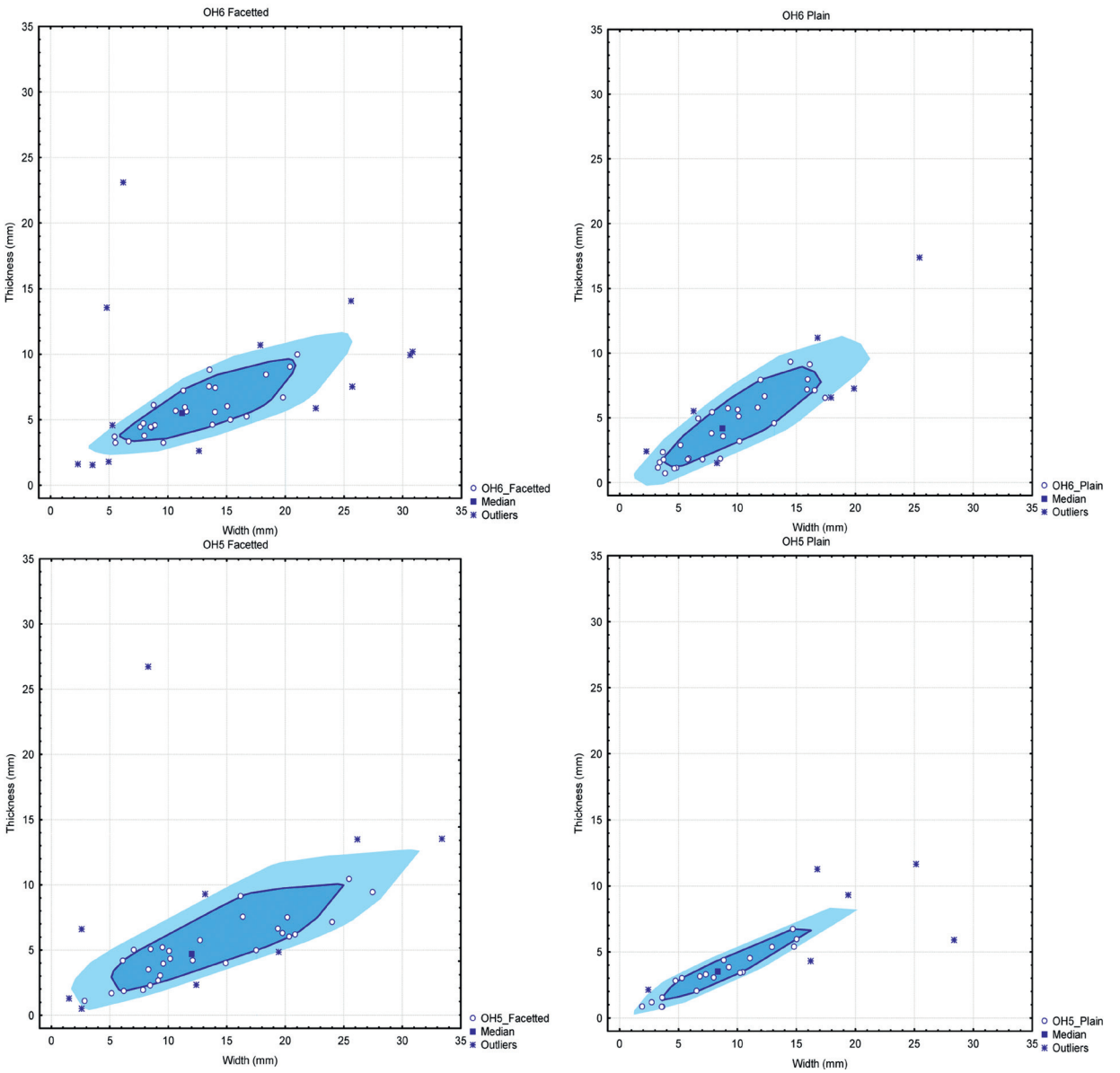

Figure 108: Kara-Bom, platform surface, comparison between OH6 and OH4

OH4 is based on a smaller sample and does not seem to differ from OH6 and OH5. Bag plots illustrate this situation (Figure 108). The first convex polygon (the bag) represents 50% of the data points which are located around the median, and the second polygon (the fence) corresponds to the bag extended by a factor of 1.5. Outliers are rejected statistically when they fall outside the fence. No bags could be drawn for the OH4 assemblage due to the small sample size.

It is however clear that facetted and plain platform medians differ. Facetted platforms are significantly thicker and wider than the plain ones.

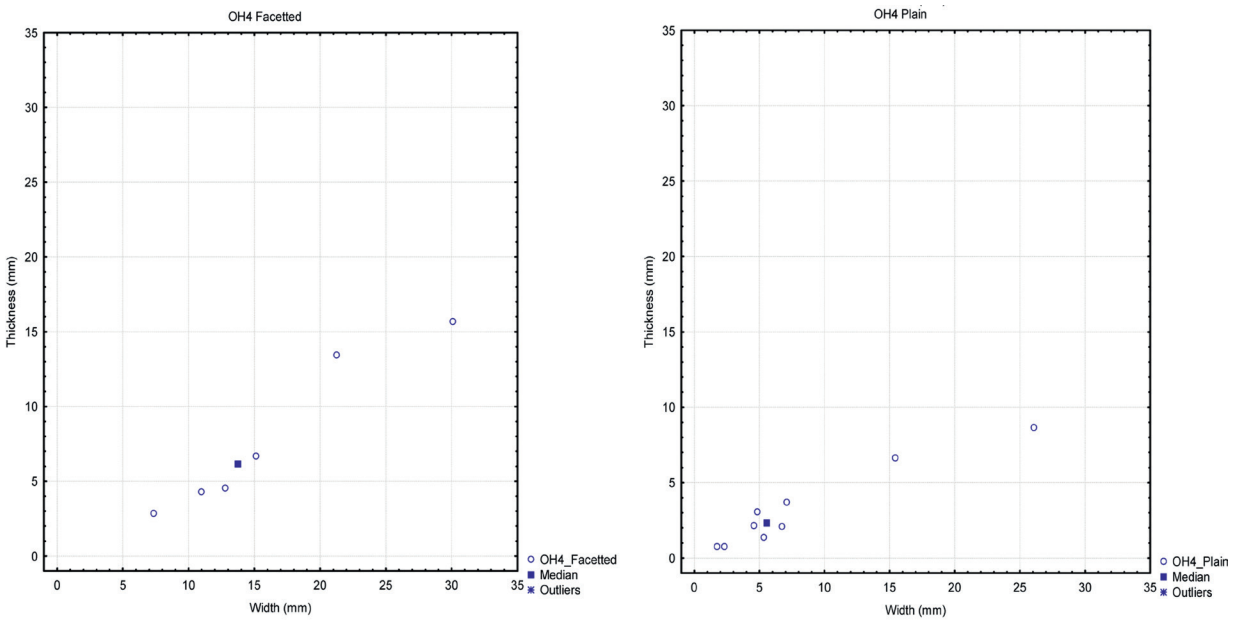

Figure 109: Kara-Bom, platform surface, OH4

Blank size attributes

LENGTH

Blank length mean does not differ from one assemblage to another ($F(2, 114) = 0.36$, $p = .69$). MPH1 could not be included in the test due to the small sample size.

WIDTH

Blank width means are similar between assemblages ($F(3, 363) = 0.38$, $p = .76$). OH6 and OH4 show a little positive skewness. Notable is the large variability observed in all assemblages except in MPH1.

THICKNESS

The mean blank thickness does not differ significantly from one level to another when considered as a whole ($F(3, 362) = 2.55$, $p = .56$).

Dorsal scar pattern

The dorsal scar patterns show similarities but also differences between assemblages. OH6 and OH5 show striking similarities for both categories and frequencies of patterning. They show a balance between uni- and bidirectional blank patterning, together with a variety of crested elements occurring in a rather low frequency. Differences between these two assemblages are minor and consist of an occurrence of bi-directional cortical elements in OH5 and a slightly higher frequency of bidirectional blanks in OH6. As previously shown, the OH5 bidirectional frequency is biased by the occurrence of numerous broken elements in the sample. The situation is reversed when considering only complete blanks; bidirectional ones becoming then statistically dominant in OH6. The MPH1 analysis is based on a small sample size and differs by a lower frequency of bidirectional blanks, by a reduced representation of crested elements and by a higher frequency of undetermined elements. OH4 shows a significant majority of bidirectional elements, including well represented bidirectional cortical blanks. Crested blank frequency is comparable to OH5 and OH6 and the unidirectional blank

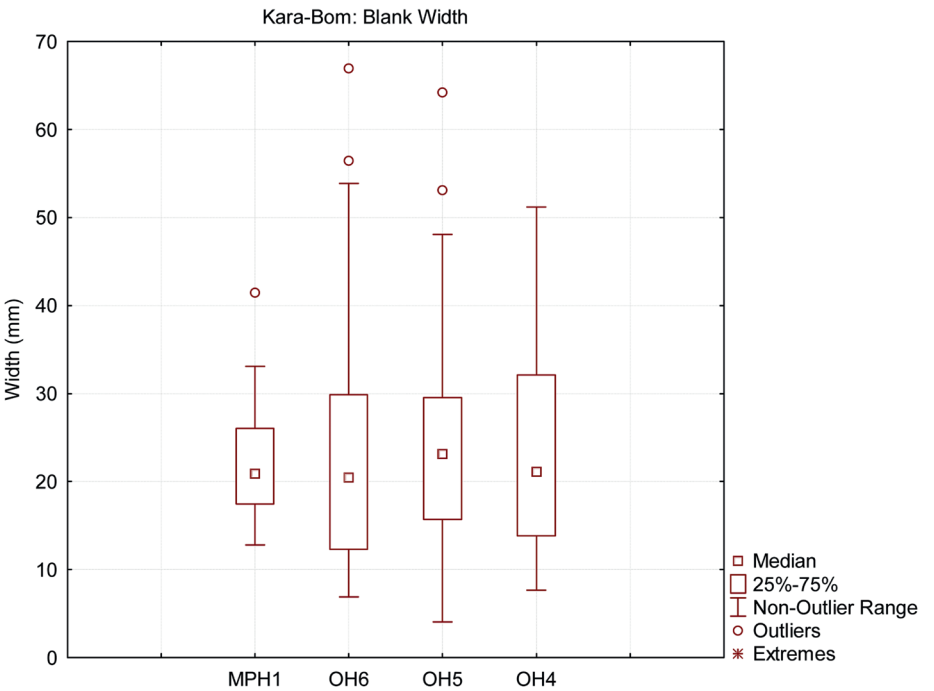

Figure 110: Kara-Bom, blank width, comparison between samples

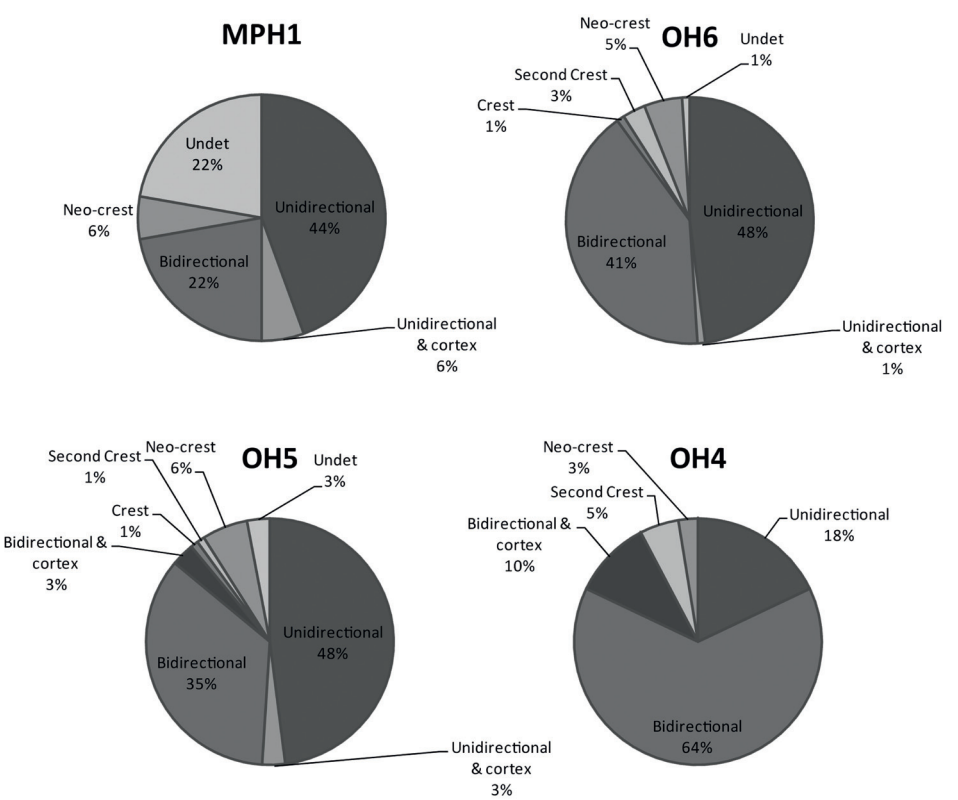

Figure 111: Kara-Bom, dorsal scar patterning, comparison between samples

frequency is significantly lower than in any of the three other assemblages.

Cross-section

MPH1 shows a majority of trapezoidal sections, although triangular ones are well represented. The situation in the OH6 assemblage is different. When considering the assemblage as a whole, triangular cross-sections are the most common, but their frequency does not statistically differ from the trapezoidal ones. The situation is similar when looking at the blade category, but the bladelets show a significant domination of triangular section. In OH5, the total sample and the blade category display a significant majority of trapezoidal sections, a situation which is reversed in the bladelet category where the triangular sections dominate significantly. OH4 shows a similar pattern with a majority of trapezoidal cross-section in the total sample and in the blade category, but the bladelet category is dominated by triangular cross-sections. So it seems that a consistent pattern is observed in the OH6, OH5 and OH4 assemblages with small laminar elements being more often produced using a single dorsal scar. MPH1 does not have any bladelets and is, therefore, not comparable.

Profile

All assemblages show a clear majority of straight profiles, usually followed by slightly curved ones. Frequencies of the other types of profile are trivial. The slight curvature of some of the blanks appears to be linked to the minimum bending or convexity of the core flaking surface necessary to proceed with a blade production, rather than a clear production oriented toward curved elements.

Orientation

Blanks are axially oriented in all the considered assemblage. No systematic off-axis blank production could be observed, although those elements occur infrequently within all assemblages.

3.7.2 CORES: REDUCTION PATTERNS AND SIZE ATTRIBUTES

The distribution of core types is uneven through the assemblage and leads to several observations.

- MPH1: the sample has yielded only two clearly identified cores. These are flake cores with one displaying radial flake scars on its dorsal face. The second one has a sub-triangular flaking surface and is mainly reduced from a single platform, although a second perpendicular platform seems to have been used to produce guiding scars. Two additional core-like tools are described. Although they look similar to Mode B cores, their core status could not be assessed.

- OH6: 29% (N=4) of the cores are classified as Mode A. The 71 % (N=10) remaining are Mode B cores.

- OH5: 20% (N=2) of the cores are classified as Mode A. The remaining 80% (N=8) are classified as Mode B cores.

- OH4: the sample includes a single core which, as it is produced on a Kombewa flake blank, is classified as Mode A.

Additional artifacts: relevant artifacts with problematic provenience, or belonging to the 1980-90 collections, although not included in the sample, are described. This set includes 10 % of Mode A cores (N=2), 76% of Mode B cores (N=16), core-like tools (N=2) and a single unclassified Mode B core.

Although this component is not directly related to laminar technology, an attempt to identify such cores in other assemblages led to the conclusion that genuine flake cores occur only within the MPH1 sample. Their frequency should be interpreted carefully as the sample size for this assemblage is rather low. They are not included in our Mode system that was designed for the categorization of blade cores. Mode A cores occur in a relatively low frequency in all assemblages except in MPH1. However, in OH4, Mode A does represent the only cores from our sam-

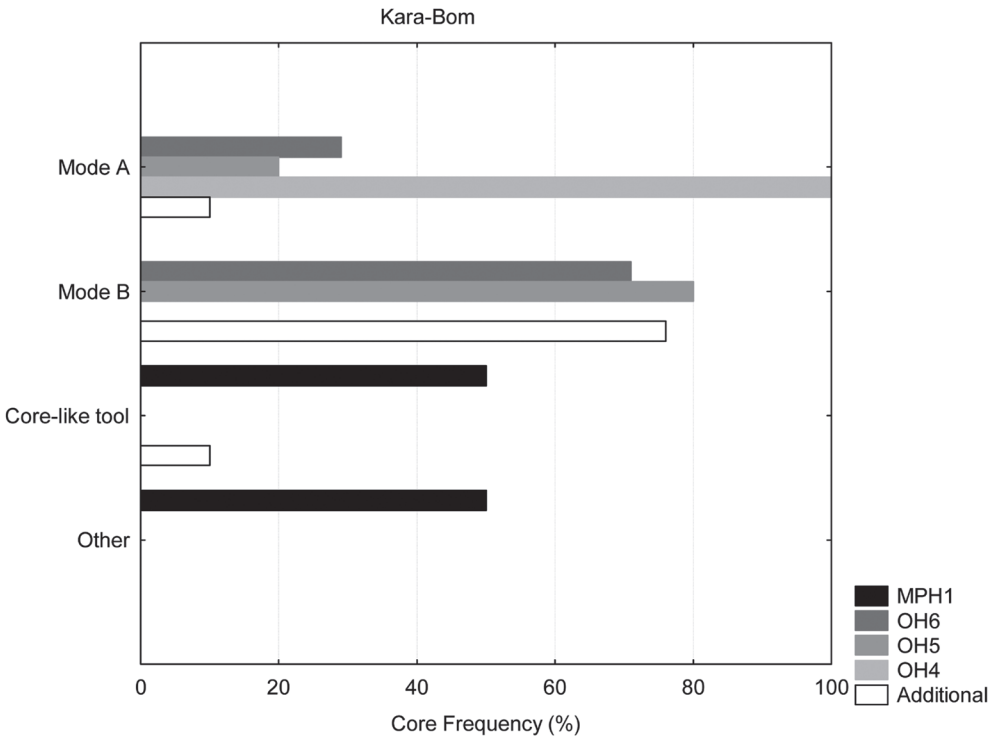

Figure 112: Kara-Bom, core Mode frequency, comparison between samples

ple and therefore, has a 100 % frequency. Mode B cores are clearly associated with OH6 and OH5, and they represent the majority of the cores. They are, however, absent in MPH1 and OH4 samples.

In OH6, differences between Mode A and Mode B cores are significant in terms of core length and flaking surface width. These differences are also observed in OH5, although their significance is not tested due to the small sample size. According to the measurement protocol described in Chapter 2, the Mode B core length is related to the thickness of the blade blank. As Mode B cores present almost exclusively a flaking surface on the narrow edge of the blank (with the exception of Mode B7), the flaking surface width depends on the blank thickness/core length. The statistical differences between core length and flaking surface width between Mode A and Mode B are then related to the type of core blanks but also reflect a reduction pattern. In fact, Mode B cores tend to show a main flaking surface on a broad face with an occasional use of a narrow face, as opposed to Mode B cores from which blanks are removed from a narrow face only.

The use of different faces is illustrated in Figure 113, where it appears that flaking surfaces do not differ in length but rather in width. 95 % confidence ellipses are drawn around each level using the full range of the axis. No ellipse was drawn for OH5 Mode A as only two data points were available. The latter, however, fall in a cluster with the OH6 Mode A ellipse. One Mode B core from OH6 falls in the range of the Mode A. It corresponds to a truncated-facetted core, which although produced on a laminar blank, displays a flaking surface located on a broad face. It is balanced by the fact that one Mode A core from OH6 falls in the range of the Mode B cores. This is a rather exhausted A10 core for which the determination of the blank was difficult. The general picture observed is that the difference between Mode A and Mode B cores seems consistent between OH. Mode B cores from OH6 and OH5 are produced on blades with a similar thicknesses (Mann-Whitney,

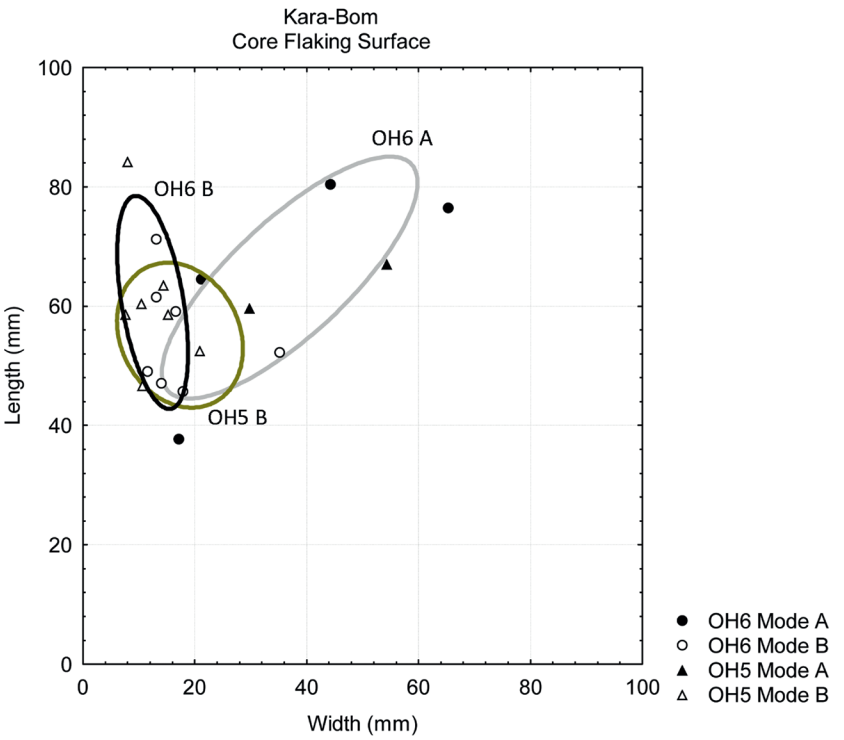

Figure 113: Kara-Bom, core flaking surface size and Mode reduction, comparisons between samples

T=Ub=30, p=.40) of minimum 10 mm. Even if they look similar between assemblages, Mode A size attributes are difficult to compare given their poor representation in the sample. Moreover, they likely represent an advanced stage of reduction and only provide a minimum size.

The only significant difference between OH5 and OH6 platform preparation stands in the Mode B cores, which are mainly facetted in OH6 (60%, N=6) and plain in OH5 (57%, N=4). A single facetted platform occurs in Mode B cores from OH5, and two plain reshaped platforms occur in OH6.

3.7.3 REDUCTION SEQUENCE RECONSTRUCTION: COMPARISONS

Blank production in MPH1 remains hard to assess. Flake production is attested to by the occurrence of radial and sub-triangular cores and occasional circular Levallois flakes and short convergent flakes. These coexist with a production of laminar elements. Laminar cores are absent from the sample, but the blank dorsal scar patterning seems to indicate a bi-directional core reduction system. This reduction system includes, at least occasionally, natural and shaped crested blanks. So the blanks used for Mode B cores are present although the two examples of core-like tools fail to be convincing enough to be considered as genuine Mode B. Small laminar blanks are not numerous. Platforms are mainly plain, but also facetted, the flake facetted platforms being significantly thicker than the laminar ones. All in all, the small sample from MPH1 does not allow a proper technological reconstruction.

Mode A cores from OH5 and OH6 show a certain degree of similarity. In OH6, they are classified as Mode A6. Mode A6 groups cores which presents two flaking surfaces treated independently. According to our analysis, the main flaking surface is located on the broad face. A second flaking surface seems to

be linked with the detachment of thick blanks, located at the intersection between the two surfaces, using a natural or a prepared crest as guiding ridge for the removal. The exploitation of the second flaking surface occurs mainly during the last stages of reduction. In both OH6 and OH5, two main types of blanks are produced.

Laminar blanks with parallel edges

Large blades are likely produced from Mode A cores, following the detachment of an initial crested blade. Judging by the dorsal scar patterning, the reduction is mainly bi-directional, showing platform switches after a short series of unidirectional removals. In the case of OH5, it seems that a platform switch may occur quickly after the beginning of the reduction, as some large blades bear on their dorsal face a combination of bi-directional scars and cortex. The occurrence of neo-crested blades of various sizes in both assemblages indicates rather frequent side preparation of the core during the course of the reduction process. Some of the largest blades can reach proportions tending to gigantism with a length reaching 180 mm. Some of the blades with a minimum of 10 mm thickness are selected and transformed into Mode B cores. These are snapped and flaked along their longitudinal axis. The variability in Mode B type is interpreted here as stages of reduction. In the sample studied, cores with a single striking platform are almost exclusively on the proximal part of the core blank (Mode B1). Mode B2 and B4, which would show respectively a single platform located on the distal part of the core blank and a flaking surface perpendicular to the axis of the core blank, are absent from both OH6 and OH5 assemblages. However, three examples are described in the additional artifact section, indicating that a distal reduction takes place when a truncation or a snapping event provides a surface thick enough to be used as a platform. Mode B5 is the most represented in both assemblages and shows a frequent switch of platform on the same flaking surface. The flaking surface is used on its entire length to detach blanks by a short series of unidirectional removals and only occasionally by an alternate bidirectional system.

The cores show, therefore, two kinds of blank production; a large blade production from which the technical blanks are used as core blanks to produce smaller laminar blanks. In such situations, a bimodal size distribution is expected. In OH6, although length and thickness show a unimodal distribution, a bimodal distribution is observed for the width. The first mode matches the size of the Mode B flaking surfaces and last removals. The second mode corresponds to the mean of the sample. In OH5, the situation is less clear. Although some signs that could indicate a bimodal distribution can be observed in the width distribution, they consist of a few artifacts only and are too weak to be significant. This could reflect the apparent overlap of flaking surface width between Mode A and Mode B. As previously mentioned, Mode B is well constrained by the thickness of the core blank, thus the width distribution of Mode A shows a greater variability. In other words, reduced Mode A cores can produce blanks comparable in size with the Mode B core early productions.

As for the large blades, small laminar blanks are detached from the intersection of two surfaces. They then display a thick triangular or trapezoidal cross-section or a natural back. Other small blanks are detached from the central part of the flaking surface and have a rather flat triangular or trapezoidal cross section. In both OH5 and OH6, cores but also blank dorsal patterning and cross-sections indicate, when possible, a rather significant number of blanks produced by Mode B cores. Cores with a few removals show traces of hinge fractures.

OH4 shows evidences of large blade production with parallel edges. As no cores can be associated with the largest artifacts, blanks only provide information on the reduction processes. Dorsal scar patterning indicates a predominance of bidirectionality. This feature is expressed more than in other assemblages.

The occurrence of bidirectional cortical blanks could indicate a use of bidirectionality in early stages of reduction. Crested artifacts and naturally backed blades indirectly indicate a sub-volumetric reduction system, with occasional readjustment of the bending and the convexities by removing thick blanks along an edge of the flaking surface. This technology pro-

duces thick blades that could potentially be used as Mode B core blanks although Mode B cores are absent. Small laminar blanks occur in the sample, some of them displaying a natural back. The only core associated with OH4 is a Kombewa flake/core tablet with a flaking surface on its narrow edge, flaked from two opposed platforms. The width histogram shows a bimodal distribution; however, this could be due to the small sample size.

Convergent blanks

All assemblages described include blanks with convergent edges. In MPH1, these are produced on short or relatively thick flakes by uni- or bidirectional reduction. One of the flake cores shows a clear triangular negative that matches the morphology of the shortest blanks. The preparation of the second flake core gives the flaking surface a triangular shape. This supports the idea that it could also have produced convergent flakes. In OH6, most of the convergent elements are on laminar blanks and show various thicknesses. Unretouched blanks are rather thin and bear bidirectional dorsal scars. Although it could not be demonstrated directly due to the lack of refits, it is assumed that the largest blades are associated with Mode A cores, especially when they are reduced by bidirectional removals from the broad flaking surface.

Platform preparation and percussion technique

Identifying the technique of percussion is problematic in most of the levels due to the mosaic of features observed. From a general point of view, none of the assemblages show traces of thin abrasion usually associated with the organic hammer. OH6 and OH5 show clear similarities with a combination of thick (mean ≥ 4mm) facetted and plain platforms associated with an occasional strong abrasion of the platform edge. In addition, a peculiar preparation described here as partial faceting occurs in both assemblages. These features suggest the use of hard and soft stone hammers. OH4 has only one case of strong abrasion, no partial faceting and only the facetted platforms can be considered as thick. The sample is too small to propose a hammer type even if some similarities with OH6 and OH5 can be observed.

For the same reasons, although MPH1 shows similarities with the OH6-OH5 sample, the technique of percussion could not be assessed. Notable is the absence of features associated with the use of a soft hammer.

Retouched tools

Retouched tools show a similar width mean and median in all sampled assemblages ($F(3, 77) = 0.433$, $p = .73$), the main differences being related to the variability within the sample. MPH1 shows a relatively narrow variability that may reflect a small sample size. The distribution displays a positive skew towards narrow blanks. By contrast, OH6 illustrates the largest variability among the samples, followed by OH5. OH4 shows a rather similar range as MPH1 although it displays the widest outlier data point.

To illustrate these differences in terms of width variability, the coefficients of variation are compared between samples. As shown in (Table 78), OH6 has the highest coefficient of variation, as MPH1 show the most standardized tool widths. Coefficients of variation are compared using Fligner-Kileen test (Fligner and Killeen 1976). The results show that only the differences between OH6 and OH4 are significantly different. Surprisingly, differences between MPH1 and OH6 appear not significant. This result could reflect the effect of MPH1 small sample size (N=9) inducing a type II error.

The coefficient of variation is here proportional to the sample size. This could explain the highly reduced variability of MPH1 sample and the largest variability of OH6. However, when considering thickness values, the opposite situation is observed. Values are inversely proportional to the sample size. Differences are not significant except between OH5 and OH6 (Mann-Whitney, T=Ub=258.5, p=.02). Except for MPH1, a monotonic trend is observed between assemblages OH6 to OH4, the toolkit tending to be thicker. When comparing the thickness of the OH4 tool kit with the thickness of the laminar blanks, no

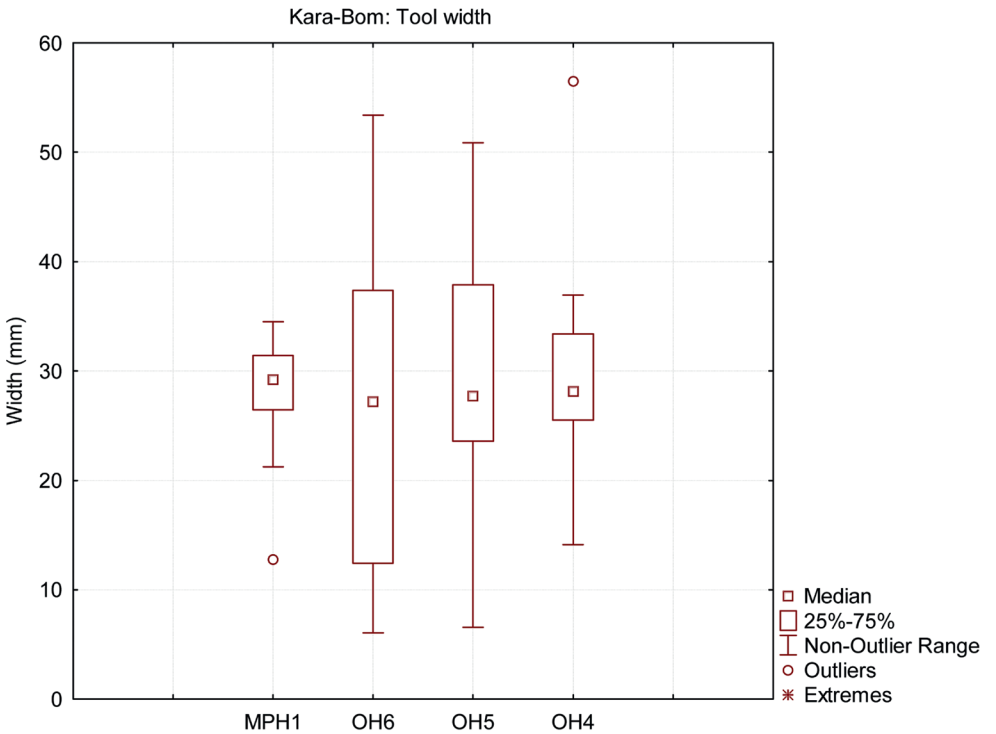

Figure 114: Kara-Bom, tool width, comparison between levels

Sample	Coefficient of variation	Fligner-Kileen test	one-tailed	two-tailed
MPH1	24%	MPH1 vs. OH6: T=2.47; E(T)=7.32; z=1.7	p=.05	p=.09
		MPH1 vs. OH5: T=5.44; E(T)=7.29; z=-0.65	p=.26	p=.51
OH6	50%	OH6 vs. OH5: T=17.25; E(T)=24.34; z=1.6	p=.05	p=.11
OH5	37%	OH5 vs. OH4: T=12.73; E(T)=13.83; z=0.3	p=.38	p=.76
OH4	32%	OH4 vs. MPH1: T=6.82; E(T)=7.06; z=-0.09	p=.46	p=.92
		OH4 vs. OH6 : T=6.35; E(T)=13.87; z=-2.04	p=.02	**p=.04**

Table 78: Kara-Bom, coefficient of variation (tool width), comparison between samples

significant difference is observed. When comparing length and width measurements between samples, it appears that OH6 differs from the other assemblages by the fact that it includes relatively small-sized tools. OH5 size distribution shows a different pattern mainly due to the occurrence of the sickle-like blades, one of which is particularly elongated and narrow. Only two MPH1 tools are complete. One is a retouched blade which matches with the OH6-OH4 range, the other one is produced on a Levallois flake blank and falls outside of all ranges, having a length roughly equal to its width.

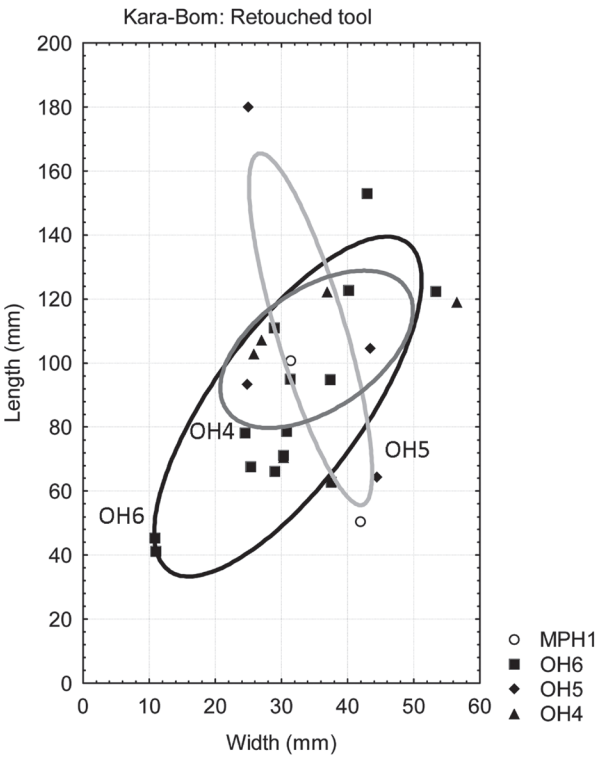

Figure 115: Kara-Bom, tool size, comparison between samples

The tool dorsal scar patterning shows a domination of bidirectional blanks, which tends to be more pronounced in the OH5 sample and less expressed in the OH6 sample. None of the differences observed are statistically significant. Artifacts bearing cortex on their dorsal face are occasionally retouched in OH5 and OH4.

The general composition of the tool kit described here shows the occurrence of retouched blades in every sample. Thet clearly dominate in MPH1, as only retouched tools are considered here. For example, Levallois flakes which are listed as tools according to Bordes's list (1961) are not included in our tool list, unless they display retouch. A single artifact is included in this category, namely a notched Levallois flake which is included in the category 'other'. The frequent occurrence of edge damage is another main feature that characterized the MPH1 toolkit. Identification of genuine retouch is not easy. Although three of the retouched blades have been typed as notched blades, they also display edge damaged along their edges.

One blade is pointed by a bilateral retouch on its distal end. The two core-like tools could represent an element of comparison with OH5 and OH6, but they could not be clearly identified as Mode B cores. The absence of retouched convergent blanks in MPH1 seems to illustrate a difference with the other assemblages. In OH6 to OH4, although a decrease of this category of tools is observed, differences in frequency between levels are not statistically significant (χ^2=(2) 168.1, p=.43). When looking at the retouched blade frequencies, there is a significant difference observed between OH6 and OH5-OH4 (χ^2=(2) 5.852, p=.05). Retouched bladelets are more frequent in OH6 than in OH5 (χ^2=(2) 3.694, p=.05) and are absent from the other samples. In fact, a single retouched bladelet occurs in OH5 and six are identified in OH6. Two Dufour bladelets (sub-type Dufour) and one atypical backed bladelet occur in OH6 sample. Due to the lack of systematic screening

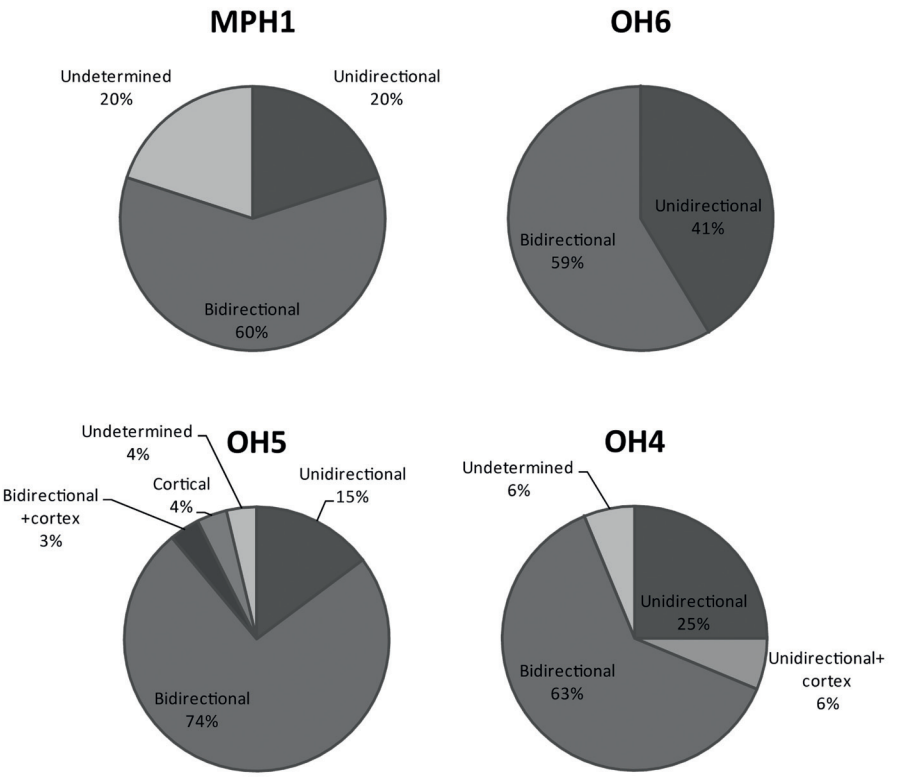

Figure 116: Kara-Bom, dorsal scar pattern, comparison between samples

during excavation campaigns, the frequency of small artifacts should be considered as a minimum.

In OH6, facetted platforms dominate but in OH5 they are as frequent as plain platforms. In OH4, all platforms are facetted with only one being dihedral. This difference may be significant; however, given the amount of undetermined platform type in OH6 and OH5, it cannot be properly tested. In MPH1, the majority of tools are mesial fragments. In OH6, retouch seems to be located mainly on the distal and proximal parts of the blanks, which could explain the lack of mesial tool fragments identified in that sample. In OH5, the retouch is mainly continuous although most of the fragments are mesio-proximal. In all samples, the retouch is mainly direct, with a infrequent occurrence of inverse retouch in OH6.

The types of retouch vary with a clear domination of thin retouch in OH6 and OH4. This observation is reinforced by the fact that combinations almost always include thin retouch. In OH6, they are associated with semi-steep retouch. In OH5 and OH4, it is associated with semi-steep, steep and scaled retouch. OH5 stands out as having significantly more scaled retouch than OH6 (χ^2=(1) 5.825, p=<.05) but this difference is not significant when compared with OH4. Notches are the most frequent type of retouch in MPH1, but they occur occasionally in other samples.

From a more general point of view, the quasi-absence of classic burin types on thin blanks is observed. No clear example of this tool class could be found in association with the studied samples. Pointed blades occur in every sample, even though they are generally not numerous. Some of these tools tend to resemble a retouched point, although they are originally produced on blanks with parallel edges. The sickle-like blades occur only in OH5 and can, therefore, be considered as typical of this assemblage.

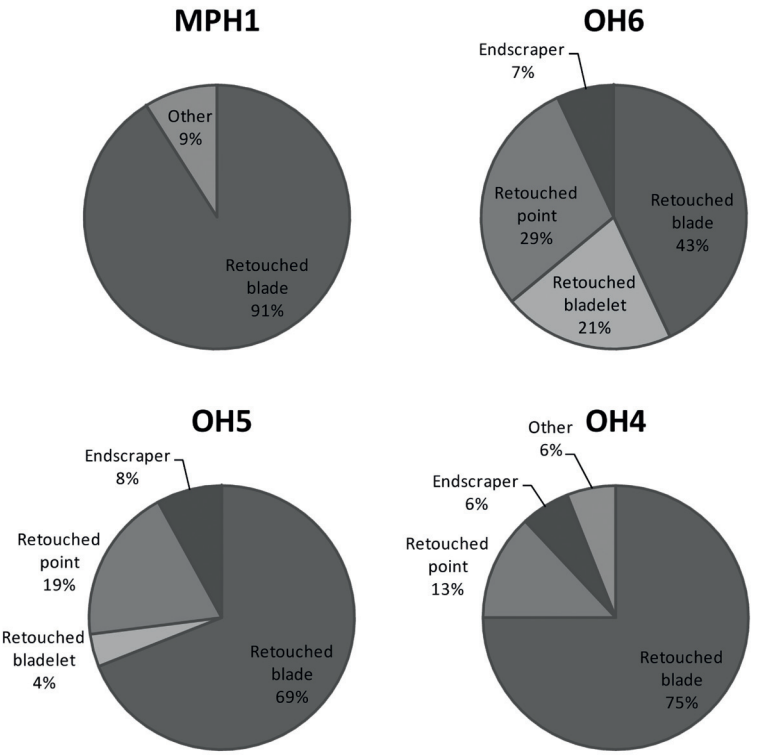

Figure 117: Kara-Bom, main categories of retouched tool, comparison between samples

	MPH1		OH6		OH5		OH4	
	N	%	N	%	N	%	N	%
Thin	1	10%	13	46%	3	12%	8	50%
Semi-steep	1	10%	2	7%	4	15%	0	0%
Steep	0	0%	0	0%	3	12%	0	0%
Scaled	0	0%	1	4%	7	27%	2	13%
Nocth	4	40%	4	14%	1	4%	1	6%
Combination	2	20%	8	29%	6	23%	4	25%
Other	2	20%	0	0%	2	8%	1	6%
	10	100%	28	100%	26	100%	16	100%

Table 79: Kara-Bom, main type of retouch, comparison between samples

	MPH1	OH6	OH5	OH4
Platform preparation	Plain + facetted	Facetted + plain	Facetted + plain	Plain + facetted
Dorsal scar pattern	Uni + bidirectional	Uni + bidirectional	Uni + bidirectional	Bidirectional
Cross-section	Trapezoidal	Triangular + trapezoidal	Trapezoidal + triangular	Trapezoidal + triangular
Profile	Straight	Straight	Straight	Straight
Orientation	None	None	None	None
Core Mode	Flake	Mode B + Mode A	Mode B + Mode A	Mode A?

Table 80: Kara-Bom, main characters of the blade production, comparison between samples

3.7.4 SUMMARY

From a technological point of view, OH6 and OH5 are highly similar. Both of these samples display an association of laminar blanks with parallel edges and laminar blanks with convergent edges. Blanks are produced following a bidirectional reduction sequence which includes Mode A sub-prismatic cores with a main flaking surface located on a broad side of the nodule interacting with a second flaking surface located on a narrow face of the nodule and likely involved in the management of convexities and bending of the broad flaking surface. Detached blanks detached are mainly large to medium size axial blades with a triangular or trapezoidal cross-section and a plain or facetted platform. Management operations occur in different stages of the reduction by the detachment of thick natural or prepared crested blades at the intersection of the two flaking surfaces. Some of the crested blades are then transformed into Mode B cores which morphologically fall into *burin d'angle* (Demars and Laurent, 1992) and *burin polyedrique* (Klaric, 2006, 2008; Klaric *et al.*, 2009) types. Those cores often illustrate a bidirectional reduction sequence system, following short series of unidirectional removals detached from two opposed platforms. The flaking surface is parallel to the longitudinal axis of the blank and is exploited on its whole length. Removals coming from the central part of the flaking surface have a triangular or trapezoidal and rather flat cross-section, as removals detached from the corner of the flaking surface are thicker and are similar to burin spalls, displaying a part of the dorsal or ventral side of the core. So far, Mode B cores can be only associated with OH6 and OH5 samples.

Convergent blanks are produced from the broad face of sub-prismatic cores, using a management system comparable with the one used for blanks with parallel edges, namely the detachment of thick side and crested blades. As the pattern of reduction is subparallel, convergent edges are likely linked with the bidirectional reduction sequence.

The MPH1 sample size is too small to offer the possibility to make robust quantified comparisons. However, it differs from OH5 and OH6 by the coexistence of a flake production from radial, flat-faced and bidirectional cores and blade blanks. Some of the flake blanks are likely Levallois flakes, showing a radial dorsal patterning and some may be represented in the sample as short convergent blanks. Blades show similarities with OH6 and OH5 in that they have a combination of uni- and bidirectional dorsal scar patterning, but also by the coexistence of plain and facetted platforms. Thick side blades and discrete crested elements may indirectly testify to a sub-volumetric reduction system. Small laminar elements are almost absent. The two core-like tools are not sufficient to suggest the use of Mode B cores,

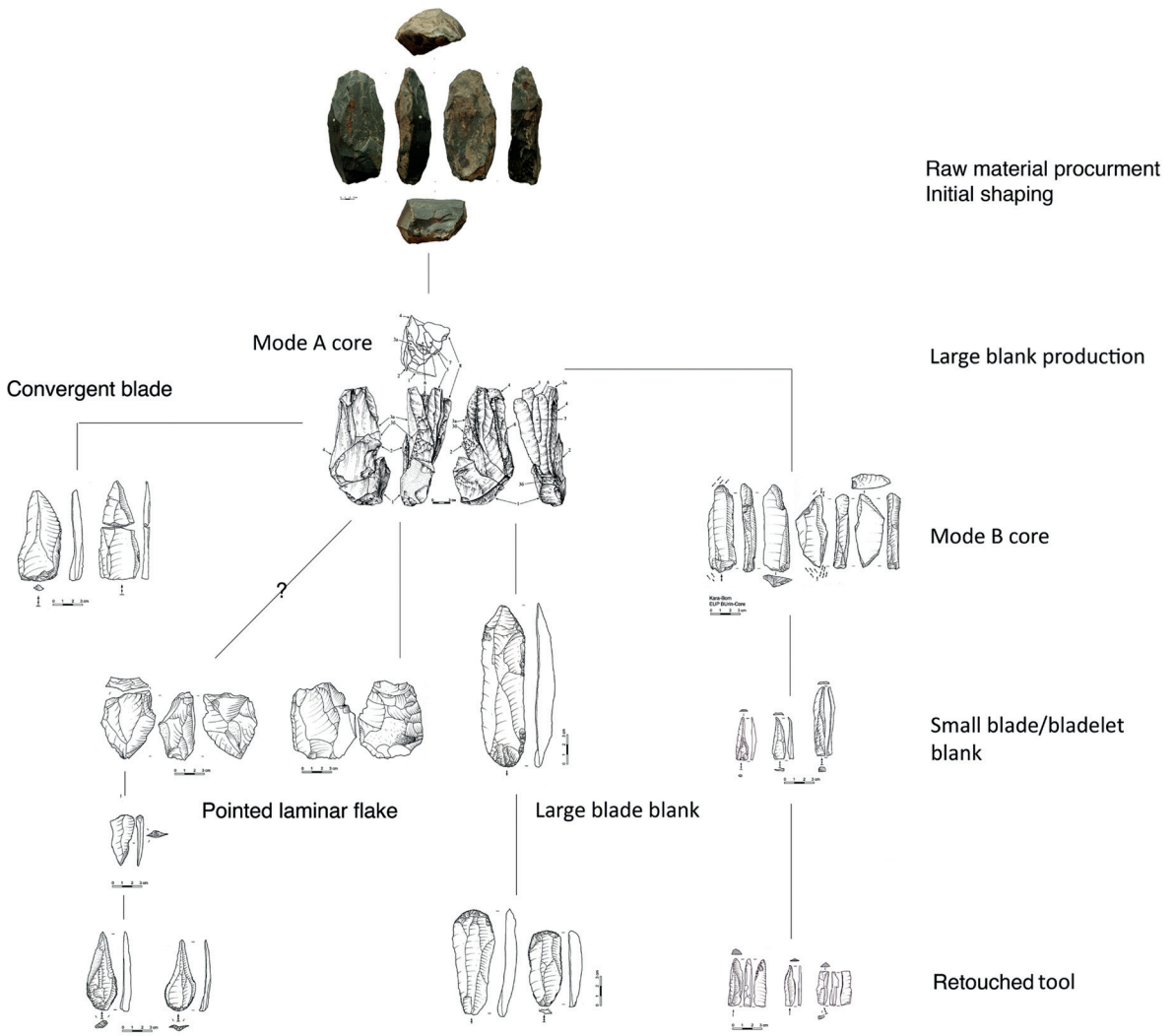

Figure 118: Kara-Bom, analytical reconstruction of the blade reduction systems from OH6 and OH5

although the situation could have been different with a larger sample.

The OH4 sample size, although larger than MPH1, remains insufficient to obtain a clear picture of the blade technology associated with this assemblage. The single Mode A core described is rather atypical and is hardly representative of the morphological diversity observed among the blanks. Blanks are similar to OH6 and OH5 except that they show a more pronounced bidirectional dorsal patterning. Platforms are facetted and plain, sometimes showing a *débordant* morphology, indicating a removal at the junction of two surfaces. Partial faceting is absent and a single blade shows strong abrasion on the platform edge. Crested, side blades and small laminar elements also occur. Looking at the general morphology of some of the small laminar blanks, a possible technology similar to Mode B is not excluded; however, none of these cores are found in association with our sample.

The MPH1 toolkit shows a frequent occurrence of edge damage on the retouched and unretouched

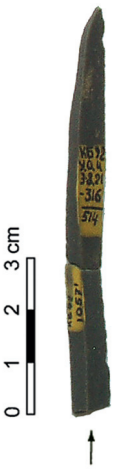

Figure 119: Kara-Bom, refitted fragments of a mesio-distal elongated spall from OH4

blanks, however, some notched tools seems to be produced intentionally. Retouched blades, especially pointed blades, are common in all samples. OH6 includes a significant series of retouched convergent blanks, showing retouch in their proximal and distal ends. The most typical elements in OH5 are the sickle-like blades, which are absent from the other samples. This sample also shows a significant amount of pieces modified by scaled retouch. Both OH6 and OH5 yielded endscrapers on medium/large blade blanks. OH4 tools are characterized by retouched blades, some being pointed by an asymmetrical truncation. Except for MPH1, all samples have yielded retouched convergent blades, however, the OH4 sample includes only a single example.

3.8 UST-KARAKOL 1 SITE DESCRIPTION AND TECHNOLOGICAL ANALYSIS OF OH5.4-5.5 ASSEMBLAGE (SECTOR1)

In this section, sector 1 (1986 excavation) and sector 2 (1993-1997 excavation) from the site of Ust-Karakol 1 are described in detail. The lithic analysis focuses on the Kara-Bom type assemblage OH5.4-5.5 from sector 1. Further descriptions of the Early Upper Paleolithic assemblages from sector 1 and sector 2 are provided in the forthcoming sections.

3.8.1 GEOGRAPHICAL SETTING

The site of Ust-Karakol 1 (51°22’ 50 N, 84° 41’ 20 E) is located 2 km southeast of Denisova Cave, at the confluence of the Karakol and Anuy rivers (Derevianko *et al.*, 1987, 2003; Derevianko, Markin, *et al.*, 2001). The Karakol and Anuy valleys cut into the relief with an approximate depth of 200 to 250 m. The geomorphology surrounding Ust-Karakol consists of an alluvial plain and steep hillside. The floodplain contains alluvial clay deposits overlying a layer of pebbles and gravels with a sandy filling. At about 7-10 m from the modern river level, the pebble layer overlies the bedrock and is located at the bottom of a 6.5 m sequence of deposits, from which about 5 m are attributed to the Pleistocene. The highest terraces reach the approximate elevation of 35-40 m above the river level (Derevianko, Markin, *et al.*, 2001; Derevianko *et al.*, 2003).

3.8.2 BACKGROUND

The site was discovered by Derevianko in 1984 and a first campaign of excavation took place in 1986, under the field direction of Markin (Derevianko *et al.*, 1987) . A surface of 120 m² (sector 1) was excavated in an area where the ground level slopes approximately 11° (UK1-1). A 4.95 m profile was exposed and divided into 10 lithological strata, 9 of which are attributed to the Pleistocene. Four horizons yielded archeological remains. Between 1993 and 1997, a second stage of research was carried out under the field direction of Postnov (Derevianko, Markin, *et al.*, 2001; Derevianko and Rybin, 2003). The new excavation (sector 2) is located 5 m east of the sector 1 limit (Slavinsky, 2007). It covers a surface of 250 m² at 7-10 m above the river level (UK1-2). A 6.5 m profile is exposed in an area where the ground level slopes approximately 13°. The stratigraphic profile is divided in 20 lithological strata, the majority of which are attributed to the Pleistocene. Ust-Karakol 2 (UK2) is located upslope at approximately 50 m from UK1-2 (Maloletko and Panichev, 1990). Zenin later connected UK1-2 and UK2 by digging a trench along the slope; however, the results of this excavation remain, up to now, unpublished. Although UK1-1 was reported as being circa 5 m east of UK1-2,

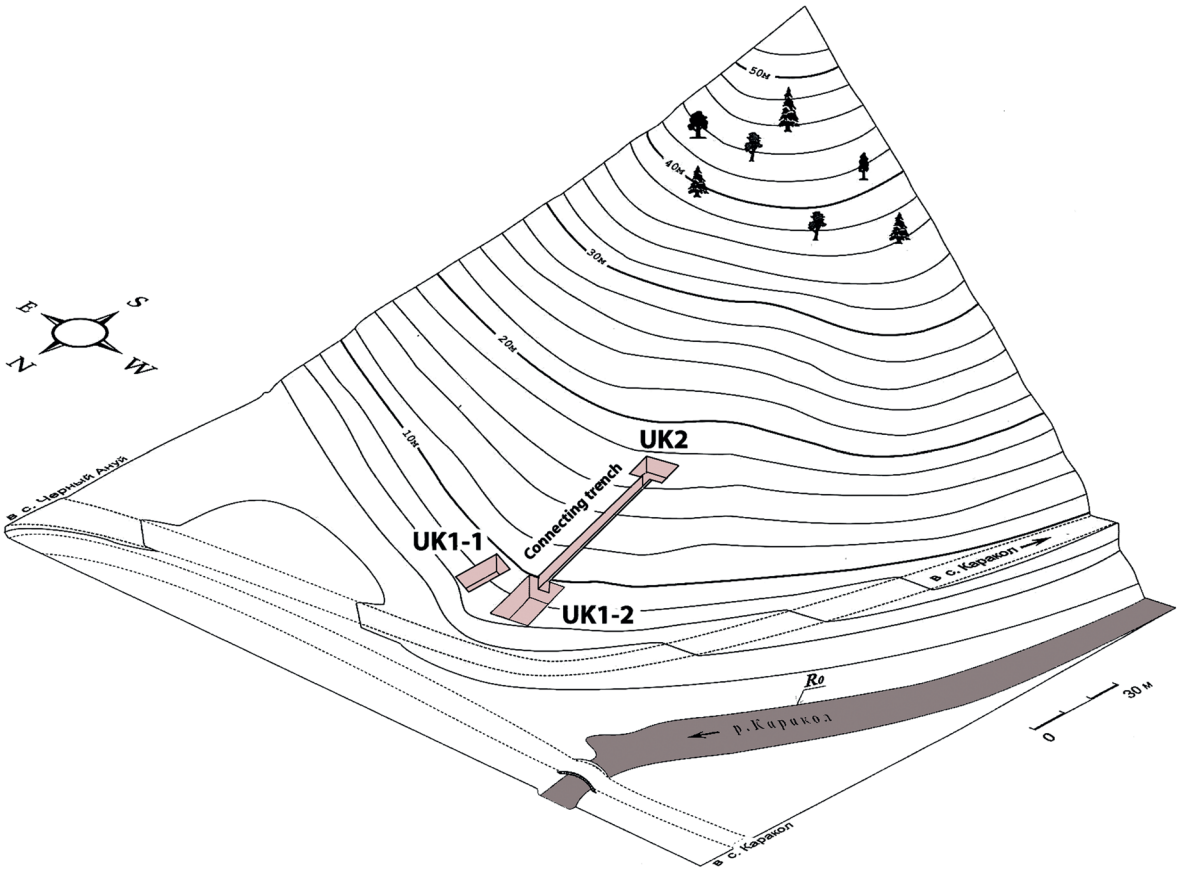

Figure 120: Ust-Karakol, general reconstruction of the excavation areas (modified after Derevianko *et al.*, 2003)

the two sectors were never connected. Based on published data, the sites are here approximately located on a general map (Figure 120).

3.8.3 STRATIGRAPHY

UK1-1

UK1-1 profile is subdivided into 10 lithostratigraphic strata (Derevianko *et al.*, 1987; Derevianko, Shimkin, *et al.*, 1998). Stratum 1 corresponds to the modern humus, Ceramic and bone fragments found in this stratum represent cultural level 1. Stratum 2 is made of light brown loam with isolated quartzite elements and limestone debris, shales and jasper. A few flakes and isolated bison and red deer remains are designated as cultural level 2. Stratum 3 contains medium size limestone blocks, pebbles and brown loam. Stratum 4 consists of silty clay sediments and contains traces of reworked humus beds. Stratum 5 is made of bedded yellowish brown loam, with small pebbles and gravels. Ferrous traces are rare and scarce. According to Derevianko and colleagues (1987), the lower part of stratum 5 contains cultural level 3. Stratum 6 contains isolated artifacts assigned to cultural level 4. The cracks are filled with sediments coming from stratum 5. Stratum 6 is composed of a gray homogenous loam and isolated limestone debris and shows the occurrence of horizontal, vertical and oblique frost cracks. Stratum 7 shows the occurrence of medium-sized limestone blocks and a dark gray loamy fill. Frost cracks are reported coming from the overlying stratum. Stratum 8 is made of homogenous dark-gray silty-loamy sediments,

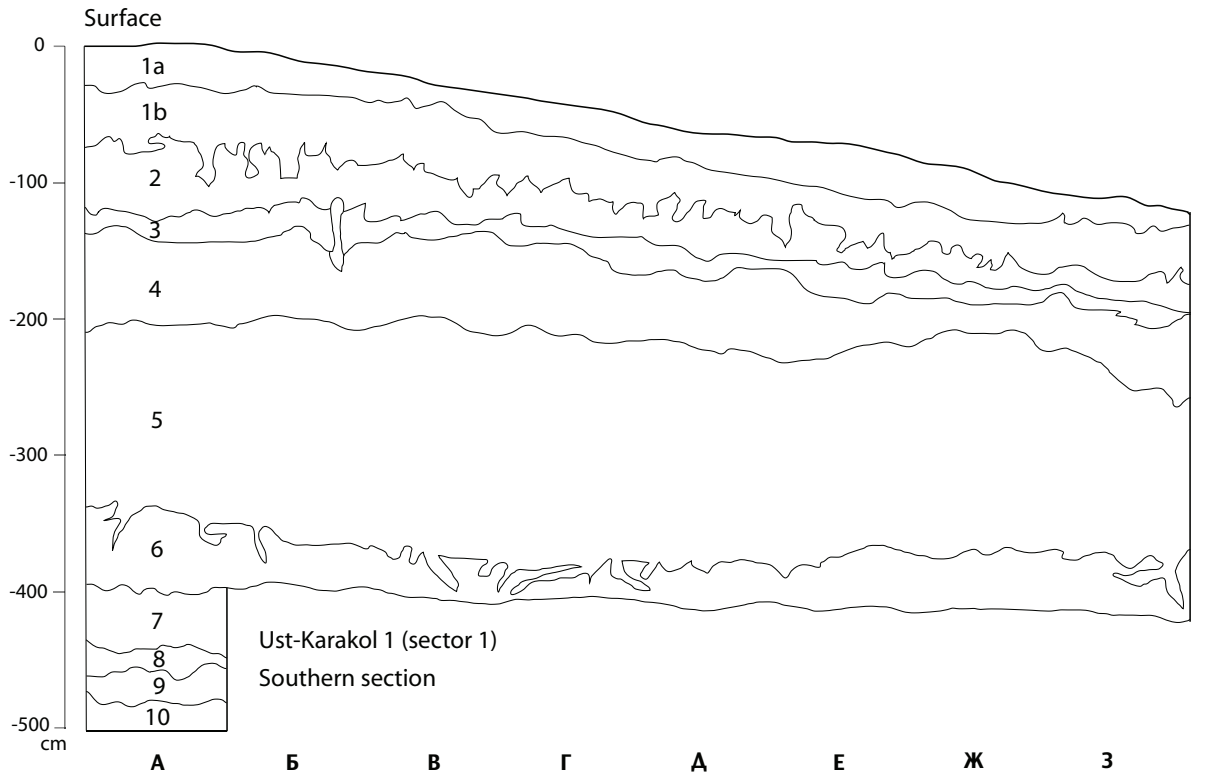

Figure 121: Ust-Karakol 1 sector 1, southern section, numbers indicate lithological strata (modified after Derevianko *et al.*, 1987)

bedded at the bottom with ferrous spots. Stratum 9 consists of gray clay with clear ferrous traces at the bottom, isolated pebbles of shale and sandstone. The lowermost stratum (10) is composed of small pebbles and boulders (sandstones and shales) with, at the top of the stratum, clay and sands. The richest human occupation is cultural level 3 from the lithological stratum 5, with an assemblage originally attributed to Early Upper Paleolithic (Derevianko *et al.*, 1987; Derevianko, Shimkin, *et al.*, 1998).

UK1-2

UK1-2 is divided in 20 lithostratigraphic strata, some of which are divided in sub-strata (Derevianko, Markin, *et al.*, 2001; Derevianko *et al.*, 2003). Stratum 1 represents the modern soil and stratum 4 is characterized by the presence of blocks and gravel. Strata 1-4 are composed of loose loess-like sediments with vertical cracks. Strata 5 and 8 are described as buried soils separated by gravels (stratum 7) and by a sandy-loam level containing evidence of soil formation. Strata 5-11 are described as loess and brown loam, containing traces of soil formation. According to Derevianko et al (2001), the deposition of stratum 11 is said to take place after a gap in the sedimentation process. Strata 12-17 includes layers of laminated red-brownish sandy loams. Laminations make the border between strata hard to follow. Stratum 18 is made of dark colored dense clayey silts containing rock debris. It is divided into two sub-strata and originates from the flood plain and from the hill side (rock). The underlying stratum 19 is divided into two sub-strata (19A and 19B). It consists of alluvial deposits and is made of sand and silt. Stratum 20 is composed of cobbles and pebbles cemented by a sandy filling. Although almost all strata have yielded archeological material, the richest assemblages are described in strata 8-11 (UP) and in strata 18-9 (MP). Strata 12-17 include small assemblages (MP) (Derevianko, Markin, *et al.*, 2001; Derevianko *et al.*, 2003).

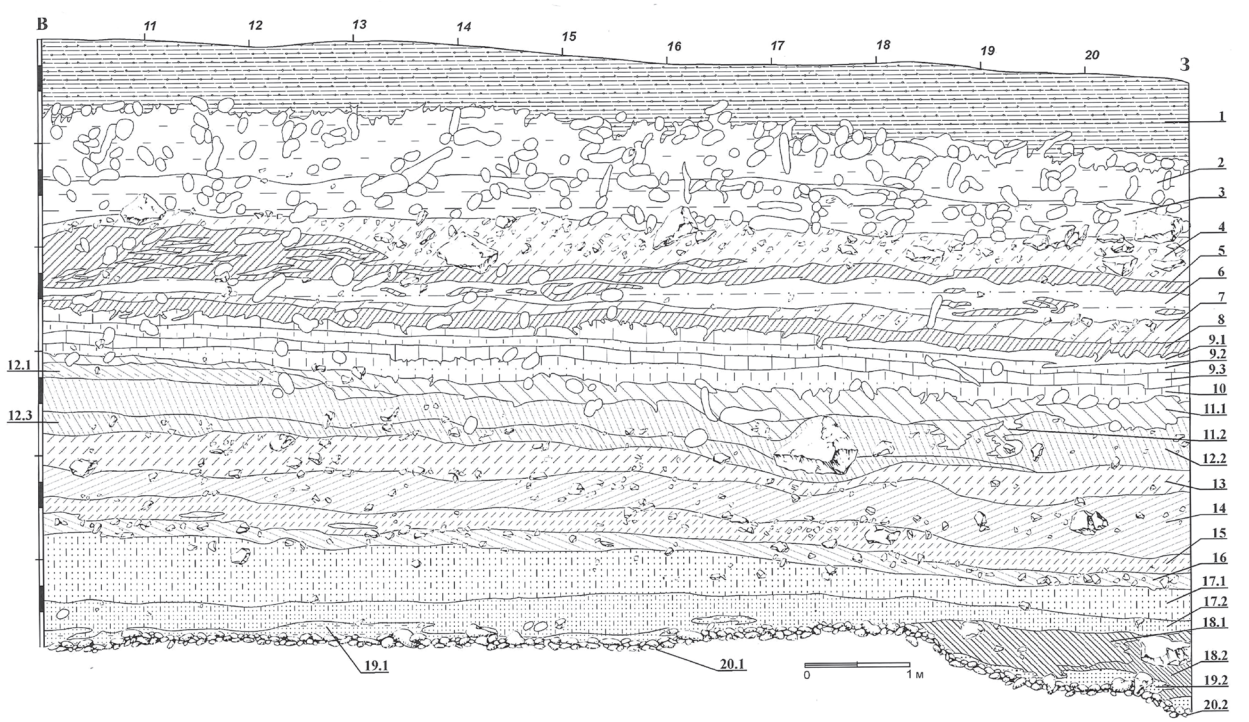

Figure 122: UK1-2, southern section (Derevianko *et al.*, 2003)

3.8.4 CHRONOLOGY

UK1-1

Two oval shaped hearths (0.7-0.8 m diameter) were identified in the lower part of stratum 5 (between -325 and -340 cm), associated with cultural level 3. Charcoal samples from two of combustion features gave conventional ages to 31, 410 ± 1,160 (SOAN-2515) and 29,900 ± 2,070 ^{14}C BP (IGAN-1077). A bison bone coming from stratum 2 was dated to 28,700 ± 850 ^{14}C BP (SOAN-2614) (Derevianko *et al.*, 1987; Derevianko, Agadjanian, Baryshnikov, *et al.*, 1998; Derevianko, Shimkin, *et al.*, 1998). Only a few unidentified bone fragments are reported as associated with the hearths. Strata 1 to 6 have yielded palynological data. Stratum 5 and 6 indicate an open forest-steppe environment with an increase in moister in stratum 4. Strata 3-1 indicate a gradual decline of arborous species in favor of the grass species. Derevianko *et al.* (1990) attribute stratum 6 to the Zyrian period (OIS5a-d/4), stratum 5 to the Karginina interstadial (OIS3) and based on the occurrence of frost cracks, stratum 2 to the Lipovsko-Novoselovo (end of OIS3).

UK1-2

This excavation area has yielded radio-thermo luminescence (RTL) and radiocarbon dates (Derevianko, Agadjanian, Baryshnikov, *et al.*, 1998). The RTL dates have yielded ages with large standard deviations, making their interpretation difficult.

Conventional radiocarbon dates indicate an age between 38 and 32.2 ka ^{14}C BP for stratum 10 and between 32 and 26 ka for stratum 5. Stratum 3 and 2 radiocarbon ages range between 32.7 and 28 ka (Derevianko, Agadjanian, Baryshnikov, *et al.*, 1998; Derevianko and Rybin, 2003). The results are problematic, as they seem to show younger ages in stratum 5 than in strata 3 and 2. However, when considering the oldest dates from each level as more reliable, the majority of the dates overlap at one sigma.

Stratum	Sample	RTL	Lab number
9	burned sediment	50±12	RTL-660
18	alluvial sediment	90±18	RTL-658
18	alluvial sediment	100±20	RTL-659
19	alluvial sediment	133±33	RTL-661
20	alluvial sediment	207±41	RTL-662
20	alluvial sediment	210±42	RTL-640

Table 81: UK1-2, RTL dates

Stratum	Sample	Radiocarbon (^{14}C BP)	Lab number
2	Bone	31,430±1,180	IGAN-1077
2	Bone	28,700±850	SOAN-2614
3	Charcoal	31,345±1,315	SOAN-2869
3	Charcoal	31,410±1,160	SOAN-2515
5	Charcoal	26,305±280	SOAN-3261
5	Humates	26,920±310	SOAN-3356
5	Charcoal	27,020±435	SOAN-3356G
5	Charcoal	30,460±2,035	SOAN-3260
9	Charcoal	29,860±355	SOAN-3358
9	Charcoal	29,720±360	SOAN-3359
9	Charcoal	33,400±1,285	SOAN-3257
10	Charcoal	35,100±2,850	SOAN-3259

Table 82: UK1-2, radiocarbon dates

Geomagnetic analyses have been performed on a stratigraphic section, indicating 3 excursions: Lachamp (44-42 ka) in stratum 11, Mono (30-25 ka) in stratum 5, and Gothenburg (13-11 ka) in stratum 2 (Derevianko *et al.*, 2003). These results are in contradiction with the radiocarbon ages of stratum 2. Palynological analysis carried out by Malayeva indicates the occurrence of eight palynozones. These results are interpreted as reflecting alternating changes between two main floral complexes, namely a birch/pine-birch environment and taiga forest. The latter would indicate a cooler and more humid climate. On the long term, Malaeva interpreted these changes interpreted as a general cooling of the climate (Derevianko *et al.*, 2003).

About 107 identifiable bone remains have been collected throughout the whole Pleistocene sequence. This poor assemblage is unevenly distributed among the strata and does not allow any diachronic recon-

struction. *Bison priscus, Carpeolus pygargus, Poephagus mutus, Crocuta spelea, Cervus elaphus, Megaloceros giganteus, Procapra gutturosa, Capra siberica* and *Ovis ammon* are the main species identified. Some of these correspond to a forest (deer and red deer) or a mountain (Siberian goat) environment or to a steppe and meadow steppe environment (Mongolian gazelle) (Derevianko *et al.*, 2003; Vasiliev, 2003). About 27 species of small mammals have been identified (Agadjanian and Serdyuk, 2005). Long-tailed squirrels *(Spermophilus undulatus)* and zokors *(Myospalax myospalax)* are the most common, respectively, in strata 19 to 11 and 11 to 1. Forest species are more present in the lower part of the sequence. More generally, strata 19 to 13 are attributed to the Ermakovo period and strata 11 to 5 are attributed to the Karga interstadial period. The strata 4-2, although attributed to the Sartan period, have yielded radiocarbon estimations, indicating a Karginian age (OIS3) (Derevianko *et al.*, 2003; Agadjanian and Serdyuk, 2005).

One conventional radiocarbon date is reported from UK2. The 31,430 ± 1,180 ^{14}C BP (IGAN-1177) age is associated with a layer correlated with the stratum 5 at UK1-1 (Cherkinskii *et al.*, 1992).

3.8.5 TAPHONOMIC APPROACH

UK1-1

In a recent study, Slavinsky (2007) produced a series of refits from cultural level 3 from UK1-1. The results that he presented have strong implications regarding the integrity of the assemblage. Based on a planimetric reconstruction of the artifact distribution, Slavinsky proposes dividing stratum 5 into five sub-strata (Slavinsky, 2007). According to him, these strata correspond to five independent occupation horizons (OH), labeled from 5.1 to 5.5. Among these occupations, he distinguishes two main technological traditions. The first one groups OH5.1 to OH5.3, and the second groups OH5.4 and OH5.5. Based on a series of refits, he also argues that OH5.4 corresponds to a homogenous short term occupation. However, Slavinsky's planimetric model does not clearly rule out a possible influence of slope effects. Using the same data, ranges of altitude have been projected on a longitudinal section A14-3 and on the transversal southern section (A14-Z14). Artifacts are plotted arbitrarily in the middle of each square. Only a few data points have been discarded from the projection

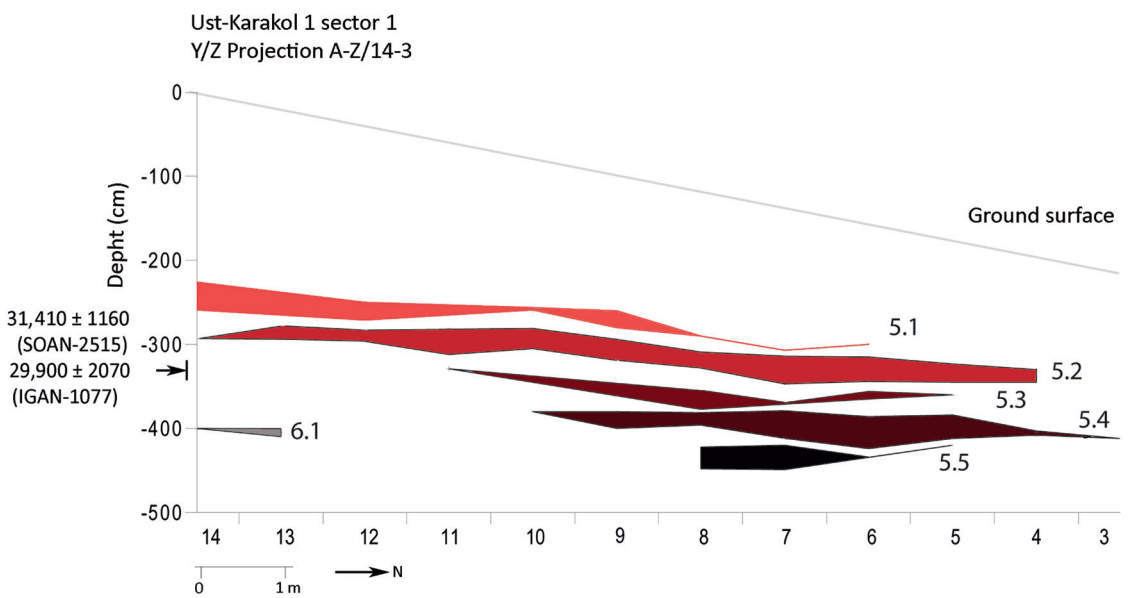

Figure 123: UK1-1, longitudinal projection of the piece-plotted artifacts based on their altitude range (data from Slavinsky, 2007)

as they had ambiguous labels. The longitudinal projection shows clearly that artifacts can be grouped in five different concentrations separated by sterile horizons ranging from circa 30cm down to a few cm in thickness. It is worth noting that none of the subunits are actually connected, although it could have been expected when projecting 8 m² on to a section. OH6.1 is reported as belonging to stratum 6 and appears here at the same altitude as OH5.4. This may imply that stratum 6 has a steeper slope then OH5.1-5.5, which appear sub-horizontal. The ground level is reconstructed using the inclination of 11° provided in the original publications (Derevianko *et al.*, 1987; Derevianko, Shimkin, *et al.*, 1998).

The transversal projection shows a similar pattern with OH5.1-5.5 clearly separated by sterile horizons. Once again, given that more than 11 m² are projected on a single profile, one would expect a certain overlap between OH. Only OH6.1 overlaps with OH5.4 due to its location higher in the slope. This reinforces the idea that stratum 5 includes individual assemblages that were grouped in the original publication under the label of 'cultural level 3'. All in all, Slavinsksi's subdivision model (Slavinsky, 2007) is validated by both transversal and longitudinal projections.

From a chronological point of view, Slavinsky argues that the dated hearth features are associated with OH5.2 as they are both reported between -324 cm and -336 cm (Slavinsky, 2007). The longitudinal projection indicates that the hearth features are either located in the interval between OH5.3 and OH5.2 or at the bottom of OH5.2. On the transversal section, the hearth features appear connected with the lowest part of the OH5.2; thereby, providing a minimal age for OH5.3-5.5.

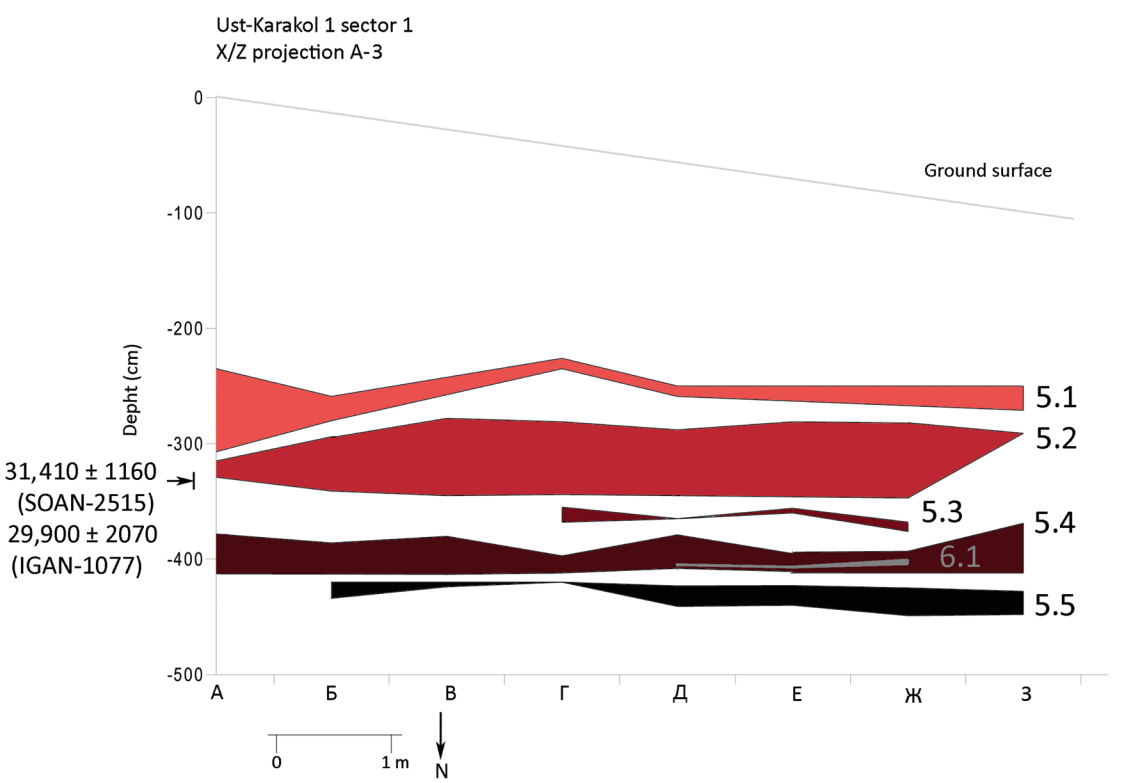

Figure 124: UK1-1, transversal projection of the piece-plotted artifacts based on their altitude range (data from Slavinsky, 2007)

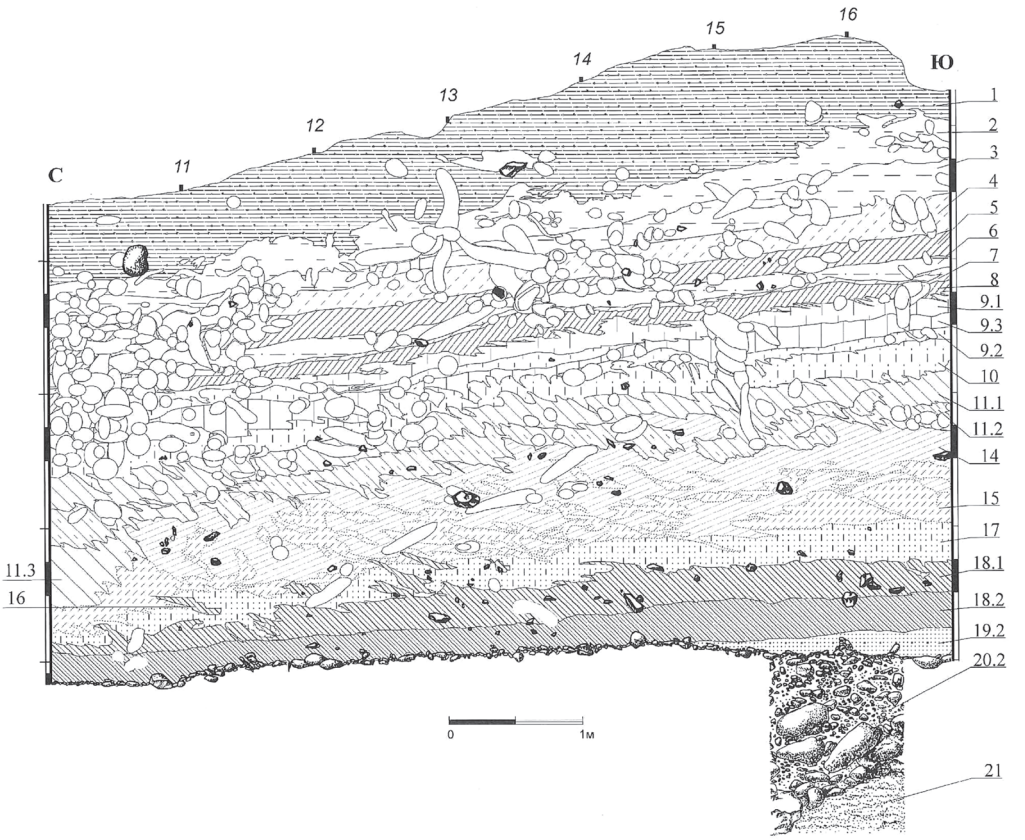

Figure 125: UK1-2, eastern section (after Derevianko *et al.*, 2003)

UK1-2

Up to now, no complete taphonomic analysis has been performed in UK1-2. However, some general comments can be formulated. As visible in the northern, southern and eastern sections, the excavated area shows a significant amount of bioturbation mainly affecting strata 2 to 14, but also more locally in the lower part of the sequence (strata 14 to 18) (Figure 125). In addition, frost cracks occur mainly between strata 9.3 and 16. These cracks are filled with sediments from the respective overlying strata. The bottom of the sequence seems relatively well preserved as stratum 18a has yielded at least one long refitted reduction sequence (Postnov, 1999) and a refit of a complete *Capra sibirica* distal foreleg (Derevianko *et al.*, 2003). Refits (Slavinsky, 2007) show movements of artifact between strata 9.1, 9.2 and 9.3, between 9.3, and 10 and between 10 and 11. In a few cases, a single sequence shows refits across several strata 9.2 to 11.1, 11b to 10 or 11.1 to 9.3. However, some long sequences are refitted within the same strata. These refits are mainly in stratum 9.3. Slavinsky notes that the Upper Paleolithic material from UK1-2 does not correspond to individual occupations, as opposed as UK1-1. He also mentions refits between strata 9-11 and 12-15 (Slavinsky, 2007). This may be linked with the facts that strata 12 and 13 are not identified on the whole site (Figure 122, Figure 125, Figure 126). Downslope, on the northern and on the eastern section, stratum 11 is directly in contact with stratum 14. Upslope, stratum 12 and 13 occur on the southern section. This likely indicates erosional processes usually affecting slope deposits. To summarize, the UK1-2 seems to show a good preservation of stratum 18 but show localized artifact movements between the middle and upper part of the sequence that are

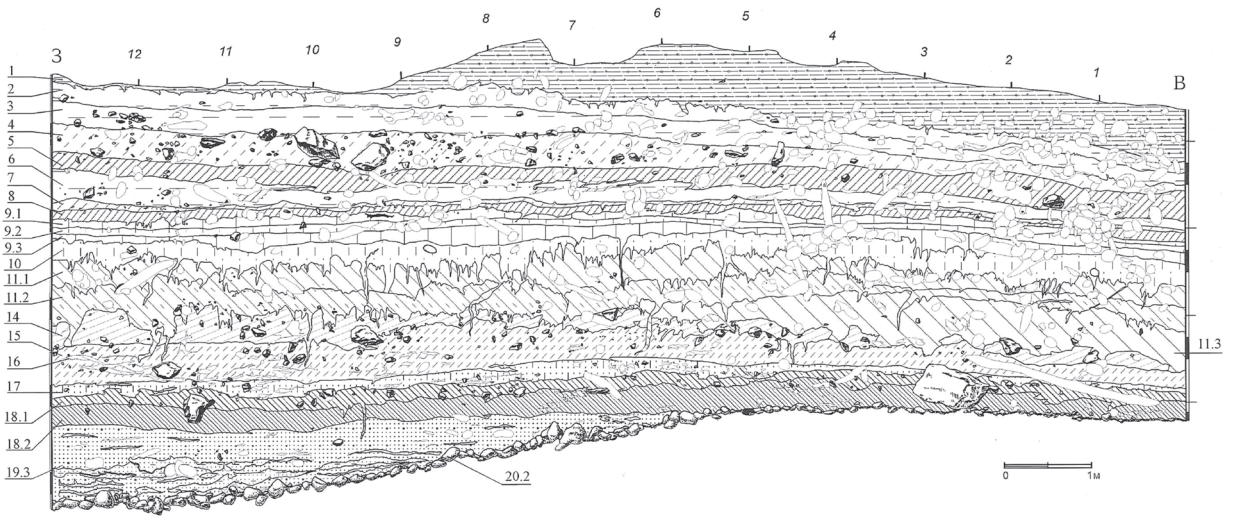

Figure 126: UK1-2, northern section

maybe due to the combine actions of slope erosion and rodent burrows.

Summary

As UK1-1 and UK1-2 trenches were not physically connected, the two sequences cannot be formaly correlated. Moreover, stratigraphic divisions are different from one trench to the other, although the two excavation areas are close to each other. The following table summarizes the available data to tentatively correlate the two in order to provide a comprehensive overview of the main chrono-cultural issues. The assemblages studied correspond to the earliest UP. Following the taphonomic assessment of UK1-1 cultural level 3, two variants of UP are recognized. OH5.1-5.3 are described here as EUP and the underlying assemblages OH5.4-5.5 are assigned to the IUP. These two variants are not differenciated at UK1-2 but are instead described as illustrating a transition from MP to UP. The interface between the MP and EUP assemblage is, however, not clear and includes erosion and slope processes as well as vertical movements of artifacts.

3.8.6 SAMPLE COMPOSITION

In this chapter, the material from UK1-1 OH5.4 and OH5.5 is described, focusing on the laminar technology. EUP assemblages from UK1-1 and UK1-2 are described in the next chapter. Initially, 657 lithic artifacts were reported as associated with cultural level 3 (Derevianko *et al.*, 1987; Derevianko, Shimkin, *et al.*, 1998). Slavinsky reported 318 artifacts for OH5.4 and 47 for OH5.5 (Slavinsky, 2007). OH5.4 has yielded 75 blades, 8 cores (including 2 fragments), 30 laminar flakes and 40 tools. For OH5.5, 6 cores, 22 blades, 2 laminar flakes and 18 tools are reported. However, this sample does not include a few pieces exhibited in the Akademia Gorodok museum (Novosibirsk, Russia).

Differences in the number of pieces between the present and the previous studies may be due to several factors. Some are due to ambiguities in terms of artifact labels and others are due to the fact that a part of the artifacts were not available at the moment of this study, as they were in the local museum. The sample studied does include the large majority of the material previously published, with the relevant remaining artifacts, including some from the museum, being discussed in the forthcoming chapters.

UK1-1				UK1-2			
Lithological stratum	**Cultural level**	**Cultural Attribution**	**Chronological attribution**	**Lithological stratum**	**Cultural level**	**Cultural Attribution**	**Chronological attribution**
1	1	?	Modern	1			Modern
2	2	?	OI2/3?	2	2-4	LUP	OIS2/3
				3			
				4			
				5	5	UP	
3	/			6	/	/	
4	/			7	/	/	
5	3 (OH5.1-5.3)	EUP	OIS3	8	11-8	EUP	OIS3
				9			
				10			
	3 (OH5.4-5.5)	IUP	OIS3/4?	11			
				12	12-17	MP?	OIS4
6	4	MP?		13			
7-10	/	/	?	14			
				15			
				16			
				17			
				18	18a-18b	MP	OIS5e(-d?)
				19	19	MP	
				20			

Table 83: Ust-Karakol 1, summary and comprehensive correlation of UK1-1 and UK1-2 sequences. Shaded rows represent assemblages studied

First observations on the lithic material from OH5.4 and OH5.5 by Slavinsky and the results of the present analysis indicate a high degree of similarity between OH5.4 and OH5.5. In order to obtain a statistically relevant sample, these two sub-levels are grouped in the following technological analysis under the label OH5.4-5.5. Petrographic data collected on the UK1-2 assemblage indicate that volcanic rocks, aleurolits and sandstones dominate, accounting for respectively 41%, 30% and 21.5 % of the archeological material. Volcanic rocks are found as pebbles along the Anuy ridge and in the Karakol and Muta River watersheds. These materials vary from dark grey to black. Aleurolits and sandstone being more com-

	N	*f*
Blade	58	64%
Bladelet	3	3%
Microblade	0	0%
Flake	1	1%
Core	9	10%
Tool	19	21%
	90	100%

Table 84: UK1-1, OH5.4-5.5, sample composition

mon in the Anuy and Karakol rivers, the data suggest an intentional selection of the volcanic rocks. Such a pattern is also observed in Denisova Cave and in Anuy II (Postnov *et al.*, 2000; Anoikin and Postnov, 2005).

3.9 LAMINAR TECHNOLOGY: OH5.4-5.5

3.9.1 BLANK ATTRIBUTES

Breakage

The distribution of both blades and bladelets indicates a majority of mesial and mesioproximal fragments (Table 85). Based on these observations, an MNI of 35 blades is calculated on a total sample of 62 laminar artifacts recorded.

Platform size and preparation

Based on observations from the MNI sample, OH5.4-5.5 blades show a majority of facetted platforms, followed by plain platforms and an insignificant occurrence of flat, dihedral platforms (Table 86).

Considering all platform types together, the mean thickness is 6.1 ± 3.5 mm and the mean width is 15.5 ± 9.6 mm.

Facetted platforms (Table 87) show a higher mean thickness and width than the MNI sample and than the plain platforms (Table 88). This difference is, however, not statistically significant. Dihedral plat-

	Total		Blade		Bladelet	
	N	*f*	N	*f*	N	*f*
Distal	0	0%	0	0%	0	0%
Mesiodistal	5	8%	4	7%	1	33%
Mesial	22	35%	20	34%	2	67%
Mesioproximal	16	26%	16	27%	0	0%
Proximal	8	13%	8	14%	0	0%
Complete	11	18%	11	19%	0	0%
	62	100%	59	100%	3	100%

Table 85: UK1-1, OH5.4-5.5, breakage

	N	*f*
Plain	11	31%
Facetted	20	57%
Dihedral Flat	3	9%
Undetermined	1	3%
	35	100%

Table 86: UK1-1, OH5.4-5.5, platform preparation

forms have a mean thickness of 5.8 ± 3.2 mm and a mean width of 14.2 ± 6.1 mm

Thin abrasion is almost absent (N=1), but some blanks for which a strong abrasion smoothed the external platform edge (N=5).

Blank size attributes

Length

As length is measured only on complete elements, the results presented are based on a smaller sample that includes only blades (Table 89). In spite of the small sample, the distribution of length measurements appears to be normally distributed (Shapiro-Wilk, W=0.91, p= .22).

	Total (blade)
Sample size	11
Mean (mm)	82.4
Standard deviation (mm)	22.1
Range (mm)	55.7 to 133.4

Table 89: UK1-1, OH5.4-5.5, blank length

Facetted platform	Total (blade)	
	Thickness	Width
Sample size	20	
Mean (mm)	7	18
Standard deviation (mm)	3.9	10.8
Range (mm)	1.4 to 13.6	4.8 to 52.4

Table 87: UK1-1, OH5.4-5.5, facetted platform size

Plain platform	Total (blade)	
	Thickness	Width
Sample size	11	
Mean (mm)	5.3	12.8
Standard deviation (mm)	2.4	6.3
Range (mm)	3 to 9.1	5.5 to 25.7

Table 88: UK1-1, OH5.4-5.5, plain platform size

Width	Total	Blade	Bladelet	Total MNI (Blade)
Sample size	62	59	3	35
Mean (mm)	27.3	28.2	9.4	30
Standard deviation (mm)	10.6	10.1	2	9.5
Range (mm)	7.5 to 52.1	12.7 to 52.1	7.5 to 11.5	14 to 52.1

Table 90: UK1-1, OH5.4-5.5, blank width

Width

The MNI mean width appears to be larger than for the total sample (Table 90) although the difference is not significant, meaning that there is no direct relationship between the width of the blank and the rate of breakage. The total sample (Shapiro-Wilk, W=0.96, p=<.05) and the MNI (Shapiro-Wilk, W=0.92, p=<.05) are not normally distributed. This is due to the combine effects of a positive skewness (0.52 for the total sample and 0.87 for the MNI) and to the presence of artifacts of more than 50 mm width, although the general distribution pattern is unimodal (Figure 127). The sample size may also play a role.

Thickness

The total sample (Shapiro-Wilk, W=0.94, p=<.05) and the MNI (Shapiro-Wilk, W=0.93, p=<.05) are not normally distributed (Table 91). This situation reflects the positive skewness of the distributions (0.91 for the total sample and 0.85 for the MNI) but also the occurrence of a second mode between 4 and 6 mm.

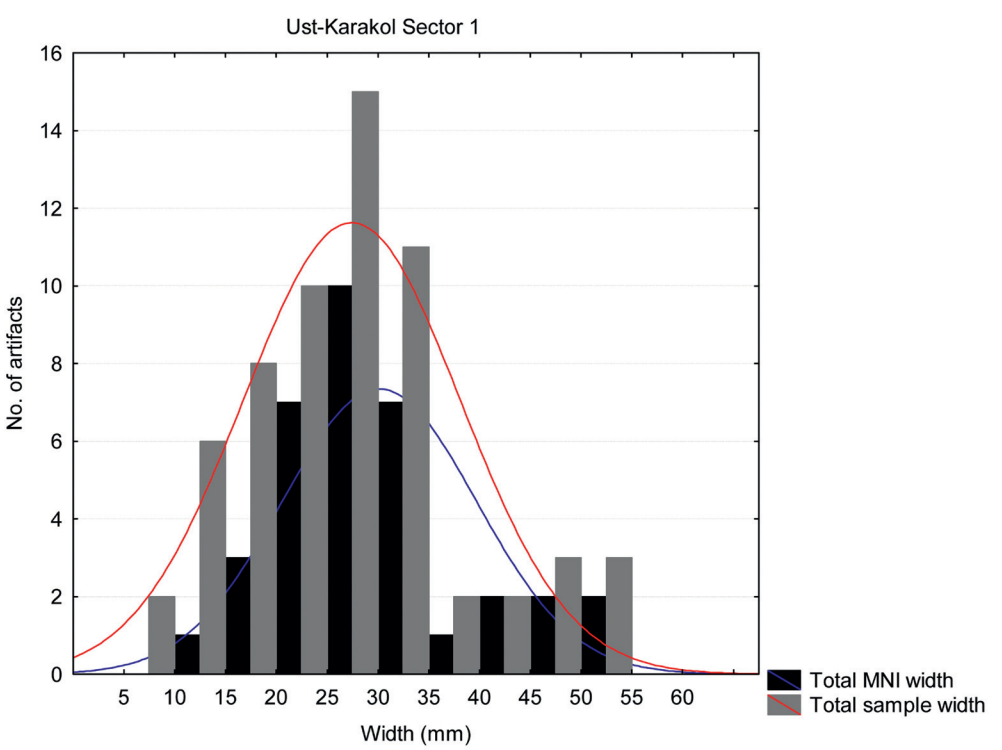

Figure 127: UK1-1, OH5.4-5.5, blank width distribution

	Total	Blade	Bladelet	Total MNI (Blade)
Sample size	62	59	3	35
Mean (mm)	8.9	9.2	3.2	10.3
Standard deviation (mm)	4.8	4.7	1.6	5
Range (mm)	1.7 to 24.3	2.1 to 24.3	1.7 to 5	3.4 to 24.3

Table 91: UK1-1, OH5.4-5.5, blank thickness

As was shown for the width, the mean thickness is larger for the MNI than for the total sample, but without showing significant differences. The thickness distribution may suggest that thinner blanks are more fragmented (Figure 128).

Dorsal scar pattern

Unidirectional and bidirectional scar patterns have similar frequencies in the total sample (χ^2 (1)= 0.314, p=.57) (Table 92). This suggests that the main reduction sequences are not strictly unidirectional or alternate bidirectional. The occurrence of crested and neo-crested blanks illustrates the initial reduction stages and the core management operations. The relatively large amount of undetermined patterns is mainly due to the frequent occurrence of concretion on the artifacts. When considering only the complete blanks, the sample size is sharply reduced and indicates a good presence of bidirectional blanks (N=5) and crested blanks (N=4) followed by unidirectional ones (N=2).

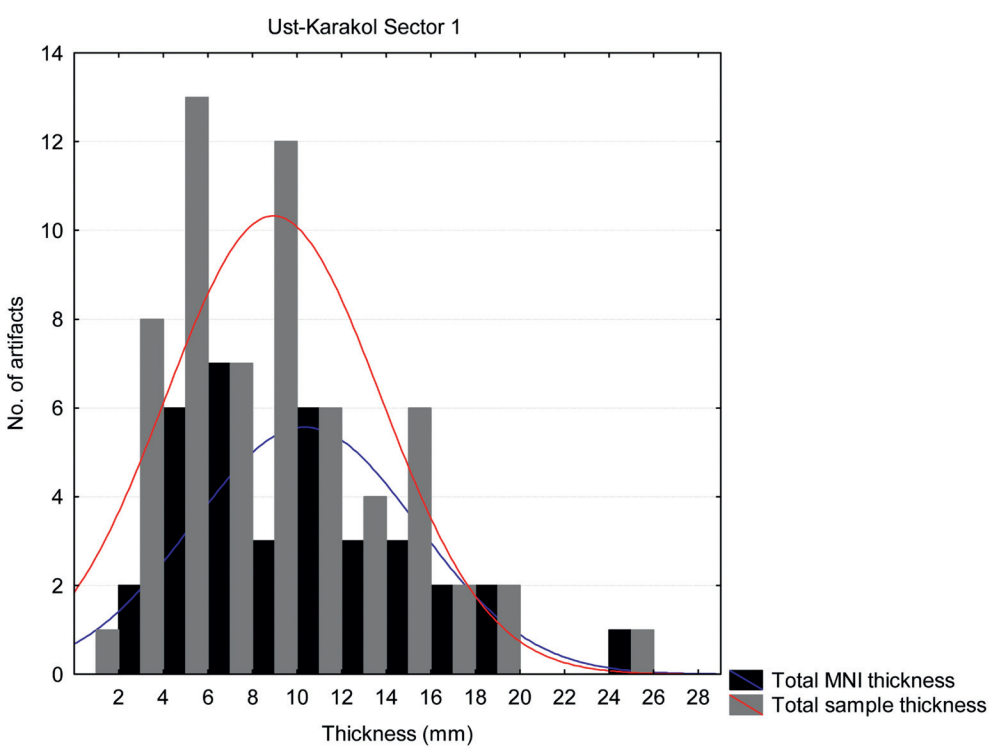

Figure 128: UK1-1, OH5.4-5.5, blank thickness distribution

	Total		Blade		Bladelet	
	N	*f*	N	*f*	N	*f*
Unidirectional	21	34%	20	34%	1	33%
Unidirectional and cortex	2	3%	2	3%	0	0%
Bidirectional	24	39%	23	39%	1	33%
Bidirectional and cortex	0	0%	0	0%	0	0%
Crest	4	6%	4	7%	0	0%
Second Crest	0	0%	0	0%	0	0%
Neo-crest	1	2%	1	2%	0	0%
Undetermined	10	16%	9	15%	1	33%
	62	100%	59	100%	3	100%

Table 92: UK1-1, OH5.4-5.5, dorsal scar pattern

Cross-section

Cross-sections appear to be mainly trapezoidal when considering the total sample (χ^2 (1)= 0.18, p=<.05) and the blade category (χ^2 (1)= 24.74, p=<.05)(Table 93). All bladelets have a triangular cross-section.

Profile

When considering the total sample, profiles appear to be mainly straight (χ^2 (2)= 22.31, p=<.05). Curved and slightly curved blanks occur with at equal frequencies, and the presence of twisted profiles is rare (Table 94).

	Total		Blade		Bladelet	
	N	*f*	N	*f*	N	*f*
Flat	1	2%	1	2%	0	0%
Rectangular	0	0%	0	0%	0	0%
Triangular	18	29%	15	25%	3	100%
Trapezoidal	42	68%	42	71%	0	0%
Polyhedral	1	2%	1	2%	0	0%
	62	100%	59	100%	3	100%

Table 93: UK1-1, OH5.4-5.5, blank cross-sections

	Total		Blade		Bladelet	
	N	*f*	N	*f*	N	*f*
Straight	33	53%	31	53%	2	67%
Slightly Curved	12	19%	12	20%	0	0%
Curved	12	19%	11	19%	1	33%
Twisted	4	6%	4	7%	0	0%
Undet	1	2%	1	2%	0	0%
	62	100%	59	100%	3	100%

Table 94: UK1-1, OH5.4-5.5, blank profiles

	Total MNI (blade)	
	N	*f*
Straight	17	49%
Slightly Curved	8	23%
Curved	7	20%
Twisted	2	6%
Undet	1	3%
	35	100%

Table 95: UK1-1, OH5.4-5.5, blank MNI profiles

These trends are similar when considering the MNI sample (χ^2 (2)= 8.18, p=<.05), indicating that breakage does not bias the values recorded on the total sample.

Orientation

When considering the total sample, most of the blanks are categorized as axial directly followed by the right and left-oriented blanks (Table 96). Differences between these categories are insignificant (χ^2 (2)= 0.83, p=.66).

	Total		Blade		Bladelet	
	N	*f*	N	*f*	N	*f*
Right	12	19%	12	20%	0	0%
Left	10	16%	10	17%	0	0%
None	14	23%	14	24%	0	0%
Undetermined	26	42%	23	39%	3	100%
	62	100%	59	100%	3	100%

Table 96: UK1-1, OH5.4-5.5, blank orientation

This observation is reinforced by the MNI (Table 97) where, except the undetermined artifacts, all categories show similar frequencies (χ^2 (2)= 0.63, p=.73).

	N	*f*
Right	12	34%
Left	9	26%
None	11	31%
Undet	3	9%
	35	100%

Table 97: UK1-1, OH5.4-5.5, blank MNI orientation

3.9.2 CORES: REDUCTION PATTERNS AND SIZE ATTRIBUTES

Nine cores have been recognized in the OH5.4-5.5 sample (Figure 129). Six cores belong to Mode A as they are on block/slab blanks, and two of them are on blade blanks, and, therefore, are classified as Mode B. One is a flake core which is described but not included in the Mode classification.

Mode	*n*	%
A1	2	25%
A2	1	13%
A3		
A4		
A5	1	13%
A6	2	25%
A7		
A8		
A9		
A10		
A11		
A12		
B1		
B2		
B3		
B4		
B5	1	13%
B6		
B7	1	13%
	8	100%

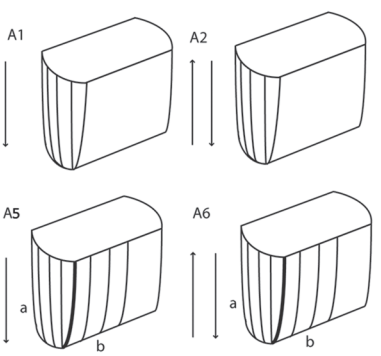

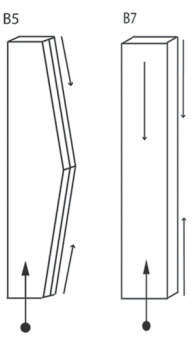

Figure 129: UK1-1, OH5.4-5.5, frequencies of cores per Mode

	Mode A		
	Mean	σ	N
Core length	35.7	22.3	6
Core width	45.2	18.7	6
Core thickness	91.5	35.1	6
Flaking surface length	91	35.5	6
Flaking surface width	44.7	20.8	6
Last removal length	67.6	5.5	5
Last removal width	27.2	15.9	5

Table 98: UK1-1, OH5.4-5.5, core size attributes

Size attributes

Only Mode A attributes are listed here, as the sample of Mode B cores is too small for the relevant statistics. The Mode B7 core is 21.0 mm long, 34.6 mm wide and 87.2 mm thick. The Mode B5 core is 32.3 mm long, 30.6 mm wide and 92.7 mm thick. The flaking surface is 91.8 mm long and 30.6 mm wide.

All measurements are recorded according to the system described in Chapter 2 which does not take into account the type of blank on which the core is produced. As a result, measurements are comparable, but in the case of Mode B cores, the thickness corresponds to the length of the blade blank, and the length of the core represents the thickness of the blade.

Striking platform preparation

Mode A cores show either a combination of a plain platform partially modified by faceting (N=4) or complete faceting (N=2). Mode B cores have plain platforms, one of them shows traces of a tablet removal.

Core descriptions

Mode A1 (N=2)

∗ YK-86-705-16

This core is produced on a block still covered by cortex (up to 70%)(Figure 130). With four surfaces displaying roughly equal width and a natural platform, the original block is a suitable shape for blade reduction with minimal preparation. It represents the early stages of a blade reduction process, with a first sub-cortical hinged blade removed from the corner between two surfaces followed by another one extending on one of the surfaces. The upper striking platform is prepared by the removal of two sub-cortical flakes and shows a series of unsuccessful attempts to remove a cortical side blade. These attempts, marked by the stepped morphology of the platform edge, have the effect of creating an oblique angle leading to a change of platform. An opposed platform is prepared by the removal of a large flake and a series of small hinged flakes illustrates the last attempts to remove a cortical blade, following the scar left by a previous removal.

∗ YK-86-673-1

This core is produced on a chert block that shows a series of removals detached from a platform prepared by the removal of a large flake (Figure 131).

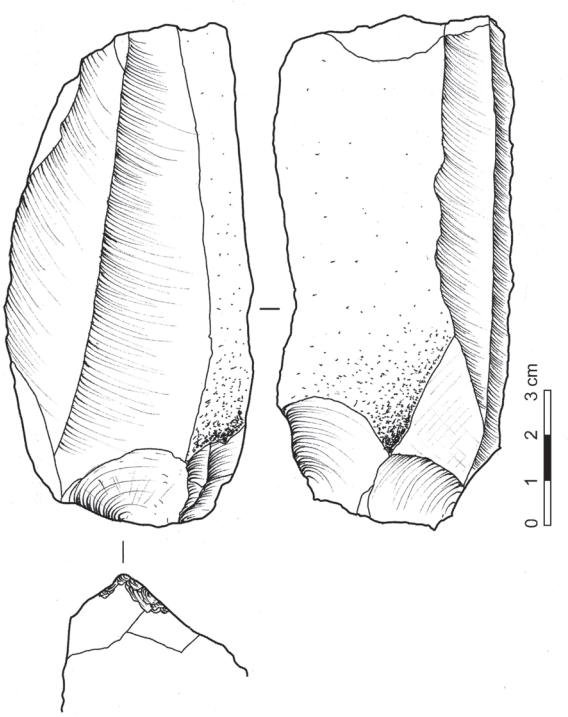

Figure 130: UK1-1, OH5.4-5.5, YK-86-705-16

The flaking surface is located on a narrow side of the nodule and displays negatives of two sub-cortical removals followed by a series of three hinged removals ending the reduction. A second opposed platform is shaped by the removal of a large flake, and although no blade was removed, a series of stepped small negatives testifies to a clear attempt to remove a thick blade from the intersection of the flaking surface and a cortical surface.

Mode A2 (N=1)

* YK-86-319-1

This core is made on an elongated cortical flake and shows two opposed platforms. A single removal is visible, detached from the upper platform and following a narrow edge of the blank.The second platform is prepared, but no removals were detached, probably due to a problem with the EPA.

Mode A6 (N=3)

* YK-86-678-1

This core is produced on a block/slab (Figure 133) and shows a main flaking surface on a broad side of the core, opposed to a cortical back. The reduction follows two opposed platforms, the upper one is prepared by the removal and faceting of the platform edge. The lower platform bear traces of a percussive event. A second flaking surface located on a narrow face illustrates attempts to remove a postero-lateral crested blade.

* YK-86-631-1

This core is produced on a block/slab with two separate flaking surfaces and two opposed platforms (Figure 134). Blade blanks are mainly detached from the broad flaking surface opposed to a cortical back. Two blades are detached from the upper platform (1, 2) and are followed by the detachment of a blank from the lower platform at the junction between the

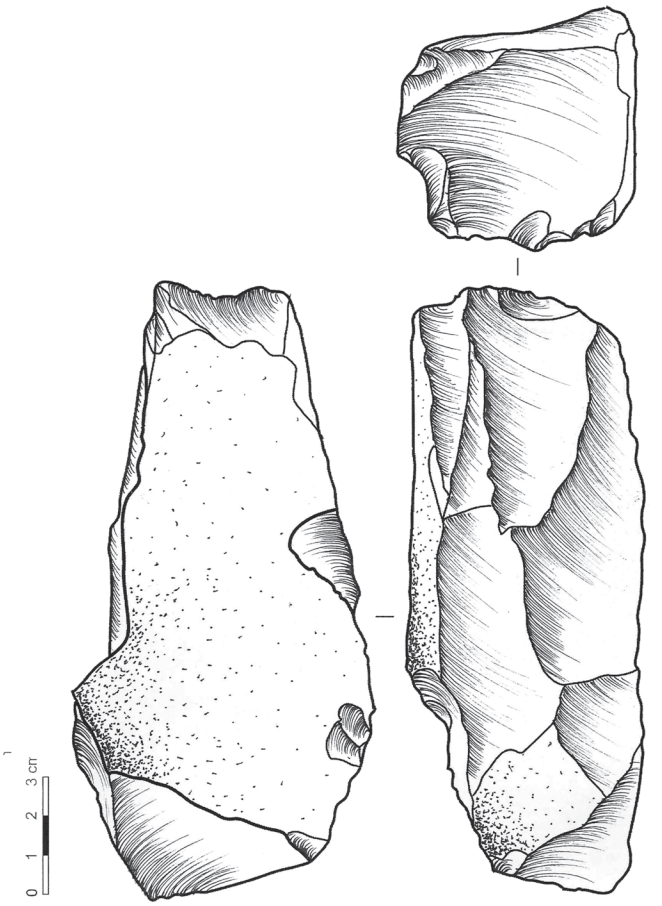

Figure 131: UK1-1, OH5.4-5.5, YK-86-673-1

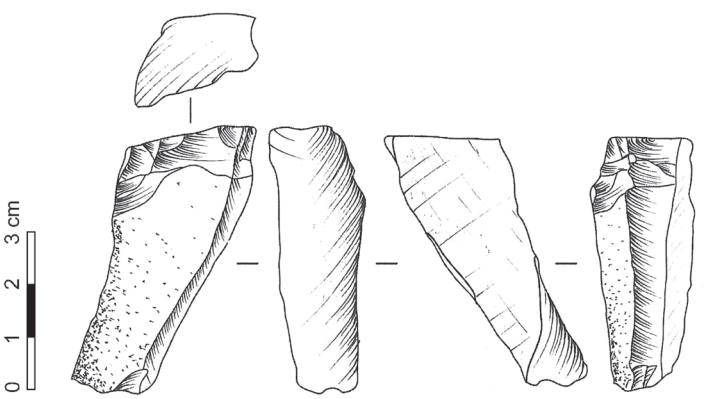

Figure 132: UK1-1, OH5.4-5.5. YK-86-319-1

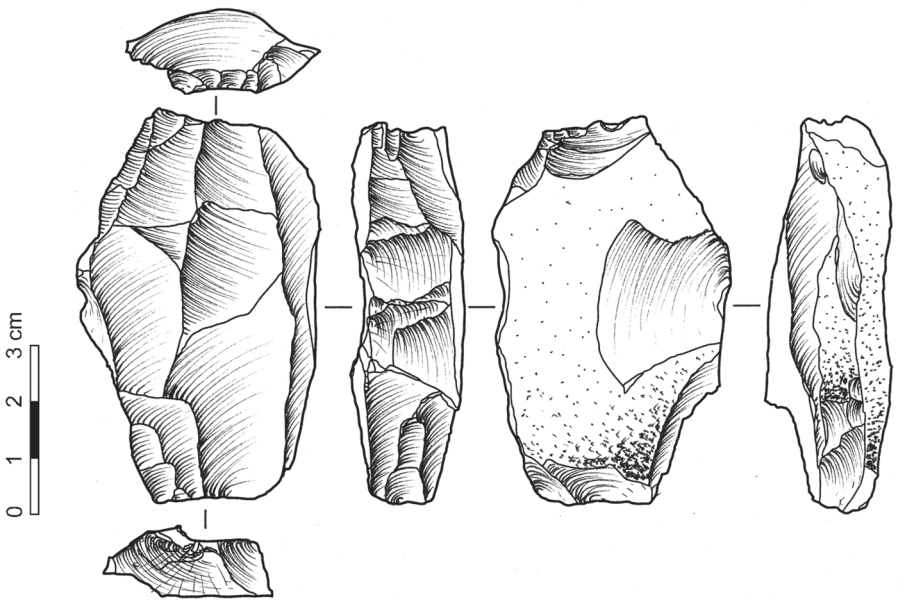

Figure 133: UK1-1, OH5.4-5.5, YK-86-678-1

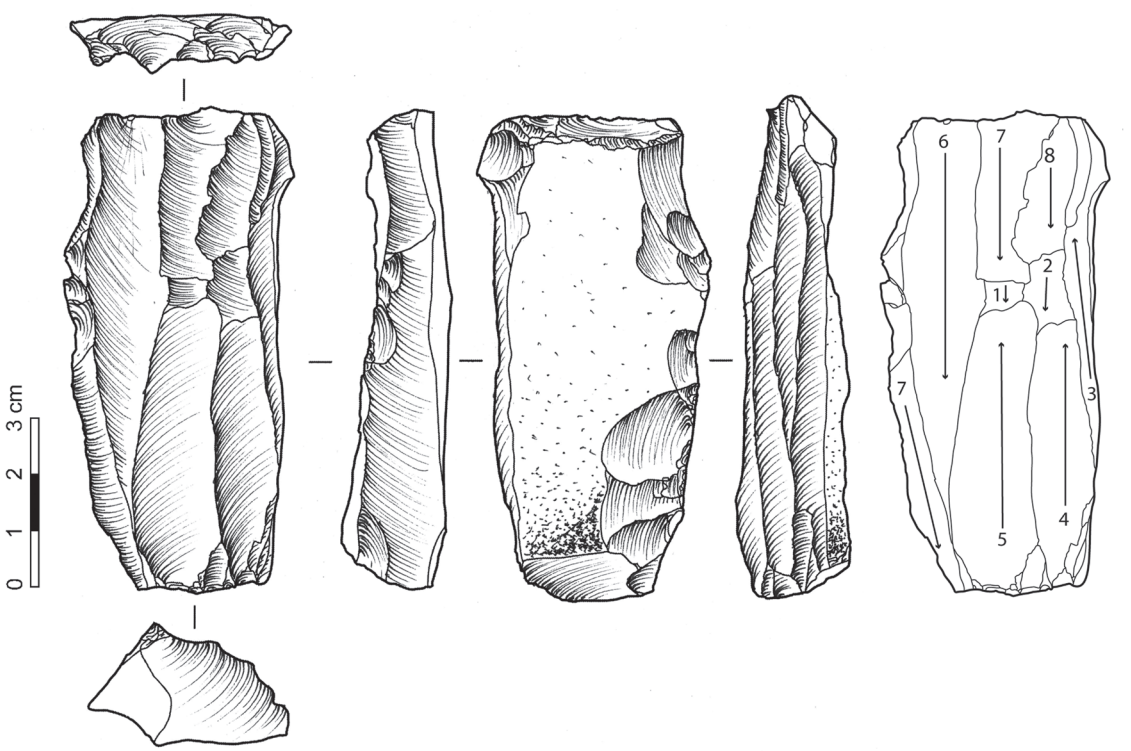

Figure 134: UK1-1, OH5.4-5.5, YK-86-631-1

broad and the narrow flaking surface (3). It is followed by the removal of a hinged blade from the upper and the lower platform, extending on the broad surface (4). Then, a hinged blade blank is struck from the lower platform, in the middle of the flaking surface (5). A platform switch occurs, with a first blade (6) followed by a blank removed from the corner of the flaking surface and two hinged fractures (7, 8).

The left corner of the flaking surface is then prepared as an antero-lateral crest by removing sub-cortical flakes from the back of the core. A single hinged removal represents the last attempt to resume the reduction sequence by creating a new flaking surface on the left narrow edge of the core. Judging by the number of removals visible on the right narrow edge, this seems to happen frequently in the course of the reduction.

The upper striking platform is rather thin and is prepared by faceting. The acute angle between the flaking surface and the striking platform is similar to an inverse truncation. The lower platform is plain and much thicker and is prepared by the removal of a sub-cortical flake and by a thin faceting still visible around the beginning of the next guiding ridge.

∗ YK-86-710-3

This core is produced on a block and has two distinct flaking surfaces (Figure 135). The main flaking surface is located on a broad face of the block and opposed to a semi-prepared and cortical back. The pattern of reduction is unidirectional. A first removal (1) is followed by an overshot (2) taking away the central part of the flaking surface. Removals are then detached from the left end of the broad flaking surface and from the perpendicular narrow flaking surface (3). The reduction ends with two hinged fractures (4, 5).

The striking platform is rather thin and is prepared by faceting, and a completely prepared platform is still visible on the left corner of the flaking surface and is posterior to removal 4.

Mode B7 (N=1)

∗ YK-86-721-11

This core is produced on a thick, bidirectional, asymmetric blade with a sub-triangular cross-section (Figure 136). It shows traces of a mesiodistal snapping event followed by two removals that prepare a strik-

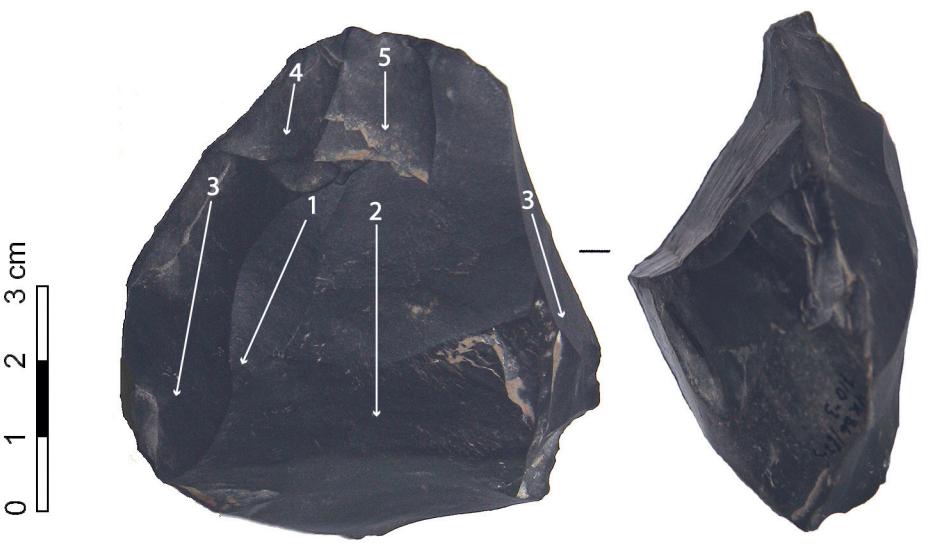

Figure 135: UK1-1, OH5.4-5.5, YK-86-710-3

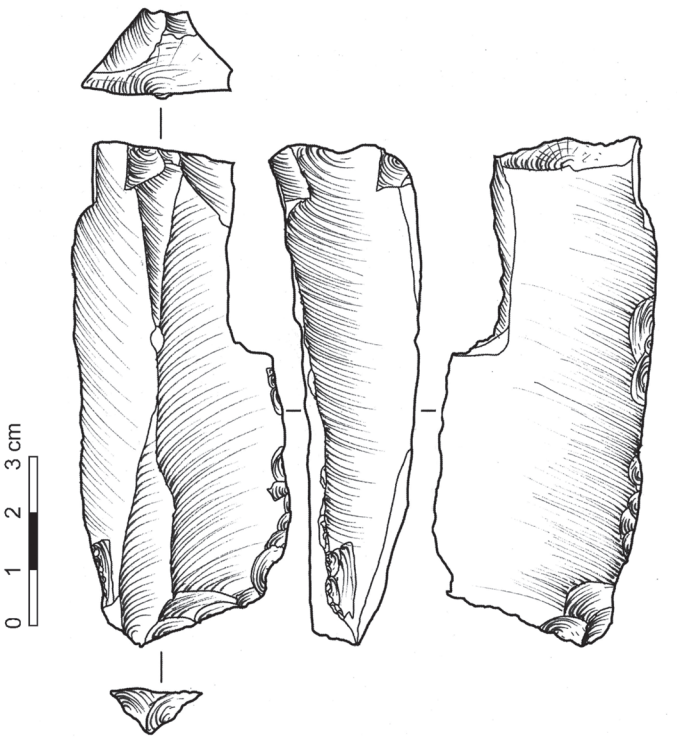

Figure 136: UK1-1, OH5.4-5.5, YK-86-721-11

ing surface. A hinged removal is detached along the right edge from a plain striking surface. More attempted removals are visible along the right edge, one using the ridge edge of the blank, the others trying to remove blanks from the central ridge.

The lower platform is a proximal truncation from which is struck a single removal following the central scar of the blank (Figure 137). Direct sporadic retouch is located along the right edge down to the proximal end. Inverse retouch is located along the left edge. This retouch may play the role of a crest.

Mode B5 (N=1)

* YK-86-619-6

This core is produced on a large bidirectional asymmetric blade which shows traces of snapping events at the lower end (Figure 138). The bidirectional reduction takes place along the right edge from two opposed platforms. The earliest phase of reduction (1) shows a removal detached from the lower platform which follows the left edge and covers the whole length of the flaking surface. Another early removal is located at the center of the flaking surface. The second phase is represented by a single removal detached from the upper platform (2). The following phase (3) includes removal from both platforms, the lower one displaying a deeply hinged negative. It is followed by a second hinged fracture (4) which ends the reduction from the lower platform. From the upper platforms, two removals including one hinged fracture (4), are followed by two hinged removals (5, 6). The upper platform is fragmented by the removal of a large flake and stepped negatives. The remaining part is elongated and shows traces of a tablet removal and lateral stepped removals. The lower platform is plain. Notable is the retouch located along the left edge that in this context is considered as a posterior crest.

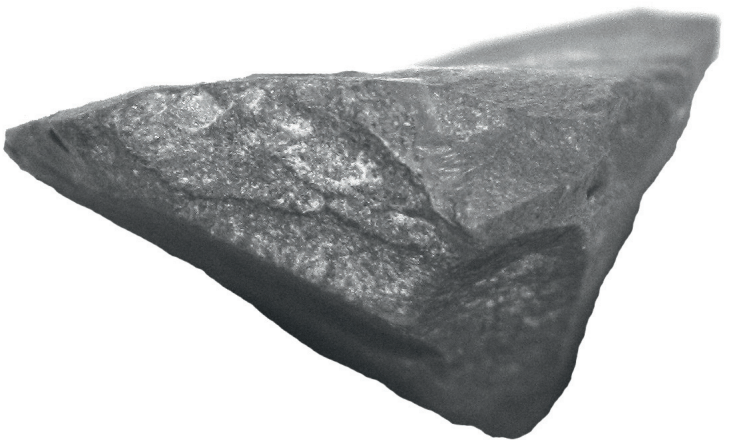

Figure 137: UK1-1, OH5.4-5.5, YK-86-721-11

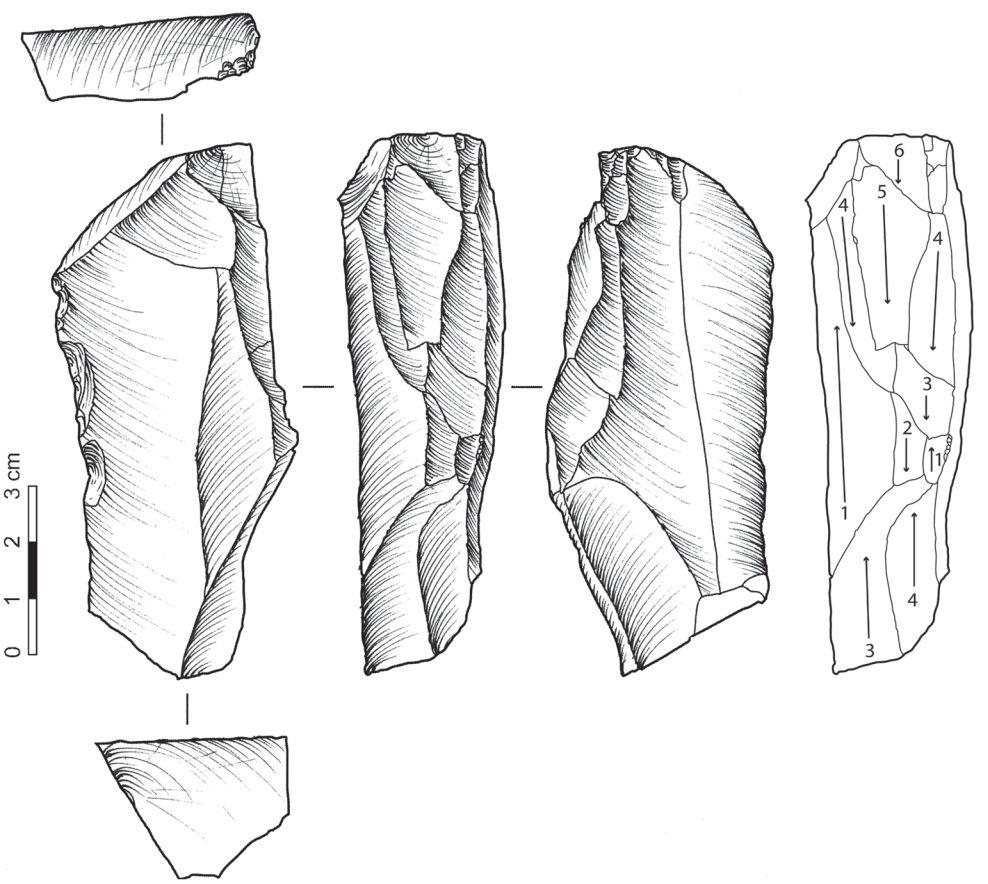

Figure 138: UK1-1, OH5.4-5.5, YK-86-619-6

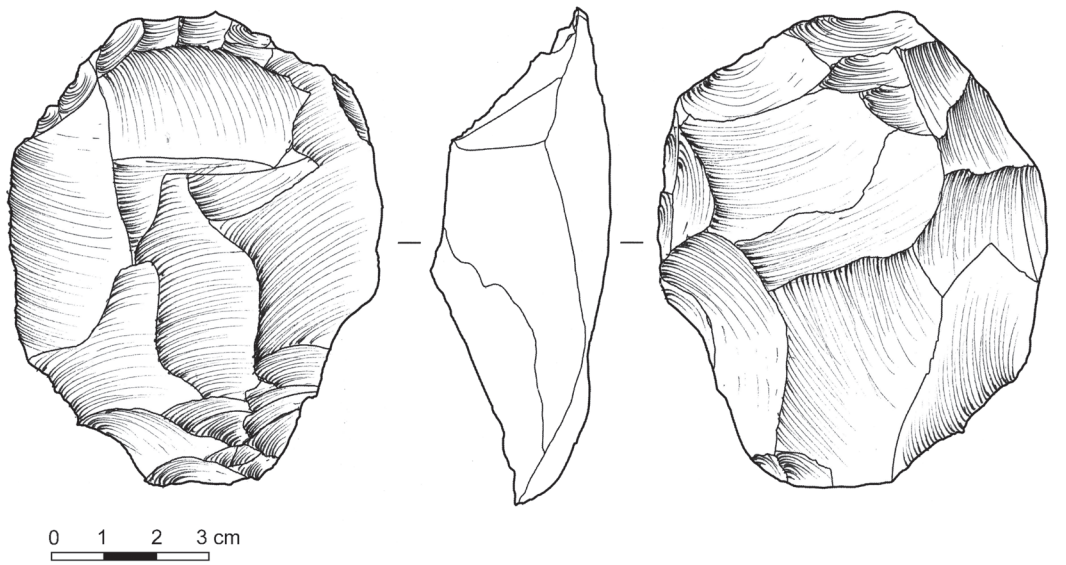

Figure 139: UK1-1, OH5.4-5.5, YK-86-625-1

Flake core (N=1)

∗ YK-86-625-1

A single Levallois flake core is associated with the sample. It shows a flat broad flaking surface opposed to a convex back shaped by radial flaking. The reduction seems to correspond to a bidirectional pattern, with blanks struck from two opposed platforms. This core show a strict surface treatment and no part of the narrow face has been used as flaking surface.

3.9.3 REDUCTION SEQUENCE RECONSTRUCTION

Following the result of the blank attribute analysis and the core descriptions, an analytical reconstruction of the individual reduction sequences is proposed in the following section.

Laminar blanks with parallel edges

Two main categories of blade can be recognized among the sample: parallel and convergent edge blanks. The first one is described as blades with parallel edges. These blades have a straight or slightly curved profile, show a roughly equal unidirectional and bidirectional patterning, and have a triangular or trapezoidal section. Some of these blades are relatively massive and the maximum length observed in the sample is 130 mm. Crested elements of various sizes testify of the initiation of the reduction, but also to core management in the course of the reduction (neocrest). Then the reduction starts by removing a blank that follows a natural edge, guiding the detachment of elongated blanks. Mode A core reduction starts from cortical blocks or nodules from which a striking platform is prepared by the removal of a large flake. Mode A1 cores are unidirectional, although they present clear traces of preparation of an opposed platform. The observed removal negatives indicate that the blanks produced are medium/large

blades with parallel edges. Mode A6 cores illustrate a more advanced stage of reduction. They clearly show the use of two flaking surfaces, the main one being located on a broad face of the nodule and the second one being located on a narrow face. The main pattern of reduction is bidirectional, using two opposed striking platform with short sequences of two-three unidirectional removals followed by a platform switch. As illustred on Figure 134, the removal of a blank from the intersection of the broad and the narrow face occurs frequently in the course of the reduction. This type of blank is generally thick (Figure 140) and is either guided by a previous scar or by the shaping of a postero-lateral or antero-lateral crest. As the use of the narrow flaking surface is embedded in the reduction of the broad surface, it is assumed that it plays a role in the management of the core, allowing a certain control on the convexity of the main flaking surface. This idea is reinforced by the fact that at the end of the core reduction, numerous attempts are made to remove such a thick blank to resume the reduction process. It seems that mostly one narrow face is used in combination with the broad face; however, the preparation of the second narrow face may occur in order to keep the reduction going.

Two of the thickest management blades (over 30 mm thick) have been subsequently transformed into Mode B cores. Core blanks are visibly snapped at both ends, snapped surface being prepared by flake removals. Another variant is the use of a truncation, which implies a preparation of the platform by facetting. Mode B cores show the use of a narrow face of the blade blank as a flaking surface. First removals then follow natural scars or edges, sometimes prepared as a crest by discontinuous retouch. The back of the core (core blank edge opposed to the flaking surface) is sometimes modified by retouch. The reduction is bidirectional, with two opposed platforms using the same flaking surface. The flaking surface is considered as a whole, as complete removals cover the entire length of the surface.

Mode B cores have a more constrained distribution of the flaking surface width than do Mode A cores. This is due to the fact that Mode B flaking surfaces are located only on the narrow edge of a blade,

Figure 140: UK1-1, OH5.4-5.5, YK-86/-378-1-633-2, refit of a thick side-blade with parallel edges

sometimes slightly extending on the broad face (B7). The maximal width of the flaking surface reflects the thickness of the blade blank. Mode A cores have a more variable flaking surface width, between 75 (early stages of reduction) and 40 mm (reduced blade cores). The single example of a narrow flaking surface core shows a Mode B core reduction strategy applied to a cortical flake and testifies to occasional production of narrow blanks.

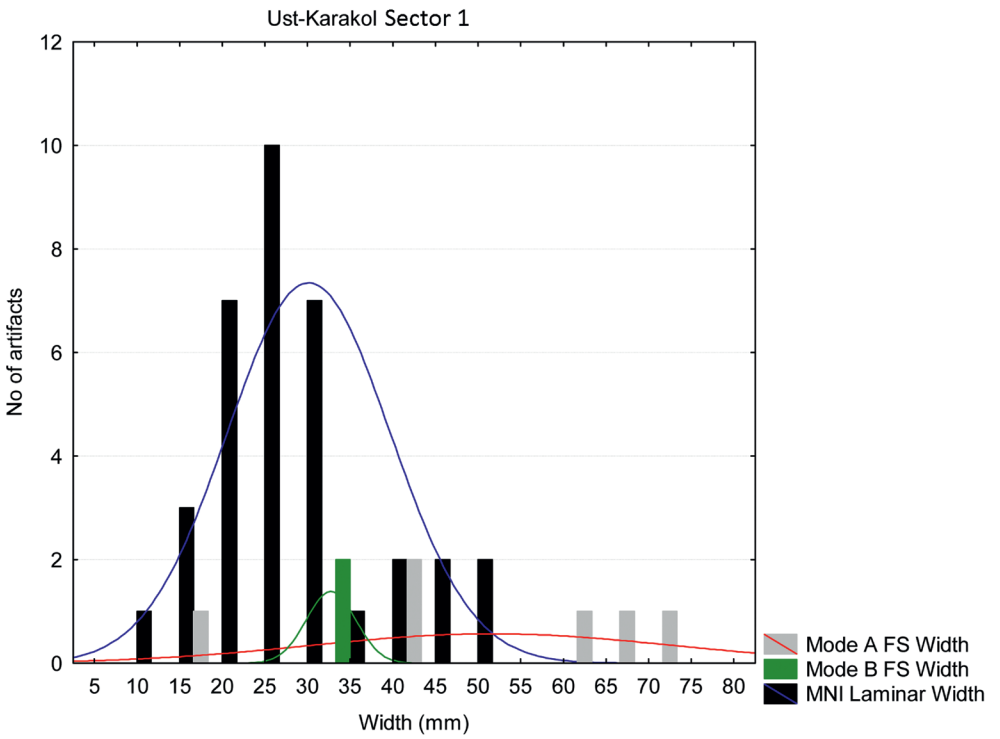

Figure 141: UK1-1, OH5.4-5.5, YK-86/-378-1-633-2, core flaking surface and MNI width distributions

The size of the blanks produced by Mode B cores overlaps with the blanks detached from Mode A cores during the advanced stages of reduction (Figure 141). However, some of them with a natural back (N=3) may testify to a detachment from the narrow face of a core. The widths range between 12 and 24 mm, and they all display a bidirectional dorsal patterning. The flaking surface length of Mode A and is comparable with the two Mode B cores, with a maximum length around 95 mm.

Convergent blanks

A second type of laminar blank showing convergent mesiodistal edges is attested to (N=4) (Figure 142, Figure 143). Two blanks are mesioproximal, one is proximal and one is a mesial fragment. One is bidirectional, two are unidirectional and one has an undetermined dorsal patterning. They all show trapezoidal sections and their profiles are curved or slightly curved. Their widths range between 24 and 56 mm, and they have a maximum thickness around 16 mm. This platform size does not differ from the variability observed on the overall blade sample, although it is notable that one of the two facetted platforms is *débordant* and represents the thickest recorded in the sample. The other facetted platform shows a partial faceting by marginal perpendicular flake removals.

It is assumed that these blanks are produced from a Mode A type of core, which displays a flaking surface wide enough and shows traces of three unidirectional sub-convergent removals or three bidirectional removals. Bidirectionality makes it easier to obtain pointed blanks from a broad surface whereas unidirectionality requires a convergence of the removals or a distal shaping of the core. Such a convergent orientation is unusual in the studied sample.

Figure 142: UK1-1, OH5.4-5.5, YK-86/D7-683-9, convergent blank with partial faceting platform preparation

Figure 143: UK1-1, OH5.4-5.5, YK-86/713-6, convergent blank

Platform preparation and percussion technique

No clear traces of abrasion have been observed in the sample, with the exception of a strong abrasion that smooths the external ridge of the platform (N=5). About 40% (N=14) of the MNI shows a macroscopic lip, and a single case of flaking on the bulb is observed combined with a lip. Lips occasionally occur in combination with extreme abrasion (N=4). Among the facetted platforms, some artifacts show only a partial faceting of the external edge and are flaked from a flat surface. All types of platforms show a mean thickness greater than 4 mm. Considering all these elements, the use of organic hammer seems unlikely. However, some features (extreme abrasion, lip, flaking of the bulb) may indicate the occasional use of a soft-stone hammer combined with a hard hammer.

Retouched tools

The main categories of retouched tools included here only tools on laminar elements. The three tools classified as others are one bifacial leaf-point on an undetermined blank, one sidescraper on slab and one sidescraper on laminar flake.

	N	*f* (among tools)	*f* (on total)
Retouched blade	15	83%	19%
Retouched bladelet	0	0%	0%
Retouched point	0	0%	0%
Endscraper	0	0%	0%
Other	3	17%	4%
	18	100%	23%

Table 99: UK1-1, OH5.4-5.5, composition of the retouched tool kit

The breakage pattern shows a majority of mesioproximal artifacts followed by mesial ones. Proximal and mesiodistal frequencies are low. The main differences between the unretouched and the retouched blanks is that mesioproximal fragments occur in a slightly higher frequency, and the mesial elements are less numerous. These variations are, however, not statistically significant.

	N	*f*
Distal	0	0%
Mesiodistal	2	11%
Mesial	4	22%
Mesioproximal	8	44%
Proximal	1	6%
Complete	3	17%
	18	100%

Table 100: UK1-1, OH5.4-5.5, tool breakage

The distribution of tool widths seems to indicate that, even after the retouch, tools are still wider than the overall blank population. This difference is statistically significant (Mann-Whitney, T=Ub=261, p=<.05). The single leaf-point on a blade has a width of 31 mm, which after retouch falls near the mean width of the blank production. The second leaf-point is 37 mm wide and falls near the mean width of the tools, and the sidescraper has a 41 mm width that roughly equals the mean width of the tools. Even when leaving out the two bifacial elements which are not on blade blanks, the difference between tool and blank width remains significant (Mann-Whitney, T=Ub=245, p=<.05).

The tool thickness distribution shows a similar picture, with a significant difference between tools and blanks (Mann-Whitney, T=Ub=250, p=<.05). The leaf-point on blade falls in the range of thickness of the blanks, with a thickness of 12 mm, the second leaf-point is 14.6 mm thick and falls in the mean thickness of the tool category, and the side-

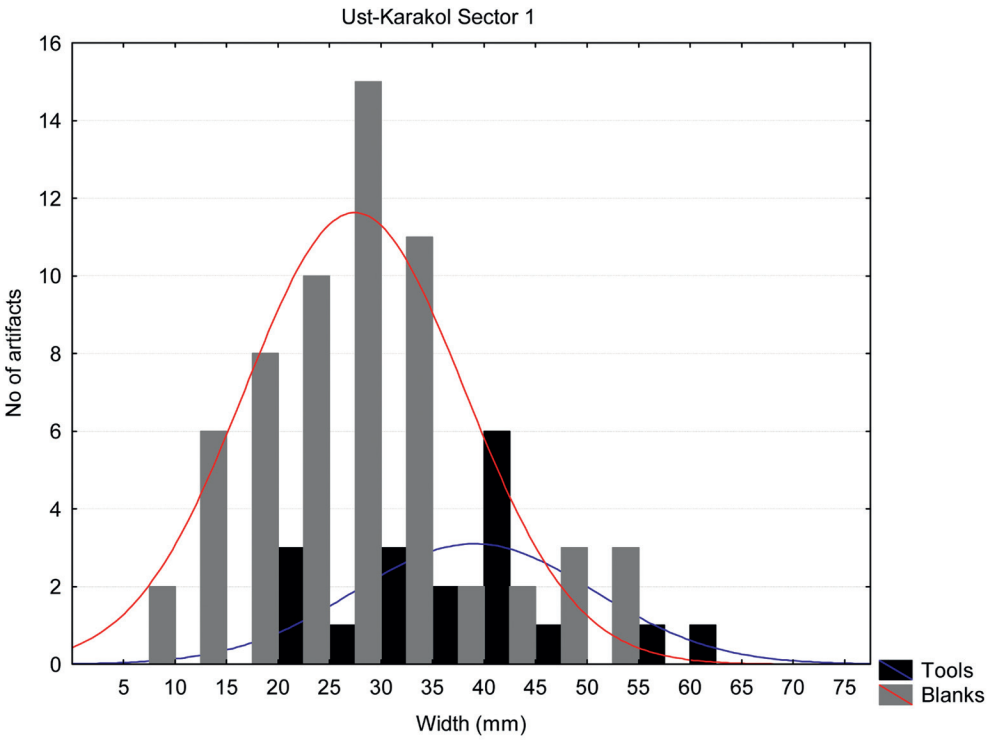

Figure 144: UK1-1, OH5.4-5.5, retouched tool and blank width distributions

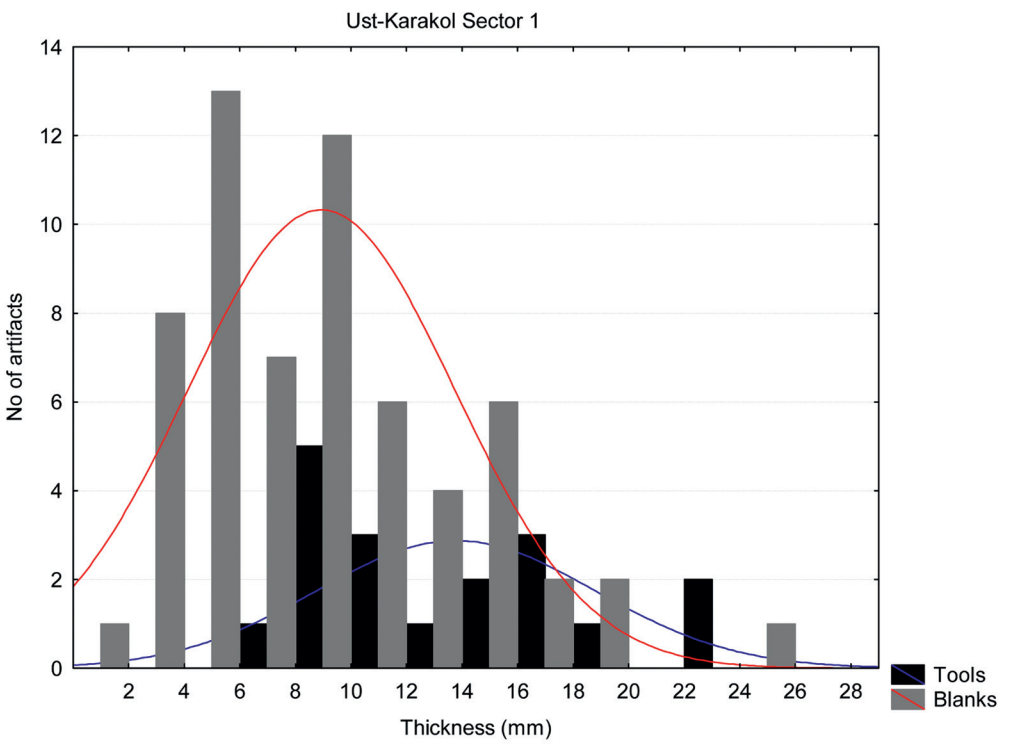

Figure 145: UK1-1, OH5.4-5.5, retouched tool and blank thickness distributions

scraper appears as one of the thickest tools with a thickness of 24 mm. When ignoring the leaf-points and the sidescraper which are not on blade blanks, the difference between the tool and the blank categories remains significant (Mann-Whitney, T=Ub=241, p=<.05), indicating that the tools tend to be thicker than the unretouched blanks.

Dorsal scar patterns indicate that most of the tool blanks are bidirectional and that a few crested elements are retouched. These results contrast with the observations made on the blank total sample; however, frequencies do not differ significantly. When comparing the tool patterning with the complete blanks, the results are in good agreement.

	N	*f*
Unidirectional	3	17%
Unidirectional and cortex	1	6%
Bidirectional	9	50%
Bidirectional and cortex	0	0%
Crest	0	0%
Second Crest	2	11%
Neo-crest	0	0%
Undet	3	17%
	18	100%

Table 101: UK1-1, OH5.4-5.5, tool dorsal pattern

Platform preparations are mainly undetermined partly due to the concretion covering some artifacts, and among the five observable cases the three different types of platforms occur. The mean platform thickness (N=5) is 4.8 ± 2.1 mm and the mean width is 14.4 ± 6.6 mm. The differences in platform thickness medians between the blanks and the tools appears not significant (Mann-Whitney, T=Ub=68, p=.43); however, the reduced sample of tool platforms makes the risk of type II error rather high.

	N	*f*
Plain	1	9%
Facetted	3	27%
Dihedral Flat	1	9%
Undetermined	6	55%
	11	100%

Table 102: UK1-1, OH5.4-5.5, tool platform preparation

The cross-sections are mostly trapezoidal (N=10), triangular (N=4) and polyhedral (N=4). The polyhedral category includes the leaf-points and the sidescraper. Tools are mainly axial (N=8) and undetermined (N=8) and generally display a straight profile (N=12).

Retouch is mainly direct, however, inverse retouch is well represented. Alternate retouch corresponds to a bifacial treatment, including two leaf-points and a sidescrpaer with bifacial retouch.

	N	*f*
Direct	9	50%
Inverse	6	33%
Alternate	3	17%
	18	100%

Table 103: UK1-1, OH5.4-5.5, tool retouch location (face)

Direct retouch is located on different parts of the blanks without any clear pattern is may be due to fragmentation and to a relatively reduced sample. Three main categories are observed, with a majority of mesial and continuous retouch (including two bilateral ones). For the inverse retouch, a clear pattern is observed with more retouch located on the proximal end of the blank. One leaf-point produced on a blade blank is included, as the two others artifacts

	Dorsal		Ventral	
	N	*f*	N	*f*
Distal	0	0%	0	0%
Mesial	3	27%	1	13%
Proximal	2	18%	5	63%
Combination	1	9%	0	0%
Continuous	3	27%	0	0%
Undetermined	2	18%	2	25%
	11	100%	8	100%

Table 104: UK1-1, OH5.4-5.5, tool retouch location (edge)

with bifacial treatment are included in the undetermined category.

From a morphological point of view, some of the tools need to be described in detail. In the sample considered, three tools show bifacial retouch.

One of the bifacial tools is a mesioproximal fragment produced on a thick blade blank (Figure 146). The dorsal face shows extensive flat retouch which mostly hinged in the thick proximal part. The ventral face shows continuous flat retouch along both edges, but the proximal part is less retouched. Typologically, it can be compared with a Jerzmanowice point, even if

Figure 146: UK1-1, OH5.4-5.5, YK-86/443-12, leaf-point on blade blank

Figure 147: UK1-1, OH5.4-5.5, YK-86/369-8, atypical leaf-point

the ventral retouch on the latter is usually located on the proximal end (Flas, 2008).

One bifacial element is likely produced on block/slab or a large flake. It shows bifacial, invasive, flat retouch. Although this artifact is classified based on its general morphology as a bifacial leaf-point (*e.g.* Freund, 1952; Koslowski, 1990; Flas, 2008), it is atypical as the preserved end is not pointed and the section is rather thick. It could also be typed as a biface. Another artifact (Figure 148) is produced on a thick slab and shows bifacial invasive retouches

Figure 148: UK1-1, OH5.4-5.5, YK-86/622-9, sidescraper

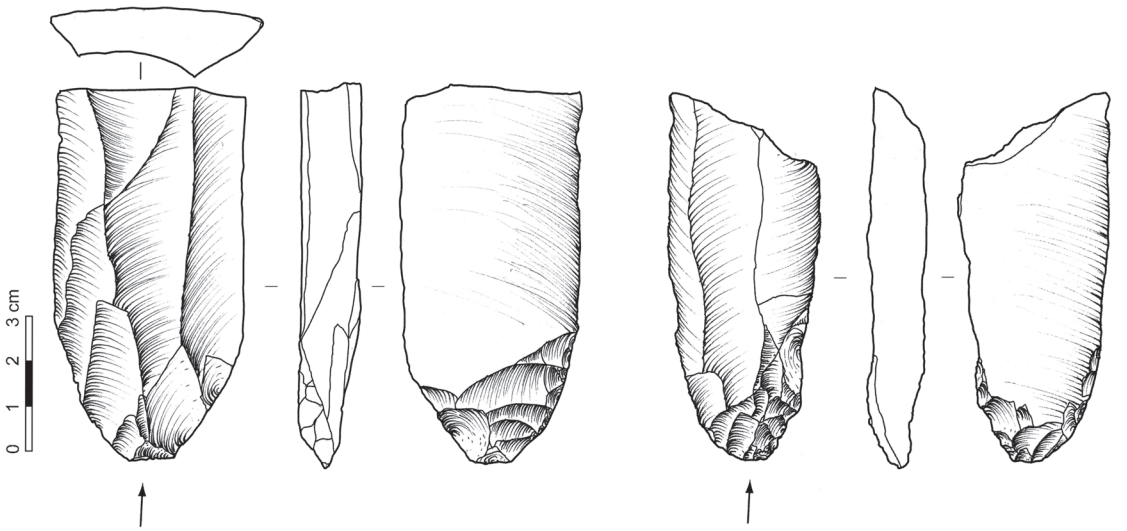

Figure 149: UK1-1, OH5.4-5.5, YK-86/B5-5-675-7 (left) and YK-86/392 (right), blades with basal thinning

along one edge, opposed to a natural back. This artifact is typed as a sidescraper.

In the sample, three blade fragments displaying proximal thinning have been identified (Figure 149). The blanks used are bidirectional blades with parallel edges bearing inverse flat retouch on their proximal end. One of them displays some direct proximal retouch similar to the Emireh point basal thinning (Garrod, 1955; Marks and Volkman, 1983; Volkman and Kaufman, 1983; Copeland, 2000). These tools can be typed as unifacial leaf points and are somewhat comparable with Jerzmanowice points, although the retouch is here not invasive (Flas, 2008).

Figure 150: UK1-1, OH5.4-5.5, YK-86/B7-719-12, large laminar flakes with inverse flat retouch

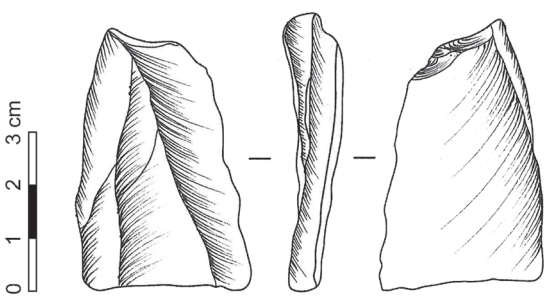

Figure 151: UK1-1, OH5.4-5.5, angle burin on oblique truncation

One of the tools is produced on a wide overshot laminar flake which bears some discontinuous direct retouch on the proximal end and along the left edge (Figure 150). The ventral side displays proximal scalar retouch and continuous and invasive flat retouch extending along the right edge. The left edge shows continuous retouch flat retouch. It can be typed as a bifacial sidescraper.

A tool is produced on proximal fragment of a bidirectional blade (Figure 151). It displays a truncation on its proximal end and a two lamellar removals slightly extending toward the ventral face. This tool can be typed as an angle burin on an oblique truncation. Some tertiary modifications of the burin edge can be observed and therefore can also be typed as a modified burin on a truncation (Demars and Laurent, 1992). Due to the reduced number of burin spall removals and to its general morphology, this burin cannot be typed as a Bassaler burin or classified as a core.